Pertanika Journal of

SCIENCE & TECHNOLOGY

JST

VOLUME 17 NO. 1 • JANUARY 2009

A scientific journal published by Universiti Putra Malaysia Press

About the Journal
Pertanika is an international peer-reviewed journal devoted to the publication of original papers, and it serves as a forum for practical approaches to improving quality in issues pertaining to tropical agriculture and its related fields. Pertanika Journal of Tropical Agricultural Science began publication in 1978. In 1992, a decision was made to streamline Pertanika into three journals to meet the need for specialised journals in areas of study aligned with the interdisciplinary strengths of the university. The revamped, Pertanika Journal of Science & Technology (JST) is now focusing on research in science and engineering, and its related fields. Other Pertanika series include Pertanika Journal of Tropical Agricultural Science (JTAS); and Pertanika Journal of Social Sciences and Humanities (JSSH).

JST is published in **English** and it is open to authors around the world regardless of the nationality. It is currently published two times a year i.e. in **January** and **July**.

Goal of Pertanika
Our goal is to bring the highest quality research to the widest possible audience.

Quality
We aim for excellence, sustained by a responsible and professional approach to journal publishing. Submissions are guaranteed to receive a decision within 12 weeks. The elapsed time from submission to publication for the articles averages 5-6 months. JST is an international journal indexed in EBSCO.

Future vision
We are continuously improving access to our journal archives, content, and research services. We have the drive to realise exciting new horizons that will benefit not only the academic community, but society itself.

We also have views on the future of our journals. The emergence of the online medium as the predominant vehicle for the 'consumption' and distribution of much academic research will be the ultimate instrument in the dissemination of the research news to our scientists and readers.

Aims and scope
Pertanika Journal of Science and Technology aims to provide a forum for high quality research related to science and engineering research. Areas relevant to the scope of the journal include: *bioinformatics, bioscience, biotechnology and bio-molecular sciences, chemistry, computer science, ecology, engineering, engineering design, environmental control and management, mathematics and statistics, medicine and health sciences, nanotechnology, physics, safety and emergency management*, and related fields of study.

Editorial Statement
Pertanika is the official journal of Universiti Putra Malaysia. The abbreviation for Pertanika Journal of Science & Technology is *Pertanika J. Sci. Technol.*

Editorial Office
Pertanika, Research Management Centre (RMC), 4th Floor, Administration Building
Universiti Putra Malaysia, 43400 Serdang, Selangor, Malaysia
Tel: +603 8946 6192, 8946 6185 • Fax: +603 8947 2075
E-mail: *ndeeps@admin.upm.edu.my*

Publisher
The UPM Press
Universiti Putra Malaysia
43400 UPM, Serdang, Selangor, Malaysia
Tel: +603 8946 8855, 8946 8854 • Fax: +603 8941 6172
penerbit@putra.upm.edu.my
URL : *http://penerbit.upm.edu.my*

Pertanika Journal of Sciences and Technology
Vol. 17(1) Jan. 2009

Contents

Regular Articles

Selected Articles from the World Engineering Congress 2007
Guest Editors: Siti Mazlina Mustapa Kamal, Farah Saleena Taip and Siti Aslina Hussain

ISSN: 0128-7680
Pertanika J. Sci. & Technol. **17 (1)**: 1 – 8 (2009)

Antimicrobial Effects on Starch-Based Films Incorporated with Lysozymes

Nozieana Khairuddin* **and Ida Idayu Muhamad**
Department of Bioprocess Engineering,
Faculty of Chemical & Natural Resources Engineering,
Universiti Teknologi Malaysia, 81310 UTM, Skudai, Johor, Malaysia
**E-mail: idayu@fkkksa.utm.my*

ABSTRACT

An antimicrobial (AM) Active Packaging can be made by incorporating and immobilizing suitable AM agents into food package matrices and applying a bio switch concept. A starch-based film was prepared and incorporated with an antimicrobial agent, *i.e.* lysozyme with EDTA as a chelating agent. This film was then inoculated with the bacteria *Escherichia coli* and *Bacillus subtilis* to carry out the microbial contamination study. The inhibition of both *E. coli* and *B. subtilis* by the AM film was clearly observed as a clear zone formation in the culture agar test. The film appearance showed that lysozymes could give a better inhibition to the growth of *E. coli* and to *B. subtilis,* at a satisfying inhibition rate. From the broth test, the decreased in the optical densities were found to be 65.83% and 91.30%, suggesting an effective growth inhibition of *E. coli* and *B. subtilis,* respectively. Physically, the film which was incorporated with lysozymes was found to be slightly different from the control film. The moisture content of the film, with lysozymes, was found to be below 10.5%, as compared to the control, after 24 hours of formation in the storage at ambient temperature.

Keywords: Antimicrobial agent, antimicrobial film, bio-switch concept, *Bacillus subtilis*, *Escherichia coli*, lysozymes

INTRODUCTION

Starches are polymers which naturally occur in a variety of botanical sources such as wheat, corn, potatoes and tapioca (Avella *et al.*, 2005; Fama *et al.*, 2005). It is a naturally abundant nutrient carbohydrate, $(C_6H_{10}O_5)_n$, which is found mainly in seeds, fruits, tubers, roots, and stems pith of plants, particularly in corn, potatoes, wheat, and rice, and this varies widely in appearance, depending on its sources; however, it is commonly prepared as a white amorphous tasteless powder. Starch is composed of repeating 1,4-α-D glucopyranosyl units: amylose and amylopectin (Avella *et al.*, 2005; Fringant, Desbrieres and Rinaudo, 1996; Mali *et al.*, 2006), where relative amounts of amylose and amylopectin, depending on the plant source (Avella *et al.*, 2005). In industry, it is used in the manufacture of adhesives, paper and textiles (Kim, Na and Park, 2003). The chemical structure of simple starch is presented in *Fig. 1.*

As a packaging material, starch alone does not form films with adequate mechanical properties (high percentage elongation, tensile, and flexural strength), unless it is first treated by either plasticization, blending with other materials, genetic or chemical modification or combinations of the above approaches. Plasticizing agents such as glycerol, sorbitol or polyethylene glycol,

Received: 6 June 2007
Accepted: 22 July 2008
*Corresponding Author

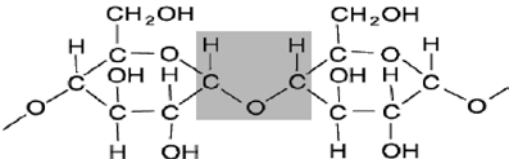

Fig. 1: Chemical structure of starch

mono-, di- or oligosaccharides, fatty acids, lipids and derivatives, are usually used to overcome film brittleness and improve its flexibility and extensibility (Flores, in press).

Antimicrobial packaging (AM) is a form of active packaging which also acts to reduce, inhibit or retard the growth of microorganisms which may be present in the packed food or packaging material itself (Appendini and Hotchkiss, 2002). Among common antimicrobial substances for food products are preservative organic acids, antimycotics (fungicide), enzymes, oxygen absorber, alcohol, etc. (Han, 2000). Many AMs are incorporated, at 0.1%-5% w/w of the packaging material, particularly films (Appendini and Hotchkiss, 2002).

Lysozyme (*Fig. 2*) is 129 amino acid residue enzyme (EC 3.2.1.17) which catalyse the hydrolysis of 1,4-beta-linkages between N-acetylmuramic acid and N-acetyl-D-glucosamine residues in a peptidoglycan and between N-acetyl-D-glucosamine residues in chitodextrins. Lysozyme is an enzyme found in egg white, tears and other secretions. The enzyme is antibacterial because it degrades the polysaccharide found in the cell walls of many bacteria. It does this by catalyzing the insertion of a water molecule at the position indicated by the arrow (a glycosidic bond), as indicated in *Fig. 3*. This hydrolysis breaks the chain at that point. Some investigations reveal that compounds like lysozyme is active against Gram-positive bacteria, and can target Gram-negative bacteria when combined with chelating agents (*i.e.* EDTA). Gram-negative bacteria possess an outer cell membrane which must be penetrated before the antimicrobial compound can reach the effective membrane suite. Penetration through the outer membrane can be accomplished by the use of a chelating

Fig. 2: The primary structure of egg white, lysozymes

agent (*i.e.* EDTA) or by osmotic shock (Padgett *et al.*, 1998). A previous study showed that the outer membrane of Gram-negative bacteria possesses divalent cations which stabilize the lipopolysaccharide association within the membrane, which is believed to hinder the ability of nisin and other molecules to reach the cytoplasmic membranes (Padgett *et al.*, 1998; Hancock, 1984). However, an addition of EDTA to edible film, containing nisin or lysozymes, had little inhibition effect on *E. coli* (Padgett, 2000) and *S. typhimurium* (Natrajan and Sheldon, 2000).

The present paper discusses the inhibitory effects of starch-based film incorporated with lysozymes against test strains of gram-positive bacteria and gram-negative bacteria. The moisture content of the film was also determined to observe the differences between the control film and the AM film.

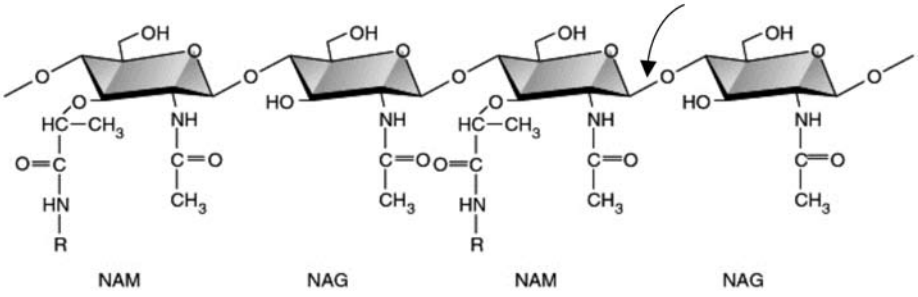

Fig. 3: Bacterial polysaccharides consists of long chains of alternating amino sugars; N-acetylglucosamine (NAG) and N-acetylmuramic acid (NAM)

MATERIALS AND METHODS

The Preparation of Antimicrobial Starch-Based Film

Starch-based films were prepared by dissolving and stirring 8.35 g starch in 80 mL of 20% ethanol. After the solution was completely dissolved, 3.8 mL glycerin (HmbG Chemicals) was added as plasticizer and the mixture was slowly heated to a mild boiling. For antimicrobial incorporated films, antimicrobial agents, lysozymes (Fluka) were mixed with 10 mL of the film solution in a separated beaker just before casting. Five milliliters of the film mixture was pipetted into petri dishes (100 mm diameter by 15 mm depth). The petri dishes were placed for 24 hour in an oven (Memmert) set at 70°C.

The Inhibition of Escherichia coli *and* Bacillus subtilis *on Agar Plate Test*

The strain selection represented the typical spoilage organism groups which commonly occur in various kinds of food products. The strains were as follows: (1) *Escherichia coli*, a conventional hygiene indicator organism, a Gram-negative rod belonging to the same family of *Enterobacteriaceae* such as *Salmonella*; and (2) *Bacillus subtilis*, a Gram-positive rod capable of forming heat-resistant spores. Spores and vegetative cells of *Bacillus* species are widely distributed in nature and are common particularly in cereals. As for the agar plate test, the AM starch-based films were cut into six squares (0.5 cm x 0.5 cm). Six sample squares were then placed onto the plate which was spread with bacteria (0.1 mL per plate). The same tests were performed using a control film. Duplicate agar plates were also prepared for each type of films and control films. The agar plates were incubated for 48 hours at 37°C in

the appropriate incubator. The plates were visually examined for the "zones of inhibition" around the film, and the results were recorded.

Enumeration

For the liquid culture test, each film was cut into squares (1 cm x 1 cm). Three sample squares were immersed in 20 mL nutrient broth (Merck, Germany) in a 25 mL universal bottle. The medium was inoculated with 200µL of *E. coli / B. subtilis* in its late exponential phase, and then transferred to an orbital shaker and rotated at 30°C at 200 rpm. The culture was periodically sampled (0, 2, 4, 8, 12, 24 hours) during the incubation to obtain the profiles of the microbial growth. The same procedure was repeated for the control starch-based film. The optical density ($o.d._{600}$) was measured at $\lambda = 600_{nm}$ using a spectrophotometer (Model UV-160, Shimadzu, Japan).

Moisture Content Determination

The determination of moisture content in this study was according to the method proposed by Finkenstadt and Willet (2004). A Moisture Determination Balance FD-620 was used to determine the moisture content (MC) of the starch products by gravimetric methods using the following equation:

$$MC = \frac{M_f - M_i}{M_i} \times 100 \quad (1)$$

For powder and thin sheet samples, the sample was heated for 25 min at 110°C. The determination of moisture content was performed in 3 replicates and the average was then reported.

RESULTS AND DISCUSSION

Antimicrobial Starch-based Film Formation

In general, a translucent starch-based film, incorporated with lysozymes which presented a good flexibility than the purely starch-based film, was formulated and formed *(Fig. 4)*. The average thickness of different films, obtained by this procedure, changed between film thicknesses which ranged from 0.16 and 0.18 mm (almost 10 measurements were conducted at different points of each kind of films with a micrometer).

The Inhibition of Escherichia coli *and* Bacillus subtilis *on Agar Plate Test*

All the samples were examined, for possible inhibition zones, after incubation at 37°C for 48 hours. *Fig. 5* shows the agar plate which contained AM incorporated film in comparison to the control film which did not consist any AM compound at all. From the observations, the AM-incorporated films revealed a clear zone which was formed on the agar plate after being in contact with the microbe colonies. For this test, the measurement of inhibition zones on/around the film squares on the inoculated bacteria was determined.

Table 1 lists the calculated inhibition area for each plate test. The control films showed that no inhibition area and colonies were formed all over the plate. The AM film showed the inhibitory growth of both *E. coli* and *B. subtilis*. Obviously, the inhibition area of *E. coli* was 27.29% larger than *B. subtilis*. The incorporation of EDTA into the film was found

Fig. 4: A translucent starch-based film incorporated with lysozymes

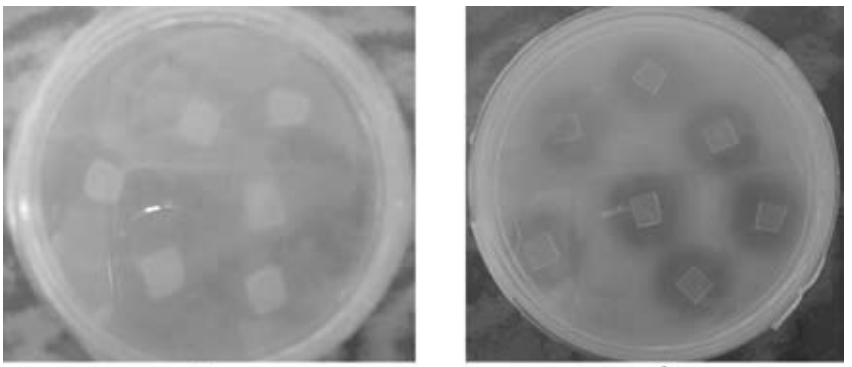

Fig. 5: A comparison of the inhibition area of (a) control film, and (b) AM incorporated film

to enhance the effectiveness against *E. coli*. The EDTA alters the outer membrane of the bacteria cell by disrupting the magnesium ions which make it stable (Dawson *et al.*, 1996).

Liquid Culture Test

In this particular test, the decrease in the optical turbidity showed that the AM had inhibited the bacteria growth. *Fig. 6a* shows the inhibition of *E. coli,* by the AM films, in a liquid culture broth at 37°C. At the stationary growth phase, the cell concentration in the control medium (OD_{600nm} = 1.355) was about 3 times higher than the cell concentration in the medium containing lysozymes incorporated film (OD_{600nm} = 0.463). *Fig. 6b* depicts the inhibition of *B. subtilis,* by the AM starch-based film, in a liquid culture broth at 37°C. Similarly, the decrease in turbidity showed that the starch-based film, containing lysozymes, had inhibited the growth of *B. subtilis*. At the stationary growth phase, the cell concentration in the control medium (OD_{600nm} = 1.127) was about eleven times higher as compared to the cell concentration in the medium containing AM film (OD_{600nm} = 0.098). Clearly, the inhibition of *B. subtilis* was found to be higher than *E. coli* because lysozymes is known as active against

TABLE 1
The inhibition of *E. coli* and *B. subtilis* on the agar plates, expressed as an area (cm^2) of inhibition zone

Film	*B. subtilis* (48 hours @ 37°C)	*E. coli* (48 hours @ 37°C)
Control	NI	NI
AM Film	15.00	20.63

NI = No inhibitory effect

Gram-positive bacteria and could target this particular bacteria type when combined with chelating agents (*i.e.* EDTA). The EDTA altered the outer membrane of the bacterial cell by disrupting the magnesium ions which stabilized the membrane (as previously reported) to increase permeability (Padgett, 1998).

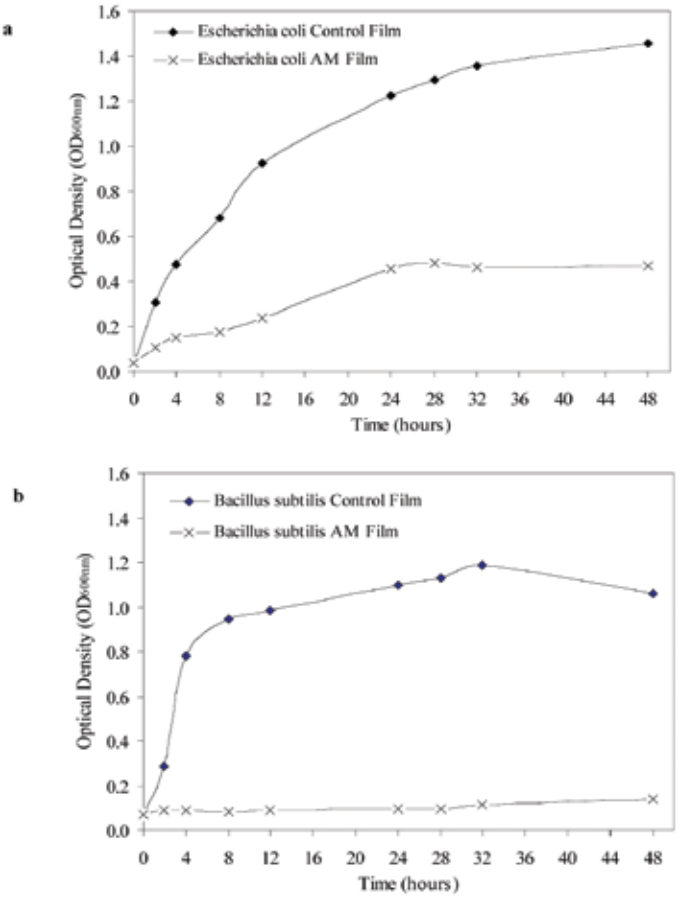

Fig. 6: The inhibition of the microbial growth by the starch-based film containing AM agents: (a) in a liquid culture medium containing E. coli *at 37°C, (b) in a liquid culture medium containing* B. subtilis *at 37°C*

Moisture Content Determination

The results showed a decrease of 10.5% in the moisture content 24 hours after the samples were incorporated with lysozyme, as compared to the control film which contained no AM agent *(Fig. 7)*. A previous study suggested that the increase in the crystalline phase of a semi-crystalline material was highly related to or associated with the decrease in its moisture content (Chang *et al.*, 2000). Consequently, the increase in the crystalline fraction with the addition of antimicrobial, and perhaps moisture or water molecules are used as the carrier to diffuse out the AM substances from the film matrices to obtain the inhibition action, which was significantly observed for the moisture content in this study. Therefore, the percentage of the moisture content was shown to decrease for the film with antimicrobial agent (Famal *et al.*, 2006).

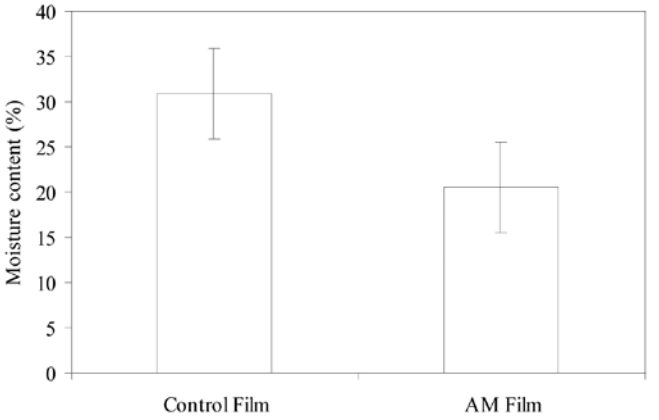

Fig. 7: A comparison of the moisture content (%) between control starch-based film and AM starch-based film

CONCLUSIONS

From the above discussion, it can be concluded that lysozymes, when combined with EDTA, enable the inhibition of both bacteria growth, but this was found to be more effectively in the inhibition of *E. coli*. As a chelating agent, EDTA plays an important role for the antimicrobial to function in the film matrix. The reduction in the moisture content of the AM film indicated the relationship between lysozymes and water molecules in the diffusion mechanism throughout the film matrices.

ACKNOWLEDGEMENT

The authors would like to thank the Ministry of Science and Innovation (MOSTI) Malaysia, the Ministry of Higher Education (MOHE) and Research Management Centre, UTM for the financial support rendered to carry out this project.

REFERENCES

Avella, M., De Vlieger, J.J., Errico, M.E., Fischer, S., Vacca, P. and Volpe, M.G. (2005). Biodegradable starch/clay nanocomposites films for food packaging applications. *Food Chemistry, 93*, 467-474.

Fama 1, L., Flores, Rojas, A.M, Goyanes, S. and Gerschenson, L. (2005). Mechanical properties of tapioca-starch edible films containing sorbates. *LWT, 38,* 631-639.

Fringant, C., Desbrieres, J. and Rinaudo, M. (1996). Physical properties of acetylated starch-based materials: Relation with their molecular characteristics. *Polymer, 37,* 2663-2673.

Mali, S., Grosmann, M.V.E., Garcia, M.A., Martino, M.N. and Zaritzky, N.E. (2006). Effects of controlled storage on thermal, mechanical and barrier properties of plasticized films from different starch sources. *Journal of Food Engineering, 75,* 453-460.

Kim, D.H., Na, S.K. and Park, J.S. (2003). Preparation and characterization of modified starch-based plastic film reinforced with short pulp fiber. II. Mechanical properties. *Journal of Applied Polymer Science, 88,* 2108-2117.

Flores, S., Fama1, L., Rojas, A.M., Goyanes, S. and Gerchenson, L. (in press). Physical properties of tapioca-starch edible films. Influence of film making and potassium sorbate. *Food Research International.*

Appendini, P. and Hotchkiss, J.H. (2002). Review of antimicrobial food packaging. *Innovative Food Science & Emerging Technologies, 3,* 113-126.

Han, J.H. (2000). Antimicrobial food packaging. *Food Technologies, 53*(3), 56-65.

Padgett, T., Han, I.Y. and Dawson, P.L. (1998). Incorporation of food-grade antimicrobial compounds into biodegradable packaging films. *Journal of Food Protection, 61*(10), 1330-1335.

Hancock, R.E.W. (1984). Alterations in outer membrane permeability. *Ann. Rev. Microbiol., 38,* 237-264.

Padgett, T., Han, I. and Dawson, P. (2000). Effect of lauric acid addition on the antimicrobial efficacy and water permeability of corn zein films containing nisin. *Journal of Food Processing and Preservation, 24,* 423-432.

Natrajan, N. and Sheldon, B. (2000). Efficacy of nisin-coated polymer films to inactive *Salmonella typhimurium* on fresh broiler skin. *Journal of Food Protection, 63*(9), 1189-1196.

Finkenstadt, V.L. and Willet, J.L. (2004). A direct-current resistance technique for determining moisture content in native starches and starch-based plasticized materials. *Carbohydrate Polymers, 55,* 149-154.

Dawson, P.L., Acton, J.C., Han, I.Y., Padgett, T., Orr, R. and Larsen, T. (1996). Incorporation of antibacterial compounds into edible and biodegradable packaging films. *Proceedings, Novel Technologies and Ingredients in Food,* Massachusetts.

Chang, P., Chea, P.B. and Seow, C.C. (2000). Plasticizing-antiplasticizing effects of water on physical properties of tapioca starch films in the glassy state. *Journal of Food Science, 65*(3), 445-451.

Fama1, L., Flores, S.K., Gerchenson, L. and Goyanes, S. (2006). Physical characterization of cassava starch biofilm with special reference to dynamic mechanical properties at low temperatures. *Carbohydrate Polymers, 66,* 8-15.

ISSN: 0128-7680
Pertanika J. Sci. & Technol. **17 (1)**: 9 – 20 (2009)

The Important Role of Concurrent Engineering in Product Development Process

A. Hambali[1*], S.M. Sapuan[1], N. Ismail[1], Y. Nukman[2] and M.S. Abdul Karim[3]
[1]Department of Mechanical and Manufacturing, Faculty of Engineering, Universiti Putra Malaysia,43400 UPM, Serdang, Selangor, Malaysia
[2]Department of Engineering Design and Manufacture, University of Malaya, 50603 Kuala Lumpur, Malaysia
[3]School of Mechanical Engineering, Faculty of Mechanical and Computer Sciences, Nottingham University Malaysia Campus, 43500 Semenyih, Selangor, Malaysia
[*]E-mail: hambali@utem.edu.my

ABSTRACT

Nowadays, Concurrent Engineering (CE) is becoming more important as companies compete in the worldwide market. Reduced time in product development process, higher product quality, lower cost in manufacturing process and fulfilment of customers' requirements are the key factors to determine the success of a company. To produce excellent products, the concept of Concurrent Engineering must be implemented. Concurrent Engineering is a systematic approach which can be achieved when all design activities are integrated and executed in a parallel manner. The CE approach has radically changed the method used in product development process in many companies. Thus, this paper reviews the basic principles and tools of Concurrent Engineering and discusses how to employ them. Similarly, to ensure a product development process in the CE environment to run smoothly and efficiently, some modifications of the existing product development processes are proposed; these should start from market investigation to detail design.

Keywords: Concurrent engineering (CE), product development process (PDP), CE principles and tools

INTRODUCTION

Concurrent Engineering (CE) is sometimes called simultaneous engineering, integrated engineering or life-cycle engineering, which is more a philosophy than a method (Tummala *et al.*, 1997). The concept of CE was initially proposed as a means to minimize product development time (Winner *et al.*, 1988).
Some common definitions are as follows:

> "Concurrent engineering is the extent to which product and process designs are generated simultaneously in the early stages of the product development process"
> (Koufteros *et al.*, 2001).

Received: 2 August 2007
Accepted: 1 November 2008
[*]Corresponding Author

Another definition of CE was presented by Junjie *et al.* (2006), as:

> "Concurrent engineering is an advanced manufacture technology in modern product design and development, which is a compact and concurrent systematic method of product design and its corresponding process (including manufacturing process and supporting process)."

Nowadays, CE is regarded as a key factor in determining the success of a company. CE involves overlapping various stages of developing new products to reduce delays. This reduction of delays is achieved by intensively implementing the CE principles. These CE principles have been cited as the main keys for the rapid new product development process and it was introduced by the Japanese firms (Bowonder and Miyake, 1993).

However, employing CE has not always been proven easy. As the popularity of CE grows and its applications have become more diverse, the core principles which define CE have become more and more vague. The CE approach is sometimes viewed as expensive in the short term, requiring resources and levels of commitment which may not be available.

According to Sapuan (2006), implementing the CE can reduce costs, shorten the time of product development process and improve product quality (CTQ), if all design activities are performed in a parallel manner and the decision making among different groups are integrated. However, CE does not mean a simultaneous undertaking of all activities in the product development process at the same time.

The objectives of this paper were to present the findings of the research on the use of CE in the product development process, review several CE principles and tools in solving product development process problems as well as propose some modifications of the existing product development process.

CONCURRENT ENGINEERING (CE) VERSUS SEQUENTIAL ENGINEERING (SE)

The method where each design phase mostly starts, when the previous one has been completed, is called sequential engineering' (SE), as shown in *Fig. 1.* The SE can also be defined as a process, in which different stages such as customer investigation, product design specification, detail design, manufacturing, and testing are separately and sequentially conducted (Portioli-Staudacher *et al.,* 2003). Therefore, some problems which may arise during product development process may cause the need for the product to be redesigned and this redesigning activity will increase development time and cost of the product (Bhuiyan *et al.*, 2006). Moreover, a critical issue in this approach is how much the requirements and design have been modified in order to be finally accepted for manufacturing and production. These factors will weaken the competitiveness of products (Kamrani and Vijayan, 2006).

In order to improve the efficiency of the product development process, CE approach must be implemented; this is shown in *Fig. 2.* In this method, all the activities in the product development process are integrated and run in parallel with the feedback when needed, and

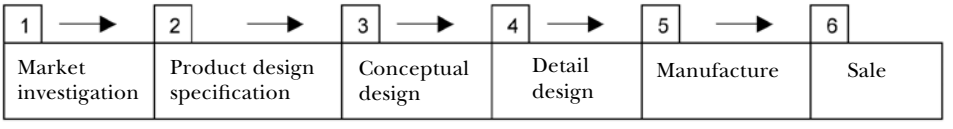

Fig. 1: Steps in product development process with serial engineering

the information and CE tools continuously flow along with all the activities in the product development process. Consequently, many of the problems which can occur under the sequential engineering process can be completely prevented after a proper consideration.

A recent study carried out by Bhuiyan *et al.* (2006), by means of comparison between the CE and SE projects in terms of process, tools and technology, communication, time to market, project performance, etc., showed that the use of the CE project was more successful than the SE project at Telcom, where tremendous improvements in terms of time to market, project development, cost and product quality were achieved.

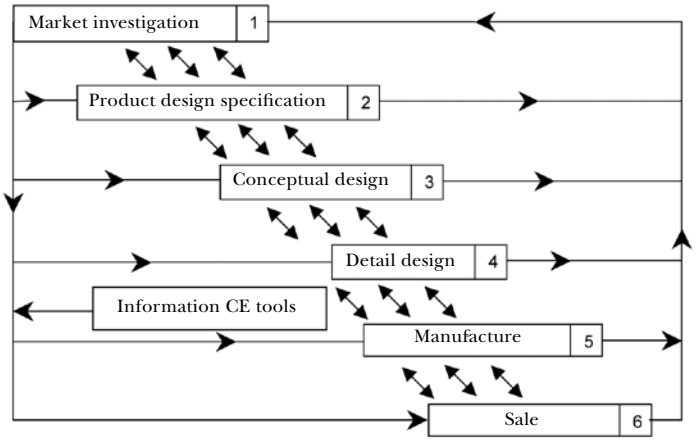

Fig. 2: Steps in product development process with CE environment

THE PRINCIPLES OF CE

In general, CE principle can be divided into three key factors which can contribute to time reduction, cost reduction, improve product quality and fulfil customer's need, as shown in *Fig. 3* (Portioli-Staudacher *et al.*, 2003; Kalkowska *et al.*, 2005; Bhuiyan *et al.*, 2006).

People

In the CE approach, utilizing the appropriate human resource at the right time is critical and it accelerates development by keeping rework to a minimum. To be successful in CE implementation requires some factors have to be considered as follows:

i. Teamwork

Team work is the basic principle of the CE (Lettice *et al.*, 1995; Kusar *et al.*, 2004). Teamwork emphasizes interpersonal relationship, cooperation, negotiation and collaboration decision making. Teamwork is an integral part of CE, as it represents the means for organizational integration.

ii. Multidisciplinary teams

CE is based on multidisciplinary product development team. Multidisciplinary teams, involving experts from all stages of the product development process such as design, process, production, marketing, manufacturing, etc., are very important in order to

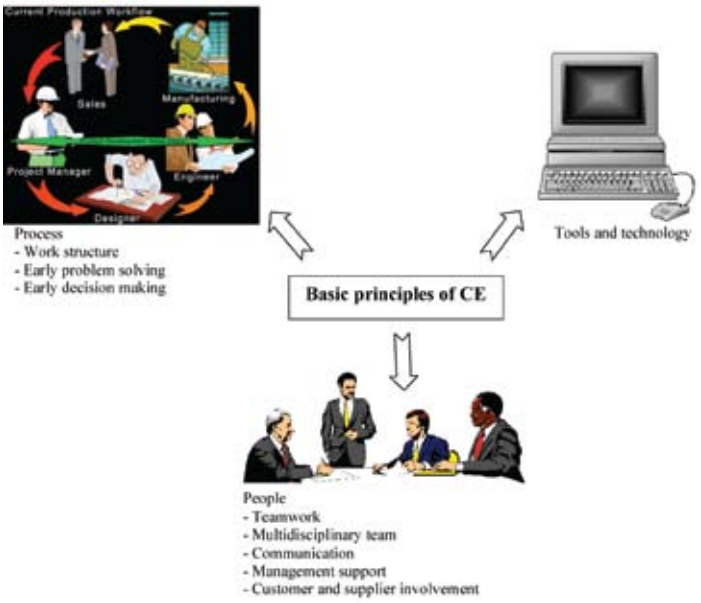

Fig. 3: Basic principles of CE

succeed in CE implementation. Multidisciplinary teams can break down the barriers between departments and provide effective means of communications.

iii. Communication

Communication is the basic principle for success in CE. Teams will work better if they know what other members are doing. Team members have regular meetings which allow fast and efficient exchange of information (Kusar *et al.*, 2004). Communication between suppliers, customers and manufacturer is also a basic principle in the implementation of CE at the early stage of product development process (Portioli-Staudacher *et al.*, 2003; Hamid *et al.*, 2005). However, according to Bhuiyan *et al.* (2006), less communication can result in less time spent and lower the potential for confusion.

iv. Management Support

According to Abdalla (1999), the main problem during practicing CE was the commitment of management in implementing CE. Thus, the lead and support from the top management is important to realize the implementation of a successful CE. The top management must not only support the CE initiative, but also actively participate in formulating and implementing the CE goals.

v. The Involvement of Customers and Suppliers

In designing and manufacturing a product, the integration between the customers, suppliers and manufacturer is essential in determining the success of a product. This CE principle can reduce a significant portion of design error and rework due to misunderstandings or miscommunication between the company, the customers, and the suppliers, at the early stage of product development process.

Process

A key in implementing the CE approach is to have a single well-defined process with clear ownership and goals. Thus, the process and the related schedule of activities must be based on some basic principles, as follows:

i. Work structure

In general, all activities in product development process must be performed in a parallel and simultaneous approach. In order to construct a clear work structure or framework, some factors have to be worked out such as defining and formalizing the CE process, defining overlapping activities, identifying process ownership and setting goals clearly.

ii. Early Problem Discovery

Problems which are discovered at the early stage of the product development process (particularly during the first 20% of the cycle time) are easier to solve than those which are discovered later.

iii. Early Decision Making

The 'window of opportunity' to affect a design is much wider during an early design stage than in a later stage, i.e. when some of the decisions are frozen and the design is matured.

Tools and Technology

An appropriate set of tools and technology should be chosen to help achieve the maximum benefits which enable integrated product development. For an effective CE implementation to be accomplished, the use of tools and technology is greatly required. However, there are two aspects which need to be considered when implementing the tools and technology; firstly, the tools and technology which enable an effective implementation of CE need to be identified, and secondly, people who will use these tools and technologies should be trained.

PRODUCT DEVELOPMENT PROCESS WITH CONCURRENT ENGINEERING

Concurrent engineering (CE) is a very important concept in the world of new product development. It is a methodology used for creating timely products, while maintaining the highest quality, lowest cost and most customers' satisfaction. In conventional product development, activities such as market investigation, product design specification, conceptual design, detail design, manufacturing and sales are sequentially performed and the trend is to complete 100% of each stage before performing the next. In this approach, a large number of modifications have to be made in the later stages of the product development process. Consequently, this can contribute to the increase in the time and cost involved in the product development process. Meanwhile, CE is a systematic approach to integrate all the design activities, and it provides a framework to make changes in design.

Basically, product development process is a process for translating customers' requirements into product design and manufacturing. Product development process provides a roadmap to designers for the activities or processes and deliverable required in designing, developing and manufacturing a particular product. The main objectives of a product development process are to minimize the life-cycle cost, maximize product quality, as well as maximize customers' satisfaction, maximize flexibility and minimize lead

time (Mazumdar, 2002). Product development process can be categorized into two main processes, firstly, deal with development of a product and secondly, deal with its production (Kusar *et al.*, 2004). However, this paper only describes the development of a product, which is initially started from market investigation up to the detail in the designing stage.

In the literature, there has been no standard product development process or designing process in the context of the CE environment. Nevertheless, various product development processes, within a CE environment, have been developed and proposed in the literature. There are a number of well-known and established product development models which are being implemented by most product designers or engineers, such as the Pugh's model (Pugh, 1991), Pahl & Beitz' model (2007), French's model (1985) and Shigley's model (Groover and Zimmers, 1984). These models are intended to be general and aim to guide designers to traverse a series of design stages and carry out a number of design activities in order to understand and solve design problems. These models are included under the umbrella of CE. However, most product development models developed, as mentioned above, merely provide a guideline or design flow to assist designers or engineers in performing designing activities, but they still lack in terms of addressing the CE tools, which is a key factor to success in the new product development in the CE environment.

The design flow of the product development process used in this research was based on the total design method or the Pugh's method (Pugh, 1991). This method has widely been used by most designers or researchers in developing a new product or automotive components. However, this method does not specifically show development in terms of the CE tools needed, but are rather descriptive of design activities; whereas, the CE tools and its flow are key elements which must really be addressed in the product development process in the CE environment. Sapuan (1996) criticized on the sequential flow of the designing process and stressed that the concept of CE must be implemented in a clear manner in this method.

There are some examples which show the importance of addressing the use of the CE tools in product development process under the CE environment in the literature. Among others, Sapuan (1998) developed a concurrent engineering design system for polymeric-based composites automotive components. The system was developed in order to assist designers to determine the materials which would satisfy a set of pre-defined design constraints, particularly in terms of reduction of weight and cost. The system comprised the integration of various CE tools, such knowledge-based system (KBS), solid modelling, material database and design analysis tools. Meanwhile, Yan (2003) developed an innovative design process model for a computer-based engineering design through an integrated and coherent use of computer-aided design (CAD) systems. The design approach which was based on the computer multiperspective modelling and evaluation derived from the above design process model could provide a comprehensive and integrated design support for various engineering design activities. Rozlina *et al.* (2004) proposed a product development model by integrating various CE techniques such as quality function deployment (QFD), morphological chart, concept convergence and design for assembly (DFA). The proposed model allows users' requirements to be identified, generates various design concepts and its evaluation; based on which, the chosen design is then optimized for manufacturing assembly. Thus, it has been proven that the CE tools should be clearly addressed at every stage of product development process under the CE environment.

A literature review of the existing studies shows the importance of addressing the CE tools in product development process, and none of the above researchers have addressed the use of the CE tools in their proposed product development process, i.e. starting from

market investigation until the detail in the designing stage. To overcome these limitations, this paper proposed a model which could provide some basic steps in the CE tools required, starting from market investigation to detail design in order to assist design teams to perform their design activities more effectively and efficiently.

The Proposed Modification of the Modelling of Concurrent Engineering System in Product Development Process

Product development process can be further divided into two main processes; firstly, it deals with the development of a product and secondly, it deals with its production (Kusar *et al.*, 2004). It has generally been known that approximately 80% of the manufacturing cost of a product is determined by the design of the product (Mikkola and Skjoett-Larsen, 2003). Thus, this paper only describes the development of a product which is started from market investigation to detail design. *Fig. 4* shows the product development process being practiced by most manufacturers; this process does not specifically show development in terms of the CE tools needed, but it is rather a description of the design activities. Meanwhile, the CE tools and their flow are key elements which must really be addressed in the product development process in the CE environment.

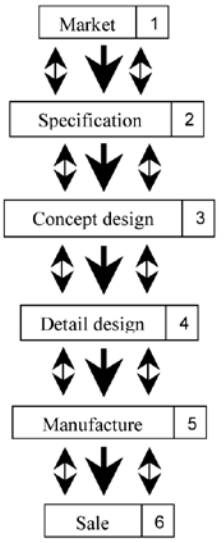

Fig. 4: Total design activity model (Pugh, 1990)

The proposed model of product development process in the CE environment is shown in *Fig. 5*. Several CE tools should be addressed and implemented to produce a product with good quality. Typically, all designing phases in this model are operated in parallel, simultaneously and iteratively but systematically operating within the design phase will minimize unnecessary iteration. From this proposed model, those who are involved in the product development process - begin with market investigation and end with detail design - will be able to understand the process flow of the product development in the CE environment. The proposed product development process, in the CE environment process, consists of four main phases, as follows:

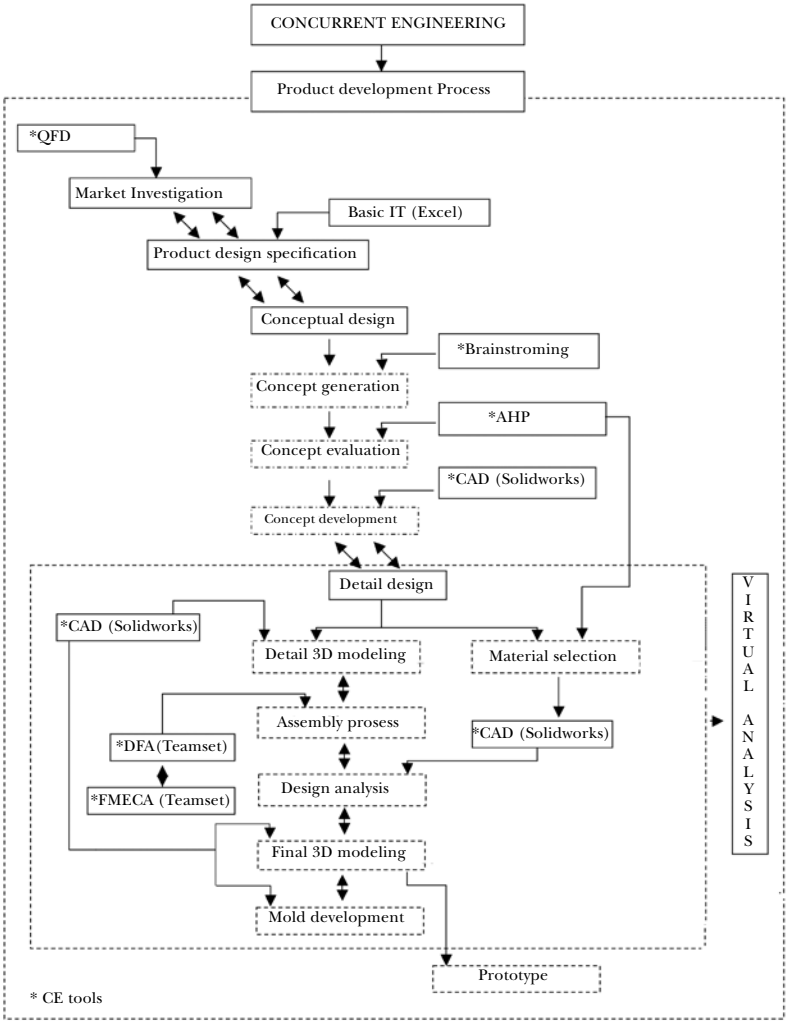

Fig. 5: Proposed product development process with CE environment

i. Market investigation

Market investigation phase is the first step in product development process and it is essential in determining the success of a product. There are many products which have been reported as unsuccessful in the marketplace because they do not meet the customers' expectation (Cooper, 2003). It is necessary to implement a tool which can ensure a better understanding of the customers' needs and requirements. One of the useful and familiar methods is quality function deployment (QFD) (Hsiao, 2002; Chen and Yang, 2004). QFD is a customer-oriented approach to product development. It supports design teams in developing new products in a structured way, based on the assessment of customers' needs.

ii. Product Design Specification (PDS)

The design specification or product design specification (PDS) is constructed after analyzing the marketplace and customers' needs. PSD is a document prepared early in the product

development process; it sets out the requirements which the design will have to satisfy. In a way, PDS acts as the control for the total design activity because it places the boundaries on the subsequent designs (Pugh, 1991). As PDS is a control document, basic computer applications have to be employed.

iii. Conceptual Design

Conceptual design is carried out within the envelope of the PDS. The conceptual design phase is more essential as compared to other design phases in product development process. This is because it forms the background work and involves many complex evaluation and decision making tasks (Sapuan, 2005a; Xu *et al.*, 2007) at this stage. In general, conceptual design consists of three steps; these are concept generation, concept evaluation and concept development.

– Concept Generation

One of the tools which can generate ideas to meet the PDS is brainstorming. This method involves generating ideas, which is typically done in small groups. By the end of a brainstorming session, there will be a list of ideas, most useless, but some may have the potential to be developed into a concept. This brainstorming session can work better if the most of the teams have different areas of expertise.

– Concept Evaluation

Once a suitable number of concepts have been generated, it is necessary to choose the most suitable design or alternative to fulfil the requirement to set out the PDS. There are many useful tools to be used in evaluating and making the best decision; these include expert system, fuzzy logic, neural network, analytical hierarchy process, etc. In the concept development phase, the chosen concept or alternative can be further developed in detail.

– Concept Development

After evaluating and decision making have been accomplished, the product should be developed in detail. At this phase, the CE tool such as the computer aided design (CAD) is essential and it must be implemented actively. The chosen concept design is designed in detail, by considering all the dimensions and specifications until the final design is carried out.

iv. Detail Design

At this phase, 3D modelling must go through five processes before the product can be manufactured. This 3D modelling and material selection analysis must be performed simultaneously, as shown in *Fig. 5*. The CE tools (such as computer aided design, or CAD) have to be applied so as to create a detail 3D modelling and for design analysis purposes. The products which have a number of parts must be analyzed using design for assembly (DFA) method in order to reduce the number of parts which are not necessary to be manufactured. After that, the product will be analyzed by employing failure mode effects critical analysis (FMECA) to evaluate the potential failure of a particular product or process. Based on the results gathered from the material selection, the 3D modelling must be analyzed to ensure the selected material is able to be manufactured easily. Then, the final detail of the 3D modelling, using the CAD, will be carried out once the design analysis is completed. Finally, the mould design of the product will be developed using the CAD applications. Generally, all the processes in the detail design phase are known as the virtual analysis because all these designing aspects can be simulated and analyzed using design simulation software.

CONCLUSIONS

This research supports the claims that CE is very important in product development process. The application of the CE concept and its tools in the product development process can help the designers to manufacture products more efficiently and effectively. The firms which have been implementing CE tool in their product development have gained tremendous benefits, particularly in terms of reducing cost incurred, reducing time for product development process, improving product quality and fulfilling customers' requirements. Moreover, some design uncertainties can be reduced using this method, and the product can be designed in a more transparent process.

ACKNOWLEDGEMENTS

The authors wish to thank Universiti Teknikal Malaysia Melaka (UTeM) and Universiti Putra Malaysia (UPM) for the support granted for this research.

REFERENCES

Abdalla, H.S. (1999). Concurrent engineering for global manufacturing. *Journal of Production Economics,* 60-61, 251-260.

Bowonder, B. and Miyake, T. (1993). Japanese innovations in advanced technologies: An analysis of functional integration. *Journal of Technology Management, 8*(2), 135-156.

Bhuiyan, N., Thomson, V. and Gerwin, D. (2006). Implementing concurrent engineering, *Journal of Research Technology Management, 49*(1), 38-43.

Chen, S.H. and Yang, C.C. (2004). Applications of Web-QFD and Delphi method in the higher education system. *Journal of Human Systems Management, 23*, 245–256.

Cooper, L.P. (2003). A research agenda to reduce risk in new product development through knowledge management: A practitioner's perspective. *Journal of Engineering and Technological Management, 20*(1-2), 117–140.

Curran, R., Price, M., Raghunathan, S., Benard, E., Crosby, S., Castagne, S. and Mawhinney, P. (2005). Integrating aircraft cost modelling into conceptual design. Journal of Concurrent Engineering, *13*(4), 321-330.

French, M.J. (1985). *Conceptual Design for Engineers*. London: Springer-Verlag.

Groover, M.P. and Zimmers. E.W. (1984). *CAD/CAM Computer Aided Design and Manufacture*. California: Prentice Hall International.

Hamid, A.B.A., Sabri, A.H.M., Mun, N.K., Shen, Y.S. and Sapuan, S.M. (2005). The implementation of early supplier involvement (ESI) in Malaysia Manufacturing Industry. *Journal of Applied Technology, 3*(2), 77-83.

Hsiao, S.W. (2002). Concurrent design method for developing a new product. *International Journal of Industrial Ergonomics, 29*(1), 41–55.

Huanga, X., Soutarb, G. N. and Browna, A. (2004). Measuring new product success: An empirical investigation of Australian SMEs. *Journal of Industrial Marketing Management, 33*(2), 117– 123.

Junjie, X., Xiaolan, J., Zhong, W. and Huahui, C. (2006). Research on green design of complex product based on concurrent engineering. *International Conference on Computer-aided Industrial Design Conceptual Design* (p. 1-5). China.

Kalkowska, J., Trzcieliniski, S. and Wlodarkiewicz-Klimek, H. (2005). Investigation of concurrent engineering in Polish manufacturing companies -some results of pilot research. *Fifth International Workshop on Robot Motion and Control* (p. 315-319). Poland.

Kamrani, A. and Vijayan, A. (2006). A methodology for integrated product development using design and manufacturing templates. *Journal of Manufacturing Technology Management, 17*(5), 656-672.

Koufteros, X.A., Vonderembse, M.A. and Doll, W.J. (2001). Concurrent engineering and its consequences. *Journal of Operations Management, 19*(1), 97–115.

Kusar, J., Duhovnik, J., Grum, J. and Starbek, M. (2004). How to reduce new product development time. *Journal of Robotics and Computer-Integrated Manufacturing, 20*(1), 1-15.

Mikkola, J.H. and Skjoett-Larsen, T. (2003). Early supplier involvement: Implication for new product development outsourcing and supplier-buyer interdependence. *Global Journal of Flexible Systems Management, 4*(4), 31-41.

Mazumdar, S.K. (2002). *Composites Manufacturing: Materials, Products, and Process Engineering*. New York: CRC Press.

Pahl, G., Beitz, W., Feldhusen, J. and Grote, K.H. (2007). *Engineering Design: A Systematic Approach*, Berlin: Springer.

Portioli-Staudachera, A., Landeghemb, H.V., Mappellic, M. and Redaellid, C.E. (2003). Implementation of concurrent engineering: A survey in Italy and Belgium. *Journal of Robotics and Computer Integrated Manufacturing,19*(3), 225–238.

Pugh, S. (1991). *Total Design: Integrated Methods for Successful Product Engineering*. Wokingham, England: Addison Wesley Limited.

Rozlina, M.S., Shahoroun, A.M., Tap, M.M. and Ishak, N. (2004). A new approach towards achieving total product design from concept to manufacture. In *Proceeding of ICPDD 2004 the 1st International Conference on Product Design and Development*, 20-24 December, Kota Kinabalu, Sabah.

Sapuan, S.M., Maleque, M.A., Hameedullah, M., Suddin, M.N. and Ismail, N. (2005). A note on the conceptual design of polymeric composite automotive bumper system. *Journal of Material Processing Technology, 159*(2), 145-151.

Sapuan, S.M. (1996). The improvement of design and manufacture in total design studies. *AEESEAP Journal of Engineering Education, 26*, 52-61.

Sapuan, S.M. (1998). A concurrent engineering design system for polymeric-based composite automotive components (PhD Thesis, University of De Montfort. United Kingdom).

Sapuan, S.M., Osman, M.R. and Nukman, Y. (2006). State of the art of the concurrent techniques in the automotive industry. *Journal of Engineering Design, 17*(2), 143-157.

Tan, C.L. and Vonderembse, M.A. (2006). Mediating effects of computer-aided design usage: From concurrent engineering to product development performance. *Journal of Operations Management, 24*(5), 494–510.

Trzcieliniski, S. (2003). Lean management and virtuality of Enterprise. Scientific Papers of the Institute of Organization and Management of Wroclaw University of Technology, No. 73.

Tummala, V.M.R., Chin, K.S. and Ho, S.H. (1997). Assessing success factors for implementing concurrent engineering a case study in Hong Kong electronics industry by analytical hierarchy process. *International Journal of Production Economics, 49*(3), 265-283.

Xu, L., Li, Z., Shancang, L. and Fengming, T. (2007). A decision support system for product design in concurrent engineering. *Journal of Decision Support Systems, 42*(4), 2029– 2042.

Yan, X.T. (2003). A multiple perspective product modelling and simulation approach to engineering design support. *Concurrent Engineering: Research And Applications, 11*, 221-234.

Winner, R.I., Pennel, J.P., Bertrend, H.E. and Slussarczuk, M.M.G. (1988). The role Concurrent Engineering in weapon system Acquisition. IDA report R-338. Alexandria, VA: Institute for Defense Analyses.

ISSN: 0128-7680
Pertanika J. Sci. & Technol. **17 (1)**: 21 – 32 (2009)

A Spatial Decision Support Tool for Oil Palm Plantation Management

Loh Kok Fook[1*], Ragu Ponusamy[2], Shattri Mansor[1] and Jamil Ismail[3]
[1] Spatial and Numerical Modelling Laboratory (SNML), Institute of Advanced Technology, Universiti Putra Malaysia, 43400 UPM, Serdang, Selangor, Malaysia
[2] Wisma FELCRA, Lot PT 4780, Jalan Rejang, Setapak Jaya, Peti Surat 12254, 50772 Kuala Lumpur, Malaysia
[3] Espatial Resources Sdn. Bhd., 6-1-1 Jalan 3/50, Diamond Square Commercial Centre, Off Jalan Gombak, 53000 Kuala Lumpur, Malaysia
[*] E-mail: kfloh03@yahoo.com

ABSTRACT

Malaysia is in the process of modernizing its oil palm plantation management, by implementing geo-information technologies which include Remote Sensing (RS), Geographic Information System (GIS), and Spatial Decision Support System (DSS). Agencies with large oil palm plantations such as the Federal Land Development Authority (FELDA), Federal Land Consolidation and Rehabilitation Authority (FELCRA), Guthrie Sdn. Bhd., and Golden Hope Sdn. Bhd. have already incorporated GIS in their plantation management, with limited use of RS and DSS. In 2005, FELCRA, Universiti Putra Malaysia (UPM) and Espatial Resources Sdn. Bhd. (ESR) collaborated in a research project to explore the potentials of geo-informatics for oil palm plantation management. The research was conducted in FELCRA located in Seberang Perak Oil Palm Scheme. In that research, a tool integrating RS, GIS and Analytical Hierarchy Process (AHP) was developed to support decision making for replanting of the existing old palms. RS was used to extract productive stand per hectare; AHP was used to compute the criteria weights for the development of a suitable model; and GIS was used for spatial modelling so as to generate the decision support layer for replanting. This paper highlights the approach adopted in developing the tool with special emphasis on the AHP computation.

Keywords: Remote Sensing, Geographic Information System, Analytical Hierarchical Process, Spatial Modelling and Spatial Decision Support Tool

ABBREVIATIONS

Analytical Hierarchy Process	– AHP
Remote Sensing	– RS
Geographic Information System	– GIS
Spatial Decision Support Tool	– SDST
Federal Land Development Authority	– FELDA
Federal Land Consolidation and Rehabilitation Authority	– FELCRA
Universiti Putra Malaysia	– UPM

Received: 6 August 2007
Accepted: 10 October 2008
[*]Corresponding Author

INTRODUCTION

Malaysia is regarded as the world's largest exporter of palm oil and its production is increasing annually due to the potential world bio-fuel markets. The cultivation of oil palm in Malaysia is largely based on private plantation management such as Guthrie Sdn. Bhd. and Golden Hope Sdn. Bhd., or organized mini estates under the supervision of some government agencies like Federal Land Development Authority (FELDA), and Federal Land Consolidation and Rehabilitation Authority (FELCRA). This has enabled a better utilization of resources through the application of advanced management statistically based tools currently and widely accepted in the palm oil industry.

In the current digital era, there is a need to modernize the management of oil palm estates in Malaysia, i.e. using state-of-the-art spatial technologies, which include Remote Sensing (RS), Geographic Information System (GIS), Global Positioning System (GPS) and Spatial Decision Support Tool (SDST), to enable reliable, cost effective and timely data collection and analysis, thus supporting more accurate decision making.

In recent years, researchers in Malaysia have embarked into the use of RS technologies in extracting oil palm crop performance indicators such as tree inventorying (Loh *et al.*, 2005), oil palm phenology (Ibrahim *et al.*, 2002) and palm macro-nutrient assessment (Nor Azleen *et al.*, 2002). The RS, GIS and GPS tools have also been developed to generate spatial layers relevant for integrated oil palm plantation management (Tey and Chew, 1997; Mariamni *et al.*, 2002; Wahid *et al.*, 2002). However, no effort has been carried out in developing the SDST for the management of oil palm plantation, despite the fact that the tool has been made operational for land use planning in several other countries (Diamond and Wright, 1988; Loh, 1991; Parker *et al.*, 2003).

The widely accepted decision making process comprises three major phases (Simon, 1960; Malczewski, 1999). These include intelligence (problem surveillance), design (setting alternatives) and choice (choosing the most attractive/best alternative). RS provides a powerful capacity to capture data through a variety of earth observation satellites. These data are then organized in the GIS to provide selection, integration, manipulation, exploration, and confirmation and generate useful information for the analysis of various processes. However, given the present RS-GIS technology level, the information generated as such mostly does not fulfil the requirements of the different phases of the decision making process, particularly in the choice phase.

FELCRA, Universiti Putra Malaysia (UPM) and Espatial Resources Sdn. Bhd. (ESR) collaborated in conducting a research project to explore the potentials of geo-informatics for the management of oil palm plantation in 2005. The overriding objective of the project was to establish a software spatial-based tool to support decision making for the replanting which is already existing in the old oil palm plantations in FELCRA; to-date, there are some 180000 hectares of oil palm plantations in Malaysia. In phase 1 of the project, which was completed in 2006, the researchers developed and integrated a database for the oil palm plantation management using the RS and GIS technologies (Loh *et al.*, 2005). Phase 2, which was currently implemented, focused on the development of the SDST.

MATERIALS AND METHODS

The flowchart of the methodology used is depicted in *Fig. 1*; it comprises of essentially four components – base information collection through RS, spatial layers generation in GIS, model development using AHP and spatial modelling to generate the decision support layer in the GIS environment.

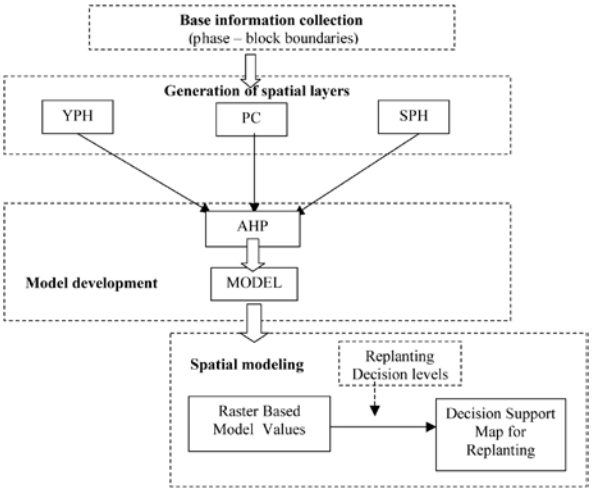

Fig. 1: The flowchart of the methodology used in the study

Study Area

Seberang Perak, comprising of some 7800 hectares of matured oil palms, was selected as the study area. It is located in the state of Perak, Malaysia, and located between the latitudes of 4.0735 and 4.2647 N, and the longitudes between 100.7983 and 100.9525 E (see *Fig. 2*). The area is situated on a gentle terrain, having basically peat soils and riverine alluvia. The mean monthly rainfall exceeds 120mm, except for July, which is regarded as a dry month, with the rainfall below 75mm. For the purpose of this study, Phase 15 covered about 1785 hectares of old oil palms, was selected for the development of the SDST, using the RS-GIS and Analytical Hierarchy Process (AHP).

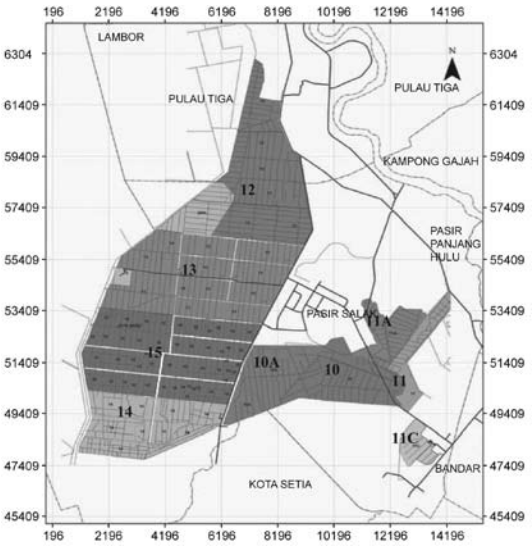

Fig. 2: The study area

Base Information Collection

IKONOS satellite imageries, dated July 21 2004, were acquired. The images were enhanced and geo-coded to conform to the Malaysian's Cassini Map Projection specifically designed for large scale map production, using 20 ground control points. An interactive linear contrast stretch was also applied to the image enhancement of the features of interest such as healthy and diseased palm trees, while the geo-coding process adopted the 1st polynomial transformation and the nearest neighbour re-sampling algorithm.

Plantation phase-block boundaries were extracted from the IKONOS imageries through a manual digitization and input into the GIS as arcs and polygon files with topology built.

Spatial Layer Generation

Three spatial layers were generated in the GIS – yield per hectare (YPH), production cost per fresh fruit bunch (PC) and stand per hectare (SPH). The data for YPH and PC were provided by FELCRA, while the SPH was extracted from the IKONOS datasets through a manual digitization of individual trees, as shown in *Fig. 3*.

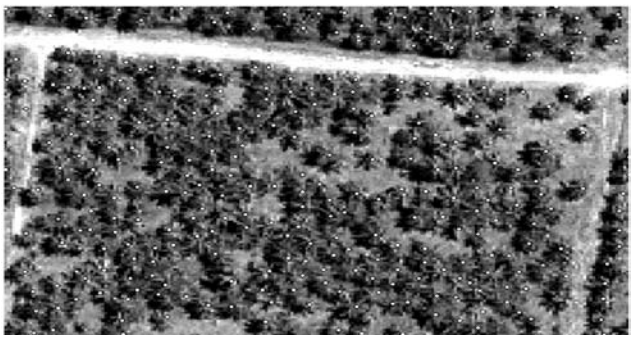

Fig. 3: Manually digitized trees from IKONOS data

Model Development Using the AHP

The AHP approach (Saaty, 1977; Saaty, 1980; Saaty, 1982) was adopted to determine the criteria priorities (weight) for the development of a model to support the decision making in replanting the existing old oil palm stand. The AHP incorporated both the qualitative and quantitative aspects of human thinking. It particularly involves (i) hierarchical structuring of the issue at hand, breaking it into separated and related structural elements or criteria; (ii) prioritizing criteria through a mathematical means; and (iii) ensuring consistency in criteria prioritization mathematically.

Spatial Modelling

A spatial weighted linear model was adopted for the generation of the decision support map for replanting, as given in equation 1. It represents the summation value of the products of criteria weights and sub-criteria scores to be assigned to each pixel of the composite spatial layer to support replanting. Weighted linear combination analysis is a common procedure in the GIS-based multi-criteria analysis. It has been adopted in the resource and disaster management studies (Chuvieco and Congalton, 1989; Graeme, 1996; Hall *et al.*, 1997; Feick and Hall, 1999).

$$R = \sum WiXi \quad (1)$$

Where, *R* represents the composite value for replanting; Wi is the criteria weight, and Xi is a sub-criteria score.

RESULTS AND DISCUSSION

AHP Computations

In this study, a 3-level hierarchy structure was designed to support the decision making for replanting. The alternatives for decision making in replanting, including (i) replant, (ii) under observation and (iii) status quo, were placed at the 3rd or bottom level of the hierarchical structure, as shown in *Fig. 4*. The next level consisted of the criteria selected for judging the alternatives; these were (i) yield per ha (YPH), (ii) production cost per ton of fresh fruit bunch (PC), and (iii) stand per ha (SPH). The top level was a single element – the decision support for replanting.

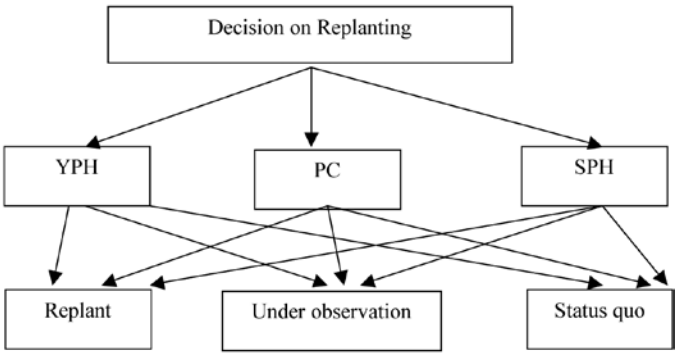

Fig. 4: Hierarchical structure for replanting decision

Although the three criteria selected influences one another, their respective impacts on decision making for replanting differ in importance. The justifications for the selection of these criteria are given in Table 1. Terrain, which is important in determining whether replanting an area with oil palm is an acceptable choice, was not selected as a criterion as the entire study area was flat, and therefore, suitable for the oil palm cultivation.

Prioritizing the criteria was done using the pair-wise comparison ratings developed by Saaty (1980), as presented in Table 2. The method employs an underlying scale, with ratings from 1 to 9, to rate the relative importance or preference for two criteria to be compared. The matrix depicted in Table 3 shows the ratings assigned to YPH, PC and SPH, by oil palm agronomists from FELCRA. The comparison was based on the relative preference of the two elements in a pair to the decision on replanting. The YPH was equal to moderately preferred over PC, and therefore, was given a rating of 2. Further YPH was moderately preferred over the SPH, and was assigned a rating of 3. Finally, PC was equal to moderately preferred over SPH, and given a rating of 2. If the same element was compared to itself, it was considered to be of equal importance and therefore, a value of 1 was assigned. The reciprocal comparisons of the paired criteria were also assigned ratings accordingly.

TABLE 1
Criteria justification

No.	Criteria	Justification
1	Yield per hectare (YPH)	Yield per unit area is very important because it determines whether return to management is economical, given the existing price of palm oil.
2	Production cost per ton fresh fruit bunch (PC)	Production cost is important as it is influenced by prices of variables such as input prices and labour cost. It is also influenced by YPH.
3	Productive stand per hectare (SPH)	Productive stand per hectare (SPH) is moderately important as it reflects the number of healthy trees uninfected by Ganoderma disease and bagworms, which are common in the study area. It also influences YPH and PC.

TABLE 2
Scale for the pair-wise comparison

Intensity of Importance	Definitions
1	Equal importance
2	Equal to moderate importance
3	Moderate importance
4	Moderate to strong importance
5	Strong importance
6	Strong to very strong importance
7	Very strong importance
8	Very to extremely strong importance
9	Extreme importance

Source: Saaty (1980)

TABLE 3
Pair-wise comparison matrix to assess the importance of criteria

Criteria	YPH	PC	SPH
YPH	1	2	3
PC	0.5	1	2
SPH	0.333	0.5	1
Total	1.833	3.5	6

The summarized field records for the SPH, YPH and PC, from an adjacent phase (Phase 13) of similar soil and climatic conditions, are presented in Table 4 below. The table shows that a 32 % drop in the YPH had caused a 15% increase in the PC. However, the drop in the SPH was insignificant, and had a slight influence on the drop in the YPH; this was mainly attributed to the occurrence of a pronounced dry period in Jun, Jul and Aug, 2005. This

greatly affected bunch formation and flower initiation. Based on this argument, agronomists at FELCRA have rated YPH >PC>SPH in terms of their importance in decision making for replanting the existing matured oil palm areas.

To synthesize these values for more meaningful comparisons, the matrix values given in Table 3 were first normalized as given in Table 5, followed by the computation of the average normalized values for each criterion provided in Columns 4 of Table 6. These average normalized values are essentially the more meaningful weights to be used in comparing the level of importance assigned for the YPH, PC and SPH, which are respectively 0.539, 0.297 and 0.164.

TABLE 4
Field records for the SPH, YPH and PC of Phase 13 - 2006 and 2007

Criteria	Jan.-Jun. 2006	Jan-Jun. 2007	Percent change
YPH (tonne per hectare)	9.79	6.65	- 32.07
PC (RM per tonne FFB)	127.67	146.25	+ 14.55
SPH (trees per hectare)	123	117	- 4.88

Source: FELCRA Seberang Perak Report for June 2006 and June 2007

TABLE 5
Normalised pair-wise comparison matrix

Criterion	YPH	PC	SPH
YPH	0.545	0.571	0.500
PC	0.273	0.286	0.333
SPH	0.182	0.143	0.167
Total	1.000	1.000	1.000

TABLE 6
Relative weights assigned to the criteria

Criterion	YPH	PC	SPH	Weights
YPH	0.545	0.571	0.500	0.539
PC	0.273	0.286	0.333	0.297
SPH	0.182	0.143	0.167	0.164
Total	1.000	1.000	1.000	1.000

The AHP measures the consistency of the judgments, in setting up priorities for the elements, with respect to a criterion by means of a consistency ratio (CR). If the ratio is < 0.1, the judgments are considered as consistent. However, if the ratio is >0.1, the judgments are considered to be inconsistent and somewhat random and it should therefore be reviewed (Saaty, 1982; Malczewski, 1999).

The step by step procedure adopted by both Saaty (1982) and Malczewski (1999) to compute the CR is as follows:

(i) The weighted sum vectors were computed by multiplying the pair-wise comparison matrix with the criteria weights;

$$\begin{pmatrix} 1 & 2 & 3 \\ 0.5 & 1 & 2 \\ 0.333 & 0.5 & 1 \end{pmatrix} \times \begin{pmatrix} 0.539 \\ 0.297 \\ 0.164 \end{pmatrix} = \begin{pmatrix} 0.539 & 0.504 & 0.492 \\ 0.269 & 0.297 & 0.328 \\ 0.179 & 0.149 & 0.164 \end{pmatrix} = \begin{pmatrix} 1.625 \\ 1.894 \\ 0.492 \end{pmatrix}$$

(ii) The consistency vector (λ_{max}) was calculated by averaging the weighted sum vectors, as shown below:

$$\begin{pmatrix} 1.625 \\ 0.894 \\ 0.492 \end{pmatrix} \div \begin{pmatrix} 0.539 \\ 0.297 \\ 0.164 \end{pmatrix} = \begin{pmatrix} 3.015 \\ 3.010 \\ 3.000 \end{pmatrix}$$

Next, the average value for the consistency vector (λ_{max}) was calculated as:
λ_{max} = (3.015+3.010+ 3.000) ÷ 3 = 3.008

(iii) The consistency index (CI) was calculated according to equation 2 below:

$$CI = (\lambda_{max} - n) / n - 1 \quad (2)$$

Where, λ_{max} is the principle eigenvalue of the matrix, and n is the order of the pair-wise comparison matrix. The CI was computed as:

$$CI = (3.008 - 3)/2 = 0.004$$

(iv) The consistency ratio was then computed using equation 3.

$$CR = CI/RI \quad (3)$$

Where, CI is the consistency index and RI is the random index value, which is dependent on the matrix order provided by Saaty (1980), as given in Table 7. The CI provides a measure of departure from consistency, while the RI is the CI of a randomly generated pair-wise comparison matrix.

Therefore, the CR determines the level of consistency and it should be < 0.10, so as to permit a reasonable level of consistency in the pair-wise comparison judgments (Saaty, 1982; Malczewski, 1999).

The CR in this study was computed as (0.004 ÷ 0.58) = 0.069, which is significantly below the threshold value of 0.1, and this indicates a high level of consistency. Hence, the criteria weights were accepted.

Spatial Modelling

The digital layers for the YPH, PC and SPH were generated in a GIS environment, as depicted in *Figs. 5, 6* and *7*, respectively.

TABLE 7
Random index values (Saaty, 1980)

N (matrix order)	RI
2	0.00
3	0.58a
4	0.90
5	1.12
6	1.24
7	1.32
8	1.41a

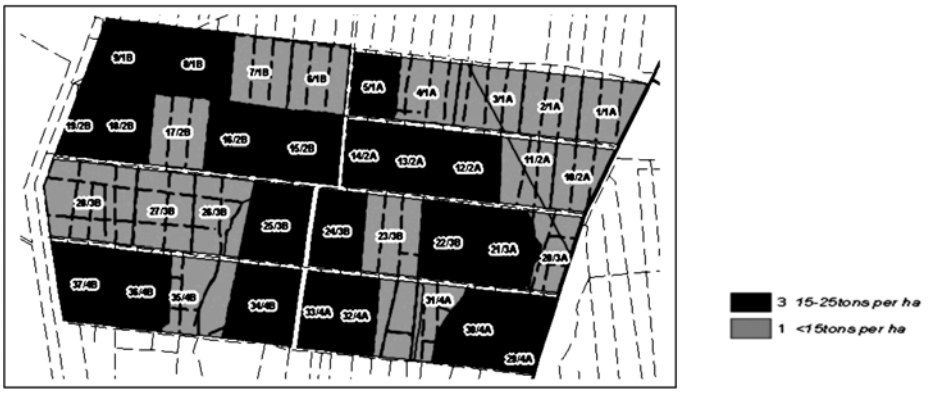

Fig. 5: Yield per hectare map of phase 15

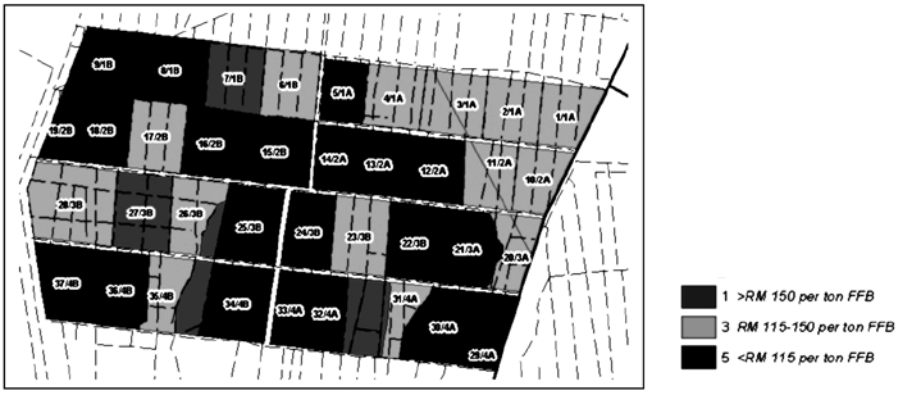

Fig. 6: Production cost map of phase 15

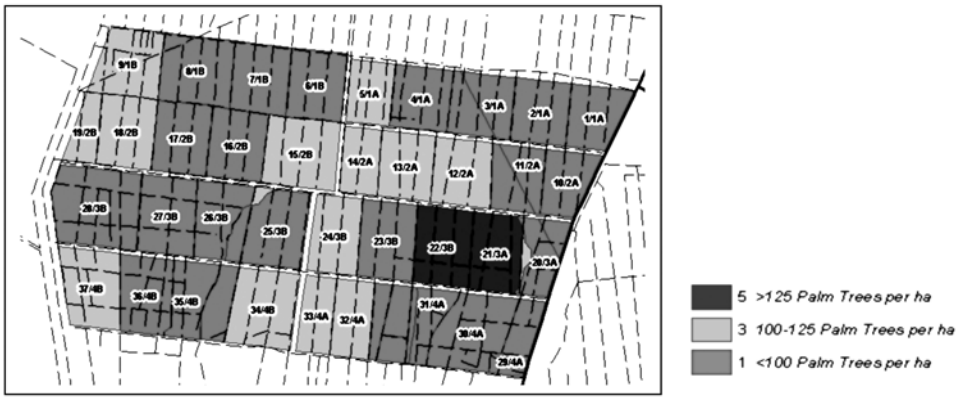

Fig. 7: Stand per hectare map of phase 15

The sub-criteria scores for the YPH, PC and SPH determined by the agronomists at FELCRA are shown in Table 8.

Equation 1 was rewritten as equation 4, considering the criteria weights, which were computed using the AHP.

$$R = 0.539\ YPH + 0.297\ PC + 0.164\ SPH \quad (4)$$

In this study, the setting of the R limits for the three alternative classes of decision making for replanting (Table 9) was done after the consultation with the local oil palm agronomists and plantation managers.

Through the map calculator tool in the GIS, the final replanting decision support map was then generated using equation 4 and the associated sub-criteria scores for the YPH, PC and STP. This map is depicted in *Fig. 8*.

TABLE 8
Sub-criteria scores

Criteria	Sub-criteria scores
Yield per hectare	3 for 15-25 tons per ha
	1 for < 15 tons per ha
Production cost	5 for < RM 115 per ton FFB
	3 for RM 115 – 150 per ton FFB
	1 for > RM 150 per ton FFB
Stand per hectare	5 for > 125 palm trees per ha
	3 for 100 – 125 palm trees per ha
	1 for < 100 palm trees per ha

TABLE 9
Replanting decision classes

No.	Replanting Decision Classes	R Values
1	Replant	< 1.9
2	Under Observation	>1.9 – 3.8
3	No Replant	> 3.8

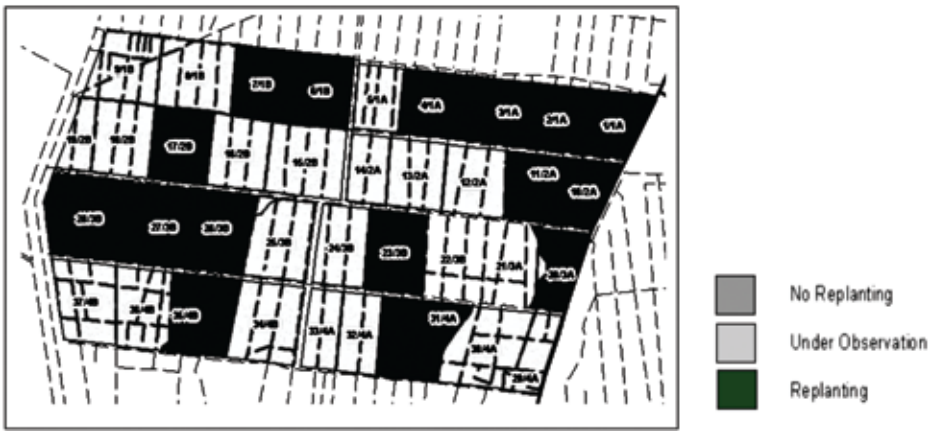

Fig. 8: Decision support map of Phase 15

CONCLUSIONS

In this study, a decision support tool for replanting of the existing old palms was developed using the integration of the RS, GIS and AHP technologies. The tool has been made operational to support the decision making for replanting in FELCRA.

For future research works in the study area, the automatic RS based algorithms will be developed to estimate yield of oil palm, stand per hectare, age of palm trees and height of palm trees. The criteria–age of the palm tree and the height of palm tree will also be considered in the AHP analysis and the spatial modelling to refine the SDST tool for replanting.

REFERENCES

Chuvieco, E. and Congalton, R.G. (1989). Application of remote sensing and Geographic Information System to forest fire hazard mapping. *Remote Sensing Environ.*, *29*, 147–159.

Diamond, J.T. and Wright, J.R. (1988). Design of an integrated spatial information system for multi-objective land-use planning. *Env. and Planning B, 15*(2), 205-214.

FELCRA. (2007). Pembentangan Prestasi hasil 2006/2007 (June), FELCRA Bhd., Seberang Perak 13, 2007.

Graeme, F.B.C. (1996). *Geographic Information Systems for Geoscientists – Modeling with GIS.* Elsevier Science Inc.

Ibrahim, S., Zainal, A.H., Mariamni, H. and Shahruddin, A. (2004). Oil palm phenology characterization using optical Remote Sensing. *Seminar on Applications of Remote Sensing, GIS and Related Technologies for Precision Farming*, Sept. 9- 11, 2002, K.L., Malaysia.

Ibrahim S., Zainal, A.H., Mariamni, H. and Shahruddin, A. (2002). Oil palm phenology characterization using optical Remote Sensing. *Seminar on Applications of Remote Sensing, GIS and Related Technologies for Precision Farming*, Sept. 9- 11, K.L., Malaysia.

Hall,G.B., Bowerman, R.L. and Feick, R.D. (1997). GIS-based decision support architecture and applications for developing countries. *South African Journal of Geo-information, 17*(3), 73-80.

Malczewski, J. (1999). *GIS and Multi-criteria Decision Analysis.* New York: John Wiley & Sons.

Loh, K.F. (1991). Crop suitability assessment and planning of part of Bantul, Yogjakarta using Remote Sensing and Geographic Information System. *Workshop on Land Use Planning*, 13 May, Yogjakarta, Indonesia.

Loh, K.F., Ponusamy, R. and Ismail, J. (2005). Geo-informatics for Oil Palm Plantation Management. *ISPRS Int. workshop on Spatial Planning and Decision Support System*, Dec. 8-9, K.L., Malaysia.

Nor Azleen, A.R., A. Tarmizi Mohamed and Wahid, O. (2002). Assessment of foliar-nitrogen content in oil palm using Remote Sensing techniques. *Seminar on Applications of Remote Sensing, GIS and Related Technologies for Precision Farming*, Sept., 9- 11, K.L., Malaysia.

Mariamni, H., Zainal, A., Ibrahim, S. and R. Zainal. (2002). GIS technology in precision farming project. *Seminar on Applications of Remote Sensing, GIS and Related Technologies for Precision Farming*, Sept., 9-11, K.L., Malaysia.

Parker, D.C., Manson, S.M., Janssen, M.A., Hoffmann, M. and Deadman, P. (2003). Multi-agent systems for the simulation of land-use and land-cover change: A review. *Annals of the Association of American Geographers, 93*(2), 314-337.

Feick, R.D. and Hall, G.B. (1999). Consensus-building in a Multi-Participant Spatial Decision Support System. *URISA Journal, 11/2.*

Saaty, T.L. (1982). *Decision Making for Leaders – The Analytical Hierarchy Process for Decision Making in a Complex World.* USA: Wadsworth, Inc.

Saaty, T.L. (1980). *The Analytical Hierarchy Process.* McGraw-Hill Inc, pp 17-34.

Saaty, T.L. (1977). A scaling method for priorities in hierarchy structure. *Journal of Mathematical Psychology, 15*, 234-2402.

Simon, H.A. (1960). *The New Science of Management Decision.* New York: Harper & Row.

Tey, S.H. and Chew, P.S. (1997). GIS and GPS technologies for research and management in plantation crops. In E. Pushparajah (Ed.), *Plantation management for the 21st century,* (Vol. 1, p.47–59). Kuala Lumpur: The Incorporated Society of Planters.

Wahid, O., Xaviar, A., Tarmizi, A.M. and Ibrahim, S. (2002). Application of precision agriculture to foliar nutrient analysis. *Seminar on Applications of Remote Sensing, GIS and Related Technologies for Precision Farming*, Sept., 9- 11, K.L., Malaysia.

ISSN: 0128-7680
Pertanika J. Sci. & Technol. **17 (1)**: 33 – 42 (2009)

Evaluation of Yield and Groundwater Quality for Selected Wells in Malaysia

Thamer Ahmed Mohammed* **and Abdul Halim Ghazali**
Department of Civil Engineering, Faculty of Engineering, Universiti Putra Malaysia, 43400 UPM, Serdang, Selangor, Malaysia
**E-mail: thamer@eng.upm.edu.my*

ABSTRACT

In Malaysia, the use of groundwater can help to meet the increasing water demand. The utilization of the aquifers is currently contributing in water supplies, particularly for the northern states. In this study, quantitative and qualitative assessments were carried out for the groundwater exploitation in the states of Kelantan, Melaka, Terengganu and Perak. The relevant data was acquired from the Department of Mineral and Geoscience, Malaysia. The quantitative assessment mainly included the determination of the use to yield ratio (UTY). The formula was proposed to determine the UTY ratio for aquifers in Malaysia. The proposed formula was applied to determine the maximum UTY ratios for the aquifers located in the states of Kelantan, Melaka, and Terengganu, and were found to be 4.2, 5.2 and 0.6, respectively. This indicated that exploitation of groundwater was beyond the safe limit in the states of Kelantan and Melaka. The qualitative assessment showed that the groundwater is slightly acidic. In addition, the concentrations of iron and manganese were found to be higher than the allowable limits, but the chloride concentration was found within the allowable limit.

Keywords: Quantitative, qualitative, assessment, groundwater, aquifers, tropical region

ABBREVIATIONS

ASR: Aquifer Storage Recovery
UTY: Use to Yield Ratio
USEPA: United States Environmental Protection Agency

INTRODUCTION

Groundwater is an important component of the natural water resources system and human beings have utilized it ever since ancient days. The development in drilling and pumping technologies make the usage of groundwater easier, and this enables human beings to use the storage of very deep aquifers. Groundwater may be cheaper than the treated surface water. Beside the advantage of low turbidity, it also contains nutrients which are good for health. The utilization of groundwater can help to solve the water shortage in areas where surface water is limited. Similarly, it can be used to supplement the surface water supplies. However, pollution may restrict and affect the exploitation of groundwater for potable uses.

Malaysia is a tropical country with an abundant amount of surface water. Most of the states in Malaysia are using surface water to meet the various water demands. Due to the global weather changes, the increasing demand and severe pollution of the surface water

Received: 21 August 2007
Accepted: 17 October 2008
*Corresponding Author

groundwater become an important source for water supply. In Malaysia, the groundwater storage is estimated to be 5000 billions m^3 and only less than 2% of the present storage has been used (Azuhan, 1999). Generally, the lack of extensive exploitation for groundwater in Malaysia can be related to:

1. the failure to recognise the vast potentials of the groundwater resources
2. the misconception that groundwater exploitation is not sustainable
3. the lack of full assessment of the groundwater resources

The use of groundwater for domestic purposes is mainly confined to rural areas, where there is no piped water supply. However, groundwater is being significantly utilised for public water supply in Kelantan and Perlis. The other states, which supplement the water supply systems groundwater, are Terengganu, Pahang, Sarawak and Sabah. In Kelantan, groundwater plays a very important role in the public water supply system. About 70% of the total water supply in the state is derived from groundwater, primarily in the Kota Bharu areas. The rural population is dependent very much on groundwater for their daily requirements, and they obtain it from the shallow dug wells. In Malaysia and during the 1998 dry spell, groundwater has provided relief for the people, especially in Selangor and Sarawak. So, there is a great potential in the use groundwater supplies to meet the increasing demand, and for this reason, a special emphasis must be given to sustainable development of groundwater.

In this study, the exploitation of groundwater from aquifers located in the four states in Malaysia was assessed using the proposed formula, and a qualitative assessment was conducted in order to evaluate the quality of the groundwater.

LITERATURE REVIEW

Groundwater is a very important component of water resources in nature. It is the main source of water supplies in many countries, and this justifies the efforts given by the researchers to improve the studies conducted on groundwater. In this study, relevant selected studies were also reviewed.

Hutchison and Hibbs (2008) analysed groundwater budget in arid basins and substantially aided by integrating the use of numerical models and environmental isotopes. Strassberg *et al.* (2007) developed and applied a data model, for spatial and temporal groundwater information, within a geographical information system (GIS). Wehrmann *et al.* (2003) used the GIS technology to determine the township use to yield ratios for the three aquifer types (sand-gravel, shallow bedrock and deep bedrock). For this purpose, they suggested the following equation to determine the ratio:

$$Y_T = a_1 y_1 + a_2 y_2 + \ldots + a_n y_n \quad (1)$$

where,

Y_T = Area-weighted total township potential aquifer yield, gallon per day (gpd)

a_n = Area within the township containing a particular potential aquifer yield, square miles (mi^2)

y_n = Potential aquifer yield of selected polygon, gallons per day per square mile (gpd/mi^2)

Bisson and Lehr (2004) proposed modern technologies for groundwater exploration, which were adapted from the oil and mineral exploration industries for evaluating, developing and managing previously undiscovered massive sustainable groundwater. In

addition, the remote sensing technique was also used for the groundwater exploration in Egypt by El-Baz *et al.* (2004). Lubczynski and Roy (2004) applied the nuclear magnetic resonance (NMR) in the determination of the subsurface free water content and hydraulic properties of the media.

Burbeg (2008) conducted a 62 day controlled aquifer test, in thick alluvial deposits at Mesquite, Nevada in USA, using a high-precision global positioning system (GPS) network to evaluate the aquifer systems during an aquifer test.

Rutledqe (2007) proposed a mathematical method to improve the reliability of recharge estimates of the groundwater. Rainfall is an important source of groundwater recharging. Fleckenstien *et al.* (2006) studied the impact of the low river flow on aquifer recharge. Cui and Shao (2005) studied the role of ground water in the ecosystems, including the effect of water condensation and water table depth on the growth of plants and the degree of soil salinity.

USEPA (1994) outlined the guidelines for delineating the captured zone. This could help to identify the wellhead protection areas, with designated land uses, to reduce the potential for groundwater contamination. The delineation of the captured zone could be simple and just a fixed radius from the well or complex, which needed hydrogeologic modelling. The captured zone or the source of waters to a well or well field must be identified in order to evaluate the quality of groundwater which would be obtained from it. The evaluation would reveal if any contamination occurred.

Fass *et al.* (2007) conducted a study on the unconfined coastal aquifer of the tropical Burdekin River delta, located in the north-eastern of Australia. They found that groundwater, in this areas, was high in chloride concentrations up to almost three times that of the sea water; this occurred up to 15 km of the present coastline. They attributed this to the transpiration by mangrove vegetation during the periods of high sea level. They found that Radiogenic (14C) carbon isotope analyses indicated that groundwater, with chloride concentrations between 15,000 and 35,000 mg/L, was mostly between 4000 and 6000 years old, at which time, the sea level was 2 to 3 m higher than the present.

Marin (2002) conducted an appraisal study on groundwater exploitation in Mexico and he reported that 1/3 of the total water use for agriculture, drinking water supplies and industrial purposes came from the ground water. In Mexico, about 70% of the drinking water supplies came from groundwater, and 75 millions out of 100 millions of the population were dependent mainly on groundwater as a source of water supply. In agriculture, groundwater used to irrigate 2 million hectares of land. The main problems of groundwater are overexploitation, contamination and slatwater intrusion. About 8000 km has significant slatwater intrusion problems in nine aquifers.

STUDIED AQUIFERS AND METHODOLOGY

In Malaysia, groundwater exploitation can help to meet parts of the increasing demand. Currently, groundwater is being used to meet various types of demand *(Fig. 1)*. The integration of surface water and groundwater usage are needed to ensure a sustainable utilization of water resources. In this study, the exploitation of groundwater, from four states in Malaysia, was evaluated. The related data was acquired from the Department of Mineral and Geosciences, Malaysia and this Department is responsible for monitoring and the management of groundwater in Malaysia.

The characteristics of aquifers in the four states in Malaysia, namely Kelantan, Melaka, Terengganu and Perak, were also presented. The aquifer in Kota Bharu, Kelantan is defined by alluvium quaternary and it is based on granite rock or metamorphic rock. The thickness

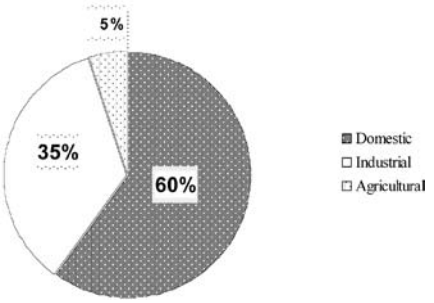

Fig. 1: Various demands for the exploited groundwater in Peninsular Malaysia

of the alluvium quaternary has several meters near the foot of a hill and more than 150 m close to the sea. The alluvium layer consists of clay, sand, silt and gravel. There are two systems of aquifer - these are shallow and deep aquifers. The shallow aquifer includes all aquifers with a thickness of lesser than 15 m and it is categorized as an unconfined aquifer and semi-confined aquifer. The deep aquifers include all the aquifers with a thickness of more than 15 m. This can be found in a semi-confined aquifer or confined aquifer. The shallow aquifer system consists of water, except for the groundwater near to the sea. As for the deep aquifer, salty water can be found near the seaside, and at a depth of 30 m to 50 m, with a distance of about 5 km from the sea.

The aquifers in Melaka are metamorphic rock, igneous rock, and consolidated alluvium layer, which is built of clay or sand at the seaside area. The main limestone is found forward the northwest, at the centre and east Tengah district and the minor limestones found in various directions in metamorphic rock or granite. The wells were constructed either in alluvium or in rock aquifers. The thickness of the alluvium layer is between 2.25 m – 19.5 m.

The aquifers in Terengganu are alluvium quaternary aquifer with silt and soft sand, with a base rock at depth of about 28 m. Due to the fact that the silt layer is thin and less than 5 m, the aquifer is mainly categorized as semi-confined aquifer. The aquifer in Perak is categorized by granite and metamorphic rocks, which are represented by limestone, shale, sandstone and tuff layers.

The methodology used was based on computing the use so as to yield the ratio (UTY) for selected aquifers in the studied area. In addition, the quality of the groundwater, from each aquifer, was assessed based on the standards set for drinking water. *Fig. 2* is used to determine the potential yield of each aquifer, while the data related to the pumping from the wells were used to compute the UTY ratio. In the present study, the following formula was proposed to compute the UTY ratio for the Malaysian aquifers:

$$UTY = \frac{\sum_{i=1}^{i=n} y_{wi}}{(y_m)(n)} \qquad (2)$$

where

y_w is the actual discharge pumped from a well i in m^3/ hr, y_m is the potential yield in m^3/hr/ well from a particular aquifer, and n is the number of wells in the aquifer.

The high UTY was found to be almost 1, suggesting a groundwater exploitation problem in the area.

Fig. 2: Yield of the aquifers in Peninsular Malaysia
(*Source*: Department of Minerals and Geoscience, Malaysia)

The assessment of groundwater quality was carried out based on the available data; few parameters were studied and these parameters included iron, pH, chloride, and manganese. The concentrations of these parameters in the groundwater were compared with the guidelines for drinking water. The methodology would help to conduct the qualitative and quantitative assessments to identify the groundwater exploitation in the studied area. At the same time, the acquired data was subjected to the processing and cataloging so that it could be more useful in the assessment process. *Fig. 3* shows a schematic flowchart for the methodology used.

RESULTS AND DISCUSSION

Quantitative Analysis

In 1995, about 98000 m^3/ day of groundwater was pumped from more than 60 wells to meet the demand of about 30% of the population of Kelantan. Considering this fact, nine more well fields will need to be constructed in order to meet the increasing demand by 2010. For the state of Melaka, the groundwater supply from the district plain can produce 1256 m^3/day to meet the demand of about 9000 people, and it was developed to produce 1430 m^3/day to

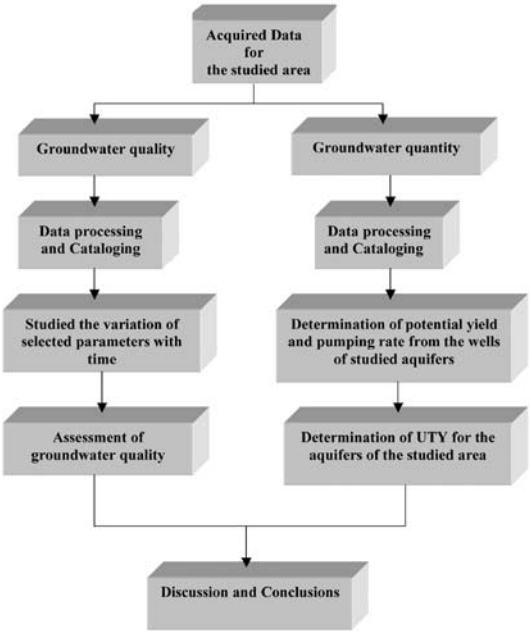

Fig. 3: Schematic flowchart of the methodology

meet the demand of 10210 persons. The discharge of salty groundwater, which is used for non-potable uses, is not included in the quantitative analysis. For the state of Terengganu, groundwater is being used in the Marang district, and the pumping is estimated to be 2200 m^3/day, and this meets the demand of 2200 people. Pumping from various well fields ranges form 160 m^3/ hr to 8 m^3/ hr. As for the state of Perak, groundwater is mainly used to meet the demand of the villages located in the rural areas. The pumping of groundwater is 180 m^3/ day, and this amount is used to meet the demand of 1278 people. *Fig. 2* shows the location of the aquifers with the potential yields. For industrial purposes, groundwater is utilized for cleaning, washing and cooling. Major areas such as Shah Alam and Bukit Rajah in Selangor use groundwater substantially for their operations. The utilization of groundwater for agricultural purposes is not very well developed, and this is normally confined to isolated agricultural areas or other areas outside many irrigation schemes.

Nevertheless, groundwater is being extensively used by Agricultural Commodities Centre in Terengganu and in aquaculture farm in Pekan, in Pahang. *Fig. 4* shows the daily consumption of the groundwater, distributed among various uses, while *Fig. 5* exhibits the number of wells allocated for various uses. *Fig. 6* shows the average yield for various wells in Peninsular Malaysia.

Safe yield is defined as a long-term balance between the natural and artificial recharge of an aquifer and the discharge from it by pumping. When more water is discharged than is recharged, the aquifer is described as being out-of-safe yield. The mining of groundwater occurred when there is a significant drop in the groundwater level of the aquifer. Safe yield can be achieved by a combination of methods. Water conservation will reduce the demand, and stormwater storage facilities can help in recharging the aquifers, since the average annual rainfall in Malaysia is 2500 mm. Achieving safe yield is important primarily because a continuous reduction in the groundwater level in an aquifer will make the supply of water to

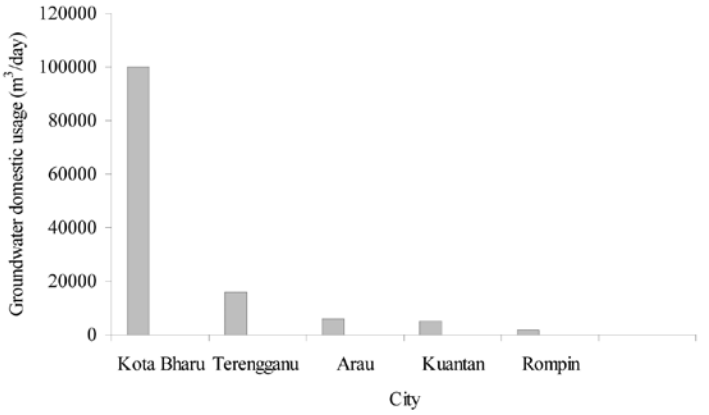

Fig. 4: Daily consumption of groundwater for domestic uses in selected cities in Malaysia

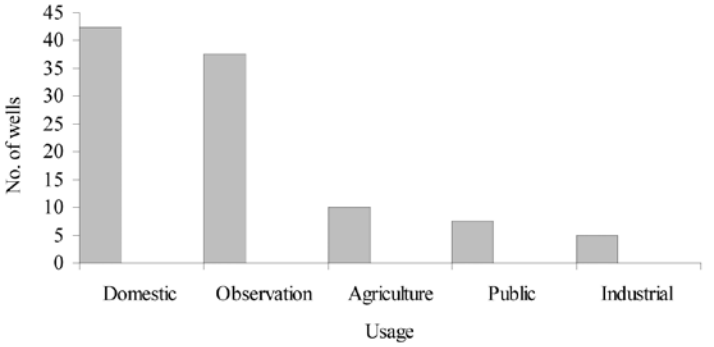

Fig. 5: Number of wells distributed based on the usage of groundwater

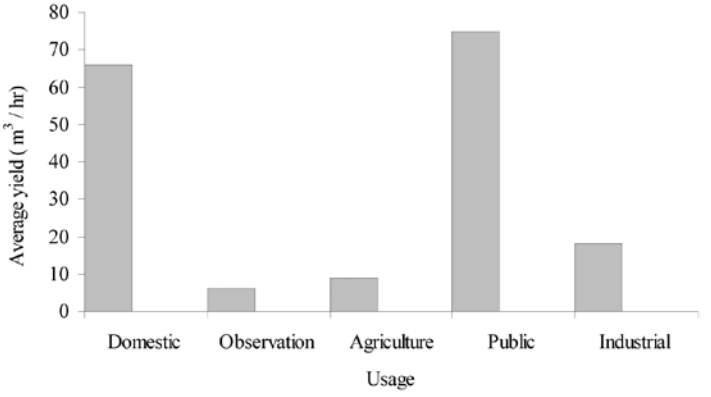

Fig. 6: Average well yield for various uses

be uneconomical. In addition, the drop in the groundwater level will damage the structure of the aquifer material. Wehrmann *et al.* (2003) made a comparison of the groundwater use to the aquifer yield, and as a result, they proposed a ratio called use-to-yield (UTY) and its values ranged from 0.5 to 0.9 for sand and gravel aquifers, but they also found that UTY was more than 0.9 for some areas within Illinois, USA. At the same time, they discovered that the estimated potential yield of deep bedrock aquifer system was 246025 m^3/ day.

In this study, Equation (2) is used to compute the UTY ratio to assess the pumping from the wells for the studied aquifers in Malaysia. The UTY ratios for the places utilizing the groundwater are shown in Table 1. The UTY ratio greater than 0.9 is not preferable because the high ratio suggests the existence or impendence of problems related to groundwater availability in a particular area. Wehrmann *et al.* (2003) proposed the UTY ratio of 0.9 for any critical case. The UTY ratios are acceptable for the wells in Terengganu. Lowy and Anderson (2006) proposed storage recovery (ASR) to optimize the available water resources and reduce adverse effects of pumping on the aquifer.

TABLE 1
Values of the use to yield ratios for the groundwater wells in Malaysia

State	Maximum UTY ratio	Minimum UTY ratio
Kelantan	4.2	0.51
Melaka	5.2	0.09
Terengganu	0.66	0.04

Qualitative Analysis

From the acquired data, it was found that the quality of the groundwater in some of the wells contained a high concentration of iron (up to 6 mg/l), while the recommended value is 0.3 mg/l. It is recommended to use the water for non-potable purposes. *Fig. 7* shows the variation of pH for the groundwater pumped from the wells located at Kelantan, Melaka and Terengganu. The low pH indicates the acidity of the groundwater. The recommended pH value for drinking water is 6.5. Guan *et al.* (2003) proposed the concept of critical pH which could assist in the design of geologic barriers to prevent viral contamination in groundwater. A critical pH value is 0.5 unit, which is below the highest isoelectric point of the virus and porous medium. The proposal of Guan *et al.* (2003) was based on the experimental and field data.

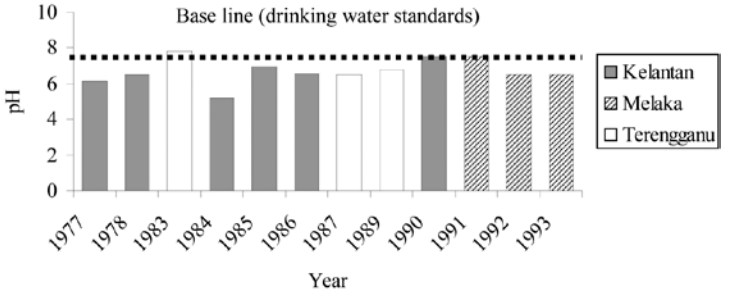

Fig. 7: Variations in the pH of the groundwater

The chloride content in groundwater is less than the recommended value for the drinking water, which is 250 mg/l, as shown in *Fig. 8.* Similarly, it is much lesser than the chloride concentration in groundwater of other areas in the Asia Pacific regions such as Northeast costal aquifers of Australia (chloride concentrations range from 15,000 to 35,000 mg/l), as reported by Fass *et al.* (2007).

The manganese concentration in the ground water is higher than the acceptable limits for drinking water, which is 0.05 mg/l (*Fig. 9*). Definitely, treatment is required for potable uses, although the concentration of the manganese is not very high (0.3 mg/l and less). Moreover, salty groundwater was found from the wells located near the coastal areas. Usually, the groundwater wells which are located near the coastal areas are affected by the salt intrusion phenomenon. Higher pumping rates will make groundwater of higher density (salt water) to be discharged from a well. So, high pumping rates and continuous pumping from the wells near the coastal areas will lead to saltwater intrusion and groundwater contamination unless precautionary measures are taken. Usually, the concentration of dissolved solids, in the groundwater, is high because it may pass through layers containing solvable materials. Wehrmann et al. (2003) found that the groundwater for the areas in Illinois contained more than 2500 mg/l of dissolved solids.

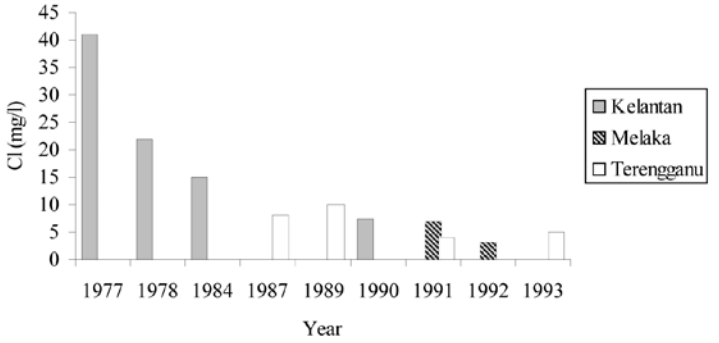

Fig. 8: Variations in the chloride concentrations in groundwater

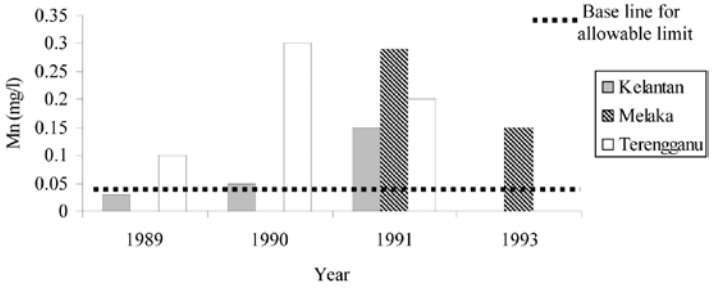

Fig. 9: Variations of manganese concentrations in groundwater

CONCLUSIONS

Although Malaysia is blessed with abundant of surface water, due to its high annual rainfall (about 2500 mm), the country still experiences increasing water demand. Many states in Malaysia use groundwater as a supplementary source to surface water to meet the demand for water supply. In the state of Kelantan, about 70% of the total domestic water demand is

met using groundwater. Meanwhile, Melaka and Terengganu are also using groundwater to meet parts of the demand in the two states. The maximum use to yield the ratios (UTY) for the wells under use in the state of Kelantan was found to be 4.2, while the minimum is 0.51. This is an indication that the concept of safe yield and sustainability has not been considered in the utilization of the aquifers in the areas. In the state of Melaka, the UTY is also high, while this is rather low in Terengganu, indicating that the aquifer is under safe yield. The quality of groundwater may determine the type of usage (potable or non-potable). According to the acquired data, groundwater needs some kind of treatment in case that it is planned to be used for domestic purposes.

REFERENCES

Azuhan, M. (1999). Malaysian groundwater in the next millennium. *Proceeding of Groundfos Dealers Conference,* Shah Alam, Malaysia.

Bisson, R. and Lehr, J.H. (2004). *Modern Groundwater Exploration.* John Wiley and Sons Publishing Company.

Burbeg, T. (2008). The influence of geologic structures on deformation due to groundwater withdrawal. *Journal of Ground Water, 46*(2), 202-211.

Cui, Y. and Shao, J. (2005). The role of groundwater in arid/semiarid ecosystems, Northwest of China. *Journal of Ground Water, 43*(4), 471-477.

El-Baz, F., Maxwell T.A. and Himida, I.H. (2004). Groundwater Exploration in Egypt. Report, Center of Remote Sensing, Boston University, USA.

Fleckenstien, J.F., Niswonger R.G. and Foqq, E.G. (2006). River-aquifer interaction, geologic heterogenity and low flow. *Journal of Ground Water, 46*(6), 837-852.

Fass, T., Cook, P.G., Stieglitz, T. and Herczeg, A.L. (2007). Development of saline groundwater through transpiration of seawater. *Journal of Ground Water, 45*(6): 703-710.

Guan, H., Schulze-Makuch, D., Schaffer, S. and Pillai, S.D. (2003). The effect of critical pH on virus fate and transport in saturated porous media. *Journal of Ground Water, 41*(5), 701-708.

Hutchison, W.R. and Hibbs, B.J. (2008). Groundwater budget analysis and cross-formational leakage in arid basin. *Journal of Ground Water, 46*(3), 384-395.

Lowy C.S. and Anderson M.P. (2006). An assessment to aquifer storage recovery using groundwater flow models. *Journal of Groundwater, 44*(5), 661-667.

Lubczynski, M. and Roy, J. (2004). Megnetic resonance sounding: New method for groundwater assessment. *Journal of Ground Water, 42*(2), 291-309.

Marin, L.E. (2002). Prespectives on Mexican groundwater resources. *Journal of Ground Water, 40*(6), 570-571.

Rutledqe, A.T. (2007). Update of the use of RORA Program for recharge estimation. *Journal of Ground Water, 45*(3), 374-382.

Strassberg, G., Maidment, D.R. and Jones, N.L. (2007). A geographic data model for representing groundwater systems. *Journal of Ground Water, 45*(4), 515-518.

USEPA. (1994). Handbook: Groundwater and Wellhead Protection. Technical Report No. EPA/625/R-94-001, Environmental Protection Agency, Office of Research and Development, Cincinnati, OH, USA.

Wehrmann, H.A., Sinclair, S.V. and Bryant, T.P. (2003). An Analysis of Groundwater Use to Aquifer Yield in Illinois. Report, Groundwater Section, Illinois, USA.

ISSN: 0128-7680
Pertanika J. Sci. & Technol. **17 (1)**: 43 – 51 (2009)

Development of Core Collection for Perennial Mulberry (*Morus* spp.) Germplasm

A.Tikader* **and C.K. Kamble**
Central Sericultural Germplasm Resources Centre,
Hosur - 635 109 P.B.No.44, Tamil Nadu, India
**E-mail: atikader_csgrc@yahoo.co.in*

ABSTRACT

Improvement of mulberry (crop) depends on the availability of suitable parents and breeders' thorough knowledge on the database of mulberry germplasm. To develop suitable varieties which are tolerant to stress condition in different agro climatic regions and resistant to pest and diseases, broad spectrum genetic variability is a pre-requisite. In this study, a total of 628 mulberry accessions were collected from 23 different countries and classified into 5 geographical groups, based on the qualitative and quantitative database. The grouping represented tropical wet (237), tropical dry (121), sub-tropical humid (215), semi-arid (10), arid (04), highland (25) and others (16). A core collection was made to compare the data, following the combined cluster analysis. The K-clustering procedure was followed to classify the mulberry accessions and 10 clusters were formed. The results indicated that cluster VIII had more number of accessions (125), whereas cluster II was minimum (27). In other clusters, mulberry accessions were distributed randomly irrespective of geographical origin and genetic diversity. Based on the geographical origin, genetic diversity and avoiding repetitiveness, a core collection was developed for the utilization of mulberry crop improvement programme in the future.

Keywords: Mulberry germplasm, core collection, geographical distribution, statistical analysis

INTRODUCTION

The germplasm collections are many and large that they diffuse and discourage effective evaluation of the accessions and thus hinder their utilization. As a solution to the problem, Frankel and Brown (1984) suggested that a core collection could be developed from the available germplasm. The core collection is the representative with the minimum repetitiveness of genetic diversity of a crop species and its relatives. The accessions, which are not included in the core, are retained as a reserve sub set for future need and searching for rare alleles (Basigalup *et al.*, 1995). The first core collection was developed from the Australian collection of perennial *Glycine* spp. Subsequently, the core collection was also developed in other crops (Holbrook *et al.*, 1993). Prior to develop a core collection, decision regarding the size of the core, sampling procedure, maintenance and improvement of the designated core has to be made (Brown, 1989). It was suggested that the number of entries in the core should be about 10 % of the total collection.

CSGRC, Hosur is maintaining 1100 mulberry accessions at present, which is large and hinders a thorough evaluation of its potential for improving important traits. The objective of this research was to evaluate and characterize the accession to designate a possible core collection for the evaluation and breeding programmes in the future.

Received: 12 September 2008
Accepted: 30 June 2008
*Corresponding Author

MATERIALS AND METHODS

The study was carried out at the Central Sericultural Germplasm Resources Centre, Hosur, in Tamil Nadu. It is situated around 12.45° N and 77.15° E, with an altitude of 942m above the mean sea level, and a dry tropical climatic condition. The average rainfall ranges from 1000 mm per anum. The mulberry plantations, at the field gene bank, are maintained as dwarf trees, spacing 2.4 x 2.4 m with two prunings/ year. The recommended agronomical package of practices was followed to maintain the plantation (Tikader *et al.*, 1999, 2000). The experiment was set up in an augmented block design to accommodate more number of mulberry plants. Each accession was represented by 4 plants and the materials used for this study represented 23 countries accessions including India (*see* Table 1). The data on growth behaviour and related growth traits were recorded after 90 days of plant pruning. The intercultural operation and pruning were conducted after the plants were attained at two years of age. The leaf moisture and the retention capacity of the leaf moisture of the harvested leaf were calculated as per standard procedure (Vijayan *et al.*, 1997).

The observation carried out on the important growth traits was recorded at the field gene bank for two seasons per year, over a period of three years. The data was computed and the multivariate statistical methods i.e., the analysis of variance, correlation, combined cluster analysis based on correlation, principal component analysis within each geographical group with random selection of entities in each cluster, were applied. A stratified random sampling procedure was used to divide the collection into a number of non-overlapping strata. The mulberry accessions were grouped based on the requirement such as the geographical origin, sexual behaviour, as well as qualitative and quantitative traits. As such, 455 indigenous and 173 exotic accessions were grouped based on origin in different zones (Johnson, 1978). The accessions were placed into different zones, i.e., tropical wet, tropical dry, sub-tropical humid, semi-arid, arid, high land and others. The multivariate analysis was done to group the mulberry accessions (628) using the Statistical Package for Social Science (SPSS).

RESULTS AND DISCUSSION

The mulberry accessions, representing different geographic regions, are presented in Table 1. The geographical distribution indicates that the maximum accession fall in the Tropical wet (237 acc.), followed by the sub-tropical humid (215 acc.), tropical dry (121 acc.), high land (25 acc.), and others (16 acc.); while the minimum in the semi-arid zone (10 acc.). The analysis of variance, indicating a high degree of variability and the relationship of different growth traits, were established through the correlation coefficient analysis (Table 2). The leaf yield of mulberry is a complex trait and it depends on several factors. The correlation matrix indicated that the leaf yield was highly associated with a number of primary branches (0.60**), total shoot length (0.74**), length of the longest shoot (0.64**), 100-leaf weight (0.22**), total biomass yield (0.99**), leaf moisture content (0.25**) and leaf moisture retention capacity (0.25**). Nevertheless, the leaf yield showed a negative significant association with the leaf shoot ratio (-0.29**) and laminar index (-0.18**). Other traits were also found to associate with each other and showed a complex relationship. Similar results had also been reported earlier by several authors (Tikader *et al.*, 1999; Vijayan *et al.*, 1997).

There are different ways which can be used to classify and group the mulberry accessions. For this, different authors have worked on mulberry and grouped the accessions in different ways, according to the clustering packages (Tikader *et al.*, 1999; Tikader and Rao, 2001a;

TABLE 1
Geographic distribution of mulberry accessions (628 accessions) of different countries

Zones	States/ Territory of India	Accessions	Country	Accessions
	Andaman & Nicobar Islands	02	Bangladesh	05
	Assam	10	Burma (Myanmar)	06
	Kerala	48	France	15
	West Bengal	125	Indonesia	05
Tropical wet			Italy	08
			Papua New Guinea	01
			Philippines	01
			Portugal	01
			Spain	02
			Thailand	04
			Venezuela	01
			Vietnam	03
Total		**185**		**52**
	Gujarat	01	Pakistan	07
	Karnataka	68	Zimbabwe	09
Tropical dry	Maharastra	02		
	Madhya Pradesh	12		
	Tamil Nadu	22		
Total		**105**		**16**
	Arunachal Pradesh	05	Australia	02
	Manipur	12	China	11
	Meghalaya	21	Cyprus	01
Sub-tropical humid	Nagaland	01	Hungary	01
	Uttar Pradesh	91	Japan	59
			Paraguay	04
			Russia	01
			South Korea	06
Total		**130**		**85**
	Punjab	05		
Semi-arid	Rajasthan	05		
Total		10		(–)
	Himachal Pradesh	02		
High land	Jammu & Kashmir	22		
	Sikkim	01		
Total		**25**		**(–)**
Others				16
Grand total		455		173

TABLE 2
Correlation coefficient matrix for different growth parameters in mulberry germplasm

Trait	X1	X2	X3	X4	X5	X6	X7	X8	X9	X10	X11	X12
X1	—											
X2	0.93**	—										
X3	-0.19**	-0.08	—									
X4	-0.14**	-0.08	0.47**	—								
X5	-0.35**	-0.23**	0.54**	0.48**	—							
X6	0.55**	0.71**	0.06	-0.04	-0.03	—						
X7	-0.01**	0.07	0.13**	-0.13**	0.32**	0.36**	—					
X8	-0.36**	-0.25**	0.51**	0.45**	0.94**	-0.01	0.37**	—				
X9	-0.43**	-0.44**	0.19**	0.12**	0.16**	-0.51**	-0.11**	0.17**	—			
X10	0.60**	0.74**	0.25**	0.25**	0.22**	0.64**	0.08*	0.18**	-0.29**	—		
X11	-0.15**	-0.13**	-0.08	-0.13**	0.01	-0.07	0.18**	0.16**	0.05	-0.18**	—	
X12	0.64**	0.78**	0.22**	0.23**	0.18**	0.67**	0.07	0.15**	-0.35**	0.99**	-0.17**	—

X1 = No. of the primary branches, X2 = Total shoot length, X3 = Leaf moisture retention capacity, X4 =Leaf moisture content , X5 = 100 leaf weight, X6 =Length of the longest shoot X7 = Internodal distance, X8 = Lamina weight, X9 = Leaf shoot ratio, X10 = Leaf yield, X11 = Laminar index, X12 = Total biomass weight

Tikader and Roy, 2001b, 2002). The accessions were grouped using the K clustering method in the SPSS package (version 11). The accessions were distributed into ten clusters, with the representative of different regions (Table 3). The cluster-wise distribution of mulberry indicated that the maximum accessions were grouped in cluster VIII (125 acc.), followed by VII (89 acc.), VI (76 acc.), III (70 acc.); I (62 acc.), IX (54 acc.), X (35 acc.) and IV (29 acc.). The minimum accessions were grouped in cluster II (27). The mulberry accessions, which were grouped with each other irrespective of their geographical distribution and genetic diversity. The distance between the final cluster centres are shown in Table 4. The distances between the final cluster centres indicated the maximum inter cluster distance between clusters IV and X (8.81), suggesting that the accessions grouped in these clusters are genetically divergent. The minimum inter-cluster distance was observed between cluster III and IV (1.97), indicating the accessions which were grouped in these cluster are genetically similar. The intra-cluster distances showed no variation between them. The different cluster groups provided a scope for the selection of accessions for further mulberry crop improvement programme (Tikader and Roy, 2002). During cluster analysis. the variability was also partitioned and presented character wise (Table 5). However, the F - test should be used only for descriptive purposes because the clusters were chosen to maximize the differences between the cases in the different clusters. The observed significance levels were not corrected for this, and could not be interpreted as the test of hypothesis that the cluster means were equal.

Two methods were found suitable to be used for designating the core collection; these are (a) combined cluster analysis based on correlation, PCA within each geographical group with a random selection of entries with each cluster, and (b) direct selection from the entries within each geographical group. Nevertheless, to run the multivariate statistical package, complete set of data is required. On the other hand, the principal component and cluster analysis can be performed according to a complete set of data and these are excellent tools to be used in grouping the accessions by degree of similarity (Brown, 1989; Smith *et al.*, 1995: Peeters and Martinelli, 1989).

TABLE 3
Region-wise distribution of mulberry accessions in different clusters

Region	Mulberry accessions in each cluster										
	I	II	III	IV	V	VI	VII	VIII	IX	X	Total
Tropical dry	18	8	14	4	13	8	11	38	4	3	121
Tropical wet	23	8	26	17	29	34	22	52	24	2	237
Sub-tropical (Humid)	14	8	22	7	13	33	48	24	23	22	214
Semi-arid	–	–	–	–	–	–	2	7	1	–	10
Arid	–	1	–	–	1	–	–	–	–	2	4
High land	5	–	7	–	1	1	5	1	1	4	25
Unknown	2	2	1	1	4	–	1	3	1	2	17
Total	62	27	70	29	61	76	89	125	54	35	628

TABLE 4
Distances between the final cluster centres

Clusters	I	II	III	IV	V	VI	VII	VIII	IX	X
I	00	3.74	3.09	5.94	3.05	3.79	2.49	3.49	2.59	4.50
II		00	6.41	6.95	4.64	6.94	5.18	6.24	5.22	6.34
III			00	7.13	4.60	1.97	2.54	3.60	3.54	4.49
IV				00	3.37	6.17	6.60	3.78	5.16	8.81
V					00	4.33	3.46	2.53	2.35	5.94
VI						00	3.52	2.59	3.51	5.94
VII							00	3.79	2.54	3.72
VIII								00	2.90	6.39
IX									00	5.12
X										00

TABLE 5
Variability partitioned during cluster analysis

	Cluster		Error		F – value
Characters	Mean square	df	Mean square	df	
Z score (NBR)	48.745	9	0.305	618	159.988
Z score (TSL)	54.320	9	0.223	618	243.044
Z score (MRC)	38.073	9	0.460	618	82.747
Z score (MC)	31.352	9	0.558	618	56.188
Z score (HUNLF)	48.013	9	0.315	618	152.254
Z score (LLS)	40.761	9	0.421	618	96.830
Z score (INTNOD)	26.487	9	0.629	618	42.12
Z score (WTLAM)	50.309	9	0.282	618	178.456
Z score (LSR)	45.133	9	0.357	618	126.324
Z score (YIELD)	52.637	9	0.248	618	212.249
Z score (TBIO)	54.382	9	0.223	618	244.306
Z score (LAMINDEX)	24.207	9	0.662	618	36.566

NBR = No of primary branches, TSL = Total shoot length, MRC = Leaf moisture retention, MC =Leaf moisture content, HUNLF = 100 leaf weight, LLS = length of the longest shoot, INTNOD = Internodal distance, WTLAM = Lamina weight, LSR = Leaf shoot ratio, YIELD = Leaf yield, TBIO = Total biomass weight, LAMINDEX = Laminar index.

Based on its geographical origin and variability, a core collection was developed. This collection consists of 135 accessions which represent different countries, geographical regions, variability and avoid repetitiveness for further mulberry improvement programme (Table 6). The core collection was also developed for the perennial *Medicago* plant introductions, following a similar procedure (Basigulap *et al.*, 1995; Diwan *et al.*, 1994).

TABLE 6
List of the core collection of mulberry based on its geographical origin and variability for 12 traits (135 accessions)

Sl.	Accessions	Country	Sl. no	Accessions	Country	Sl. no	Accessions	Country
1	ME-0132	Zimbabwe	46	MI-0275	India	91	MI-0121	India
2	MI-0018	India	47	MI-0322	India	92	MI-0160	India
3	MI-0107	India	48	ME-0053	Japan	93	MI-0287	India
4	MI-0141	India	49	ME-0147	Italy	94	MI-0291	India
5	ME-0003	Burma	50	MI-0366	India	95	MI-0305	India
6	ME-0006	Indonesia	51	ME-0157	Unknown	96	MI-0319	India
7	MI-0090	India	52	MI-0042	India	97	ME-0007	Bangladesh
8	MI-0188	India	53	MI-0155	India	98	ME-0033	Thailand
9	MI-0199	India	54	MI-0056	India	99	ME-0084	Bangladesh
10	ME-0018	Indonesia	55	MI-0091	India	100	MI-0024	India
11	MI-0142	India	56	MI-0112	India	101	MI-0039	India
12	MI-0345	India	57	MI-0163	India	102	MI-0074	India
13	MI-0156	India	58	MI-0187	India	103	MI-0102	India
14	MI-0299	India	59	MI-0193	India	104	MI-0220	India
15	MI-0330	India	60	MI-0203	India	105	MI-0267	India
16	ME-0144	France	61	MI-0106	India	106	MI-0274	India
17	MI-0364	India	62	MI-0113	India	107	MI-0312	India
18	MI-0427	India	63	MI-0122	India	108	MI-0344	India
19	ME-0030	Pakistan	64	MI-0128	India	109	MI-0398	India
20	MI-0057	India	65	MI-0137	India	110	MI-0412	India
21	MI-0450	India	66	MI-0151	India	111	ME-0027	Japan
22	ME-0055	Cyprus	67	MI-0066	India	112	MI-0004	India
23	MI-0048	India	68	MI-0400	India	113	MI-0145	India
24	MI-0103	India	69	ME-0082	France	114	MI-0154	India
25	MI-0147	India	70	MI-0209	India	115	MI-0349	India
26	MI-0030	India	71	MI-0236	India	116	MI-0370	India
27	MI-0053	India	72	MI-0449	India	117	MI-0017	India
28	ME-0020	Burma	73	ME-0040	Japan	118	MI-0319	India
29	MI-0060	India	73	ME-0049	Japan	119	ME-0129	Zimbabwe
30	MI-0087	India	75	ME-0054	China	120	ME-0052	Papua New Guinea
31	MI-0183	India	76	ME-0068	Japan	121	MI-0045	India
32	MI-0234	India	77	ME-0114	Japan	122	MI-0150	India

Cont. Table 6

33	MI-0301	India	78	ME-0139	South Korea	123	MI-0244	India
34	ME-0065	Burma	79	ME-0154	South Korea	124	MI-0333	India
35	MI-0214	India	80	MI-0373	India	125	ME-0057	Paraguay
36	ME-0156	China	81	MI-0431	India	126	MI-0034	India
37	MI-0254	India	82	MI-0439	India	127	MI-0139	India
38	MI-0310	India	83	MI-0206	India	128	MI-0437	India
39	ME-0155	Unknown	84	MI-0222	India	129	MI-0438	India
40	MI-0292	India	85	ME-0012	Pakistan	130	ME-0166	France
41	MI-0298	India	86	MI-0012	India	131	ME-0047	Japan
42	MI-0308	India	87	MI-0014	India	132	ME-0061	Russia
43	MI-0266	India	88	MI-0016	India	133	ME-0078	Japan
44	MI-0245	India	89	MI-0031	India	134	ME-0094	Japan
45	MI-0264	India	90	MI-0036	India	135	ME-0153	France

CONCLUSIONS

Any statistical package requires a complete database for a proper analysis and interpretation to be done. In other words, the number of accession is to be reduced to designate a core collection. Moreover, a limited number of accessions will not represent the geographical zones. A collection of 15 – 20 % of most variable, representing different geographical regions and core group, can be made and used for further evaluation and breeding purposes. The new collection/ introductions are dependent on variability, which can be added to the present core collections from time to time, considering 15 - 20% of the samples.

REFERENCES

Basigalup, D.H., Barnes, D.K. and Stucker, R.E. (1995). Development of a core collection for perennial *Medicago* plant introductions. *Crop Science, 35*, 1163 – 1168.

Brown, A.H.D. (1989). The case of core collections. In A.H.D. Brown *et al.* (Eds). *The use of plant genetic resources*, (pp. 136–156). Cambridge: Cambridge University Press.

Brown, J.S. (1991). Principal component analyses of cotton cultivar variability across the V.S. cotton belt. *Crop Science, 31*, 915 – 922.

Diwan, N., Baucher, G.R. and McIntosh, M.S. (1994). A core collection for the United States annual *Medicago* germplasm collection. *Crop Science, 34,* 279 – 285.

Frankel, O.H. and Brown, A.H.D. (1984). Current plant genetic resources: a critical appraisal. In *Genetics: New frontiers* (pp.1-11). New Delhi: Oxford & IBH Publication Company.

Holbrook, C.C., Anderson, W.F. and Pitman, R.N. (1993). Selection of a core collection from the U.S. germplasm collections. *Crop Science, 33,* 859 – 861.

Johnson, B.L.C. (1978). India Resources and Development.

Peeters, J.P. and Martinelli, J.A. (1989). Hierachical cluster analysis as a tool to manage variation in germplasm collections. *Theoretical Applied Genetics, 78,* 42- 48.

Smith, S.E., Guarino, L., Al-Doss, A. and Conta, D.M. (1995). Morphological and agronomic affinities among the Middle Eastern Alfalfas accessions for Oman and Yemen. *Crop Science, 35,* 1188 – 1194.

Tikader, A., Rao, A.A., Ravindran, S., Naik, V.G., Mukherjee, P and Thangavelu, K. (1999). Divergence analysis in different mulberry species. *Indian J. Genetics, 50,* 87 – 93.

Tikader. A., Rao, A.A. and Mukherjee, P. (2000). Phenotypic characterisation of mulberry (*Morus* spp.) germplasm. In *Proceedings of 4th China International Silk Conference (*pp. 114 – 125). Soochoow University, China.

Tikader, A. and Rao, A.A. (2001a). Analysis of divergence in mulberry species through different clustering technique. *Sericologia, 41,* 109 – 116.

Tikader, A. and Roy, B.N. (2001b). Multivariate analysis in some mulberry (*Morus* spp.) germplasm accessions. *Indian J. Sericulture, 40*(2), 71 – 74.

Tikader, A. and Roy, B.N. (2002). Genetic divergence in mulberry (*Morus* spp.). *Indian J. Genetics, 62,* 52 – 54.

Vijayan, K., Tikader, A., Das, K.K., Chakroborti, S.P. and Roy, B.N. (1997). Correlation studies in mulberry (*Morus* spp.) *Indian J. Genetics, 57,* 455 – 460.

ISSN: 0128-7680
Pertanika J. Sci. & Technol. **17 (1)**: 53 – 59 (2009)

Spectrophotometric Determination of Trace Arsenic (III) Ion Based on Complex Formation with Gallocyanine

Nor Azah Yusof* **and Zainab Omar**
Department of Chemistry, Faculty of Science,
Universiti Putra Malaysia, 43400 UPM, Serdang,
Selangor, Malaysia
**E-mail: azah@science.upm.edu.my*

ABSTRACT

In this study, a simple, selective and sensitive method, for spectrophotometric determination of As(III) with gallocyanine as the sensitive reagent was developed. The wavelength of an analytical measurement, for the determination of As (III), using gallocyanine was at 630 nm with an optimum response at pH 2. The RSD for the reproducibility of 100 ppm As (III) was 2.3%. The LOD was 0.04 ppm with linear dynamic range in As(III) concentration of 0.2 - 1.5 ppm. The developed method has been validated against Atomic Absorption Spectrophotometry (AAS). The interference study of several metal ions was carried out and it revealed that that Mn (II) ion was interfered the most.

Keywords: Gallocyanine, arsenic determination, metal toxicity

INTRODUCTION

Arsenic occurs in the environment in organic and inorganic forms. In more specific, arsenic is generally found in the inorganic form of arsenite and arsenate. Arsenic usually contaminates ground and surface water. The concentration of arsenic in both surface and ground waters generally ranges from 0.001 to 0.01 ppm, but elevated levels (1-50 ppm) have also been reported in groundwaters in China, India and Bangladesh (The Arsenic Crisis, 1998).

A long-term exposure to low concentration of arsenic has been linked to increased risk of cancer and can lead to death if ingested in large dose. Arsenic is usually exposed to human being through food and water. The maximum contaminant level (MCL) of arsenic, which is recommended for the implementation in the USA for drinking water, is 0.01 ppm (Arsenic, 2000).

Numerous analytical techniques have been employed to detect arsenic including spectrophotometry (Hashemi *et al.*, 2007; Afkhami *et al.*, 2001; Kundu *et al.*, 2002), chromatography technique (Sun *et al.*, 2007), atomic absorption spectrometry (Dang *et al.*, 1999) and inductively coupled plasma mass spectrometry (Steely *et al.*, 2007). Among these techniques, spectrophotometry offers the simplest and cheapest way for the detection of arsenic and it is readily amenable to portable instrumentation.

In the trioxide As_2O_3, As has valence +3, while in the pentoxide As_2O_5, the valence is +5. When oxides such as these are dissolved in water, they attract H^+ and OH^- ions, and may rearrange their structures. In the case of As_2O_5, the equation involved is:

Received: 19 September 2007
Accepted: 24 October 2008
*Corresponding Author

$$As_2O_5 + 3H_2O \rightarrow 2H_3AsO_4 \quad (1.1)$$

The molecule formed is orthoarsenic acid, which dissociates to give H^+ ions, and an acidic solution. Here, arsenic behaves as a non-metal, like phosphorus, and can form salts with metals or positively charged compound.

Gallocyanine or 7-dimethylamino-4-hydroxy-3-oxo-phenoxazine-1-carboxylic is an oxazine derivative. It is also known as alizarin navy blue, mordant blue and anthracene blue. The dye is soluble in acid and alkaline solutions, and partially soluble in water. In acidic solution, this reagent is present in a cationic form. Solutions can also be prepared in dioxane, pyridine, acetic anhydride and concentrated sulfuric acid (Feigl *et al.*, 1972). *Fig. 1* shows the structure of the reagent in both neutral and ionic forms. Gallocynine has been used in a few analytical applications such as the determination of iodate and periodate (Ensafi *et al.,* 2000) and boron (Skaar, 1964).

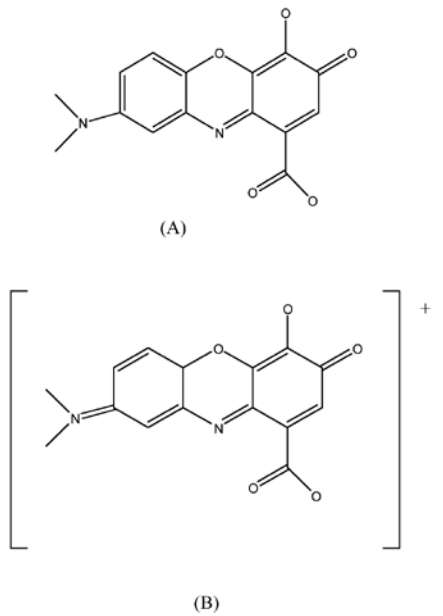

Fig. 1: Structure of gallocynine in neutral (A) and ionic form (B)

In this work, a simple way of detecting arsenic, based on the usage of gallocyanine in cationic form is proposed. The method proposed is indeed suitable for a particular need of fast and *in situ* analytical test.

The Experiment

(i) Reagent

All chemicals used were of analytical grade (BDH), and deionised water was also employed for solution preparation in the present study. Gallocyanine solution of 1.0×10^{-4} M was prepared by dissolving 0.006 g of gallocyanine in 200 ml of deionised water. Working standard solutions of As (III) were prepared by an appropriate dilution of stock solution

before use. Buffer solutions were prepared according to the method suggested in the *Handbook of Basis Tables for Chemical Analysis* (Svoronos and Svoronos, 1989).

(ii) Instrumentation

The measurements were made using the Ultraviolet-Visible Spectrophotometer (Varian-Cary Win UV 100). For this purpose, the Atomic Absorption Spectrophotometer was used for the validation study.

(iii) Procedure

The absorption spectra of gallocyanine were recorded before and after the reaction with 100 ppm As (III). The effects of pH on the complex formation was studied by mixing 2.5 ml of gallocyanine solution with 1.0 ml of 100ppm As(III) solution containing 0.5 ml of buffer at different pH values (pH 1.0 – 10.0).

The effect of gallocyanine concentration, on the As (III) complex formation, was studied by adding 1.0 ml of 100 ppm As (III) solution into a volumetric flask containing 5.0 ml of different concentrations (2.0×10^{-6} M to 3.8×10^{-5} M) of gallocyanine, and diluted to the mark with deionised water.

A dynamic range of As (III) concentration was studied by introducing different concentrations (0.1 – 10.0 ppm) of As (III) to a cuvette containing 3.0 ml of gallocyanine (3.0×10^{-5} M).

The interferences, from both anion and cation, were studied by introducing 0.5 ml of 100 ppm As (III) to a cuvette containing 3.0 ml of 3.0×10^{-5} M of gallocyanine and interfering ions [the ratio of As (III) : interfering ion is 1:1]. Another cuvette, containing the similar proportion except for the interfering ion displaced with deionised water, was prepared as a control.

RESULTS AND DISCUSSION

Fig. 2 shows the absorbance spectra of gallocyanine and gallocyanine-As(III) complex. It was observed that the formation of the complex caused a decrease in the absorbance, due to a sharp colour change, i.e. from dark blue to light violet. Gallocyanine showed its maximum absorbance at 630 nm, while gallocyanine-As (III) complex showed the maximum absorption at 525 nm and very low absorption at 630 nm. The difference in the absorbance between gallocyanine and gallocyanine-As (III) complex at 630 nm was used for further analytical measurement. The biggest difference between gallocyanine and complex was obtained at pH 2. Therefore, this pH was used throughout the study.

The reproducibility study was carried out by running 10 replicates of similar proportion of As (III), gallocyanine and buffer. This was done to estimate the discrepancies in its response. The RSD was calculated to be 2.3%, suggesting that the developed method is reproducible.

The effect of the reagent concentration was studied using different initial concentrations of the reagent (2.0×10^{-6} M to 3.8×10^{-5} M). From *Fig. 3*, it is observed that the absorbance increased with the increasing amount of reagent, until it reached a point where the absorbance became almost constant. The same observation was also reported by Satienperakul *et al.* (2005) who studied the chemiluminisence determination of As (III). They reported that with the increase of the volume of reagents involved, the signal increased rapidly to a plateau.

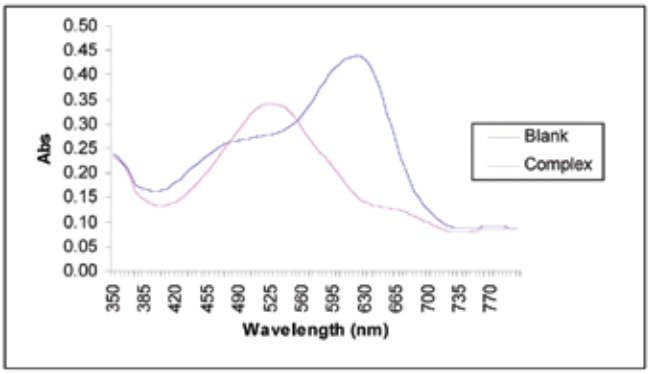

Fig. 2: Absorption spectra of gallocyanine (blank) and As (III)-gallocyanine complex

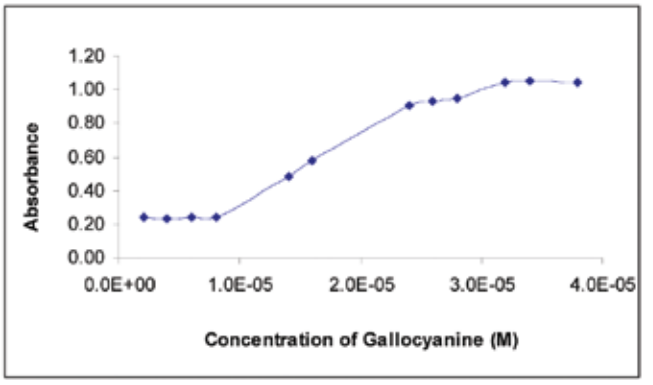

Fig. 3: The effect of the concentration of gallocyanine on the absorbance of As (III)-gallocyanine

Fig. 4 shows the response curve of the reagent towards different concentrations of As (III). It shows that the developed method produced a linear response when the As (III) concentration was within the range of 0.02 to 2.00 ppm. In the present study, the limit of detection (LOD) of As (III), defined as the concentration equivalent to a signal blank, plus three times the standard deviation of the blank, was calculated to be 0.04 ppm. Hashemi and Modasser (2007), who carried out a study on the detection of arsenic based on hydride generation and bleaching of permanganate, achieved LOD as low as 3.0 ppb; whereas, Afkhami *et al.* (2001) utilized the inhibitory effect of arsenic on the redox reaction, between bromate and hydrochloric acid, were able to detect arsenic at sub ppb level. Meanwhile, Kundu *et al.* (2002) proposed a simpler method for arsenic detection, based on the colour bleaching of methylene blue in micellar medium, with LOD of 0.03 ppm. Even though better LOD has been reported by these researchers, the use of multiple step reaction (hydride generation, inhibitory effect and arsine release for colour bleaching) usually imposes some effects on the response time. The use of the multiple reagents also limits the possibilities of miniaturization. When a comparison was carried out with the findings of these researches, the current research offered a single step detection with a short response time and fairly good LOD.

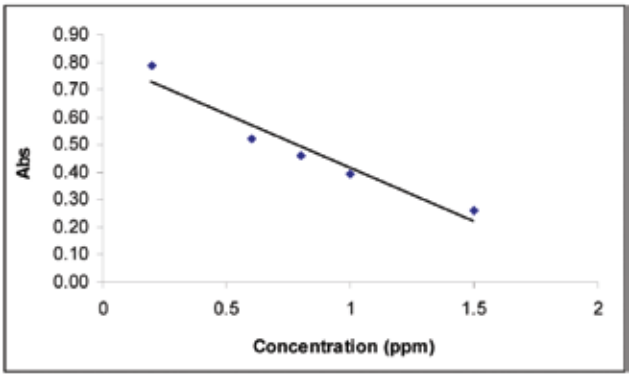

Fig. 4: The linear response towards different concentrations of As (III)

The degree of interference, measured from some foreign ions at 1:1 mole ratio of As (III):ion, is summarized in Table 1. The main cation interference was obtained from Mn(II). It was also found that NH_4^+ gave a high degree of interference since they are chemically reactive and capable of forming complex with lots of metal. Negative interference was observed for anions, whereas cation showed a positive interference. Musa and Narayanaswamy (1995) reported that the most common type of such interference was the complexing of the analyte by the interfering ion.

In this study, the developed method was validated against the AAS. The data for the developed method and AAS are shown in Table 2. Based on the data shown, the developed method was proven to be comparable with the conventional method (AAS).

TABLE 1
The percentage of interference from foreign ions

Anions/ cations	% Interference
Mn(II)	8.33
Cd(II)	6.79
Co(II)	1.84
Pb(II)	1.46
NH4+	7.84
Citrate	7.16
Phosphate	2.71

TABLE 2
Result of the comparative study of the developed method and AAS

Method	Concentration (mean), ppm
AAS	1.01 ppm
Developed sensor	0.97 ppm

CONCLUSIONS

The limit of detection of As (III), using the developed method, was found to be 0.04 ppm. The relative standard deviation (RSD), for the reproducibility of determination of As (III), was calculated to be 2.3%. In addition, it was also found that Mn(II) ion interfered most in the determination of As (III). An excellent agreement with the AAS method was achieved, when the proposed method was applied in the determination of As (III). The characteristic of the method, i.e. simplicity, selectivity and rapid calibration, has made it especially suitable for a routine analysis.

ACKNOWLEDGEMENT

The author would like to acknowledge the Ministry of Environment and Science Department of Malaysia for funding this research with an IRPA research grant, 09-02-04-0818.

REFERENCES

Ahmad, M. and Narayanaswamy, R. (1995). Development of an optical fibre Al (III) sensor, based on immobilised chrome azurol S. *Talanta*, *42*, 1337-1344.

Arsenic, [web page], 2000: available at http://www.du.edu/~jcalvert/phys/arsenic.htm. Accessed in January, 2006.

Afkhami, T., Madrakian, A.A. and Assl. (2001). Kinetic-spectrophotometric determination of trace amounts of As (III), based on its inhibitory effect on the redox reaction between bromate and hydrochloric acid. *Talanta, 55*(1), 55-60.

Dang, T.M.N., Tran, Q.T. and Vu, K.V. (1999). Determination of arsenic in urine by atomic absorption spectrophotometry for biological monitoring of occupational exposure to arsenic. *Toxicology Letters, 108*(2-3, 5), 179-183.

Ensafi, A.A. and Gadamali. B.D. (2000). Flow injection simultaneous determination of iodate and periodate by spectrophotometric and spectrofluorometric detection. *Analytical Sciences, 16,* 61-64.

Feigl, F. (1958). *Spot Test in Inorganic Chemistry,* (5th Ed.). Amsterdam. Elsevier.

Hashemi, M. and Modasser, P. (2007). Sequential spectrophotometric determination of inorganic arsenic species by hydride generation from selective medium reactions and colour bleaching of permanganate. *Talanta.* (In Press).

Kundu, S., Ghosh, S.K., Mandal, M., Pal, T. and Pal, A. (2002). Spectrophotometric determination of arsenic via arsine generation and in-situ colour bleaching of methylene blue (MB) in micellar medium. *Talanta*, *58*(5), 935-942.

Satienperakul, S., Cardwell, T.J., Kolev, S.D., Lenehan, C.E. and Barnett, N. W. (2005). A sensitive procedure for the rapid determination of arsenic (III) by flow injection analysis and chemiluminescence detection. *Analytica Chimica Acta, 554*, 25-30.

Skaar, O.B. (1965). Photometric Determination with Oxazine Derivatives. *Anal. Chim. Acta, 32,* 508-514.

Steely, S., Amarasiriwardena, D., Jones, J. and Yañez, J. (2007). A rapid approach for assessment of arsenic exposure by elemental analysis of single strand of hair using laser ablation-inductively coupled plasma-mass spectrometry. *Microchemical Journal*, *86*(2), 235-240.

Svoronos, T.J. and Svoronos, P.D.N. (1989). *CRC Handbook of Basis Tables for Chemical Analysis*. USA: CRC Press. Inc. 50.

Sun, Y.C., Chen, Y.J. and Tsai, Y.N. (2007). Determination of urinary arsenic species using an on-line nano-TiO_2 photooxidation device coupled with microbore LC and hydride generation-ICP-MS system. *Microchemical Journal, 86*(1), 140-145.

The Arsenic Crisis, [web page], (1998): available at http://www.es.ucl.uk/ research/lag/as/pdf., accessed in January 2006.

ISSN: 0128-7680
Pertanika J. Sci. & Technol. **17 (1)**: 61 – 68 (2009)

Effect of Body Size on Heavy Metal Contents and Concentrations in Green-Lipped Mussel *Perna viridis* (Linnaeus) from Malaysian Coastal Waters

Yap, C.K.[1*], Ismail, A.[1] and Tan, S.G.[2]
[1]Department of Biology, Faculty of Science, Universiti Putra Malaysia,
[2]Department of Cell and Molecular Biology, Faculty of Biotechnology and Biomolecular Science, Universiti Putra Malaysia,
43400 UPM, Serdang, Selangor, Malaysia
[*]E-mail: yapckong@hotmail.com

ABSTRACT

The concentrations of cadmium, copper, zinc and lead, in the total soft tissues of green-lipped mussel *Perna viridis* of a wide range of sizes (2-11 cm), were determined from a population at Pasir Panjang. The metal contents (μg per individual) and concentrations (μg per g) of cadmium, lead, copper and zinc were studied in *P. viridis* to find the relationships with body sizes. Smaller and younger mussels showed higher concentrations (μg per g) of Cd, Pb and Zn than the larger and older ones. The results of the present study showed that the plotting of the metal content, against dry body flesh weight on a double logarithmic basis, gave good positive straight lines; this observation is in agreement with Boyden's formula (1977). This indicated that *P. viridis* showed a different physiological strategy for each metal being studied, which is related to age.

Keywords: *Perna viridis*, metal contents, metal concentrations, shell length, total dry body weight, shell thickness

INTRODUCTION

The green-lipped mussel, *Perna viridis,* is an established biomonitor of heavy metal contamination in the coastal waters of Asia-Pacific (Tanabe, 2000), and particularly in Malaysia (Yap *et al.*, 2003; 2006). From the literature, the heavy metal concentrations measured in the soft tissues of mussels could be used as biomonitors of heavy metal bioavailabilities and contamination in the coastal environment, in which the mussels live (Yap *et al.*, 2006). However, the accumulation of heavy metal concentrations in the tissues of mussels is also affected by a number of intrinsic and extrinsic factors. The extrinsic factors include spawning season (Dare and Edwards, 1975; Phillips, 1980; Lobel *et al.*, 1991) and mussel size (Boyden, 1977; Cossa *et al.*, 1980; Williamson, 1980; Lobel and Wright, 1982; Propham and D'Auria, 1983; Lobel *et al.*, 1991; Riget *et al.*, 1996).

Previous studies revealed that the body size might change the heavy metal uptake due to the changes in the kinetic steady-states as mussels grew (Lobel *et al.*, 1991; Riget *et al.*, 1996). Obviously, body size would affect metal bioaccumulation in the rates of uptake and excretion (Phillips and Rainbow, 1993). Besides, the effects of the body size on different physiological rates such as pumping, filtration and respiration, have been reported in the mussel, *Mytilus edulis* (Winter, 1978; MΦhlenberg and Riisgard, 1979; Bayne and Newell, 1983; Jones *et al.*, 1992).

Received: 4 September 2008
Accepted: 19 September 2008
[*]Corresponding Author

The relationships between heavy metal concentrations and body sizes in temperate molluscs have been well documented (Boyden, 1974, 1977; Simpson, 1979; Cossa *et al.*, 1980; Lobel and Wright, 1982), but such information for tropical and sub-tropical species is rather limited. Therefore, the present study aimed to provide comparative information in understanding the physiological strategies for the accumulation of Cd, Pb, Cu and Zn in relation to body size of a tropical mussel. The objective of the present study was to investigate the effects of the length, thickness and total dry flesh body weight of shells on metal contents (μg per individual) and concentrations (μg per g) in *P. viridis*.

MATERIALS AND METHODS

Mussels, having a wide range of body sizes (2-11 cm), were collected from a local mariculture site in Pasir Panjang between August and October, 1998. All samples were stored at -10°C until metal analysis was conducted. The samples were thawed at room temperature, on a clean tissue paper, with the posterior margins placed downwards to drain away the excess water (Chan, 1988). The total soft tissues were carefully removed by de-shelling the mussels with a stainless steel knife. The dry weight of the soft tissues was determined by drying the whole soft tissues individually for at least 72 hours at 105°C to constant weights (Mo and Neilson, 1994). The samples were pooled to get enough samples for the metal analyses.

The samples were digested in concentrated nitric acid (Yap *et al.*, 2003, 2006). They were placed in a hot-block digestor at a low temperature (40°C) for 1 hr, and digested at a high temperature (140°C) for 3 hrs. The digested samples were then diluted to a known volume with double distilled water. After filtration, the prepared samples were subjected to Cd, Cu, Pb and Zn analyses in an air-acetylene flame atomic absorption spectrophotometer (Perkin-Elmer Model 4100). The data are presented in μg g^{-1} dry weight basis. To avoid possible contamination, all glassware and equipment used were acid-washed, and the accuracy of the analysis was checked using the blank and standard addition testing procedure. The percentages of recoveries for heavy metal analyses were found to be 92% for Zn, 110% for Cd, 92.5% for Pb and 96% for Cu. The samples were also checked with the Certified Reference Material for Soil (International Atomic Energy Agency, Soil-5, Vienna, Austria). Standard solutions were prepared from 1000 mgL^{-1} stock solutions of each metal (MERCK Titrisol).

The effects of body size on heavy metal concentrations were investigated in the mussels using a linear regression analysis of logarithmic transformed data (Boyden, 1974, 1977). Regression analyses are better interpretations than simple correlations because they can predict fluctuation, shape of curve and accuracy between variables; whereas the degree of closeness between X and Y is not easy to grasp (Snedecor and Cochran, 1979). Boyden (1974, 1977) suggested that plotting the metal contents (μg per individual) or concentrations (μg g^{-1}) against body size on double logarithmic scales generally produces a straight-line relationship which can easily be defined using an equation, thus:

$$\text{Log (metal)} = \text{Log(a)} + \text{b Log(body size)}.$$

where (a) = intercept and (b) = slope. In the present study, body sizes (flesh dry weight, shell length and shell thickness) were plotted against metal contents and metal concentrations of the tested animal.

Shell thickness, which is considered as an age measure (Cossa *et al.*, 1980; Frew *et al.*, 1989), was calculated according to the following formula:

$$\text{Shell Thickness } (g.cm^{-3}) = \frac{\text{shell weight (g)}}{\text{shell length (cm)} \times \text{shell height (cm)}}$$

RESULTS AND DISCUSSION

Fig. 1 shows that all metal contents (Y) (µg per individual) were related to body dry flesh weights (X) by the following relation, $Y = aX^b$ [$Log(Y) = a + bLog(X)$], where $b < 1$. According to Boyden (1977), by plotting metal contents (Y) (µg per individual) against body size, an equation with a slope (b) less than 1 is explained by larger individuals containing less metal, and a logarithmic transformation of this equation yields a straight-line relationship. The results of present study are similar to those of other studies carried out in blue mussels, snails, fish and clams (Table 1). Cd showed the weakest relationship with an increasing dry flesh body weight ($r = 0.62$, $p < 0.01$) and it had a similar concentration (Y) (µg per g) to that of a study on mussel *M. edulis* which reported a coefficient correlation of 0.65 (Cossa *et al.*, 1980). In other aquatic organisms, this non-essential metal (Cd) was not regulated and kept accumulating until it reached a threshold level (Kraak *et al.*, 1994; Lukyanova *et al.*, 1993; Tessier *et al.*, 1994). The Cu content was positively correlated ($r = 0.94$, $p < 0.001$) with the increasing body weight. Similar positive relationships for Cu were also reported for *M. edulis*, *Mercenaria mercenaria* and *Venerupis decussata* (Boyden, 1974).

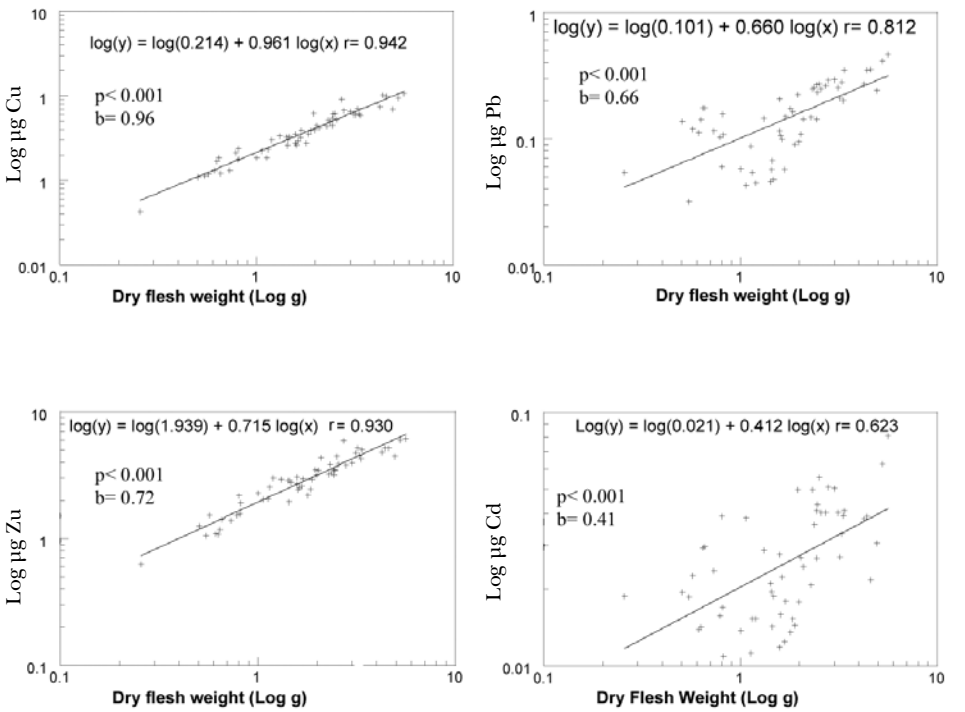

Fig. 1: The relationships between Cd, Cu, Pb and Zn content (log µg) and the total soft tissue dry weight (log g) of mussel P. viridis *from Pasir Panjang, Port Dickson, (with a positive regressive equation as log(Y)= log(a) + b log(X), 0 < b< 1)*

Fig. 2 shows the double logarithmic transformations, in which metal concentrations (Y) (µg per g) were found to be related to the length and shell thickness of shell, as X by the relation $Y= aX^b$, where the slopes (b) were negative. Boyden (1977) described this equation, by plotting metal concentrations (Y) (µg per g) against body size, as having negative slopes (b) when larger mussels were indicated to accumulate less heavy metal as compared to smaller ones. The concentrations of Cd and Zn showed significant ($p< 0.001$) decrease with the increasing shell length ($r= -0.69$ and $r= -0.65$) and thickness ($r= -0.68$ and $r= -0.66$).

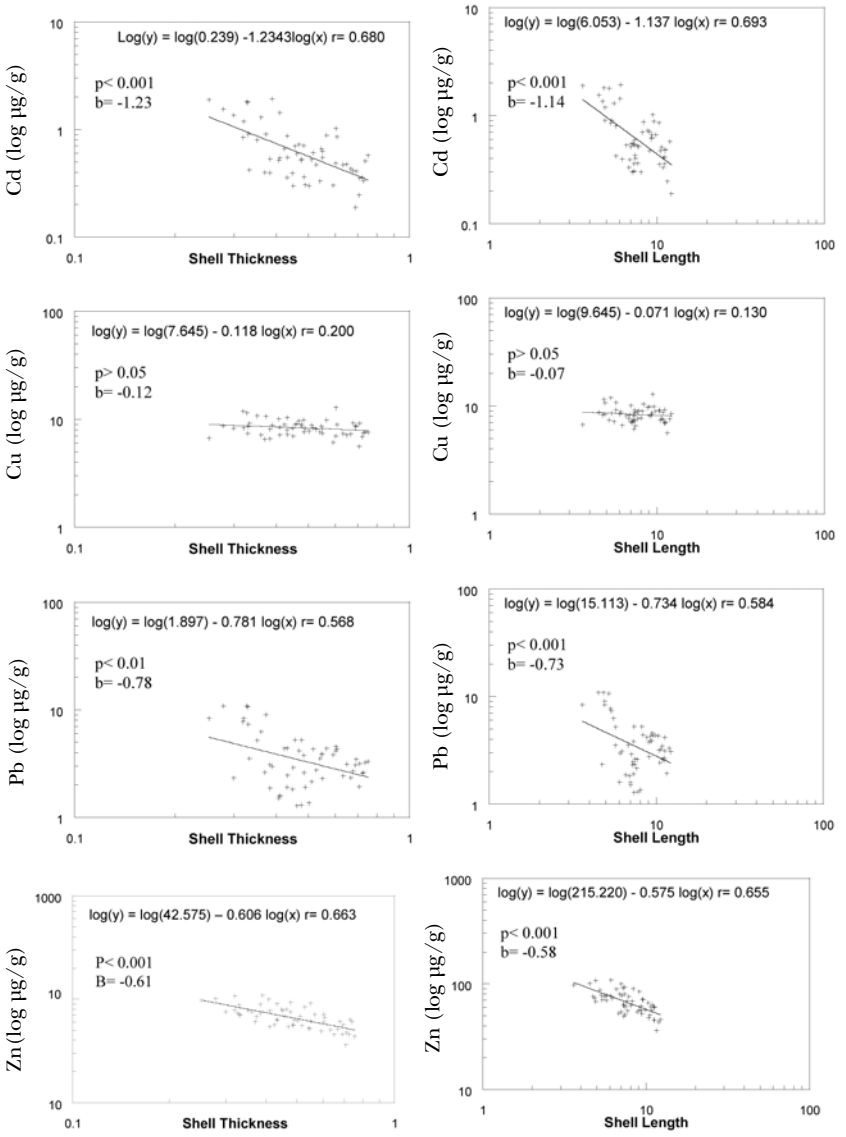

Fig. 2: The relationships between the concentrations of Cd, Cu, Pb and Zn (log µg.g^{-1}) and the thickness (log g.cm^{-2}) and length (log cm) of mussel P. viridis *from Pasir Panjang, Port Dickson (with negative regressive equation as log(Y)= log(a) - b log(X), b< 0)*

Pb showed an intermediate decrease with the increasing shell length (r= -0.58) and shell thickness (r= -0.57). The concentration of Cu illustrated an insignificant ($p > 0.05$), weak and decreasing relationship with the shell length (r= -0.13) and thickness (r= -0.20).

Boyden (1977) explained that the metal concentrations in older mussels would be lower when compared to the younger ones *(Fig. 1)*. The results could be due to the older individuals which had experienced longer terms of exposure, as compared to younger mussels. Further studies should be conducted to prove this hypothesis.

In previous studies, many authors reported negative relationships between body size and the accumulation of aquatic contaminants in suspension-feeding bivalves (Williamson, 1980; Amiard *et al.*, 1986; Martincic *et al.*, 1992). For instance, Williamson (1980) reported that higher levels of Cd, Pb and Zn were found in smaller individual snails, and suggested that this might be due to the variations in the metabolic activities at different ages of the organisms. He also suggested that the increase in metabolic rates, in relation to different body sizes, might affect the uptake and elimination of metal. The same inverse relationships between the body size and heavy metal accumulation were also observed in *Penaeus stylirostris* (Paez-Osuna and Ruiz-Fernandez, 1995) and *Corbicula fluminea* (Bilos *et al.*, 1998). Swaileh and Adelung (1994) reported that smaller individual ocean quahog *Arctica islandica* had higher concentrations of Zn than the bigger individuals. Bilos *et al.* (1998) showed significant relationships, between the body size and concentrations of Cu (positive) and Zn (negative), in clam *Corbicula fluminea.*

TABLE 1
The comparison of the correlation coefficient (r) for the metal content (μg per individual) versus the total dry soft tissue weight (g) from other studies

Species	Metals	r value	Reference
Mytilus edulis (mussel)	Cu	0.80	Boyden (1977)
Mytilus edulis (mussel)	Zn	0.85	Boyden (1977)
Mytilus edulis (mussel)	Cu	0.86	Cossa *et al.* (1980)
Mytilus edulis (mussel)	Zn	0.86	Cossa *et al.* (1980)
Mytilus edulis (mussel)	Cd	0.65	Cossa *et al.* (1980)
Cepaea hortensis (snail)	Cd	0.26	Williamson (1980)
Cepaea hortensis (snail)	Pb	0.65	Williamson (1980)
Cepaea hortensis (snail)	Zn	0.82	Williamson (1980)
Macoma balthica (clam)	Cu	0.96	Bordin *et al.* (1992)
Macoma balthica (clam)	Zn	0.98	Bordin *et al.* (1992)
Macoma balthica (clam)	Cd	no correlation	Bordin *et al.* (1992)
Arius thalassinus (fish)	Cu	0.92	Law and Singh (1991)
Arius thalassinus (fish)	Zn	0.76	Law and Singh (1991)
Arius thalassinus (fish)	Pb	0.60	Law and Singh (1991)
Perna viridis (mussel)	Cu	0.94	The present study
Perna viridis (mussel)	Zn	0.93	The present study
Perna viridis (mussel)	Pb	0.81	The present study
Perna viridis (mussel)	Cd	0.62	The present study

Since Cu and Zn are essential metals involved in several enzymatic systems, which may display partial regulation in mussels (Timmermans, 1993; Kraak *et al.*, 1994;), the relationships between body sizes (shell length and shell thickness) and concentrations of these metals observed in the mussel *P. viridis* strongly suggested different physiological requirements with size, which might be related to age.

The results gathered in the current study suggested that there might be differences in physiology between young and older mussels. Since large and aged mussels tended to pump less water, through their bodies per unit of body weight, the uptake of metals was lower than that in smaller individuals. The surface area to volume ratios decreased with size, and this affected the relative contribution of the adsorbed metal content to the total body burden of heavy metals (Cossa *et al.*, 1980; Swaileh and Adelung, 1994). Therefore, the decrease in metal concentrations with body size indicated that a significant proportion of the metal content was surface-adsorbed as smaller mussels have a larger surface area to volume ratio (Jones *et al.*, 1992). As the concentrations of heavy metal (μg per g) decreased with an increase in the body size (length and thickness of shell); this indicated that the chemical pollutants were more concentrated in young mussels due to their faster growth rate (Cossa *et al.*, 1980; Olafsson, 1986).

CONCLUSIONS

The relationships between the accumulation of heavy metal and size were observed and the correlation coefficients were found to be different between the heavy metals examined. The findings of the present study revealed that younger and smaller *P. viridis* accumulated higher concentrations of Cd, Cu, Pb and Zn. Therefore, the factor of body size should be taken into consideration in designing experiments, such as the "Mussels Watch" program in order to enhance the interpretation of ecotoxicological results, especially when these results were based on the comparisons between different mussel populations and different size groups or ages. This can be done in a number of ways; these include sampling a restricted size range of mussels at every sampling station. However, this is not a realistic approach as according to Lobel *et al.* (1991), every locality has a location-dependent maximum size. Further studies should focus on the establishment of statistical constant for each metal and the concentrations of heavy metal in different size groups, which should be normalised before valid interpretations of ecotoxicological biomonitoring data can be made.

REFERENCES

Amiard, J.C., Amiard-Triquet, C., Berthet, B. and Metayer, C. (1986). Contribution to the ecotoxicological study of cadmium, lead, copper and zinc in the mussel *Mytilus edulis* I: Field Study. *Mar. Biol.,* 90: 425-431.

Bayne, B.L. and Newell, R.C. (1983). Physiological energetics of marine molluscs. In K.M. Wilbur and A.S. Saleuddin (Eds.), *The Mollusca* (pp. 407-515). New York: Academic Press.

Bilos, C., Colombo, J.C. and Rodriguez-Presa, M.J. (1998). Trace metals in suspended particles, sediments and asiatic clams (*Corbicula fluminea*) of the Rio de la Plata Estuary, Argentina. *Environ. Pollut, 99,* 1-11.

Bordin, G., McCourt, J. and Rodriguez, A. (1992). Trace metals in the marine bivalve *Macoma balthica* in the Westerschelde Estuary, the Netherland. Part 1: analysis of total copper, cadmium, zinc and iron- locational and seasonal variations. *Sci. Tot. Environ, 127,* 225-280.

Boyden, C.R. (1974). Trace element content and body size in molluscs. *Nature, 251,* 311-314.

Boyden, C.R. (1977). Effects of size upon metals content of shellfish. *J. Mar. Biol. Assoc. U.K., 57,* 675-714.

Broman, D., Lindqvist, L. and LundberghI, I. (1991). Cadmium and zinc in *Mytilus edulis* (L.) from the Bothnian and the Northern Baltic Proper. *Environ. Pollut. 74*, 227-244.

Chan, H.M. (1988). Accumulation and tolerance of cadmium, copper, lead and zinc by the green mussel *Perna viridis. Mar. Ecol. Prog. Ser., 48,* 295-303.

Cossa, D., Bourget, E., Pouliot, D., Piuze, J. and Chanut, J.P. (1980). Geographical and seasonal variations in the relation between trace metals content and body weight in *Mytilus edulis. Mar. Biol., 58,* 7-14.

Dare, P.J. and Edwards, D.B. (1975). Seasonal changes in flesh weight and biochemical composition of the mussels (*Mytilus edulis* L.) in the Conway Estuary, North Wales. *J. Exp. Mar. Biol. Ecol., 18,* 89-97.

Frew, R.D., Hunter, K.A. and Beyer, R. (1989). Cadmium in the dredge oyster *Ostrea lutaria*- dependence on age, body weight and distribution in internal organs. *Mar. Pollut. Bull., 20,* 463-464.

Jones, H.D., Richards, O.G. and Southern, T.A. (1992). Gill dimension, water pumping rate and body size in the mussel *Mytilus edulis* (L.). *J. Exp. Mar. Biol. Ecol., 155,* 213-237.

Kraak, M.H.S., Toussaint, M., Lavey, D. and Davids, C. (1994). Short-term effects of metals on the filtration rate of the zebra mussel *Dreissena Polymorpha. Environ. Pollut, 84,* 139-143.

Law, A.T. and Singh, A. (1988). Heavy metals in fishes in the Klang Estuary, Malaysia. *Malay. Nature J., 41,* 505-513.

Lobel, P.B. and Wright, D.A. (1982). Relationship between body zinc concentration and allometric growth measurements in the mussel *Mytilus edulis. Mar. Biol., 66,* 145-150.

Lobel, P.B., Bajdik, C.D., Jackson, S. E. and Longerich, H.P. (1991). Improved protocol for collecting mussel watch specimens taking into account sex, size, condition, shell, shape and chronological age. *Arch. Environ. Contam. Toxicol., 21*, 409-414.

Lobel, P.B., Mogie, P., Wright, D.A. and Wu, B.L. (1982). Metal accumulation in four molluscs. *Mar. Pollut. Bull., 13,* 170-174.

Lukyanova, O.N., Belchera, N.N. and Chelomin, V.P. (1993). Cadmium bioaccumulation in the scallop *Mizuhopecten yessoensis* from an unpolluted environment. In R. Dallinger and P.S. Rainbow (Eds.), *Ecotoxicology of Metals in Invertebrates* (pp. 25-35). Boca Raton: SETAC Special Publication Series.

M⊕hlenberg, F. and Riisgard, H.U. (1979). Filtration rate, using a new indirect technique, in thirteen species of suspension-feeding bivalves. *Mar. Biol., 54,* 145-147.

Martincic, D., Kwokal, Z., Peharec, Z., Margus, D. and Branica, D. (1992). Distribution of Zn, Pb, Cd and Cu between sea water and transplanted mussel (*Mytilus galloprovincialis*). *Sci. Tot. Environ., 119,* 211-230.

Mo, C. and Neilson, B. (1994). Standardization of oyster soft dry weight measurements. *Wat. Res., 28,* 243-246.

Olafsson, J. (1986). Trace metal in mussels (*Mytilus edulis*) from South-East Iceland. *Mar. Biol., 90,* 223-229.

Paez-Osuna, F. and C. Ruiz-Fernandez. (1995). Comparative bioaccumulation of trace metals in *Penaues stylirostris* in estuarine and coastal environments. *Estuar. Coast. Shelf Sci., 40,* 35-44.

Phillips, D. J. H. (1980). *Quantitative Aquatic Biological Indicators: Their Use to Monitor Trace Metal and Organochlorine Pollution.* London: Applied Science Publishers.

Phillips, D. J. H. and P. S. Rainbow, P. S. (1993). *Biomonitoring of Trace Aquatic Contaminants.* London: Elsevier Science Publishers Limited.

Popham, J.D. and D'Auria, J.M. (1983). Combined effect of body size, season and location on trace element levels in mussels (*Mytilus edulis*). *Arch. Environ. Contam. Toxicol., 12,* 1-14.

Riget, F., Johansen, P. and Asmund, G. (1996). Influence of length on element concentrations in the blue mussels (*Mytilus edulis*). *Mar. Pollut. Bull., 32,* 745-751.

Simpson, R.D. (1979). Uptake and loss of zinc and lead by mussels (*Mytilus edulis*) and relationships with body weight and reproductive cycle. *Mar. Pollut. Bull., 10,* 74-78.

Snedecor, G.W. and Cochran, W.G. (1979). *Statistical Methods* (6th ed.). Iowa: The Iowa State University Press.

Swaileh, K.M. and Adelung, D. (1994). Levels of trace metals and effects of body weight on metal content and concentration in *Artica islandica* L. (Mollusca: Bivalvia) from Kiel Bay Western Baltic. *Mar. Pollut. Bull., 28,* 500-505.

Tanabe, S. (2000). Asia-Pacific Mussel Watch progress report. *Mar. Poll. Bull., 40,* 651.

Tessier, L., Vaillancourt, G. and Pazdernik, L. (1994). Comparative study of the cadmium and mercury kinetics between the short-lived gastropod *Viviparus georgianus* (Lea) and pelecypod *Elliptio complanata* (Lightfoot), under laboratory conditions. *Environ. Pollut., 85,* 271-282.

Timmermans, K.R. (1993). Accumulation and effects of trace metals in freshwater invertebrates. In R. Dallinger and P.S. Rainbow (Eds.), *Ecotoxicology of Metals in Invertebrates* (pp. 133-148). Boca Raton: SETAC Special Publication Series.

Williamson, P.D. (1980). Variables affecting body burdens of lead, zinc and cadmium in a road side population of the snail *Cepaea hortensis* Müller. Oecologia (Ber.), *44,* 213-220.

Winter, J.E. (1978). A review on the knowledge of suspension-feeding in lamellibranchiate bivalves with special reference to artificial aquaculture systems. *Aquaculture, 13,* 1-33.

Yap, C.K., Ismail, A., Edward, F.B., Tan, S.G. and Siraj, S.S. (2006). Use of different soft tissues of *Perna viridis* as biomonitors of bioavailability and contamination by heavy metals (Cd, Cu, Fe, Pb, Ni and Zn) in semi-enclosed intertidal water, the Johore Straits. *Toxicol. Environ. Chem., 88,* 683 - 695.

Yap, C.K., Ismail, A. and Tan, S.G. (2003). Background concentrations of Cd, Cu, Pb and Zn in the green-lipped mussel *Perna viridis* (Linnaeus) from Peninsular Malaysia. *Mar. Poll. Bull., 46,* 1043-1048.

ISSN: 0128-7680
Pertanika J. Sci. & Technol. **17 (1)**: 69 – 85 (2009)

Software Development for Optimal Design of Different Precast Slabs

J. Noorzaei*, J.N. Wong, W.A. Thanoon and M.S. Jaafar
Department of Civil Engineering, Faculty of Engineering, Universiti Putra Malaysia, 43400 UPM, Serdang, Selangor, Malaysia
**E-mail: jamal@eng.upm.edu.my*

ABSTRACT

Precast concrete technology forms an important part in the drive towards a full implementation of the Industrialized Building System (IBS). The IBS requires building components and their dimensions to be standardized, and preferably cast off site. Slabs are major structural elements in buildings, other than beams and columns. Standardized and optimized slabs can significantly enhance the building industries in achieving the full implementation of the IBS. Nevertheless, this requires computer techniques to achieve standardized and optimized slabs which can satisfy all building design requirements, including the standards of architectural and structural design standards. This study proposed a computer technique which analysed and designed five different types of slabs which will satisfy all the requirements in design. The most commonly used slabs included in this study were the solid one way, solid two way, ribbed, voided and composite slabs. The computer techniques enable the design of the most optimized sections for any of the slab types under any loading and span conditions. The computer technique also provides details for the reinforcements required for the slabs.

Keywords: Precast slabs, Industrialized Building System, optimized sections, building design

INTRODUCTION

For the past half century, the precast concrete components have been marketed on the basis of savings in materials and improved quality of products and workmanship, as well as the ease of construction. According to Yee (2001), the precast concrete technology has taken an important perspective in terms of its impact on both social and environment.

Architects and engineers have long hailed precast concrete for its high quality architectural and structural products. Precast concrete products can be fabricated in a large variety of shapes and sizes, while the use of prestressing provides for much longer spans than can be achieved using conventional insitu methods of construction (Yee, 2001).

Mixed construction techniques are now being used in more than 50 per cent of new multi-storey buildings in the western world, whereby the increased use of precast concrete over the past 10-15 years is due to the move towards greater offsite prefabrication of structural elements (Elliot, 2002). Some of the limitations found in precast concrete have inevitably led to it being used with other materials in a cost effective manner. Structurally, different components may either work together or independently, but they can provide many advantages over the use of a single material when used together.

Similar to the design of other structural elements, the aim of the design of a slab system is the attainment of acceptable probabilities which will not become unfit for their specified use during some defined life. Therefore, slabs should be designed to sustain, with an

Received: 10 September 2008
Accepted: 29 October 2008
*Corresponding Author

appropriate degree of safety, all loads and deformations liable to occur during construction and in service, so as to adequately perform their intended functions, and to possess an appropriate factor of safety against failure. Significant improvements in the efficiency of the overall building system can be gained by improving precast structural floor system to reduce weight, depth, and cost to better accommodate service systems (Pessiki *et al.*, 1995).

Comprehensive design formulations and procedures, for solid (one-way and two-way), ribbed, hollow core and composite slabs, are available in reinforced concrete books and British Standards (BS8110: Part 1: 1997, Allen, 1988; Kong and Evans, 1987; MacGinley and Choo, 1990; Mosley and Bungey, 1993). In order to achieve effective design of different precast slab systems and optimize the sections which consider all design requirements, a computer technique is therefore required. The objective of this study was to propose a comprehensive design using a computer technique for the most commonly used slabs in building construction, i.e. solid one-way, solid two-way, ribbed, voided and composite slabs. A computer program written in FORTRAN was developed for the purpose of achieving an optimum slab design which will fulfil all the BS8110 design requirements.

DEVELOPMENT OF COMPUTER CODE AND COMPUTATION ASPECT

A general computer code has been written in the FORTRAN language. The computer coding is done in two stages. In Stage I, individual type of slab system is programmed and validated with manual computation. Meanwhile in Stage II, all the individual programs are combined in the form of sub-routines and works under a master program. Each type of the slab systems is identified by a predefined code as:

i) NTYPE 1: Solid one-way
ii) NTYPE 2: Solid two-way
iii) NTYPE 3: Ribbed
iv) NTYPE 4: Voided (hollow core)
v) NTYPE 5: Composite (half slab)

Therefore, by merely inputting the respective code, the complete analysis, design and drafting of each slab type is carried out automatically. The design of every floor slab is started using loading and trial dimension as input. The depth of the slab is fixed based on satisfying BS8110 requirement for bending moment, shear force and deflections. *Fig. 1* shows the computational flowchart implemented for the solid one-way slab, solid two-way slab, ribbed slab, hollow core slab and composite slab, respectively. The analysis and design of the floor slabs were implemented in such a way that nine independent blocks were formed to obtain the load, moment, reinforcement, shear check, deflection check and result. All these blocks were controlled by the sub-routine MAIN. Other than these nine independent blocks, there were also five secondary sub-routines, identified as BARSIZE, INCREASEHEIGHT, DRAWLINES, DRAWSHAPES and TEXT. The function of each subroutine is explained in the Appendix.

APPLICATION AND VALIDATION OF THE COMPUTER CODE

Numerical Example 1: One-way Solid Slab

The chosen cross-section and the material properties of the slab are shown in *Fig.2.* The slab was designed to carry a selected live load of 1.5 kN/m^2, plus floor finishes and finishing load of 1.5 kN/m^2.

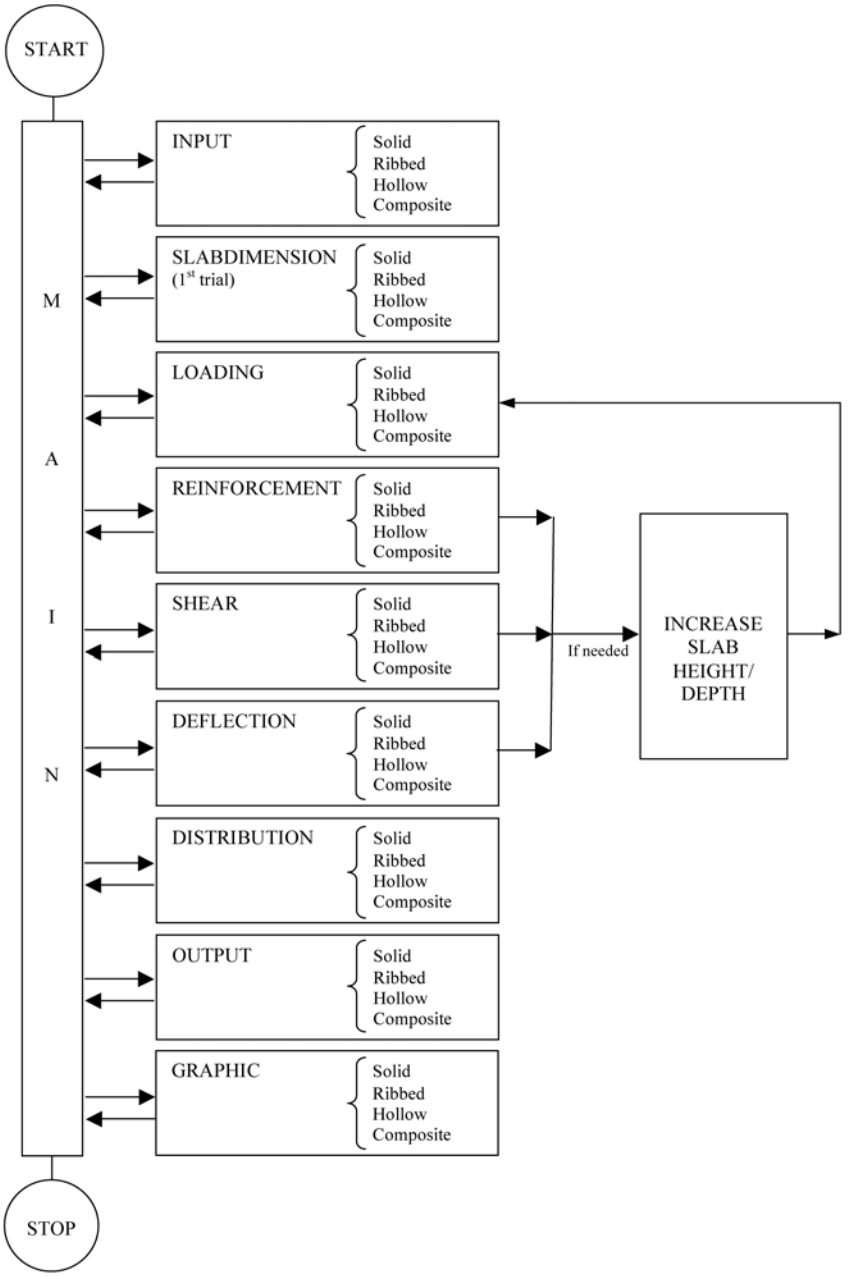

Fig. 1: Generalized flowchart for the design of different flooring

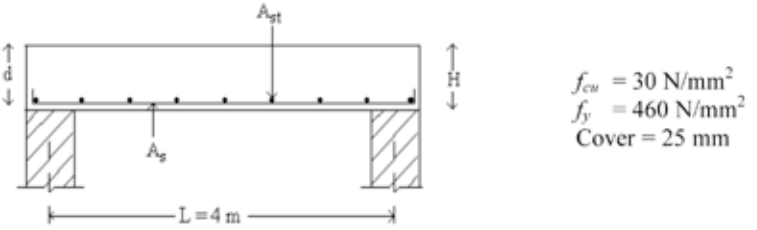

Fig. 2: Solid one-way slab for example 1

The output cross-section details evaluated through the program are shown in Table 1. Initially, the trial depth was assumed to be 80 mm. This depth represented the minimum depth which fulfilled the moment requirement (Eqn. 1, see Appendix). The program fixed the optimal depth after 19 iterations, i.e. 170 mm. This slab was designed manually and the comparisons of the various items are illustrated in Table 2. It is evident from this table that there is an excellent agreement between the results.

After deciding the final cross-section details of the floor slab, the graphic sub-routines were called and the structural members were drawn and viewed on the computer terminal. Since the FORTRAN 90 Power Station is equipped with graphic libraries, the various cross-sections can be drawn using these libraries; this is useful to the structural engineer. *Fig. 3* shows the graphical representation of the cross-section for numerical example 1.

TABLE 1
Cross-section details

Item	Value
Initial Height (mm)	80
No. of Iteration	19
Slab depth, *H* (mm)	170

Numerical Example 2: Two-way Solid Slab

A selected slab measuring 4.5 m x 7.0 m is simply supported at the edges with no provision to resist torsion at the corners or to hold the corners down (see *Fig. 4*). The characteristic dead load including finishes and the partition for this example is 1.5 kN/m^2, and the characteristic live load is 1.5 kN/m^2.

The cross-section details, evaluated through the program, are shown in Table 3. Using this cross-section, the analysis and design proceed are as shown in Table 4. Initially, the trial depth was assumed to be 85 mm. This depth represented the minimum depth which fulfilled the moment requirement. The program fixed the optimal depth after 21 iterations, i.e. 185 mm. *Fig. 5* shows the graphical representation of the cross-section for numerical example 2.

TABLE 2
Comparison of analysis and design for one-way solid slab

Item	Manual	Computer Output	Item	Manual	Computer Output
Loading & Moment			**Shear Check**		
Ultimate load, w (kN/m²)	10.212	10.212	Shear Force, V (kN)	20.424	20.424
Ultimate moment, M_u (kNm)	20.424	20.424	Shear Stress, v (N/mm²)	0.145	0.145
$A_{S(req)}$ (mm²/m)	348.913	348.913	$v < 0.8\sqrt{f_{cu}}$ or 5N/mm²	OK	OK
$A_{S(pro)}$ (mm²/m)	402.000	402.000	Shear Capacity,		
v_c (N/mm²)	0.574	0.574			
Use	Y8 @125 c/c	Y8 @ 125 c/c	$v < v_c$	OK	OK
Transverse Reinforcement			**Deflection Check**		
$A_{St(req)}$ (mm²)	221	221	Modification Factor, MF	1.462	1.462
$A_{St\ (pro)}$ (mm²)	226	226	L/d (allowable)	29.240	29.232
Use	Y6 @125 c/c	Y6 @ 125 c/c	L/d (actual)	28.369	28.369
			Actual < Allowable	OK	OK

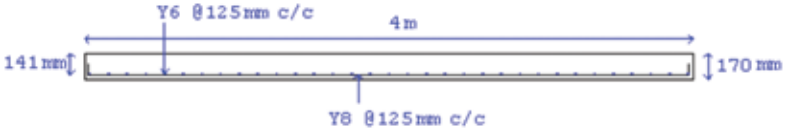

Fig. 3: Graphical representation of the solid one-way slab

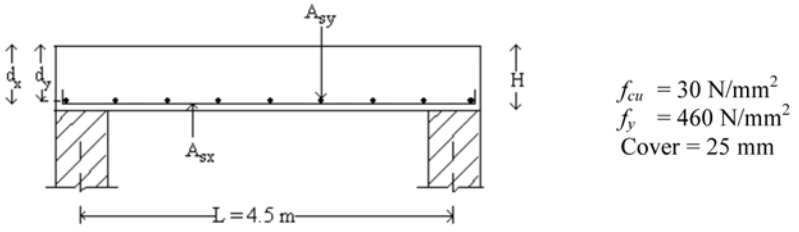

Fig. 4: Solid two-way slab for example 2

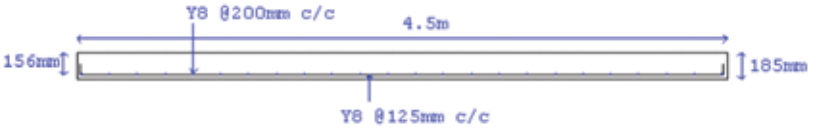

Fig. 5: Graphical representation of solid two-way slab

TABLE 3
Cross-section details

Item	Value
Initial Height (mm)	85
No. of Iteration	21
Slab depth, H (mm)	185

TABLE 4
Comparison of analysis and design for two-way solid slab

Item	Manual	Computer Output	Item	Manual	Computer Output
Loading & Moment			**Shear Check**		
Ultimate load, w (kN/m²)	10.716	10.716	Shear Force, V (kN)	24.111	24.111
Ultimate moment, M_{sx} (kNm)	23.219	23.168	Shear Stress, v (N/mm²)	0.163	0.163
Ultimate moment, M_{sy} (kNm)	9.548	9.575	$v < 0.8$ or 5N/mm²	OK	OK
Reinforcement-Short Span			Shear Capacity, v_c (N/mm²)	0.477	0.477
$A_{SX(req)}$ (mm²/m)	358.520	357.734	$v < v_c$	OK	OK
$A_{SX(pro)}$ (mm²/m)	402.000	402.000	**Deflection Check**		
Use	Y8 @125 c/c	Y8 @125 c/c	Basic *Span/Depth*	20.000	20.000
Reinforcement-Long Span			Modification Factor, *MF*	1.465	1.468
$A_{SY(req)}$ (mm²/m)	240.500	240.500	L/d (allowable)	29.300	29.368
$A_{SY(pro)}$ (mm²/m)	251.000	251.000	L/d (actual)	28.846	28.846
Use (No. & bar diameter)	Y8 @200 c/c	Y8 @ 200 c/c	Actual < Allowable	OK	OK

Numerical Example 3: Ribbed Slab

A sample precast floor slab, consists of several units of ribbed slab, is simply supported at the ends, as shown in *Fig. 6*. The effective span is 5.0 m, while the chosen characteristic dead

load includes finishes and partition is 1.5 kN/m² and the characteristic live load is 2.0 kN/m². The distance of the centre to the centre of the ribs is 300 mm.

The final cross-sections evaluated through the program are shown in Table 5. Using this cross-section, the analysis and design was proceeded, as shown in Table 6. Initially, the trial depth was assumed to be 110 mm. This depth represented the minimum depth which satisfied the moment requirement. The program fixed the optimal depth, after 21 iterations, which was 210 mm. *Fig. 7* shows the graphical representation of the cross-section for numerical example 3.

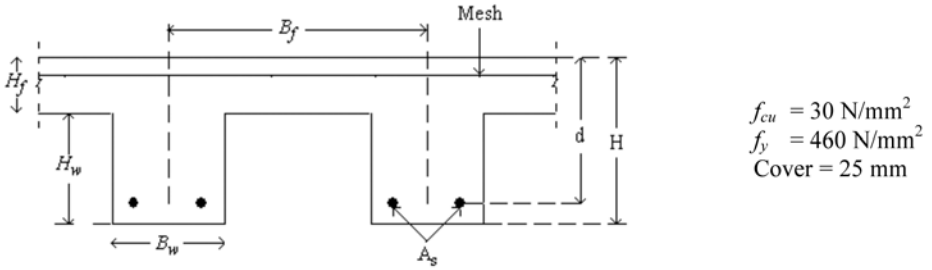

Fig. 6: Cross-section of the ribbed slab

TABLE 5
Cross section details

Item	Computation
Initial Height (mm)	110
No. of Iteration	21
Sla depth b, H (mm)	210
Flange width, B_f (mm)	300
Topping, H_f (mm)	60
Web width, B_w (mm)	125
Web height, H_w (mm)	150

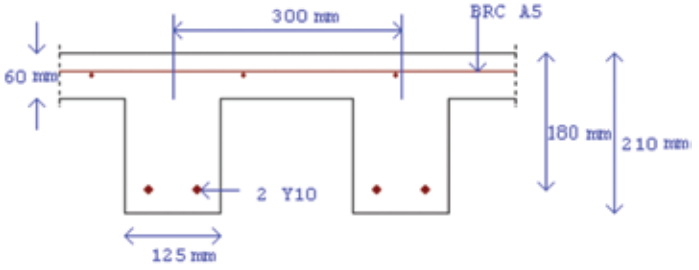

Fig. 7: Graphical representation of the ribbed slab

TABLE 6
The comparison of the analysis and design for the ribbed slab

Item	Manual	Computer Output	Item	Manual	Computer Output
Loading & Moment			Shear Check		
Ultimate load, w (kN/m²)	2.825	2.825	Shear Force, V (kN)	7.063	7.062
Ultimate moment, M_u (kNm)	8.828	8.828	Shear Stress, v (N/mm²)	0.314	0.314
Moment resistance, M_{RC} (kNm)	36.450	36.450	$v < 0.8\sqrt{f_{cu}}$ or 5N/mm²	OK	OK
Reinforcement			Shear Capacity, v_c (N/mm²)	0.727	0.727
$A_{S(req)}$ (mm²)	118.137	118.130	$v < v_c$	OK	OK
$A_{S(pro)}$ (mm²)	157.000	157.000	**Deflection Check**		
Use (No. & bar diameter)	2Y10	2Y10	Basic Span/ Depth	16.667	16.667
Topping Reinforcement			Modification Factor, MF	1.685	1.685
$A_{St(req)}$ (mm²)	72	72	$Ld/$ (allowable)	28.084	28.082
Use (Type of mesh)	A98	A98	L/d (actual)	27.778	27.778
$A_{St\ (pro)}$ (mm²)	98	98	Actual < Allowable	OK	OK

Numerical Example 4: Hollow Core Slab

A sample precast floor slab, consisting of several units of hollow core slab, is simply supported at the ends, as shown in *Fig. 8*. The characteristic dead load, including finishes and partition, is 1.0 kN/m² and the characteristic live load is 1.5 kN/m². The distance of the centre to the centre of the core is 300 mm.

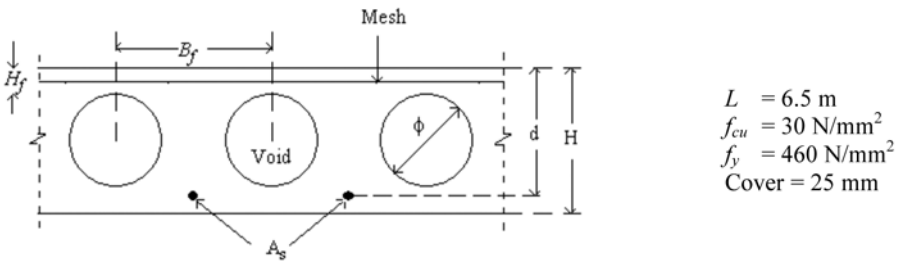

Fig.8: Cross section of hollow core slab

The cross-section details evaluated through the program are shown in Table 7. Using this cross-section, the analysis and design proceed, are as shown in Table 8. Initially, the trial depth was assumed to be 130mm. This depth represented the minimum depth which satisfied the moment requirement. The program fixed the optimal depth after 29 iterations, i.e. 270 mm. *Fig. 9* shows the graphical representation of the cross-section for numerical example 4.

TABLE 7
Cross-section details

Item	Value
Initial depth (mm)	130
No. of Iteration	29
Slab depth, H (mm)	270
Core c/c, B_f (mm)	300
Topping, H_f (mm)	50
Core Diameter., ϕ (mm)	170

TABLE 8
Comparison of analysis and design for hollow core slab

Item	Manual	Computer Output	Item	Manual	Computer Output
Loading & Moment			**Shear Check**		
Ultimate load, w (kN/m²)	3.099	3.099	Shear Force, V (kN)	10.072	10.072
Ultimate moment, M_u (kNm)	16.367	16.366	Shear Stress, v (N/mm²)	0.216	0.216
Moment resistance, M_{RC} (kNm)	42.930	42.930	$v < 0.8\sqrt{f_{cu}}$ or 5N/mm²	OK	OK
Reinforcement			Shear Capacity, v_c (N/mm²)	0.578	0.578
$A_{S(req)}$ (mm²)	166.347	166.340	$V < v_c$	OK	OK
$A_{S(prov)}$ (mm²)	201.000	201.000	**Deflection Check**		
Use (No. & bar diameter)	1Y16	1Y16	Basic Span/ Depth	18.035	18.035
Topping Reinforcement			Modification Factor, *MF*	1.544	1.544
$A_{St(req)}$ (mm²)	60.000	60.000	$L/$ (allowable)	27.846	27.847
Use (Type of mesh)	BRC A4	BRC A4	L/d (actual)	27.426	27.426
$A_{St\ (prov)}$ (mm²)	63.000	63.000	Actual < Allowable	OK	OK

As stated, the initial trial depth of 130 mm was used in the analysis and design of the voided slab following BS8110 Code. In deflection check, the slab depth does not satisfy the requirement for allowable span/depth ratio (the span/depth ratio is greater than allowable span/depth). Thus, the slab depth was increased to 135 mm and the calculations of loading, moment, reinforcement, shear check and deflection check were performed. The procedure was repeated until all the BS8110 requirements were satisfied. The optimal slab height was obtained after 29 iterations, and the final slab depth was found to be 270 mm. The comparison of analysis and design, obtained in the present study with the ones which were manually calculated, is presented in Table 8. This table clearly shows there is a good agreement between the results obtained.

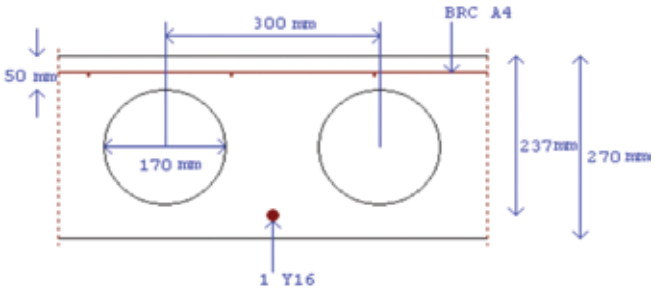

Fig. 9: Graphical representation of the computer output for hollow core slab example

Furthermore, the effects of the imposed load on the optimal void sizes and slab depth have been studied using the developed computer code to minimise the self weight, and hence, the overall cost. The correlations, between the void size and the self weight of the slab for 1 m width, are shown in *Figs. 10* to *12* for different imposed loads and floor spans. In general, when the void size increased, the self weight of the slab also decreased. All curves show similar correlations.

Table 9 presents the economical and practical design cases for the voided hollow precast slab. This includes the different span lengths of 5 m, 5.5 m and 6 m for three different imposed loads of 1.5, 2.0 and 2.5 kN/m^2.

TABLE 9
Optimal design

Span (m)	Imposed Load (kN/m^2)	depth (mm)	Void Diameter (mm)
5.0	1.5	210	110
	2.0	215	115
	2.5	225	125
5.5	1.5	235	135
	2.0	245	145
	2.5	250	150
6.0	1.5	265	160
	2.0	270	170
	2.5	275	170

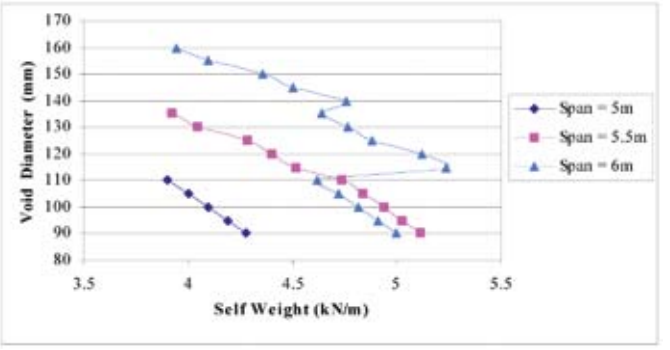

Fig. 10: Variation of self weight using IL = 1.5 kN/m² and DL = 1.5 kN/m²

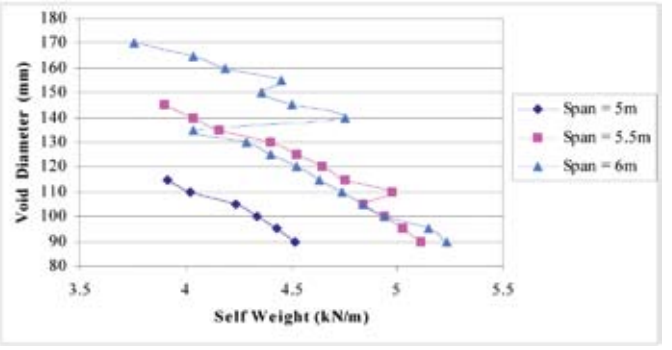

Fig. 11: Variation of self weight using IL = 2.0 kN/m² and DL = 1.5 kN/m²

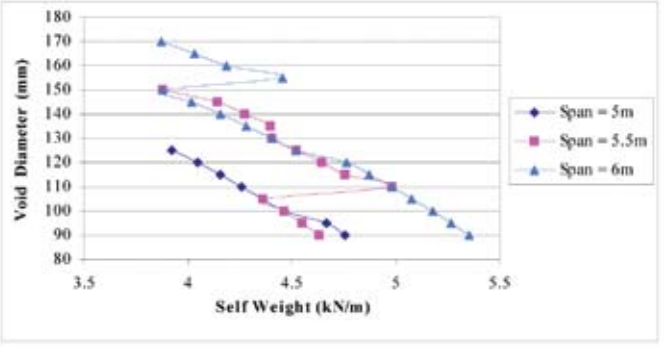

Fig. 12: Variation of self weight using IL = 2.5 kN/m² and DL = 1.5 kN/m²

Numerical Example 5: Half (Composite) Slab

The composite floor slab *(Fig. 13)* was simply supported over an effective span of 3.5 m. The characteristic dead load, including the finishes and partition, is 1.5 kN/m², while the characteristic live load is 2.5 kN/m². The allowance for the construction load = 0.75 kN/m².

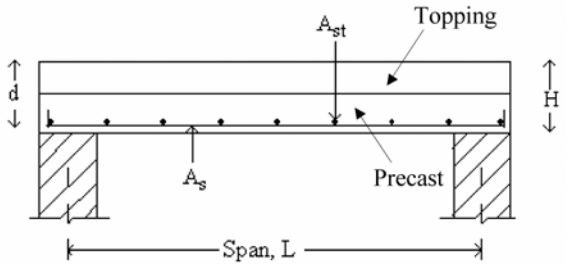

Fig. 13: The cross-section of the composite slab

The cross-section details, evaluated through the program, are shown in Table 10. Using this cross-section, the analysis and design proceed, are as shown in Table 11. Initially, the trial depth was assumed to be 75 mm. This depth represented the minimum depth which satisfied the moment requirement. The program fixed the optimal depth after 16 iterations, i.e. 150 mm. *Fig. 14* shows the graphical representation of the cross-section for numerical example 5.

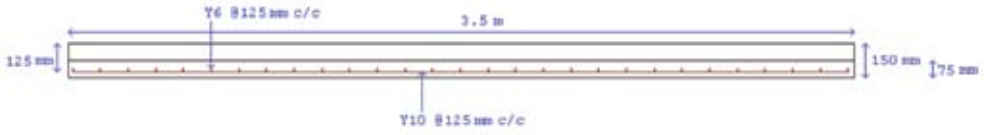

Fig. 14: Graphical representation of the composite slab

TABLE 10
Cross-section details

Item	Value
Initial depth (mm)	75
No. of Iteration	16
Slab depth, *H* (mm)	150
Precast depth (mm)	75
Insitu topping (mm)	75

TABLE 11
The comparison of analysis and design for the composite slab

Item		Manual	Computer Output	Item		Manual	Computer Output
Loading & Moment				Shear Check			
Precast	Ultimate load, w (kN/m²)	6.240	6.240	Precast	Shear Force, V (kN)	10.920	10.920
	Ultimate moment, M_u (kNm)	9.555	9.555		Shear Stress, v (N/mm²)	0.218	0.218
Composite	Ultimate load, w (kN/m²)	11.140	11.140		$v < 0.8\sqrt{f_{cu}}$ or 5N/mm²	OK	OK
	Ultimate moment, M_u (kNm)	17.058	17.058		Shear Capacity, v_c (N/mm²)	1.219	1.219
Reinforcement					$v < v_c$	OK	OK
Precast	$A_{S(req)}$ (mm²)	520.607	527.306	Composite	Shear Force, V (kN)	19.495	19.495
					Shear Stress, v (N/mm²)	0.156	0.156
Composite	$A_{S(req)}$ (mm²)	329.245	329.106		$v < 0.8\sqrt{f_{cu}}$ or 5N/mm²	OK	OK
					Shear Capacity, v_c (N/mm²)	0.672	0.672
$A_{S(req)}$ (mm²) (Choose greater value)		520.607	527.306		$v < v_c$	OK	OK
$A_{S(prov)}$ (mm²)		628.00	628.000	**Deflection Check**			
Use		Y10 @ 125 c/c	Y10 @ 125 c/c		a	9.814	9.814
Topping Reinforcement				Precast	Span/250	14.000	14.000
$A_{St(req)}$ (mm²)		195.000	195.000		$a <$ *Span/250*	OK	OK

CONCLUSIONS

The analysis, design and graphical features of the different types of precast industrialized slab systems have been presented in the form of a generalized computer code. The programme is written in FORTRAN 90 Power Station environment and can run on any small PC. The computer code is a user-friendly programme, with several options, covering different types of slab systems. The program always starts with the minimum dimension of the slabs (as defined by the code) and evaluates the most optimum sections, based on the least weight section which is represented by the sections with the smallest depth. After deciding on the details of the final cross-section of the floor slab, this software equipped with graphic facilities can draw the structural members to be viewed on the computer terminal. The illustrated examples show that the results obtained using the developed computer code and from the manual calculation are in excellent agreement. Furthermore, the application of the programme, on the voided slab, indicates that the programme can select the optimal dimension of the slab and voids for minimum weight and, thus minimum cost of the slabs.

REFERENCES

Allen A.H. (1988). *Reinforced Concrete Design To BS8110 Simply Explained.* E. & F.N. Spon.

BS 8110 Part 1. (1997). Structural use of concrete. British Standard Institution, London.

Elliot K.S. (1996). *Multi-Storey Precast Concrete Frame Structures.* Blackwell Science Ltd.

Elliot K.S. (2002). *Precast Concrete Structures.* Butterworth-Heinemann.

Fortran Power Station Programmer's Guide.

Kong, F.K. and Evans, R.H. (1987). *Reinforced and Prestressed Concrete* (3rd edition). Chapman & Hall.

MacGinley, T.J. and Choo, B.S. (1990). *Reinforced Concrete Design Theory and Examples* (2nd edition). E. & F.N. Spon.

Mosley, W.H. and. Bungey, J.H. (1993). *Reinforced Concrete Design* (4th edition). MacMillan.

Pessiki, S., Prior, R., Sause, R. and Slaughter, S. (1995). Review of existing concrete gravity load framing systems. *PCI Journal, 40*(2), 52-67.

Yee A.A. (2001). Social and environmental benefits of precast concrete technology. *PCI Journal, 46*(3), 14-19.

Yee A.A. (2001). Structural and economic benefits of precast/prestressed concrete construction. *PCI Journal, 46*(4), 34-42.

Appendix: Function of each sub-routine

Subroutine	Function
MAIN	NTYPE of slab is selected corresponding to 1. Solid slab 2. Ribbed slab 3. Hollow slab 4. Composite slab If solid slab is selected, JTYPE of slab is selected according to 1. One-way slab 2. Two-way slab
INPUT	This read the geometric data, material properties and loads. Input data for: 1. Solid slab: L, L_y (for two way slab only), cover, f_{cu}, f_y, DL, LL and % redistribution. 2. Ribbed: L, B_{flange}, cover, f_{cu}, f_y, DL, LL and % redistribution. 3. Hollow: L, centre of core distance, cover, f_{cu}, f_y, DL, LL and % redistribution. 4. Composite: L, cover, f_{cu} (precast & topping), f_y, DL, LL, construction load and % redistribution.
SLABDIMENSION	This sub-routine creates the trial dimension of the slab (including effective depth, height, web width, flange height, etc., according to the types of slabs) which satisfy the moment requirement. The trial cross-section is of a minimum value, which will be changed whenever the limiting condition is not being satisfied. $minimum\ effective\ depth = \sqrt{\frac{M}{0.156 f_{cu} b}}$ (1) $Trial\ height = minimum\ effective\ depth + cover + \phi_{bar}/2$ (2)
LOADING	The calculation of the self weight, design ultimate load, design ultimate moment and moment of resistance (for the ribbed and hollow slabs only) is carried out in this sub-routine. Ultimate load, $\omega = 1.4G_k + 1.6Q_k$ (3) Ultimate moment; (a) One-way slab, ribbed, hollow and composite: $M \frac{\omega l^2}{8}$ (4) (b) Two-way slab $m_{sx} = \alpha_{sx} n l_x^2$ in direction of span l_x (5)

$$m_{sy} = \alpha_{sy} n l_x^2 \text{ in direction of span } l_y \quad (6)$$

Moment of resistance, $M_{RC} = 0.45 f_{cu} b_f h_f \left(d - \frac{h_f}{2} \right)$ (7)

REINFORCEMENT

This sub-routine calculates the area of the tensile steel rquired, As_{req}.

$$As_{req} = \frac{M}{0.95 f_y z} \quad (8)$$

After obtaining As_{req}, this sub-routine calls upon the sub-routine BARSIZE to select the suitable bar size and bar spacing.

SHEAR

Checking of design shear stress, v and design shear capacity, v_c is done in this subroutine.

$$v = \frac{V}{bd} \quad (9)$$

$$v_c = 0.79\{100A_s/(b_v d)\}^{1/3} (400/d)^{1/4} (f_{cu}/25)^{1/3}/\gamma_m \quad (10)$$

DEFLECTION

To carry the task on deflection checking. Check *actual span/depth* should not be greater than *allowable span/depth* so that the deflection of a slab will not be excessive.

$$\textit{Allowable span / effective depth} = \textit{basic span/effective depth ratio} \times \textit{M.F.} \quad (11)$$

$$\text{where } \textit{M.F.} = 0.55 + \frac{(477 f_s)}{120\left(0.9 + \frac{M}{bd^2}\right)} \quad (12)$$

$$\textit{Actual span / effective depth} = \frac{l}{d} \quad (13)$$

DISTRIBUTION

This sub-routine calculates the distribution, which is also known as the transverse reinforcement required, Ast_{req} for the solid and composite slabs. Meanwhile, for the ribbed and hollow slabs, this sub-routine calculates the topping reinforcement required. Suitable bar size and spacing will be selected.

(a) For solid and composite slabs:

$Ast_{req} = 0.13\% \ bh$ for high-yield steel (14)

$Ast_{req} = 0.24\% \ bh$ for mild steel (15)

(b) For ribbed and hollow slabs:

A_{mesh} =0.12% of the topping cross sectional area (16)

	After obtaining Ast_{req}, this sub-routine calls upon subroutine BARSIZE to select the suitable bar size and bar spacing. In the case of the ribbed and hollow slabs, a suitable mesh is selected within the DISTRIBUTION sub-routine.
OUTPUT	All the results and values of the calculation will be presented in this sub-routine.
GRAPHICMODE	To draw the cross-section of the optimal slab dimension. This sub-routine will call upon the sub-routine DRAWLINES (), DRAWSHAPES (), and TEXT ().
BARSIZE	This sub-routine selects the bar diameter, spacing and the number of bars which satisfy the required reinforcement. The area of reinforcement provided will be calculated.
INCREASEHEIGHT	This subroutine is called whenever the limiting condition in the sub-routine REINFORCEMENT, SHEAR and DEFLECTION is not being satisfied. Examples of the limiting conditions are: *i)* $K > K'$ (subroutine REINFORCEMENT) *ii)* $v >$ lesser of $0.8\sqrt{f_{cu}}$ or $5\text{N/mm}^2\}$ (Subroutine SHEAR) *iii)* $v > v_c$ *iv)* Actual l/d > Allowable l/d (subroutine DEFLECTION) The slab height will be increased by 5mm each time this sub-routine is being called. Whenever the slab dimension is changed, the recalculation of all the parameters has to be carried out starting from the sub-routine LOADING and so on.
DRAWLINES	To draw straight lines for the slab cross-section, reinforcement and dimension lines.
DRAWSHAPES	To draw rectangular and circle shapes for the appropriate slabs.
TEXT	To write the text for the slab dimension and the type of reinforcements.

ISSN: 0128-7680
Pertanika J. Sci. & Technol. **17 (1)**: 87 – 93 (2009)

Response of *Streptococcus zooepidemicus* to Oxidative Stress in Hyaluronic Acid Fermentation

Mashitah, M.D.[1*], Masitah, H.[2] and Ramachandran, K.B.[3]
[1]School of Chemical Engineering, Engineering Campus, Universiti Sains Malaysia, Seri Ampangan, 14300 Nibong Tebal, Penang, Malaysia
[2]Department of Chemical Engineering, Faculty of Engineering, University of Malaya, 50603 Kuala Lumpur, Malaysia
[3]Department of Biotechnology, Indian Institute of Technology Madras, Chennai 600 036, India
[*]E-mail: chmashitah@eng.usm.my

ABSTRACT

Streptococcus zooepidemicus (*SZ*) is an aerotolerant bacteria and its ability to survive under reactive oxidant raises the question of the existence of a defense system against oxidative stress. As a characteristic of lactic acid bacteria, *Streptococcus* lacks an ordinary anti-oxidative stress enzyme, catalases and an electron transport chain. Whether this bacterium resists oxidative stress prior to an exposure to a higher level of an oxidizing agent H_2O_2 in hyaluronic acid fermentation is not known. This paper describes that *Streptococcus* cells, once treated with lower concentrations of H_2O_2 (i.e. 0.25, 0.50 and 1.0 mM) at least, were prepared for a subsequent higher concentrations of H_2O_2 such as 20.5 and 100 mM. At low concentrations (i.e. 0.25, 0.50 and 1.0 mM), H_2O_2 was found to act as a stimulant for HA synthesis, but it became toxic if presented at a very high level (100 mM H_2O_2). The highest HA yield to glucose consumed ($Y_{HAtotal/glu}$) was 0.017 gg^{-1} for the cells pre-treated with 0 mM of H_2O_2, and then exposed to 20.5 mM H_2O_2. Thus, this implied that this bacteria might possess a defense mechanism against oxidative stress and that this system was inducible.

Keywords: Hyaluronic acid, hydrogen peroxide, oxidative stress, protective response, *Streptococcus zooepidemicus*

ABBREVIATIONS

DNA	deoxy-ribonucleic acid
HA	hyaluronic acid
H_2O_2	hydrogen peroxide
OD	optical density
ROS	reactive oxygen species
SBA	sheep blood agar
*s*HA	soluble hyaluronic acid
*t*HA	total hyaluronic acid

Received: 29 May 2007
Accepted: 22 August 2008
[*]Corresponding Author

$Y_{HAtotal/glu}$ hyaluronic acid yield to glucose consumed

$Y_{H2O2/glu}$ hydrogen peroxide yield to glucose consumed

$Y_{X/glu}$ biomass yield to glucose consumed

INTRODUCTION

The ability to persist and thrive under oxidative stress is necessary for the growth of bacteria, under aerobic or reactive oxidant challenges. In bacteria, the association of enzymatic and non-enzymatic systems, with reactive oxygen species (ROS), provides a mechanism for a cellular response against deleterious effects of the molecules. Of the various reactive molecules (O_2^-, H_2O_2, • OH), hydrogen peroxide (H_2O_2) is particularly derived from non-radical oxygen. Though H_2O_2 is chemically less reactive, it is still a threat to the structure and function of cells (Halliwell and Gutteridge, 1989). Likewise, it can readily diffuse across the cellular membranes and oxidatively damage a number of vital cellular components, including membrane lipids, enzymes and DNA (Miller and Britigan, 1997; Porter, 1984).

An adaptation to hyperoxidative environment provides organisms with a wider selection of ecological niches for survival. Like many other lactic acid bacteria, most *Streptococcus* species have manganese form of superoxide dismutase (Mn-SOD) for detoxification of ROS (Jakubovics, Smith and Jenkinson, 2002). However, this might not be the only mechanism in bacteria. The binding of the metal ions onto superoxide dismutase (SOD) or catalases in forms, which was unable to accelerate radical (O_2-, H_2O_2, • OH) or non-radical reactions (Halliwell and Gutteridge, 1999), was thought to form the basis for an alternative chemically detoxification of H_2O_2. These involved reactions are described as (Bannister, Bannister and Rotilio, 1987): $2O_{2-} + 2H^+ \rightarrow H_2O_2 + O_2$ (Superoxide dismutase), $2(H_2O_2) \rightarrow 2H_2O_2 + O_2$ (Catalase) and $H_2O_2 + RH_2 \rightarrow 2H_2O + R$ (Non-specific peroxidase). Such a system might be necessary in reducing the levels of H_2O_2 and damaging their production. However, as is the characteristic of lactic acid bacteria, *Streptococcus* species does not synthesize heme and lacks catalase (Condon, 1987). The specific mechanisms by which they adapt to peroxide stress are still unknown.

Traditionally, hyaluronic acid (HA), which is an industrially important biopolymer, was extracted from rooster comb. However, an increasing trend to streptococcal fermentations is rapidly expending in view of its emerging applications in the medical and cosmetic industries (Lerner, 1996). Remarkly, *Streptococcus zooepidemicus* (*SZ*) were also greatly used as the risk of cross species viral infection which can be avoided (Huang *et al.*, 2006). Nevertheless, there were some drawbacks in relation to *Streptococcus* HA production routes. According to Goh (1998), under aerated conditions, HA production was found to be reduced as a result of the growth inhibition by hydrogen peroxide (H_2O_2), since this compound is inherently toxic and reactive, as well as *Streptococcus zooepidemicus* being catalase negative (Hardie and Whiley, 1995). Mashitah *et al.* (2005) reported that H_2O_2, produced by *Streptococcus zooepidemicus* cells, did not affect the growth of cell, but influenced the production of HA. Accordingly, the production of H_2O_2 took place during the growth phase, and this was only started after the growth had reached its late exponential phase, that is, when H_2O_2 in the culture media had depleted. Whether such cells are able to resist oxidative stress prior to exposure to higher level of H_2O_2, this has not been clearly defined. In this study, the researchers examined the response of *Streptococcus zooepidemicus* cells to oxidative stress, prior and during the HA fermentation. For this purpose, H_2O_2 was used as an oxidizing agent.

MATERIALS AND METHODS

Strain

Streptococcus equi sub-species *zooepidemicus* ATCC 39920 was obtained from the American Type Culture Collection (Rockville, MD., USA). It was maintained on sheep blood agar (SBA) slants and kept at 4°C.

Culture medium

The composition of the medium used in all the experiments comprised of (gl^{-1}) glucose 30, yeast extract 10, KH_2PO_4 0.5, $Na_2HPO_4.12H_2O$ 1.5, and $MgSO_4.7H_2O$ 0.5, respectively. The pH of the medium was adjusted to 7.0 with 5 M NaOH prior to autoclaving it at 121°C for 20 min. This glucose solution was autoclaved separately and mixed aseptically with the other components on cooling.

Cell suspension

Cell suspension of the shake flask culture was prepared by inoculating aseptically a stock culture of *S. zooepidemicus* onto Sheep Blood Agar (SBA)-plates and incubated overnight at 37°C. The formed colonies were punched by a sterile cork borer to obtain ten round disks of 0.85 cm in diameter. The disks were then put in a sampling bottle containing 50 ml of sterile distilled water. The sampling bottle was vortexed for 3 min so that the cells could evenly be distributed in the liquid.

The Effect of H_2O_2 Pre-treatment

20 SBA-disks full of *S. zooepidemicus* colonies, were pre-incubated with 100 ml of H_2O_2 solution (0, 0.25, 0.50 and 1.0 mM) in an orbital shaker at 37°C, 150 rpm for 30 min. These cells (15 ml) were then re-treated with H_2O_2 (15 ml) at the indicated concentrations (0, 20.5 and 100 mM) into a flask containing 120 ml culture media. The cells were left to be in contact with H_2O_2 in an orbital shaker at 37°C, 250 rpm for 24 h. After 24 h, the samples were analyzed for cell biomass, H_2O_2 and HA production, and glucose consumption. The cell biomass was taken as indices of the cells growth during the fermentation period.

Analytical Methods

The cell concentration was determined by measuring the optical density (*OD*) at 600 nm by Jenway Spectrophotometer and dry cell method. A correlation between the dry cell weight and OD_{600} was established. The concentration of H_2O_2 was analyzed using the spectrophotometric method as suggested by Emiliani and Riera (1968), with a slight modification. Hyaluronic acid (HA) and glucose concentrations were determined using the method described by Mashitah *et al.* (2002), and the hexokinase method (Sigma Diagnostic, Glucose HK, Procedure No 16-UV), respectively. The HA soluble (HA_{sol}) represented the hyaluronic acid (HA) which had been solubilised or released from *Streptococcus zooepidemicus* capsule during the fermentation. The HA total (HA_{total}) represented the combination of HA which was solubilised from the capsule during the fermentation and the HA which was released from the ruptured capsule into the solution, after being treated with sodium dodecyl sulphate and vortexed for 3 mins.

RESULTS AND DISCUSSION

The Effect of H_2O_2 Pre-treatment on Growth and Biomass Yield

The ability of *S. zooepidemicus* to respond to H_2O_2 pre-treatment, prior to HA fermentation, was investigated and the results are shown in *Fig. 1.* It was suggested that prior to treating the *Streptococcal* cells directly with a high level of H_2O_2 in the production medium, the cells were pre-treated in the absence or in the presence of 0.25, 0.50 and 1.0 mM H_2O_2 at 37°C, 150 rpm for 30 mins. This was done to allow the cells to acclimatize with the low levels of H_2O_2 before being introduced to a medium with higher H_2O_2 concentrations, since exposing to higher doses of H_2O_2 at the start of the culture would significantly decrease the growth and HA production (Mashitah *et al.,* 2005; Mashitah, 2006).

As shown in *Fig. 1(a)*, the *S. zooepidemicus* biomass was found to slightly increase when pre-treated with lower doses of H_2O_2. For a 0 mM added H_2O_2 with 1.0 mM H_2O_2 pre-treatment, it led to a slight increase in biomass as compared to the one without any pre-treatment. As for 20.5 mM added H_2O_2, with 0.5 mM H_2O_2 pre-treatment, a slightly lower level of cell biomass was detected. A similar trend was also observed for 0.25 mM pre-treated cells. However, it was also observed that with 100 mM H_2O_2 medium, not more than 1% of either 0, 0.25, 0.50 or 1.0 mM pre-treated population could survive as compared to the non-pretreated control. This showed that the treated cells when exposed to lower levels of H_2O_2, were better able to cope with subsequent toxic doses. This also meant that the growth was unaffected or even enhanced by pre-treating the cells to H_2O_2. The treatment with the highest H_2O_2 concentration (100 mM) led to a depletion of the biomass values. Thus, indicating that the organism might have been killed or destroyed at this level of added H_2O_2.

The Effect of H_2O_2 Pre-treatment on HA and Extracellular H_2O_2 Production and Glucose Consumption

As observed in *Fig. 1* (*a, b, c, d* and *e*), the biomass and HA production (HA total and HA soluble) were closely related. For the cells treated with 0 mM H_2O_2, lesser amounts of extracellular H_2O_2 and glucose consumption were detected (*Fig. 1(d)*). This could be due to the fact that during H_2O_2 exposure, *S. zooepidemicus* might consume H_2O_2 and glucose during growth. Therefore, when the maximum biomass was attained, H_2O_2 became limited, and hence the inhibition was reduced to increase the production of HA. This showed that some cells might have evolved highly efficient and often redundant repair mechanisms to remove lesion from DNA, proteins and membrane lipids. For example, all damages produced by free radical attack on DNA molecules were repaired by a universal DNA repair process known as the base-incision repair (Demple and Harrison, 1994; Thibessard *et al.*, 2001; Zhang, 2002), indicating that the appearance of ROS, H_2O_2 had led to the development of defense mechanisms which either kept the concentration of the oxygen derived radicals at acceptable levels or repaired oxidative damages.

The findings of the current study also showed that the main physiological benefit of adaptive response was clear to protect *Streptococcus* cells from higher doses of a toxic agent. Such a protective response also indicated that the cell, once exposed to the H_2O_2, expects, or at least is prepared for a subsequent lethal dose. Besides that, a protective mechanism could have occurred; the cocoid cells associated into strands by the HA capsule, where the reduced surface-to-volume ratio and the limited H_2O_2 diffusivity in the capsule shielded the cells from H_2O_2. In other words, the streptococcal cells synthesized HA excessively for a reduced rate of H_2O_2 uptake.

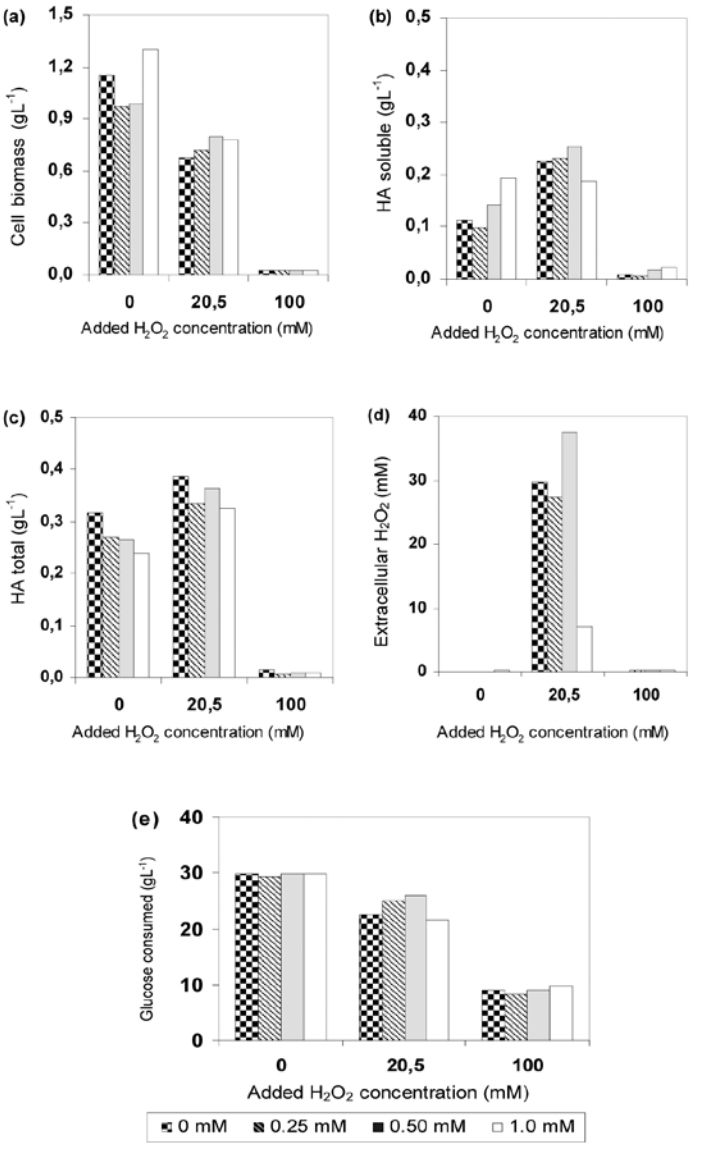

Fig. 1: The effect of hydrogen peroxide pretreatment on the growth and HA production, H_2O_2 released and glucose consumption by S. zooepidemicus *after 24 hr of fermentation period. (X-axis - concentration of treated H_2O_2; legend – concentration of the pre-treated H_2O_2)*

When pre-treated cells were treated with higher doses of H_2O_2 (100 mM), the growth and HA production was negligible (*Fig.1*). As a result, a lesser amount of glucose was utilized *(Fig. 1 (e))* and lower extracellular H_2O_2 was detected in the media. This also means that a significant damage, due to H_2O_2, indiscriminately reacted with various macromolecules in the cells had occurred, thus leading to a variety of biochemical and physiological lesions, and resulting in metabolic impairment and cell death (Totter, 1980; Harman, 1981; Ames, 1983).

From Table 1, it can be observed that the highest HA yield to glucose consumed ($Y_{HAtotal/glu}$) was 0.017 gg^{-1} for the cells pre-treated with 0 mM, and then exposed to 20.5 mM H_2O_2. As for the cells pre-treated with 0.50 mM and exposed to 20.5 mM H_2O_2 medium, the detected amount of extracellular H_2O_2 in the media was found to be the highest. The highest by-product yield ($Y_{H2O2/glu}$) to glucose consumed was 1.44 mM g^{-1}. According to Ryan and Kleinberg (1975), the concentration of H_2O_2 increased continuously during the growth due to the catabolic activity, and the categorization of this organism as H_2O_2 producer was therefore appropriate.

TABLE 1
Yield parameters of *S. zooepidemicus* at various pre-treated H_2O_2 concentrations, which were re-treated with 20.5 mM H_2O_2 medium (Condition: T = 37°C, agitation 250 rpm)

Pretreated H_2O_2 conc. (mM)	Biomass, X (gL^{-1})	Hyaluronic acid total, $HA_{tota\,l}$ (gL^{-1})	Hydrogen peroxide, H_2O_2 (mM)	$Y_{x/glu}$ (gg^{-1})	$Y_{HA/glu}$ (gg^{-1})	$Y_{H2O2/glu}$ (mM g^{-1})
0	0.672	0.388	29.7	0.0299	0.017	1.32
0.25	0.716	0.334	27.2	0.0288	0.013	1.09
0.50	0.798	0.364	37.3	0.0308	0.014	1.44
1.0	0.781	0.326	6.99	0.0362	0.015	0.32

CONCLUSIONS

In the response of *S. zooepidemicus* cells to oxidative stress in hyaluronic acid fermentation, several important features were found. Streptococcal cells were aerotolerant bacteria; when treated to lower levels of H_2O_2 (0, 0.25, 0.5 and 1.0 mM) it was better able to cope with the subsequent higher toxic levels of the oxidizing agent (20.5 mM). H_2O_2, at low level, acts as a stimulant for the cells to synthesize HA. At higher level (100mM), the cells might be destroyed or killed. Furthermore, for the Streptococcal cells to survive against the oxidative stress, a defense system which is inducible must exist.

ACKNOWLEDGEMENTS

The authors are grateful to the University Sains Malaysia, the Ministry of Higher Education (FRGS Grant) and the University of Malaya (Vote F: 0066/2001A, 0148/2002 & 0158/2003) for the financial support granted for this research.

REFERENCES

Ames, B.N. (1983) Dietary carcinogens and ant carcinogens. Oxygen radicals and degenerative diseases. *Science, 221,* 1256-1264.

Bannister, J.W., Bannister, W.H. and Rotilio, G. (1987). Aspects of structure, functions and applications of superoxide dismutase. CRC. *Critical Rev. Biochem., 22, 111-180.*

Condon, S. (1987) Response of lactic acid bacteria to oxygen, *FEMS Microbiol. Rev., 46, 269-280.*

Demple, B. and Harrison, L. (1994). Repair of oxidative damage to DNA: Enzymology and biology. *Annu. Rev. Biochem., 63,* 915-948.

Emiliani, E. and Riera, B. (1968). Enzymatic oxalate decarboxylation in *Aspergillusniger*. II. Hydrogen peroxide formation and other characteristics of the oxalate decarboxylase. *Biochimica et Biophysica Acta, 167*, 414-421.

Goh, L.T. (1998). Fermentation studies of hyaluronic acid production by *Streptococcus zooepidemicus*. (PhD Thesis. University of Queensland, Brisbane, Australia).

Halliwell, B. and Gutteridge, J.M.C. (1989). *Free Radicals in Biology and Medicine* (2nd Edition). Oxford: Clavendon Press.

Halliwell, B., Gutteridge, J.M.C. (1999). *Free Radicals in Biology and Medicine* (3rd Edition). Oxford: Oxford University Press.

Hardie, J.M. and Whiley, R.A. (1995). The genus Streptococcus. In B.J.B. Wood and W.H. Holzapfel (Eds.), *The genera of lactic acid bacteria 2* (pp. 55-124). Blackie Academic and Professional.

Harman, P. (1981). The aging process. *Proc. Natl. Acad. Sci., 78*, 7124-7128.

Huang, W.C., Chen, S.J. and Chen, T.L. (2006). The role of dissolved oxygen and function of agitation in hyaluronic acid fermentation. *Biochem. Eng. J., 32, 239-243*.

Jakubovics, N.S. and Jenkinson, H.F. (2001). Out of the iron age: new insights into the critical role of manganese homeostasis in bacteria. *Microbiology, 14*, 1709-1718.

Jakubovics, N.S., Smith, A.W. and Jenkinson, H.F. (2002). Oxidative stress tolerance is manganese (Mn^{2+}) regulated in *Streptococcus gordonii. Microbiology, 148*, 3255-3263.

Lerner, M. (1996). Hyaluronic acid market benefits from new uses. *Chemical Marketing Reporter, 250,12-13*.

Mashitah, M.D., Masitah, H. and Ramachandran, K.B. (2002). A rapid method for an identification of hyaluronic acid produced by fermentation *of Streptococcus zooepidemicus* ATCC 39920. In *15th Malaysian Analytical Chemistry Symposium and Regional Science Instrumentation Expo 2002*, 10-12 September. Bayview Beach Resort, Pulau Pinang.

Mashitah, M.D., Ramachandran, K.B. and Masitah, H. (2005). Sensitivity to hydrogen peroxide of growth and hyaluronic acid production by *Streptococcus zooepidemicus* ATCC 39920. *Dev. Chem. Eng. Mineral Process., 13(5/6),* 1-12.

Mashitah, M.D. (2006). Kinetics of hydrogen peroxide formation and its relation to hyaluronic acid production by *Streptococcus zooepidemicus*. (PhD Thesis, University of Malaya, Kuala Lumpur, Malaysia).

Miller, R.A. and Britigan, B.E. (1997). Role of oxidants in microbial physiology. *Clin. Microbiol. Rev. 10*, 1-18.

Porter, N.A. (1984). Chemistry of lipid peroxidation. *Methods Enzymol, 105*, 273-282.

Ryan, C.S. and Kleinberg, I. (1975) Bacteria in human mouths involved in the production and utilization of hydrogen peroxide. *Arch. Oral. Biol., 40(8)*, 753-763.

Thibessand, A., Fernandez, A., Gitz, B., Bourget, N.L. and Decaris, B. (2001). Hydrogen peroxide effects on *Streptococcus thermophilus* CNRZ 368 cell viability. *Res. Microbiol. 152*, 593-596.

Totter, T.R. (1980). Spontaneous cancer and its possible relationship to oxygen metabolism. *Proc. Natl. Acad. Sci. 79*, 1763-1767.

Zhang, H. (2002). Function of oxygen-resistance proteins in the anaerobic bacteria *Desulforibrio vulgaris* strain Hildenborough. *MSc Thesis*, University of 1Calgary, Canada.

ISSN: 0128-7680
Pertanika J. Sci. & Technol. **17 (1)**: 95 – 115 (2009)

Stability Study of an Exothermic Biocatalytic Reaction and its Application in Bioprocess Systems

M.R. Mohd. Radzi and M.H. Uzir*
School of Chemical Engineering, Engineering Campus, Universiti Sains Malaysia, Seri Ampangan, 14300 Nibong Tebal, Seberang Perai, Penang, Malaysia
**E-mail: chhekarl@eng.usm.my*

ABSTRACT

Biocatalytic reaction is a type of reaction which uses enzyme or whole-cell as a (bio)-catalyst to achieve a desired conversion, under controlled conditions in a bioreactor. Temperature produces opposed effects on enzyme activity and stability, and is therefore a key variable in any biocatalytic processes. An exothermic biocatalytic reaction, in a continuous-stirred-tank reactor (CSTR), was analyzed where dynamic equations (non-linear differential equations) could be derived from the Michaelis-Menten and Arrhenius equations, by performing mass and energy balances on the reactor. In this work, the effects of the different parameters such as dilution rate, proportional control constant and dimensionless total enzyme concentration, on the stability of the system, were studied. The stability of the reaction could be analyzed, based on the ODE (ordinary differential equation), solved using the numerical technique in MATLAB® and the analytical investigation using Mathematica.® The numerical analysis can be carried out by considering the phase-plane behaviour and bifurcation diagrams of the dynamic equations, while the analytical analysis using Mathematica® can be undertaken by evaluating the eigenvalues of the system. In order to model the operational stability of biocatalysts, modulation factors need to be considered so that a proper design of bioreactors can be done. Temperature, as a key variable in such bioprocess systems, can be conveniently optimized through the use of appropriate models.

Keywords: Biocatalytic reaction, dynamical analysis, bifurcation, phase-plane analysis, eigenvalues analysis

INTRODUCTION

Biocatalytic reactions, with either enzyme or whole-cell as the catalyst, have long been used to catalyse chemical synthesis in order to obtain fine chemicals with specific structures (Adrie and Patrick, 2000). Enzyme, as an active catalyst, initiates or modifies the rate of a chemical reaction, and accelerates the system without itself being affected. Accordingly, biocatalysts can be divided into cellular (whether growing, resting or non-living cells) and non-cellular (enzymes which have been removed from the cellular membrane) types. Ribozymes, abzymes and peptide mimics can also be considered as biocatalysts (Benkovic and Ballesteros, 1997).

Biocatalysts have been applied in areas such as pharmaceuticals, detergents, and food products. As a matter of fact, recent advances in genetic engineering have improved stabilisation and immobilisation techniques of enzyme as biocatalyst. A better understanding of the structure-function relationships has also attracted a number of chemists and engineers to apply such methods outside these traditional businesses. Biocatalysis differs from

Received: 18 June 2007
Accepted: 29 October 2008
*Corresponding Author

conventional processes, not only by featuring a different type of catalysts, it also constitutes a new base of technology. The raw materials of a biologically-based process is built on sugar, lignin, animal or plant waste and the product range of biotechnological processes which often encompass chiral molecules or biopolymers such as proteins, nucleic acids or carbohydrates. Biocatalysts, including isolated enzymes, micro-organisms, plants, and catalytic antibodies, offer benefits such as environmentally-friendly materials, stereoselectivity and regioselectivity, as well as new reactions beyond the traditional chemical synthesis.

The development of the new biocatalysts and improvements, in process design and engineering, has fuelled and heightened interest in biocatalysis. The main objective is to solve some critical industrial problems and create alternative synthetic routes. As these technological advances evolve, emerging markets for biocatalysts, such as fine chemicals, pharmaceuticals and consumer products will result in a significant growth.

Biocatalyst has gone a step forward and it is competing with the conventional chemical catalysts. Potential advantages of biocatalysts include high specificity, high activity under mild environmental conditions, and high turnover number. Their biodegradable nature and label, as a natural product, have also become very important assets (Polastro, 1989). Drawbacks are inherent to their complex molecular structure, making them costly to produce, and are intrinsically unstable as well.

Temperature produces opposed effects on the activity and stability of enzyme, and for this reason, it is therefore a key variable in any biocatalytic processes (Andres, 1999). In order to study the effect of temperature on the rate of an exothermic biocatalytic reaction, two factors need to be considered. The first is the influence of temperature on the reaction rate constant, and the second is the thermal denaturation of enzymes at elevated temperatures, which counteracts the enhancement in the rate constant at higher temperature. The temperature range, over which enzymes exhibit their activities, is rather limited. At temperatures above 100°C, a number of enzymes relatively show substantial activities, while near the freezing temperatures, the rates become very slow (Harvey and Douglas, 1996). The thermal deactivation of enzymes limits their useful lifetime in processing environments, and is thus of considerable importance in process design and development. The temperature range, over which thermal denaturation occurs, varies with the nature of the enzyme being considered.

High temperature induces irreversible deactivation of enzymes. It enables the thermodynamic parameters of enzyme to be determined and is used to study the mechanisms involved in the biochemical systems. For example, the effects of this factor on the stability of *Rhizomucor miehei* lipase have been investigated. The stability criterion used was the residual hydrolytic activity of the lipase. Experimental and theoretical parameters, obtained by linear regression analysis, were compared with the theoretical kinetics to validate the series-type inactivation model. Lipase obtained from *R. miehei* was deactivated by either thermal or pressure treatment (Noel and Combes, 2003). There are many types of enzyme involved in the exothermic biocatalytic reaction and some of the examples are shown in Table 1. The main objective of this work was to determine the optimum conditions and parameters, for which an exothermic biocatalytic reaction reached a stable state.

THE MICHAELIS-MENTEN MODEL

The standard Michaelis-Menten equation, based on one-substrate-one-product, is given below.

$$-r_S = \frac{k_3'[E_t]\,[S]}{[S] + K_m} \tag{1}$$

TABLE 1
Examples of exothermic biocatalyst

Biocatalyst	Temperature Range (°C)	Comments
Sulfolobus	60 - 80	Important geochemical agent in the production of sulphuric acid from sulphur in high temperature hydrothermal systems.
Sulfolobus metallicus	70 - 80	Catalyst in bioleaching of chalcopyrite at 70°C for microbial catalysis of ferrous ion oxidation.
β-glucosidase from *Sulfolobus solfataricus*	70 - 80	Catalyst in lactulose production from lactose and fructose hydrolysis.
Candida antarctica lipase B	30 - 60	Catalyst for the biocatalytic production of chiral secondary alcohols.

where [S] is the substrate concentration (mol dm^{-3}), $[E_t]$ is the total enzyme concentration (mol dm^{-3}), K_m represents Michaelis-Menten Constant (mol dm^{-3}), and $k_3' = k_3[W]$ is the rate constant (s^{-1}).

Let V_{max} represent the maximum rate of reaction, for a given total enzyme concentration, $[E_t]$. Hence,

$$V_{max} = k_3'[E_t] \tag{2}$$

From Eq. (1), the Michaelis-Menten equation can simply be rewritten as:

$$-r_s = \frac{V_{max}[S]}{[S] + K_m} \tag{3}$$

THE MODEL OF EXOTHERMIC REACTION

Considering the biocatalytic reaction in the CSTR, substrate A was converted into product B through an enzymatic reaction. Therefore, the reaction rate, based on the Michaelis-Menten equation derived previously (in respective to this particular biocatalytic reaction for the decomposing rate of substrate A) is given by:

$$r_A = \frac{k_3' C_A C_{Et}}{C_A + K_m} \tag{4}$$

where r_A represents the moles of substrate A decomposing per hour per cubic meter of reacting mixture, C_A shows the concentration of A in the reacting mixture, C_{Et} is the total enzyme concentration, and K_m represents the Michaelis-Menten constant. Applying the Arrhenius equation for the rate constant k_3',

$$k_3' = k_A e^{-E/RT} \tag{5}$$

where k_A is the reaction velocity constant (s^{-1}), E is the activation energy (J/mole), R is the universal gas law constant = 8.314 J/mole K, and T is the absolute temperature, (K). Substituting Eq. (5) with Eq. (4), the reaction rate could therefore be rewritten as:

$$r_A = \frac{k_A e^{-E/RT} C_A C_{Et}}{C_A + K_m} \tag{6}$$

For further derivation of the dynamic model of an exothermic biocatalytic reaction, a general mass balance of substrate A and energy balance on the CSTR was carried out.

The General Mass Balance of Substrate A

A general balanced equation, around the reactor system for component A, could be simply written, as:

$$F_{Ao} - F_A - \int {}^{V} r_A dV = \frac{dN_A}{dt} \tag{7}$$

hence;

$$FC_{Ao} - FC_A - r_A V = \frac{VdC_A}{dt} \tag{8}$$

where F_{Ao} represents the inlet mole flow rate of A (moles A/s), F_A is the outlet mole flow rate of A (moles A/s), F is the feed rate of the mixture to the reactor (m^3/s) C_{Ao}, is the inlet concentration of A (mle/m^3), C_A represents the outlet concentration of (A, mole/m^3) and V is the volume of the mixture (m^3). Substituting Eq. (6) with Eq. (8) leads to:

$$FC_{Ao} - FC_A - \frac{k_A e^{-E/RT} C_A C_{Et}}{C_A + K_m} V = \frac{VdC_A}{dt} \tag{9}$$

Rearranging Eq. (9), gives;

$$\Rightarrow \frac{dC_A}{dt} = \frac{F}{V}[C_{Ao} - C_A] - \frac{k_A e^{-E/RT} C_A C_{Et}}{(C_A + K_m)} \tag{10}$$

The following assumptions were made in order to arrive at Eq. (10); these include (i) the density of the reacting mixture is constant, unaffected by the conversion of A to B, (ii) the feed and product rates F are equal and constant, (iii) volume, V of the reacting mixture is constant, (iv) perfect mixing occurs, so that C_A is the same in the reactor and product stream.

The Energy Balance on the CSTR

A general heat balance around a CSTR can be represented as:

$$F\rho C_P T_o - F\rho C_P T + r_A V(\Delta H) - Q(T) = \rho V C_P \frac{dT}{dt} \tag{11}$$

where T_0 is the temperature of the feed stream, T is the temperature in the reactor, C_p is the specific heat of reacting mixture and ΔH refers to the heat of the reaction.

Substituting Eq. (6) with Eq. (11) gives:

$$F\rho C_p T_0 - F\rho C_p T + \left[\frac{k_A e^{-E/RT} C_A C_{Et}}{C_A + K_m}\right] V(\Delta H) - Q(T) = \rho V C_P \frac{dT}{dt} \tag{12}$$

Rearranging Eq. (12) leads to:

$$\rho V C_P \frac{dT}{dt} = F\rho C_p T_0 - F\rho C_p T + \left[\frac{k_A e^{-E/RT} C_A C_{Et}}{C_A + K_m}\right] V(\Delta H) - Q(T) \tag{13}$$

$$\frac{dT}{dt} = \frac{F}{V}[T_o - T] + \frac{k_A(\Delta H) e^{-E/RT} C_A C_{Et}}{\rho C_p [C_A + K_m]} - \frac{Q(T)}{\rho V C_P}$$

In arriving to Eq. (13), three important assumptions should be followed; (i) the specific heat of the reacting mixture remains constant and unaffected by the conversion of A to B, (ii) a perfect mixing is achieved such that the temperature of the reacting mixture and the product stream are the same, and (iii) the heat of the reaction ΔH is constant, which is independent of the temperature and composition.

For further analysis, the dimensionless variable for the dynamic equations of this exothermic biocatalytic reaction as obtained previously was defined.

Using Eq. (10) by defining some dimensionless variables:

$$\tau = \frac{Ft}{V} = Dt \qquad y = \frac{C_A}{C_{Ao}} \qquad \alpha = \frac{C_{Et}}{C_A + K_m}$$

$\frac{F}{V}$ is the dilution rate, and D, which refers to the rate of which the existing medium in the reactor, is replaced by a fresh medium α.

Dividing both sides of Eq. (10) with (DC_{AO}):

$$\frac{dC_A}{dt(DC_{Ao})} = \frac{D[C_{Ao} - C_A]}{DC_{Ao}} - \frac{k_A e^{-E/RT} C_A C_{Et}}{(C_A + K_m) DC_{Ao}}$$

$$\Rightarrow \frac{dy}{d\tau} = 1 - y - \frac{k_A \alpha y}{D} e^{-E/RT} \tag{14}$$

From Eq. (13):

$$\frac{dT}{dt} = \frac{F}{V}[T_o - T] + \frac{k_A(\Delta H) e^{-E/RT} C_A C_{Et}}{\rho C_p [C_A + K_m]} - \frac{Q(T)}{\rho V C_P}$$

Defining θ_0 and θ with;

$$\theta = \frac{\rho C_P T}{C_{Ao}(\Delta H)} \qquad \theta_0 = \frac{\rho C_P T_0}{C_{Ao}(\Delta H)}$$

Multiplying both sides of Eq. (13) with $\frac{V\rho C_P}{FC_{Ao}(\Delta H)}$

$$\frac{dT}{dt}\left[\frac{V\rho C_P}{FC_{Ao}(\Delta H)}\right] = \frac{F}{V}[T_0 - T]\left[\frac{V\rho C_P}{FC_{Ao}(\Delta H)}\right] + \frac{k_A(\Delta H)e^{-E/RT}C_A C_{Et}}{\rho C_P[C_A + K_m]}\left[\frac{V\rho C_P}{FC_{Ao}(\Delta H)}\right] - \frac{Q(T)}{V\rho C_P}\left[\frac{V\rho C_P}{FC_{Ao}(\Delta H)}\right]$$

$$\Rightarrow \qquad \frac{d\theta}{d\tau} = \theta_0 - \theta + \frac{k_A y\alpha}{D}e^{-E/RT} - \frac{Q(T)}{FC_{Ao}(\Delta H)} \tag{15}$$

From the dimensionless equation, $\theta = \frac{\rho C_P T}{C_{Ao}(\Delta H)}$, upon rearranging, leads to;

$$T = \frac{\theta C_{Ao}(\Delta H)}{\rho C_P} \tag{16}$$

Substitute Eq. (16) into Eq. (14);

$$\frac{dy}{d\tau} = 1 - y - \frac{k_A y\alpha}{D}e^{-\frac{E}{R\left[\frac{\theta C_{Ao}(\Delta H)}{\rho C_P}\right]}}$$

$$\Rightarrow \frac{dy}{d\tau} = 1 - y - \frac{k_A y\alpha}{D}e^{-\left[\frac{E\rho C_P}{R\theta C_{Ao}(\Delta H)}\right]} \tag{17}$$

and similarly, Eq. (16) into Eq. (15) gives:

$$\frac{d\theta}{d\tau} = \theta_0 - \theta + \frac{k_A y\alpha}{D}e^{-\left[\frac{E\rho C_P}{R\theta C_{Ao}(\Delta H)}\right]} - \frac{Q(T)}{FC_{Ao}(\Delta H)} \tag{18}$$

Eq. (17) and Eq. (18) then become:

$$\left.\begin{aligned}\frac{dy}{d\tau} &= 1 - y - r(y,\theta)\\ \frac{d\theta}{d\tau} &= \theta_0 - \theta + r(y,\theta) - q(\theta)\end{aligned}\right\} \tag{19}$$

$$r(y,\theta) = \frac{k_A y \alpha}{D} e^{-\left[\frac{E\rho C_P}{R\theta C_{Ao}(\Delta H)}\right]}$$

where;

$$q(\theta) = \frac{Q(T)}{FC_{Ao}(\Delta H)}$$

Based on the famous work by Aris and Amundson (1958), a form of control heat-removal function $q(\theta)$ was chosen and it is given by:

$$q(\theta) = U(\theta - \theta_C)\,[1 + K_C(\theta - \theta_S)] \tag{20}$$

where θ_C is the dimensionless mean temperature of water in the cooling coil which indicates that the heat removal is always proportional to the difference between the reactor temperature and the mean cooling-water temperature.

The term in brackets indicates that the proportional control on the cooling-water flow rate is present. The flow rate is increased by an amount proportional to the difference between the actual reactor temperature, θ and the desired steady-state temperature, θ_s, with K_C as the proportional control constant. The increase in the rate of the cooling-water flow is assumed for convenience to cause an approximately proportional increase in the heat removal. The constant U is a dimensionless analogue of U_0A, the overall heat-transfer rate. Defining $\beta = \frac{E\rho C_P}{RC_{Ao}(\Delta H)}$ and substituting Eq. (20) with Eq. (19), the final

dynamic equation to be studied is:

$$\left.\begin{aligned} \frac{dy}{d\tau} &= 1 - y - \frac{k_A y \alpha}{D} e^{-\frac{\beta}{\theta}} \\ \frac{d\theta}{d\tau} &= \theta_0 - \theta + \frac{k_A y \alpha}{D} e^{-\frac{\beta}{\theta}} - U(\theta - \theta_C)[1 + K_C(\theta - \theta_S)] \end{aligned}\right\} \tag{21}$$

RESULTS AND DISCUSSION

The Effect on Varying the Dilution Rate, D

The dilution rate D was the first parameter considered in this work; it refers to the rate of which the existing medium in the reactor is replaced by a fresh medium. The system was analyzed at three different values of K_C, by varying the values of the dilution rate. The difference between the stability of each system could then be analyzed.

Fig. 1 was numerically solved using the MATLAB® by applying ODE23 at a constant proportional control constant, K_C=10, and varying the value of the dilution rate D, from 20 s^{-1} to 90 s^{-1}. This simulation was undertaken in order to study the effect of the increasing values of D on the stability of the system. *Fig. 4* shows that for the system with K_C=10, the trajectory from the numerical integration resulted in a spiral focus for each value of D, but changing in the focus point. The non–formation of Hopf bifurcations resulted in no limit

cycle in this system. Increasing the value of D at K_C=10 would result in the decrease of the dimensionless temperature θ values, while reactant A conversion y was found to increase from 0 to 1. A further analysis was undertaken using the MATLAB® to study this dynamical system, as shown in *Figs. 2* (a) and *(b)*. Plotting y against D and θ against D respectively shows that θ is decreasing while y is increasing with the increment in D, and stable focus without any bifurcation behaviours. This system can easily be maintained and controlled.

Meanwhile, increasing the dilution rate would result in a higher amount of substrate added into the reactor; therefore increasing the rate of the substrate diffusion into the active sites of enzyme to initiate the reaction. The diffusion of the substrate and product, inside a porous biocatalyst, was found to occur in parallel with the catalyzed reaction. The more enzyme catalyses the reaction reduced the substrate concentration within the particles, the greater the substrate concentration gradient created between the internal microenvironment and the bulk of the solution would be. In turn, this would increase the rate, at which the substrate was delivered to the enzyme molecules towards the outside of the particles, and increase y. However, there was a decrease in θ as the dilution rate D increased from 20 s^{-1} to 90 s^{-1}. As there was a constant amount of cell in the reactor, the active sites of the enzyme would fully be utilised by the substrate. Increasing the dilution rate caused the heat (released by the reaction) to be dissipated on the excess amount of the substrate and at the same time, lowered the temperature of the reactor.

The analysis was carried out mainly to look at the effect of increasing the value of D on the stability of the system at K_C = 9. The numerical integration, using the MATLAB® from the model equations, was plotted in *Fig. 3*, indicating that the system varied in the value of the dilution rate D, i.e. from 10 s^{-1} to 80 s^{-1}. Trajectories (in the form of stable spiral focus) appeared for D, which was equal to 10 s^{-1}, 20 s^{-1}, 30 s^{-1} and 40 s^{-1}. Limit cycles were formed when the values of D were 50 s^{-1} and 60 s^{-1}. Any further increase in D would result in stable focus points with a better stability.

In addition, further analysis of this dynamical system was undertaken, based on the stability diagram of the model equations at K_C = 9, as shown in *Figs. 4 (a)* and *(b)*. It is obvious that there were Hopf bifurcations (which appeared in between the two Hopf points) in

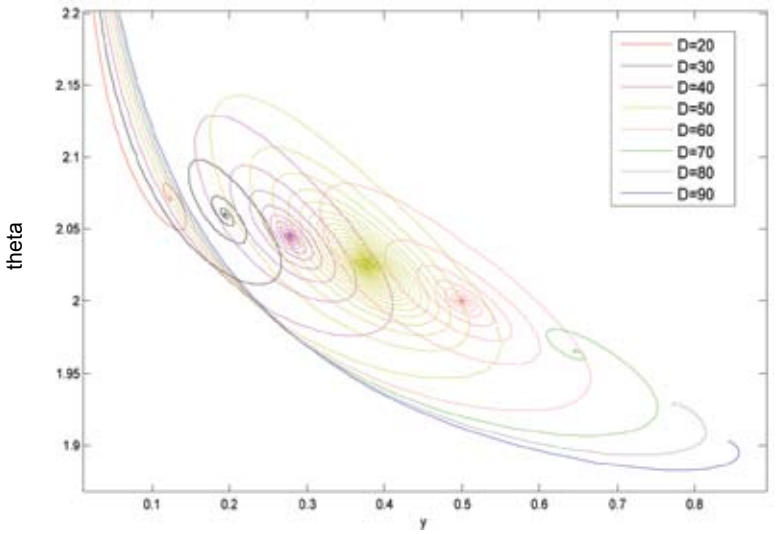

Fig. 1: Phase-plane of model equations at K_C = 10 at various dilution rates, D

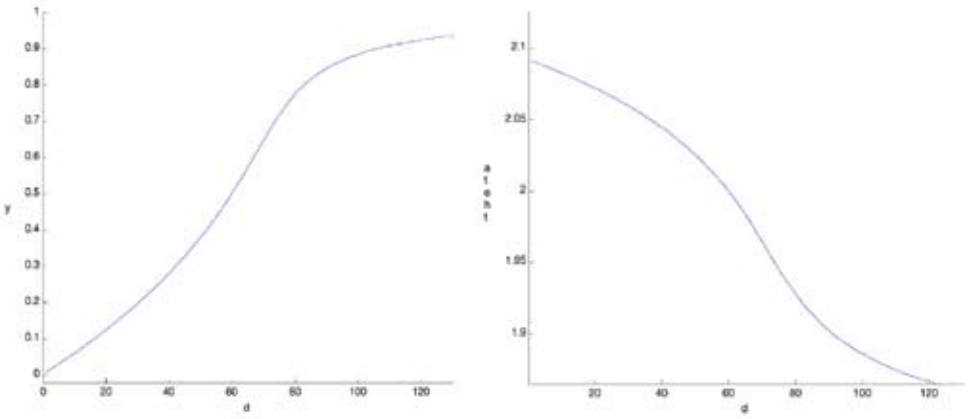

Fig. 2: Stability diagram of model equations at K_C = 10 with no bifurcations: (a) Bifurcation diagram y versus D and (b) Bifurcation diagram θ *versus D*

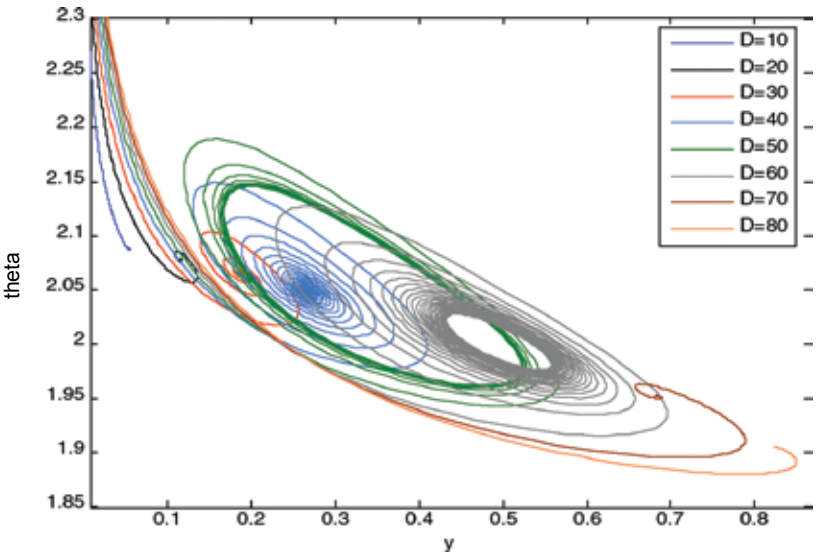

Fig. 3: Phase-plane of model equations at K_C = 9 at various dilution rates, D

this system. The first Hopf point was at y = 0.2914, θ = 2.0448 and D = 42.6748, while the second Hopf point was at y = 0.5, θ = 2.0 and D =60.00. These bifurcations occurred when there were changes in the stability of the system, i.e. from the stable node or spiral focus to the limit cycles and vice versa. Bifurcation was observed in this system because there was instability in the enzyme, under this range of conditions.

The same analysis was repeated for the purpose of studying the effect of increasing the value of D on the stability of the system at K_C = 7. *Fig. 5* shows the phase-plane of θ versus, y, at a proportional control constant, K_C = 7 with variable dilution rates D, from 20 s^{-1} to 80 s^{-1}. This system resulted in a stable spiral focus for D, which equalled to 20 $s^{-1}$and 30 s^{-1}.

The limit cycles were formed when the values of D varied at 40 s^{-1}, 50 s^{-1} and 60 s^{-1}. If the dilution rate D increased further, the limit cycles would disappear and a good control could be achieved.

Further analysis of this dynamical system was carried numerically, as shown in *Figs. 6 (a)* and *(b)*. Again, the Hopf bifurcations were observed to occur in between the two Hopf points. The first Hopf point was at $y = 0.2270$, $\theta = 2.0649$ and $D = 38.6688$, while the second Hopf point was at $y = 0.6271$, $\theta = 1.9636$ and $D = 63.5063$. These bifurcations evolved when there were changes in the stability of the system, i.e. from spiral focus to limit cycles and vice versa.

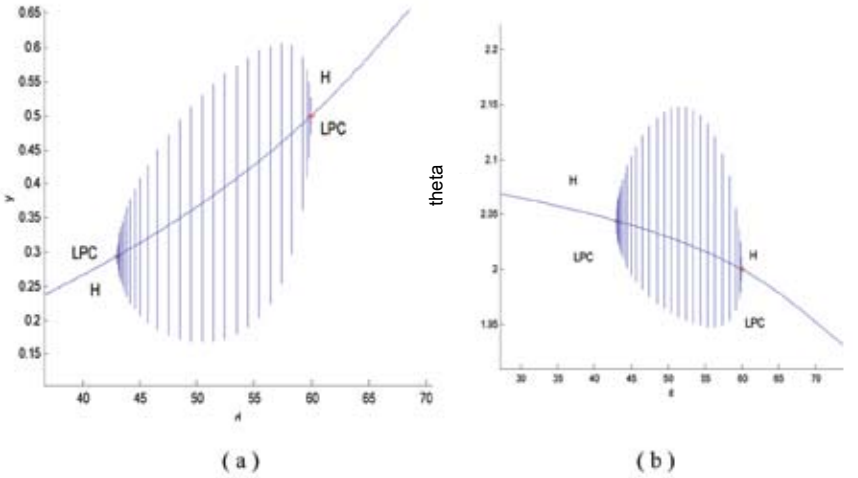

Fig. 4: Bifurcation diagram of model equations at $K_C = 9$: (a) plot y versus D and (b) plot θ versus D

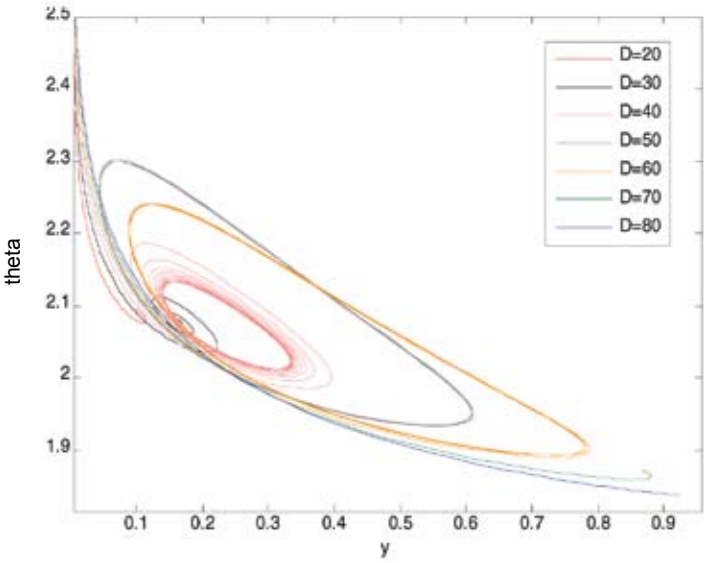

Fig. 5: Phase-plane of model equations at $K_C = 7$ at various dilution rates, D

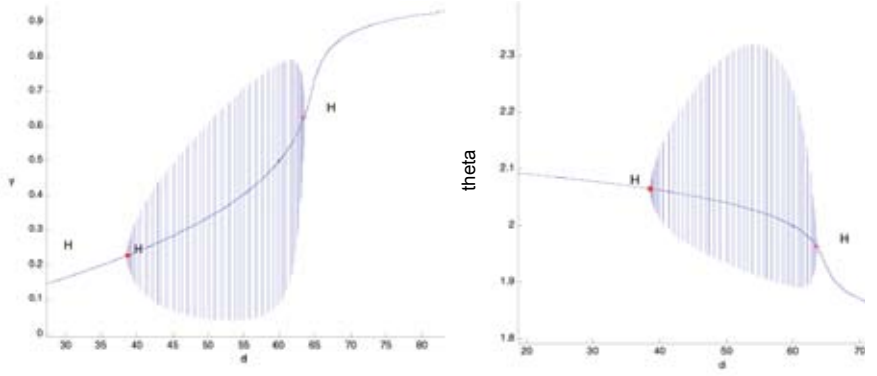

Fig. 6: Bifurcation diagram of model equations at K_C = 7: (a) plot y versus D and (b) plot θ versus D

The Effect of Changes in the Proportional Control Constant, K_C

The second parameter being considered was the proportional control constant, K_C which referred to the proportional control of the cooling-water flow rate. Such an increase in cooling water flow rate was assumed for convenience, i.e. to obtain an approximate proportional increase in heat removal (Donald, 1991). For this purpose, the system was analysed, at three different values of D, by varying the value of K_C. The difference between the stability of each system could then be analyzed. Taking an example of the system at D = 50, the results from the simulation are shown in *Figs. 7* and *8*.

Referring to the above figures, the stability of the system was analyzed at the dilution rate, D which was equal to $50s^{-1}$ and varied in the value of proportional control constant, K_C. This system resulted in a stable spiral focus for K_C =1. Limit cycles were then formed when K_C = 2. As a result, a stable steady-state, formed for K_C, was equal to 3 and 4. Limit cycles

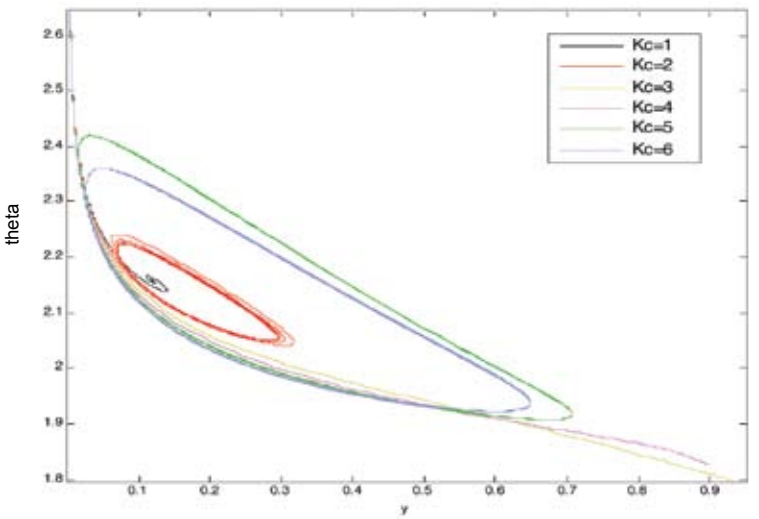

Fig. 7: Phase-plane of model equations at D = 50 at various K_C (1-6)

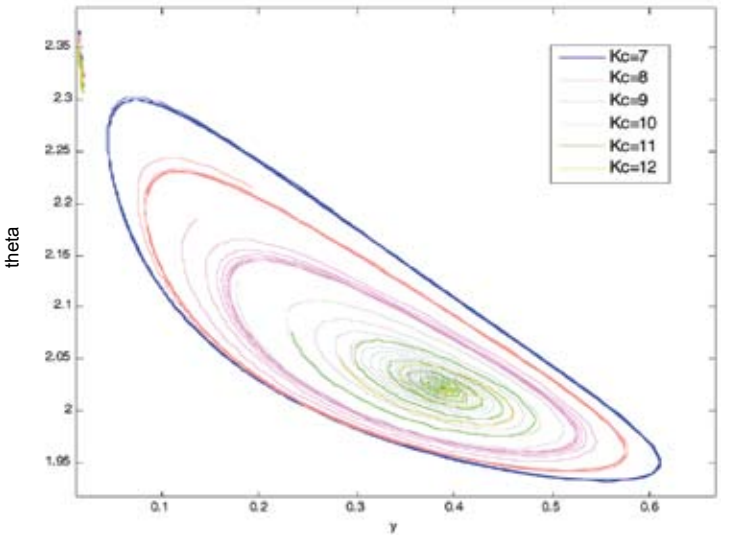

Fig. 8: Phase-plane of model equations at D = 50 at various K_C (7-12)

then appeared when the values of K_C varied from 5 to 9. Further increase in the value of K_C would result in a stable spiral focus. If the dilution rate D was increased further, the limit cycles would disappear and a stable reaction system could be achieved.

To make the observation easier, the bifurcation diagrams were plotted as shown in *Figs. 9, 10* and *11*, i.e. at three different values of D. According to the analysis carried out, and based on the phase-plane of the model equations in *Figs. 9, 11* and *13*, the dimensionless temperature of the reactor θ was found to decrease with the increase in the proportional control constant K_C. Meanwhile, the reactant conversion y increased with the increase in K_C. The limit cycles were also observed to appear in each system.

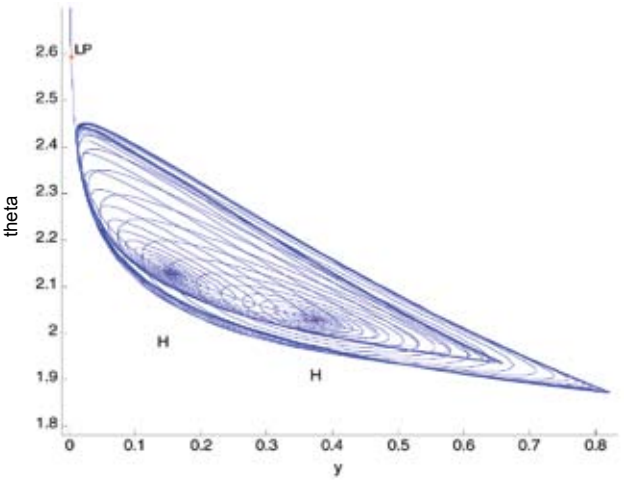

Fig. 9: Phase-plane of model equations at D = 50 at various K_C

From the bifurcation diagrams, it can be concluded that the types of bifurcation formed are different from one another. Based on the data presented in *Fig. 10,* there are Hopf bifurcations which appeared in between the two Hopf points, at D = 50. The first Hopf point was at $y = 0.1563$, $\theta = 2.1280$ and $K_C = 1.812$, while the second Hopf point was at $y = 0.3746$, $\theta = 2.0268$ and $K_C = 9.6945$. However, there is a region of stable steady-state in between this range of bifurcation. Referring to *Fig. 12* for system at D = 60, there is a small Hopf bifurcation which was formed at a Hopf point $y = 0.1483$, $\theta = 2.1504$ and $K_C = 0.847$. As for the third system analyzed at D = 40, the Hopf bifurcation re-appeared in between the two Hopf points. The first Hopf point was indicated at $y = 0.1823$, $\theta = 2.0916$ and $K_C = 4.2924$, while the second Hopf point was at $y = 0.2537$, $\theta = 2.0554$ and $K_C = 8.0131$.

As discussed in the earlier section, K_C refers to the proportional control on the cooling-water flow rate. The increase in the cooling water flow rate would cause an approximately proportional increase in the heat removal. Therefore, the amount of heat removed from

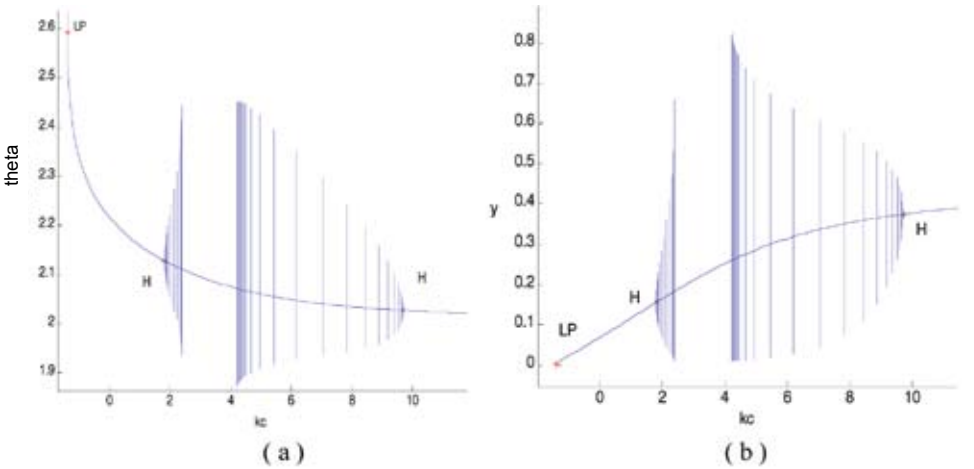

Fig. 10: Bifurcation diagram of model equations at D = 50; (a) plot θ *versus* K_C *and (b) plot y versus* K_C

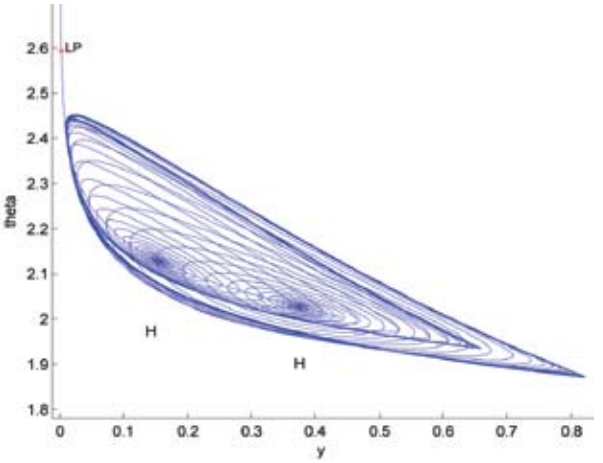

Fig. 11: Phase-plane of model equations at D = 60 at various K_C

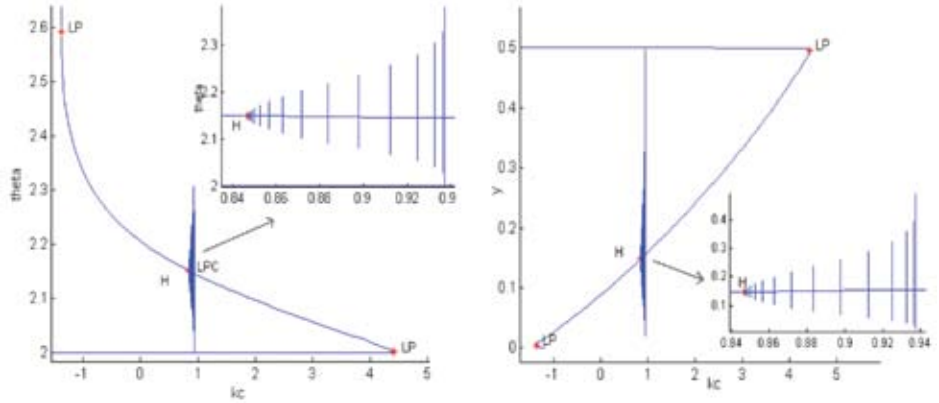

Fig. 12: Bifurcation diagram of model equations at D = 60; (a) plot θ *versus* K_C *and (b) plot y versus* K_C

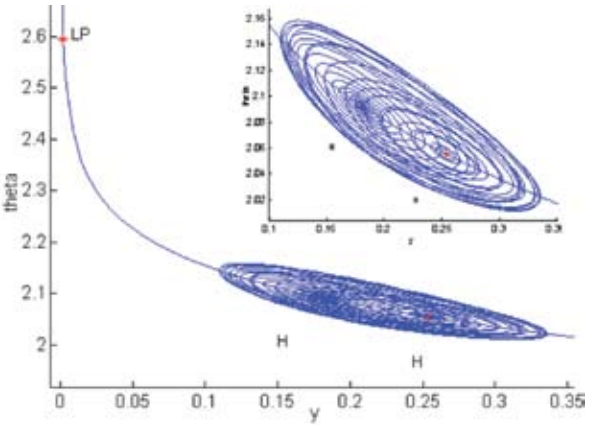

Fig. 13: Phase-plane of model equations at D = 40 at various K_C

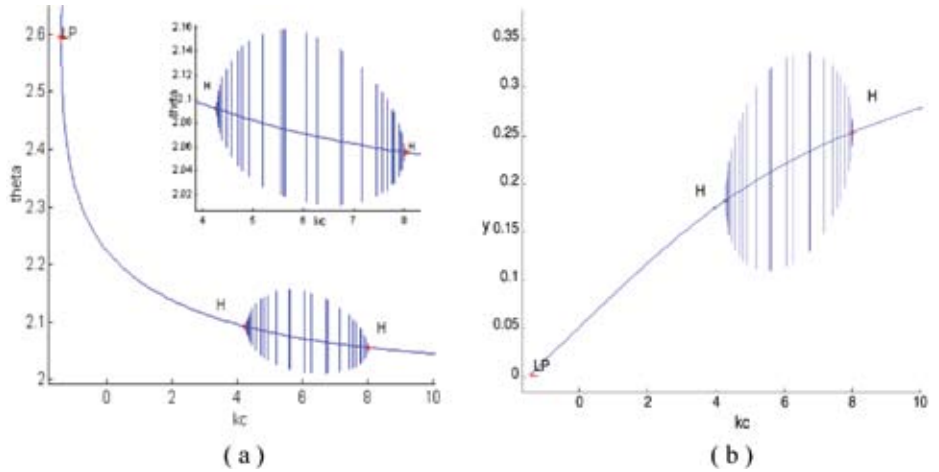

Fig. 14: Bifurcation diagram of model equations at D = 40; (a) plot θ *versus* K_C *and (b) plot y versus* K_C

the system was higher at higher values of K_C, the condition which would lower the reactor temperature. The increase in K_C resulted in the increase in the reactant conversion, as the heat removal from the system provided a suitable or an optimum temperature for the enzyme to have an optimum activity. This optimum operating condition would therefore promote more substrate to diffuse into active site of the enzyme, which further later led to substrate conversion.

At a lower value of K_C, the reactant conversion was found to be very low because the amount of heat removed was low, and this caused the temperature of the system to increase. As a result, the internal energy of the molecules in the system would also increase. The internal energy of the molecules might include the translational energy, vibrational energy and rotational energy, the energy involved in the chemical bonding of molecules as well as the energy involved in the non-bonding interactions. Some of this heat might be converted into a chemical potential energy. If this chemical potential energy increase was great enough, some of the weak bonds which determined the three dimensional shape of the active proteins might be broken. This could lead to a protein thermal denaturation and thus inactivate the enzyme. Therefore, too much of heat could also cause the rate of an enzyme-catalysed reaction to decrease, as the enzyme became denatured and inactive (Bommarius, 2004).

The effect on changes in the total enzyme concentration, α

The third parameter to be considered is the dimensionless total enzyme concentration, α which refers to the total amount of cells or enzyme in the reactor. Here, the system was analyzed at constant value of D = 50 and K_C =10 with variable values of α.

From the phase-plane plotted in *Fig.15*, it could be observed that there were no bifurcations occurred in the system; this resulted in the non formation of the limit cycles. The increase in the total cell concentration α was found to increase the reactant conversion y, since there were more cells to react with the substrate added to the reactor. Meanwhile, the increase in the reactor temperature was basically due to the increase in the metabolic rate of the cell during the growth phase. The nutrient consumed was becoming less since the cell was at a stage of reproducing new cells. For α higher than 40, oscillations started to emerge in the system before it reached the equilibrium point, due to the interaction of cell with the high temperature. The enzyme was also found to be unstable, at a certain high temperature, even when the amount of cells was relatively high.

The Effect of Different Initial Conditions

The objective of this section was to study the effect of changing the values of the dimensionless initial point $y = \frac{C_A}{C_{Ao}}$ and $\theta = \frac{\rho C_P T}{C_{Ao}(\Delta H)}$, which represented the conversion reactant A and the dimensionless reactor temperature on the stability of reaction. Phase-plane was plotted using MATLAB® for two different systems, with graphically different initial points.

Figs. 16 and *17* show that the phase-plane portrait for the system at D = 50 s^{-1} and K_C = 8 resulted in a stable limit cycle, while the spiral focus appeared for the second system. For both systems, it could be clearly seen that varying the initial values did not impose any effect on the stability of the reaction, and this was followed by the same loops of stability which moved towards the same equilibrium point.

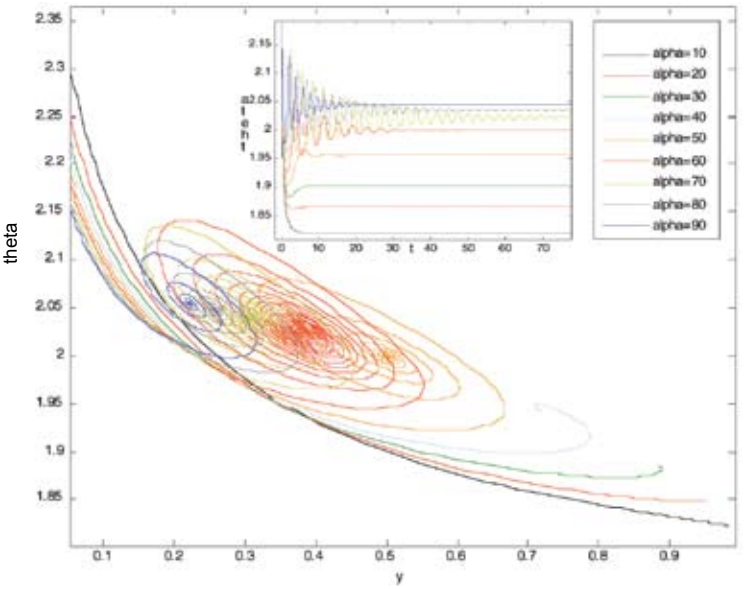

Fig. 15: Phase-plane of model equations at K_C = 10 and D = 50 at various α α

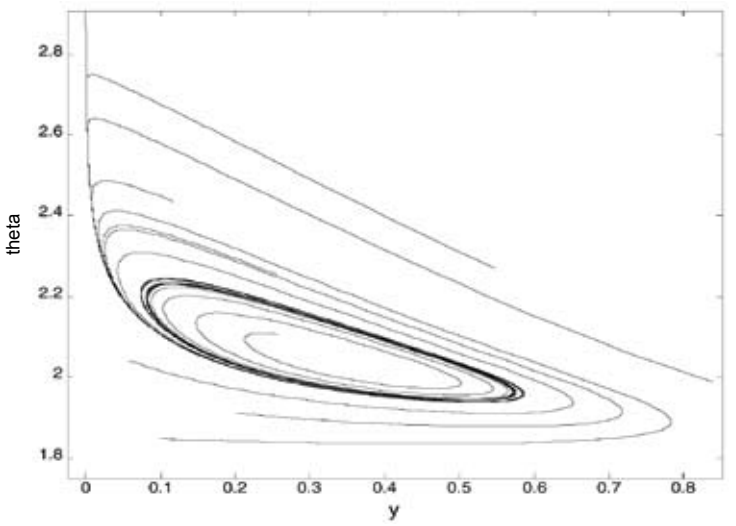

Fig. 16: Phase-plane portrait for system at D = 50 s^{-1} and K_C = 8 with changes in the initial points

The Analytical Investigation on the Thermal Stability of Biocatalytic Reaction

The results discussed previously involved the transition of the reaction stability (from the stable steady-state point and stable focus) to the formation of the limit cycles which could be proven mathematically using the eigenvalue analysis. Such an analysis was carried out using Mathematica® on two dynamic equations. Taking an example of the system at K_C = 7 and varying the value of D, the results gathered for the stability of the system could be simplified as in the Table 2 and *Fig. 20.*

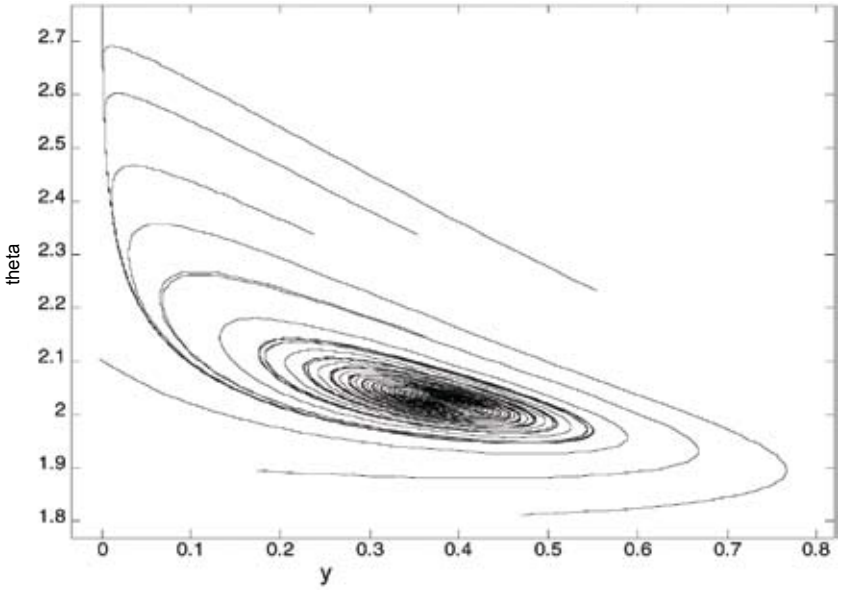

Fig. 17: Phase-plane portrait for system at D = 50 s^{-1} and K_C = 10 with changes in the initial points

TABLE 2
Equilibrium point coordinates and eigenvalues for system at K_C = 7

D (s^{-1})	Equilibrium Coordinates		Eigenvalues
	y	θ	
5	0.02310	2.10614	-10.4368
			-7.0869
20	0.10101	2.09095	-2.3210 + 5.8362i
			-2.3210 - 5.8362i
30	0.16300	2.07839	-0.6471 + 4.4308i
			-0.6471 - 4.4308i
40	0.23800	2.06256	0.0642 + 3.2368i
			0.0642 - 3.2368i
50	0.33655	2.04052	0.3392 + 2.1786i 0.3392 - 2.1786i
60	0.50010	1.99997	0.2498 + 1.0892i 0.2498 - 1.0892i
70	0.86795	1.87065	-0.7262
			-0.4782
80	0.92288	1.83861	-0.9148
			-0.5187

Based on the data presented in the table, changes were observed in the equilibrium points of this system for the different values of dilution rates D, which ranged from 5 s^{-1} to 80 s^{-1}. The dimensionless conversion y was found to increase with an increment in D, which was due to the addition of the substrate into the reactor. This had also increased the opportunity of substrate diffusion into the active sites of the enzyme to initiate the reaction. However,

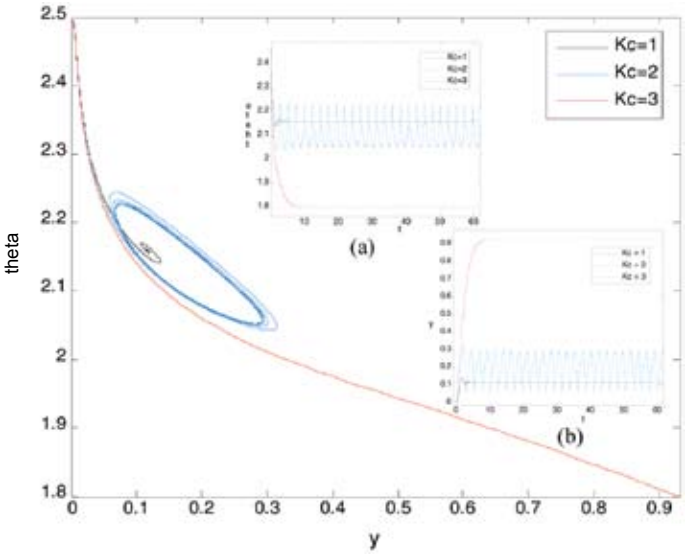

Fig. 18: Phase-plane portrait for system at D = 50 s^{-1} with varying proportional constant, K_C: (a) Plot θ versus t and (b) Plot y versus t

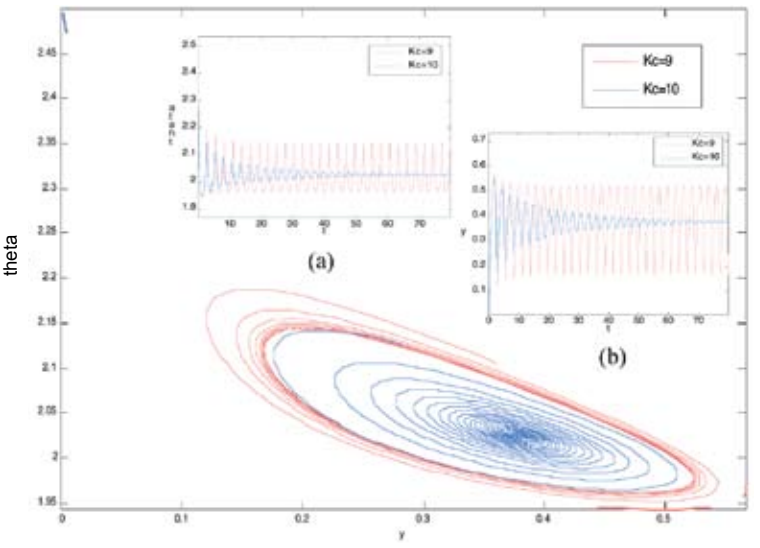

Fig. 19: Phase-plane portrait for system at D = 50 s^{-1} with varying proportional constant, K_C. (a) Plot θ versus t and (b) Plot y versus t

the values of the dimensionless temperature of the reactor were also found to decrease, as D increased from 5 s^{-1} to 80 s^{-1}. As there was a constant amount of enzyme in the reactor, the active sites of the enzyme would be fully utilized by the substrate. Increasing the dilution rate had caused the heat to release by the reaction to be dissipated on the excess amount of substrate and at the same time lowering the temperature of the reactor.

The eigenvalues obtained from the analysis were plotted in order to study the transition of the stability in the system *(Fig. 20)*. From the figure, it can be observed that for D = 5 s^{-1}, there was a stable node and for D = 20 s^{-1} there was a stable spiral focus. For the system with D = 50 s^{-1}, the eigenvalues were found to be positive in the real part which was located in the unstable region with the formation of limit cycle. Therefore, there were transition points, from the stable region to the unstable region, in between D = 20 s^{-1} and D =50 s^{-1}. The Hopf bifurcations were found to occur when a conjugated complex pair crossed the boundary of the stabile region.

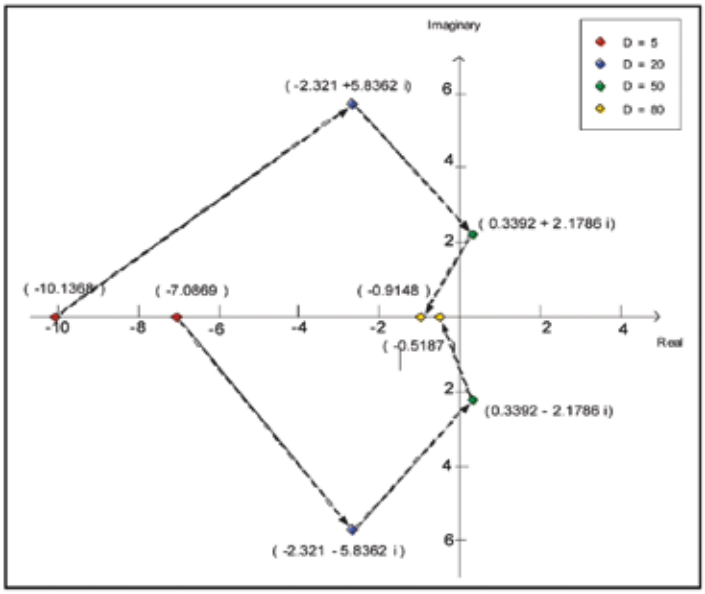

Fig. 20: Transition of stable point to limit cycle analyzed on system at K_C = 7

CONCLUSIONS

The evaluation of the model was discussed using both the graphical measures and mathematical analysis. Based on the observation of the graphs and discussions, some conclusions can therefore be put together. Modelling the operational stability of biocatalysts and considering modulation factors are required for a proper design of bioreactors. Temperature, as the key variable in such a bioprocess system, could be conveniently optimized through the use of appropriate models.

Three parameters were analyzed in this project; these were dilution rate (D), the proportional control constant (K_C) and the dimensionless total enzyme concentration (α). Each parameter discussed could have a different effect on the stability of the system, especially on the variables to be controlled in the dynamic equation, such as the dimensionless reactor

temperature (θ) and the dimensionless conversion of reactant (y). In some cases studied in this research, some Hopf bifurcations were formed in the phase-plane plot, indicating that there was a transformation in the stability loop from the stable node or spiral focus into limit cycle. The existence of the Hopf bifurcations had been successfully proven using the numerical technique and the eigenvalues analysis.

A study on the stability of such an exothermic biocatalytic reaction is very important as its results can be applied in the controlling process systems in optimum and stable conditions.

REFERENCES

Adrie J.J. Straathof and Adlercreutz, P. (2000). *Applied Biocatalysis,* 2nd ed., Harwood Academic Publishers.

Andrés I. (1999). Stability of biocatalysts. *Electronic Journal of Biotechnology, 2*(1).

Benkovic, S. and Ballesteros, A. (1997). Biocatalysts-the next generation. *Trends in Biotechnology, 15*, 385-386.

Briggs, G.E. and Haldane, J.B. (1925). A note on the kinetics of enzyme action. *Biochem J. 19*(2), 338-9.

Bommarius, A.S and Riebel, B.R. (2004). *Biocatalyst: Fundamentals and Applications*. Wiley-VCH.

Ourique, C.O., Evaristo, C.B. and Jose, C.P. (2002). The use of particle swarm optimization for dynamical analysis in chemical processes. *Computers and Chemical Engineering, 26*, 1783-1793.

Kaplan, D. and Glass, L. (1995). *Understanding Nonlinear Dynamics*. New York: Springer.

Donald, R. and Coughanowr, R. (1991). *Process Systems Analysis and Control* (2nd Edition). New York: McGraw-Hill.

Blanch, H.W. and Clark, D.S. (1996). *Biochemical Engineering*. U.S.A: Marcel Dekker Inc, U.S.A.

Henley, J. and Sadana, A. (1986). Deactivation theory. *Biotechnology and Bioengineering, 28*, 1277-1285.

Gibbs, P.R., Uehara, C.S., Neunert, U. and Bommarius, A.S. (2005). Accelerated biocatalyst stability testing for process optimization. *Biotechnol Prog* May-Jun, *21*(3), 762-74.

Koshland D.E. (1958). Application of a theory of enzyme specificity to protein synthesis. *Proc. Natl. Acad. Sci.* Feb; *44*(2), 98-104. U.S.A.

Lucia Russo and C.Silvestro. Nonlinear analysis of a network of three continuous stirred tank reactors with periodic feed switching: Symmetry and symmetry-breaking. *Int. J Bifurcation and Chaos, 14,* 1325-1341.

Noel M. and D. Combes. (2003). Effects of temperature and pressure on Rhizomucor miehei lipase stability. *Journal of Biotechnology*, 23-32.

Perez M., Font R. and Montava M.A. (2002). Regular self-oscillating and chaotic dynamics of a continuous stirred tank reactor. *Computers and Chemical Engineering, 26*, 889 – 901.

Parker H. (2005). Accelerated biocatalyst stability testing for process optimization. *Biotechnol Prog.*, *21*(3), 762-74.

Peter B. Kahn and Yair Zarmi. (1998). *Nonlinear Dynamics: Exploration through Normal Forms*. Wiley.

Polastro, E. (1989). Enzymes in the fine-chemicals industry: dreams and realities. *Bio/Technology 7,* 1238-1241.

Seborg D.E., Edgar Thomas F and Mellicamp, Duncan A. (2004). *Process Dynamic and Control. (*2nd Edition). Wiley-VCH.

Yeong S.K., Chang S.P. and Deok K. (2006). Lactulose production from lactose and fructose by a thermostable β-galactosidase from *Sulfolobus solfataricus. Enzyme and Microbial Technology, 39,* (4),903-908.

ISSN: 0128-7680
Pertanika J. Sci. & Technol. **17 (1)**: 117 – 123 (2009)

Physico-Mechanical Properties of the Josapine Pineapple Fruits

Rosnah Shamsudin[1*],Wan Ramli Wan Daud[2],
Mohd Sobri Takrif[2] and Osman Hassan[3]

[1]Department of Process and Food Engineering, Faculty of Engineering, Universiti Putra Malaysia, 43400 UPM, Serdang, Selangor, Malaysia
[2]Department of Chemical and Process Engineering, Faculty of Engineering, Universiti Kebangsaan Malaysia, 43600 UKM, Bangi, Selangor, Malaysia
[3]School of Chemical Sciences & Food Technology, Faculty of Science and Technology, Universiti Kebangsaan Malaysia, 43600 UKM, Bangi, Selangor, Malaysia
[*]E-mail: rosnahs@eng.upm.edu.my

ABSTRACT

The physico-mechanical properties data of fruits are important in the design of various handling, packing, and storage and transportation system. The physical-mechanical properties of pineapple fruit from the Josapine variety, namely the weight of the fruit (with and without peel), pulp to peel ratio, diameter of the whole fruit (with and without peel), at three different positions along the longitudinal axis of the fruit, length of the fruit (with and without peel) and the length of crown were studied using the standard method at seven stages of maturity during storage at 25°C and 52% (RH). The effect of fruit maturity on the firmness of each fruit at three different locations was measured using a cylindrical die of 6 mm in diameter with the Instron Universal Testing Machine. The results indicated that the average total weight of a single fruit is 886.86 ± 49.67 g. The average pulp to peel ratio is 1.91. The average diameter (with and without peel) was 86.83 ± 5.24 mm and 80.95 ± 4.15 mm (top section), 100.77 ± 3.84 mm and 90.19 ± 3.73 mm (middle section) and 97.17 ± 3.49 mm and 73.30 ± 5.11 mm (bottom section), respectively. The average length of the fruit (with and without peel) was 126.65 mm and 113.64 mm, respectively. The average length of crown was 89.13 mm. The firmness of the fruits was found to decrease with the stage of maturity. These data are important in determining the optimum stage of maturity for fruit processing.

Keywords: Diameter, firmness, Josapine, length, pineapple, stage of maturity

INTRODUCTION

Pineapple (*Ananas comosus* L.) is an important food crop which is planted extensively in the tropical and sub-tropical regions. It is one of the major commercial fruits in Malaysia, and is mainly used as fresh dessert fruits or for the preparation of canned pineapple in the form of slices or rings, juices and jams. There are five varieties of pineapples in Malaysia; these include Moris, Sarawak, Gandol, Josapine and N36. The Josapine is a hybrid, between 'Johor' ('Singapore Spanish' x 'Smooth Cayenne') and 'Sarawak' ('Smooth Cayenne') varieties, developed by the Malaysian Agriculture Research and Development Institute (MARDI) for the fresh fruit. It fruits very early. (120 days, after flower induction) allowing an annual plantation cycle in Malaysia. The vigorous plant produces two to three shoots and the leaves are spiny only at the tip. According to Abdullah and Rohaya (1997), the pineapple fruit can

Received: 2 July 2007
Accepted: 7 October 2008
[*]Corresponding Author

be divided into two major portions; namely, the fruit body and the crown. Each portion is different in terms of their morphological features, behaviour and characteristics.

Maturity at harvest is an important factor affecting the quality and the rate of change of quality during post harvest. The maturity indices can be determined in many ways, including the estimation of the duration of development; measurement of size, weight or density, physical attributes; (such as color, firmness and moisture content); as well as other chemical attributes such as starch, sugar or acid content or morphology evaluation (Shewfelt, 1993).

The common practice in the field for determine the ripeness fruit is by pressing with the thumb. For evaluating the mechanical properties of the fruits and vegetables, many investigators have used a rigid cylindrical die to study the load-deformation behavior of the fruit (Boussinesq, 1885; Timoshenko and Goodier, 1951; Finney, 1963). Today sophisticated devices have been developed for texture measurement in fruits and vegetables for example texture analyzers and pressure testers. The three commonly used pressure testers are the Magness-Taylor, UC Fruit Firmness testers and Instron Universal Testing Machine. Force deformation characteristics of agricultural products are important to simulate the destruction that occurs in bruising. A firmness of fruit is a useful indicator to estimate harvest maturity.

The objectives of the study were to determine (1) the physical properties, namely weight of fruit with and without peel, pulp to peel ratio, diameter of the whole fruit with and without peel at three different position along the longitudinal axis of the fruit, length of fruit with and without peel, length of crown; and (2) to determine the effect of fruit maturity on the firmness fruit, at three different locations of each fruit during storage at 25°C and 52%RH.

MATERIALS AND METHODS

Pineapple (*Ananas comosus* L.), from the Josapine variety, was obtained from a plantation in Johor, a southern state in Malaysia. The pineapples were harvested at stage of maturity 1. The stage of maturity was determined based on the standard specification and grade by Federal Agricultural Marketing Authority (FAMA, 2004). After harvesting, the fruits were stored at room temperature of 25°C, relative humidity (RH) of 52% until they reached the desired maturity stage required for the experiment. They were selected at seven different stages of maturity and the description for the various stages is given in Table 1. Each measurement was repeated three times, and the average values are reported.

Shape, Size and Weight of Fruit

The length and width of the whole Josapine pineapple fruit with and without peel were measured by keeping the fruit resting horizontal on its most stable position. The sample fruit was peeled manually using a knife. The diameter and length of the fruit with and without peel were determined by digital vernier calipers. The diameter of pineapple was recorded at three different locations of the whole fruit, i.e. top, middle and bottom section (*Fig. 1*). The top is defined as the end of the fruit where the crown is. The weight of the whole fruit with and without peel was recorded using the electronic balance. To determine the pulp to peel ratio, every individual pineapple is peel and pulp were weighed separately. The average values of three replications were reported.

Mechanical Properties of Fruit

Fruit firmness was determined by using an Instron universal testing machine (Model 5566, US) with a cylindrical die of 6 mm in diameter at 25°C. The load cell of Instron was 5000N

TABLE 1
Description on maturity stage

Maturity Stage	Description
1	immature fruit all eyes are glossy bluish dark green with reddish bractea (first day storage)
2	all eyes are glossy dark green with traces of yellow between eyes at base (4 days in storage)
3	eyes are dark green with 1-2 eyes yellowish green at base (5 days in storage)
4	about 25% of eyes, from the base, are yellow (6 days in storage)
5	about 50% of eyes are orangey yellow, half ripe fruit (7 days in storage)
6	more than 75% of the eyes are orangey yellow, three-quarter ripe fruit (8 days in storage)
7	full orangey yellow, fully ripe fruit (11 days in storage).

Source: Standard specification and Grade by FAMA

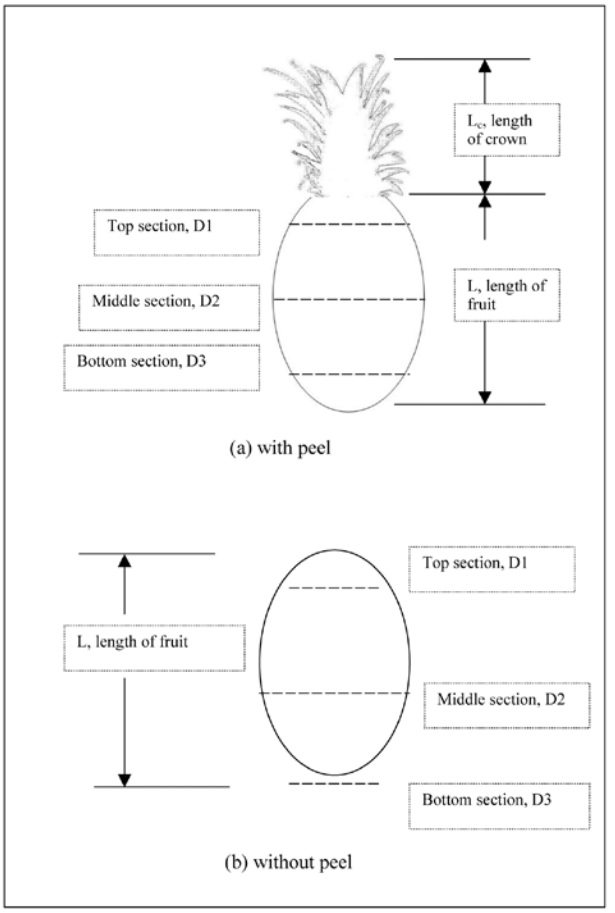

Fig. 1: Longitudinal section of pineapple fruit (a) with peel (b) without peel

with the crosshead speed fixed at 10 mm/min until rupture. The pineapple fruit was loaded in a horizontal position. Clamps were employed to hold a section of the pineapple fruit to determine the firmness of fruit. The individual pineapple fruit was compressed at three different location of each fruit namely (a) top section, (b) middle section and (c) bottom section as shown in *Fig. 2.* The three pineapple fruits were randomly taken from each stage of maturity for mechanical properties. The compression was started at the preset condition until rupture, occurred in the force-deformation curve. The rupture force was taken as the maximum peak force which required rupturing the peel of the fruit.

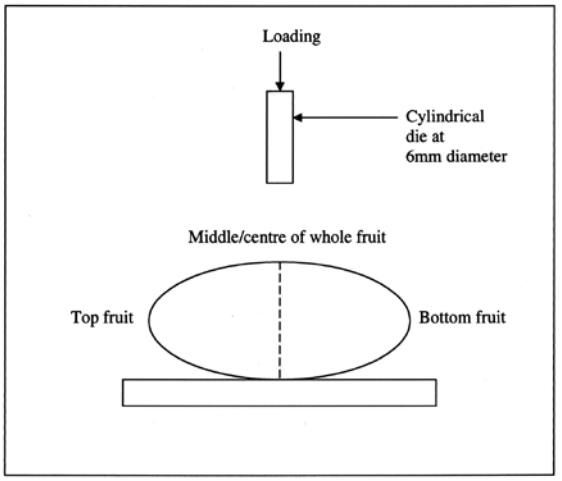

Fig. 2: Orientations of pineapple under compressive loading

RESULTS AND DISCUSSION

Table 2 shows the physical constituents of pineapple fruit from Josapine variety, as percentage of weight of the whole fruit and the pulp-peel-ratio. The total weight of a single whole fruit for pineapple varies between 800.38 g and 940.13 g with an average value of 886.86 g. The pulp to peel ratio of Josapine variety varies between 1.48 and 2.54 with an average of 1.91. According to Chan (1993), the average weight of other varieties like Gandul, Moris and Maspine are 1.6kg, 1.0kg and 1.76kg respectively. Thus, the weight of Josapine fruit was less than other varieties. The advantage of Josapine variety had improved acid content (0.63%), total soluble solid or TSS (16.8%) the plants are not spinney, ripen to full colour, yet remained firm and retained their flavours, resisted blemish and excellent in keeping quality (Chan, 1993).

Tables 3(a) and (b) shows the range of average diameter at three different locations of a whole Josapine pineapple fruit both with and without peel. The diameter of the Josapine pineapple fruit is at a maximum, in the middle portion and less at both the ends. The maximum and minimum observed diameters for this variety with peel were 106.93 mm and 77.07 mm, respectively. These values were 98.17 mm and 65.57 mm, respectively.

Tables 3(a) and (b) shows the length of fruit with and without peel. The maximum and minimum observed length of fruit with peel was 136.51 mm and 119.26 mm, respectively. These values for the fruit without peel were 124.59 mm and 103.49 mm respectively. The

TABLE 2
Constituents of pineapple fruit (Josapine variety)

	Total weight of a single fruit (g)	pulp (%)	peel (%)	Pulp/peel ratio
Maximum	940.13	67.50	37.50	2.54
Minimum	800.38	62.78	31.16	1.48
Average	886.86	65.29	34.71	1.91
Standard deviation	49.67	1.09	0.70	0.36

TABLE 3(a)
Diameter and length of Josapine pineapple fruit (with peel)

	With peel			
	Maximum	Minimum	Average	Standard deviation
D1 (mm)	94.60	77.07	86.83	5.24
D2 (mm)	106.93	93.85	100.77	3.84
D3 (mm)	101.26	90.38	97.17	3.49
L, Length of fruit (mm)	136.51	119.26	126.65	5.48
L_c, Length of crown (mm)	113.48	65.78	89.13	14.36

TABLE 3(b)
Diameter and length of Josapine pineapple fruit (without peel)

	Without peel			
	Maximum	Minimum	Average	Standard deviation
D1 (mm)	88.06	73.11	80.95	4.15
D2 (mm)	98.17	82.93	90.19	3.73
D3 (mm)	83.73	65.57	73.30	5.11
L, Length of fruit (mm)	124.59	103.49	113.64	5.39

average length for Josapine variety with and without peel was 126.65 mm and 113.64 mm respectively.

The pineapple crown is made up of a bunch of crown leaves, which physiologically behaves like leafy vegetable. The maximum and minimum length of the crown for Josapine pineapple fruit was 113.48 mm and 65.78 mm, with an the average was 89.13 mm.

Fig. 3 shows the force (N) required to rupture the peel of Josapine pineapple fruit at different stages of maturity under ambient storage. The force decreased with the stage of maturity from 74.79 N to 42.93 N (top position), 62.56 N to 37.20 N (middle position) and

57.14 N to 36.04 N (bottom position). The decrease in force is strongly influenced by the ripening process and storage period. This trend is in agreement with the results reported by Jha *et al.* (2005) for mango (32.96 N to 22.39 N, 288 hours in storage) and Krishna and Reddy (2005) for orange (15.6 N to 10.8 N, 10 days in storage). These phenomena could be due to changes in structure of the pectin polymers, during ripening in the cell wall (Jha *et al.*, 2005). Biochemical changes studies of the wall during fruit ripening indicated that there are structural changes in pectin, hemicellulose and cellulose. Fruit firmness was closely associated with the maturity stage. Mature green fruit had the highest penetration values and the yellow fruit had the lowest values (Edmundo Mercado-Silva *et. al.*, 1998; Jha, Kingsly and Sangeeta Chopra, 2005).

Fig. 3 shows the force required to rupture the peel of pineapple fruit is higher at the top position than at the bottom position. This might be due to the ripening process of pineapple fruit, which started at the bottom position and slowly propagated to the top position. Fruitlets in the lower portion of a fruit are more mature or ripe than the upper portion (Ramlah, 1981). Therefore, the force required to rupture the fruit was minimum at the bottom position.

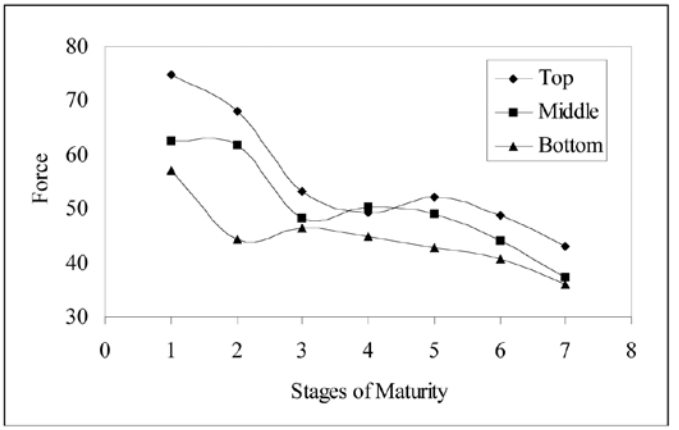

Fig. 3: Maximum load of the peel of the Josapine pineapple fruit

Fig. 3 shows the force increases after maturity 2 at bottom position maturity 3 at middle position, and maturity 4 at top position before decreasing further. According to Jha and Matsuoka (2002), during storage the fruit had started to rot and the epidermis probably loss its firmness and the inner surface provided a greater resistance to the compression and caused an increased temporarily. During storage period, the rotting process continued further and probably made the fruit softer which in turn to decrease the firmness continuously. The second phase of decreased in force was observed after stage of maturity 3, at bottom position, stage 4 at middle position and stage 5 at top position. This indicates that fruits firmness at bottom position start probably rotting 1 stage of maturity ahead of the fruits firmness at middle position. Similar trend was also observed for middle and top position. This may be attributed to the effect of ripening process.

CONCLUSIONS

As a conclusion, the average total weight of a single fruit of Josapine pineapple is 886.86 ± 49.67g. The average force observed that decreased with the stage of maturity during storage at 25°C and 52% (RH). The force required to rupture the peel of pineapple fruit is higher at the top position than at the bottom position when compressed using cylindrical die of 6 mm in diameter.

REFERENCES

Abdullah, H. and Rohaya, MA. (1997). Influence of maturity stage on quality of stored pineapple (*Ananas comosus* CV. Mauritius). *Journal of Bioscience 8*(2), 119 – 126.

Boussineq, J. (1885). Contact stresses between bodies in compression. In N.N. Mohsenin (Ed.), *Physical properties of plant and animal materials* (pp. 278-308). New York: Gordon and Breach Science Publishers.

Chan, Y. K. (1993). Recent advancements in hybridization and selection of pineapple in Malaysia. *Acta Horticulture 334 First International Pineapple Sysposium*, 33-44.

Mercado-Silva, Erdmundo, Benito-Bautista, Pedro and Ma Delus angeles Garcia-Velasco. (1998). Fruit development, harvest index and ripening changes of guavas produced in central Mexico. *Biology and Technology Post harvest, 13*, 143-150.

FAMA. (2004). *Analisis Industri Buah Nanas*. Kuala Lumpur.

Finney. (1963). Contact stresses between bodies in compression. In N.N. Mohsenin (Ed.), *Physical properties of plant and animal materials* (p. 278-308). New York: Gordon and Breach Science Publishers.

Jha S.N., Kingsly A.R.P. and Sageeta Chopra. (2005). Physical and mechanical properties of mango during growth and storage for determination of maturity. *Journal of Food Engineering, 72*, 73–76.

Jha, S.N. and Matsuoka. (2002). Surface stiffness and density of eggplant during storage. *Journal of Food Engineering, 54*, 23-26.

Ramlah, M. (1981). In H. Abdullah and M.A. Rohaya. Influence of maturity stage on quality of stored pineapple (*Ananas comosus* CV. Mauritius). *Journal of Bioscience, 8*(2), 119 – 126.

Shewfelt, R. L. (1993). Measuring quality and maturity. In *Handling Post harvest*. US: Academic Press Inc.

Timoshenko and Goodier. (1951). Contact stresses between bodies in compression. In N.N. Mohsenin (Ed.), *Physical properties of plant and animal materials* (p. 278-308). New York: Gordon and Breach Science Publishers.

ISSN: 0128-7680
Pertanika J. Sci. & Technol. **17 (1)**: 125 – 129 (2009)

Electrical Conductivity Studies in Polycrystalline $(CuSe)_{1-x}Se_x$

Zainal Abidin Talib[1*], Josephine Liew Ying Chyi[1], Zulkarnain Zainal[2], W. Mahmood Mat Yunus[1], Lim Kean Pah[1], Wan M Daud Wan Yusoff[1] and Mohd Maarof HA Moksin[1]

[1]Department of Physics, [2]Department of Chemistry, Faculty of Science, Universiti Putra Malaysia, 43400 UPM, Serdang, Selangor, Malaysia
[*]E-mail: zainalat@science.upm.edu.my

ABSTRACT

This studies are directed towards measuring the electrical conductivity of the $(CuSe)_{1-x}Se_x$ metal chalcogenide semi-conductor composites, with different stoichiometric compositions of Se (x = 0, 0.2, 0.4, 0.5, 0.6, 0.8,1.0) in bulk form. The electrical conductivity measurement was carried out at room temperature, using the parallel plate technique. The $(CuSe)_{1-x}Se_x$ composites were prepared using solid state reaction, by varying the ratio of CuSe:Se, in the reaction mixture. The electrical conductivity of $(CuSe)_{1-x}Se_x$ was determined to be in the range of 1.17×10^{-8} to 1.02×10^{-1} S/cm. The finding indicated that the electrical conductivity value tended to decrease as the concentration of Se increased. The effect of the concentration of Se, on electrical conductivity of $(CuSe)_{1-x}Se_x$ composites, is discussed in this paper.

Keywords: Electrical conductivity, $(CuSe)_{1-x}Se_x$ metal chalcogenide semi-conductor, stoichiometric, parallel plate techniques, solid state reaction

INTRODUCTION

Copper selenide (CuSe) is an interesting semi-conductor compound, with various applications in solar cells, super ionic conductors, photo-detectors, photovoltaic cells and Shottky-diodes (Lippkow and Strehblow, 1998; Pathan, Lokhande *et al.*, 2003). The attraction of copper selenide also lies in the feasibility of producing ternary material, i.e. $CuInSe_2$, by incorporating indium into this binary compound (Dhanam *et al.*, 2005). Copper selenide is a metal chalcogenide semi-conductor, with a wide range of stoichiometric compositions (CuSe, Cu_2Se, Cu_3Se_2, Cu_7Se_4, Cu_5Se_4, Cu_2Se) and non-stoichiometric composition ($Cu_{2-x}Se$) (Deevi, 2000; Dhanam *et al.*, 2005). $Cu_{2-x}Se$ or Cu_2Se is treated as copper (I) selenide, while CuSe, Cu_3Se_2 and $CuSe_2$ are treated as copper (II) selenide (Shafizade *et al.*, 1978; Nandakumar *et al.*, 1998; Hankare *et al.*, 2006). Copper (II) selenide, in the form of Cu_3Se_2, is often reported as an impurity phase, along with CuSe (Shafizade *et al.*, 1978; Pathan *et al.*, 2003). The copper selenide exists in various crystallographic forms, even at the room temperature. These include orthorhombic, monoclinic (Heyding and Murray, 1976), cubic (Grozdanov, 1994; Hankare *et al.*, 2006), tetragonal and hexagonal (Heyding and Murray, 1976; Perez-Robles *et al.*, 1999) forms, depending on the method of preparation used.

Selenium has good photovoltaic and photoconductive properties. It exhibits both photovoltaic action (where light is converted directly into electricity) and photoconductive action (where the electrical resistance decreases with the increasing illumination). These properties make selenium useful in the production of photocells and exposure meters for

Received: 11 January 2008
Accepted: 8 April 2008
[*]Corresponding Author

photographic use, as well as solar cells. In addition, selenium is extensively used in rectifiers to convert ac to dc electricity. Just like carbon and silicon, selenium is also known as a structuring element. It was expected that the mixture of the CuSe-Se composite material would affect the electrical properties, which have been extensively used in electronics, such as photocells, light meters as well as solar cells and solid-state applications. The investigation of the electrical transport phenomena, in those materials, is an important topic which is closely linked to their basic fundamental and physical properties.

In this paper, the electrical conductivity measurement of the $(CuSe)_{1-x}Se_x$ metal chalcogenide semi-conductor composites in bulk form, using the parallel plate technique, is presented to further fill in the information gap in the literature on the electrical properties of polycrystalline, $(CuSe)_{1-x}Se_x$ composites.

MATERIALS AND METHODS

The samples of $(CuSe)_{1-x}Se_x$ (x = 0, 0.2, 0.4, 0.5, 0.6, 0.8,1.0) were prepared using the solid state reaction method, with the stoichiometric mixtures of CuSe and Se. The starting CuSe (purity 99.5%) and Se (99.5%) were weighed based on the stoichiometric amount, and milled in the volumetric flasks for 24 hours with a magnetic stirrer. For this, ethanol was used as the mixing medium. The mixtures were then dried overnight in an oven, at the temperature around 75°C. After that, the dried $(CuSe)_{1-x}Se_x$ powder was weighed and placed into an 8 mm diameter mould, to form a pellet shape sample, using a hydraulic press (SPECAC USA, model 15011) of 3 tonne pressure.

The electrical conductivity of the samples used in this study was measured using the parallel plate technique. In this system, copper wires were attached to both ends of the pellet sample. Silver paint was applied to the surfaces of the pellet to serve as electrodes. The current I, which flowed through the sample, was measured by the Keithley 236 source measure unit consisting of a voltage source and current detector. The *I-V* characteristic showed a linear relationship; this indicated that a good ohmic junction was formed between the electrodes and the sample. The resistivity of the material was obtained by measuring the resistance and physical dimension of a material, based on the following expression:

$$\sigma = \frac{RA}{L} \tag{1}$$

where R is the resistance of the sample, A is surface area and L is the thickness of the sample. The electrical conductivity, σ was calculated from $\sigma = 1/\rho$.

RESULTS AND DISCUSSION

The XRD spectra of the polycrystalline $(CuSe)_{1-x}Se_x$ compounds (*Fig. 1*) show that the compound is a polycrystalline material. It can clearly be observed that the diffraction peaks corresponded to only the planes of CuSe and Se phase.

Fig. 2 shows the *I–V* curves for the $(CuSe)_{1-x}Se_x$ sample, with compositions $x = 0$, 0.2, 0.4, 0.5, 0.6, 0.8, 1. The *I-V* behaviour of this sample shows a linear behaviour for both forward and reverse bias conditions. The slope of the curve provides the conductance value which can be used to calculate the electrical conductivity of the sample.

Fig. 3 shows the electrical conductivity σ, as a function of composition x of the $(CuSe)_{1-x}Se_x$ samples. The conductivity was found to decrease drastically as Se replaced the CuSe in the $(CuSe)_{1-x}Se_x$ compound, from $x = 0$ to 1. The bulk electrical conductivity values of

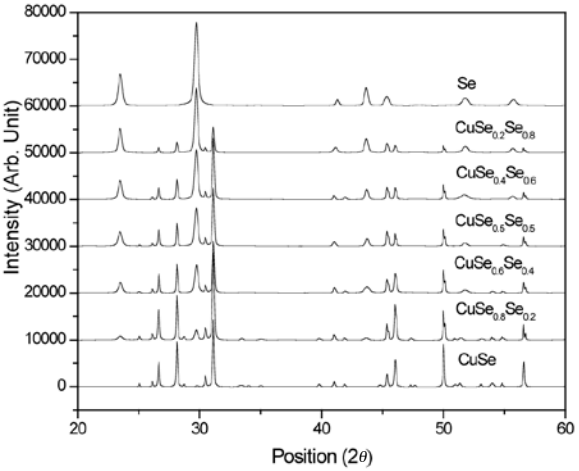

Fig.1: The XRD pattern of the $(CuSe)_{1-x}Se_x$ composites

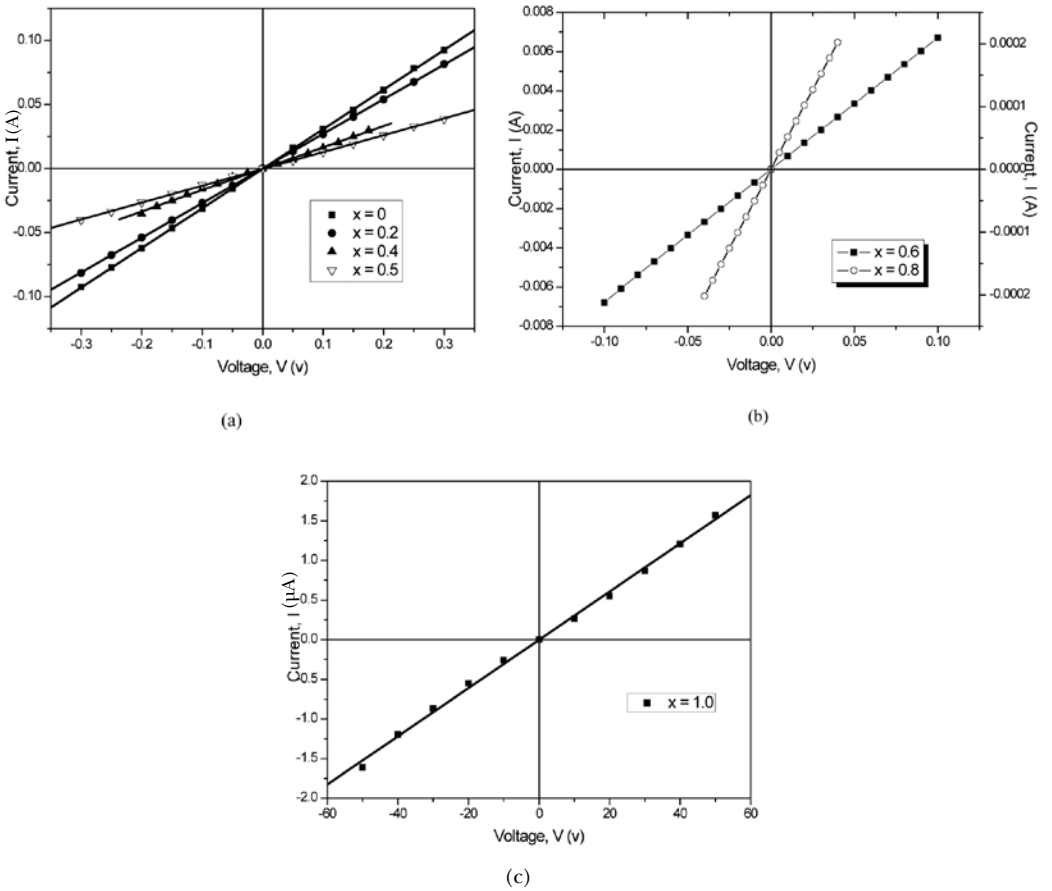

Fig. 2: The I-V characteristics for the $(CuSe)_{1-x}Se_x$ sample (a) x = 0, 0.2, 0.4, 0.5; (b) x = 0.6, 0.8; (c) x = 1

$(CuSe)_{1-x}Se_x$ were determined to be in the range of 1.17 x 10^{-8} to 1.02 x 10^{-1}S/cm. A larger value of electrical conductivity was observed at low Se content, suggesting that the electrons in the CuSe do play a role in the electrical conductivity. This is because the CuSe contains metallic copper inclusion, which positively contributes to the conductivity. The samples with higher Cu concentration were found to show a remarkably larger electrical conductivity as compared to the sample with higher Se concentration. When Se was added to $(CuSe)_{1-x}Se_x$, the Cu concentration decreased, and this in turn decreased the electrical conductivity of the composites.

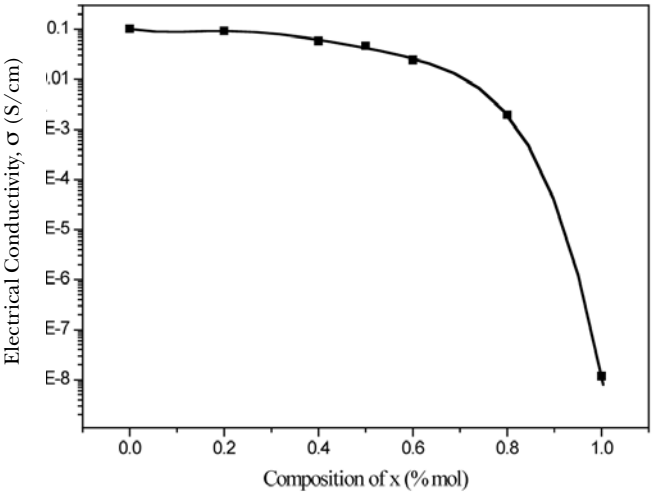

Fig. 3: The electrical conductivity σ for $(CuSe)_{1-x}Se_x$ at different compositions of x

CONCLUSIONS

$(CuSe)_{1-x}Se_x$ metal chalcogenide compounds had been successfully prepared using a solid state reaction, by varying the ratio of CuSe:Se in the reaction mixture. The electrical conductivity of $(CuSe)_{1-x}Se_x$ compounds, with different stoichiometric compositions of Se (x = 0, 0.2, 0.4, 0.5, 0.6, 0.8,1.0), was investigated using the parallel plate technique. The electrical conductivity values of the $(CuSe)_{1-x}Se_x$ compounds were determined to be in the range of 1.17 x 10^{-8} to 1.02 x 10^{-1} to S/cm, which corresponded to the compositions of Se, i.e. from x = 0 to 1.0. The electrical conductivity of the $(CuSe)_{1-x}Se_x$ composites was found to decrease when the composition of Se increased.

ACKNOWLEDGEMENTS

The authors would like to acknowledge Universiti Putra Malaysia, the Academy of Sciences, Malaysia, for their financial support - SAGA (5486512) and TORAY Foundation.

REFERENCES

Deevi, S.C. (2000). Powder processing of FeAl sheets by roll compaction. *Intermetallics, 8*(5-6), 679-685.

Dhanam, M., Manoj, P.K. and Prabhu, R.R. (2005). High-temperature conductivity in chemical bath deposited copper selenide thin films. *Journal of Crystal Growth, 280*(3-4), 425-435.

Grozdanov, I. (1994). Electroconductive copper selenide films on transparent polyester sheets. *Synthetic Metals, 63*(3), 213-216.

Hankare, P.P., Chate, P.A., Delekar, S.D., Bhuse, V.M., Asabe, M.R., Jadhav, B.V. and Garadkar, K.M. (2006). Structural and opto-electrical properties of molybdenum diselenide thin films deposited by chemical bath method. *Journal of Crystal Growth, 291*(1), 40-44.

Heyding, R.D. and Murray, R.M. (1976). The crystal structures of $Cu_{1.8}Se$, Cu_3Se_2, α- and γ CuSe, $CuSe_2$, and $CuSe_2$II. *Canadian Journal of Chemistry, 54*(6), 841-848.

Keithley Instruments, I. (2005). Determining resistivity and conductivity type using a four-point collinear probe and the Model 6221 Current Source. Application Note Series, www.keithley.com. 2615.

Lippkow, D. and Strehblow, H.H. (1998). Structural investigations of thin films of copper-selenide electrodeposited at elevated temperatures. *Electrochimica Acta, 43*(14-15), 2131-2140.

Nandakumar, P., Dhobale, A.R., Babu, Y., Sastry, M.D., Vijayan, C., Murti, Y.V.G.S., Dhanalakshmi, K. and Sundararajan, G. (1998). Photoacoustic response of CdS quantum dots in Nafion. *Solid State Communications, 106*(4), 193-196.

Pathan, H.M., Lokhande, C.D., Amalnerkar, D.P. and Seth, T. (2003). Modified chemical deposition and physico-chemical properties of copper(I) selenide thin films. *Applied Surface Science, 211*(1-4), 48-56.

Perez-Robles, J.F., Garcia-Rodriguez, F.J., Yanez-Limon, J.M., Espinoza-Beltran, F.J., Vorobiev, Y.V. and Gonzalez-Hernandez, J. (1999). Characterization of sol-gel glasses with different copper concentrations treated under oxidizing and reducing conditions. *Journal of Physics and Chemistry of Solids, 60*(10), 1729-1736.

Shafizade, R.B., Ivanova, I.V. and Kazinets, M.M. (1978). Electron diffraction study of phase transformations of the compound CuSe. *Thin Solid Films, 55*(2), 211-220.

ISSN: 0128-7680
Pertanika J. Sci. & Technol. **17 (1)**: 131 – 136 (2009)

Impedance Studies on $Ca_{0.5}Sr_{0.5}Cu_3Ti_4O_{12}$ Ceramic Oxide

Mazni Mustafa, W. Mohamad Daud W. Yusoff*, Zainal Abidin Talib, Abdul Halim Shaari and Walter Charles Primus

Department of Physics, Faculty of Science, Universiti Putra Malaysia, 43400 UPM, Serdang, Selangor, Malaysia

**E-mail: wmdaud@science.upm.edu.my*

ABSTRACT

$Ca_{0.5}Sr_{0.5}Cu_3Ti_4O_{12}$ (CSCTO) ceramic oxide was prepared using solid state reaction technique. Impedance measurement was done using High Dielectric Resolution Analyzer (Novocontrol Novotherm) from 30 °C to 250 °C, in the frequency range of 10^{-2} to 10^6 Hz. X-ray diffraction pattern showed a single phase with a cubic structure. In the complex impedance plot, three semi-circles were observed; these represented the grain, grain boundary and electrode effect responses. The semi-circles were fitted using a series network of three parallel RC circuits. The resistance was found to increase with the decreasing temperature. The activation energies, E_a, obtained from the Arrhenius plots of CSCTO, were 0.31 eV and 0.73 eV for grain and grain boundary conductivity, respectively. The value of the grain energy was revealed as smaller than the grain boundary energy, due to the semi-conducting grain and the insulating grain boundary characteristic (Sinclair *et al.,* 2002).

Keywords: CCTO, impedance, grain boundary, Arrhenius

INTRODUCTION

The $ACu_3Ti_4O_{12}$ family of compounds has been known since 1967, and most exceptional behaviour was exhibited by the $CaCu_3Ti_4O_{12}$ (CCTO) ceramics. The CCTO was first synthesized in 1979, and has a cubic perovskite structure with space group *Im*-3 (Bochu *et al.*, 1979). The CCTO shows a giant dielectric response and has an extremely high value of dielectric constant ε', at 1 kHz of about 10,000 (Subramanian *et al.*, 2000). Based on the impedance spectroscopy (IS), a high permittivity is associated to an "extrinsic" effect, due to an internal barrier layer capacitance (IBLC) effect, where insulating surfaces or grain boundaries are formed on the semi-conducting grains during the processing of the CCTO ceramics (Guillemet-Fritsch *et al.*, 2006). It was reported that most compositions of $A_{2/3}Cu_3Ti_4O_{12}$ (A = trivalent rare earth) showed dielectric constants above 1000 at 100 kHz. Those of the compositions $ACu_3Ti_4O_{12}$ (A = Ca, Sr or Ba) also showed dielectric constants above 1000, except for $BaCu_3Ti_4O_{12}$, which revealed a value below 1000 (Ohwa *et al.*, 2004). In this article, the microstructures of both CCTO and strontium substituted CCTO (CSCTO) are reported. The impedance properties of the CSCTO were also studied at different temperatures.

THEORY

The frequency dependent properties of a material can be described in four possible complex formalisms; these are complex permittivity ($\varepsilon^*=\varepsilon'-i\varepsilon''$), complex impedance ($Z^*=Z'-iZ''$),

Received: 11 January 2008
Accepted: 8 April 2008
*Corresponding Author

complex admittance ($Y^*=Y'+iY''$), and complex electric modulus ($M^*= M' + iM''$). The above formalisms are interrelated as:

$$\varepsilon^* = \frac{1}{iwZ^*C_o} = \frac{Y^*}{iwC_o} = \frac{1}{M^*} \quad (1)$$

Where, $C_o = \varepsilon_o A/d$, A is the area, d is the thickness of the sample, ω is the angular frequency ($2\pi f$) and $\varepsilon_o = 8.854 \times 10^{-14}$ Fcm^{-1} is the permittivity of free space.

The complex impedance plot was fitted using the universal capacitor $C^* = B\ (i\omega)^{n-1}$, where B is a constant, n lies in the range $0 < n < 1$, and R is the resistance. The resistivity ρ was calculated using $\rho = RA/d$, where R is the resistance value from the fitting results, A is the area and d is the distance. The conductivity σ was calculated using the resistivity data by equation $\sigma = 1/\rho$. The conductivity σ follows the Arrhenius law and can be described by the following expression:

$$\sigma = \sigma_o \exp(-E_a/kT) \quad (2)$$

where E_a is the activation energy, and k is the Bolzmann's constant.

MATERIALS AND METHODS

$CaCu_3Ti_4O_{12}$ (CCTO) and strontium substituted CCTO (CSCTO) ceramics were prepared, using solid state reaction technique, from the raw materials such as calcium carbonate ($CaCO_3$), strontium carbonate ($SrCO_3$), titanium dioxide (TiO_2) and copper (II) oxide (CuO). These materials were weighed according to the stoichiometric ratios and were ground for 3 hours. The mixed powders were calcined at 900 °C for 10 hours. The calcined powder was reground for 2 hours to improve its homogeneity, before sintering in air at 1050 °C for 24 hours in powder and pellet forms. The XRD was done on the sintered powder to monitor the phase evolution using Philips (Model PW3040). After that, these sintered pellets were polished to achieve flat and parallel surfaces and were sputtered with silver as electrode, using the RF Magnetron Sputtering. The impedance measurement was done from 30 °C to 250 °C, in the frequency range of 10^{-2} to 10^6 Hz, using a High Dielectric Resolution Analyzer (Novocontrol Novotherm).

RESULTS AND DISCUSSION

The XRD patterns for both CCTO and CSCTO are shown in *Fig. 1.* The patterns show single phases for both samples, while cubic structure with calculated lattice parameter a = 7.4041 Å was compared to 7.3590 Å (Jha *et al.,* 2003). *Fig. 2* shows the SEM images of the surfaces of the CCTO and CSCTO. The morphology shows grain and grain boundary for both the samples. The grain size for the CSCTO is much larger than the CCTO grain size.

The complex impedance provided the grain and the grain boundary effects, as well as the capacitive, C and resistive, R element of the samples. Using the fitting approach of the universal capacitor, $C^* = B\ (i\omega)^{n-1}$, the grain and grain boundary effects could be separated due to the existence of the semi-circles.

Fig. 3(a) shows complex impedance plots for the CSCTO at selected temperatures of 190 °C and 230 °C. The graphs show three semi-circles, as illustrated in *Fig. 3(b).* The high frequency semi-circle is attributed to the grain properties, while the second semi-circle is

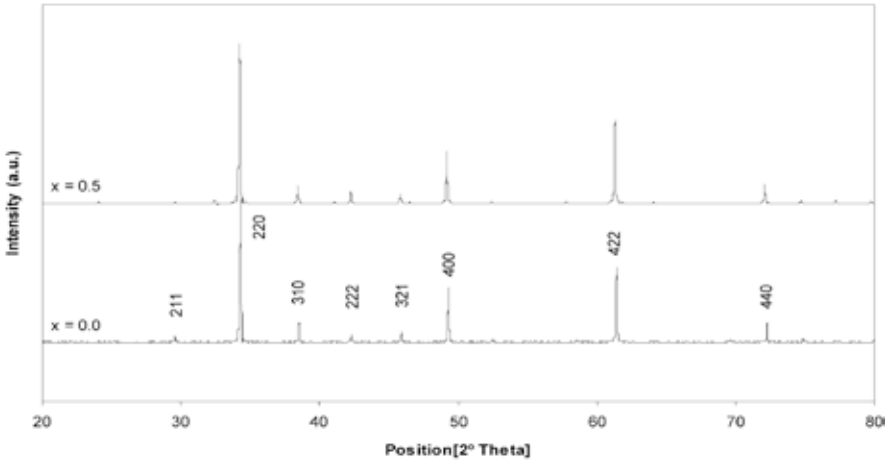

Fig. 1: X-ray diffraction patterns of both CCTO and CSCTO

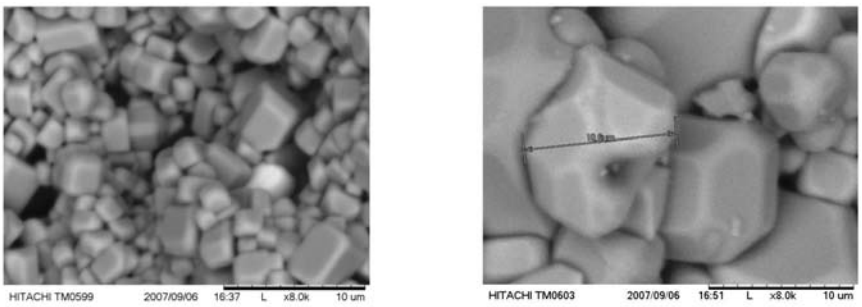

Fig. 2: Electron micrographs for (a) CCTO, and (b) CSCTO consisting of grain and grain boundary

assigned to the grain boundary properties. The third semi-circle, at the low frequency, is due to the electrode effects. The presence of the three semi-circles are modelled as an equivalent electrical circuit, which comprises a combination of the series network of three parallel RC circuits, as depicted in *Fig. 4*. The fitting parameters for the CSCTO are listed in Table 1. The grain resistance (R_g) and grain boundary resistance (R_{gb}) were obtained from the intercept of the semi-circles on the real axis, Z'. It could obviously observed that the resistance was increased when the temperature decreased from 230 °C to 70 °C. The frequency peak ω_p was also found to increase as the temperature increased. The semi-circles were inclined at an angle of $n\pi/2$, where the n values for the grain region were increased from 0.98 to 1 as the temperature decreased. The n values for the grain boundary region were in the range of 0.70 to 0.80, between 70 °C to 230 °C. If n = 1, the universal capacitor would give an ideal capacitor, where $C^* = C$. As for the grain region, a pure C was observed, while at the grain boundary region, the universal capacitor gave both capacitance and resistance.

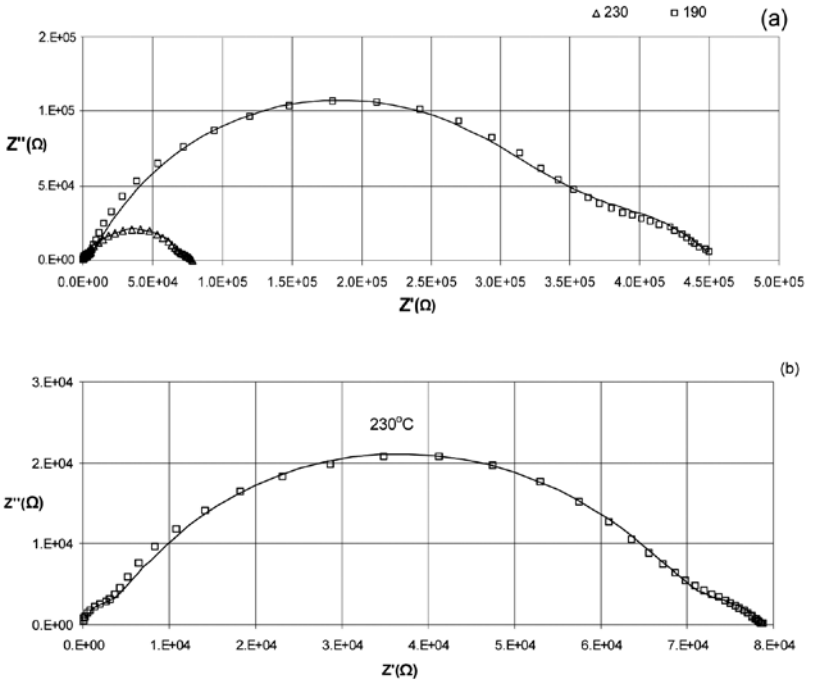

Fig. 3: (a) Complex impedance plots of CSCTO ceramics, with equivalent circuit modelling, at selected temperatures of 190 °C and 230 °C; (b) Complex impedance plots of the CSCTO ceramics, with equivalent circuit modelling at 230 °C

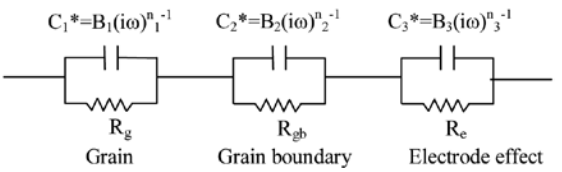

Fig. 4: The equivalent circuit used to model the CSCTO response

Fig. 5 shows the conductivity of the grain and grain boundary of the samples against the reciprocal temperature. The activation energy, E_a values for the CSCTO were 0.31 eV and 0.73 eV for the grain and grain boundary conductivity, respectively. The activation energy value of the grain is smaller than the grain boundary because of its characteristic, i.e. the grain possesses a semi-conducting behaviour, which is more conducting than the grain boundary; the grain boundary is insulating, or known also as an internal barrier layer capacitor (IBLC) which needs much lower energy to stimulate the charge carrier by thermal activation (Sinclair *et al.*, 2002).

TABLE 1
The list of fitting parameters for grain, grain boundary and electrode effects for CSCTO at 70 °C, 110 °C, 150 °C, 190 °C and 230 °C

Temperature oC	Universal Capacitor			Resistance
Grain	$B_1(\Omega Hz)^{-1}$	n_1	ω_p (Hz)	R_g (Ω)
70°C	1.81×10^{-10}	1.00	20000	44000
110°C	6.63×10^{-11}	1.00	120000	20000
150°C	9.95×10^{-11}	1.00	200000	8000
190°C	1.18×10^{-10}	1.00	320000	4200
230°C	1.72×10^{-10}	0.98	500000	2500
Grain Boundary	$B_2(\Omega Hz)^{-1}$	n_2	ω_p (Hz)	R_{gb} (Ω)
70°C	3.68×10^{-9}	0.80	0.4	130000000
110°C	6.99×10^{-9}	0.67	4	16500000
150°C	1.95×10^{-8}	0.64	20	2320000
190°C	1.76×10^{-8}	0.70	250	330000
230°C	1.99×10^{-8}	0.70	2000	68000
Electrode Effect	$B_3(\Omega Hz)^{-1}$	n_3	ω_p (Hz)	R_e (Ω)
70°C	8.07×10^{-8}	0.80	0.02	82000000
110°C	2.99×10^{-7}	0.60	0.03	9100000
150°C	1.89×10^{-6}	0.58	0.07	850000
190°C	2.29×10^{-6}	0.51	2	120000
230°C	1.71×10^{-5}	0.55	5	8800

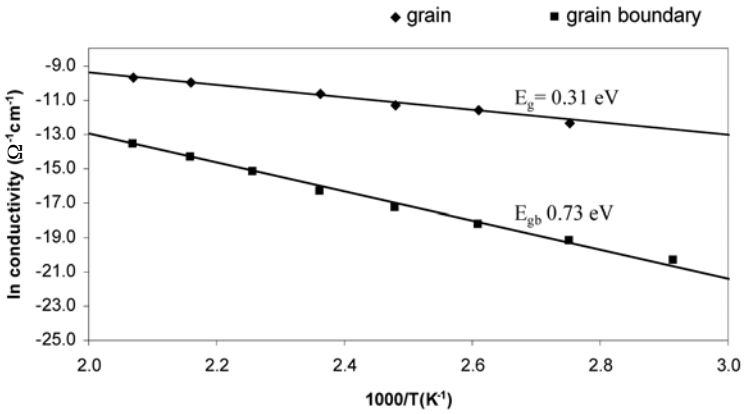

Fig. 5: The Arrhenius plots of (a) the grain conductivity, and (b) grain boundary conductivity of the CSCTO ceramic sintered at 1050°C

CONCLUSIONS

The XRD patterns for the CSCTO show a single phase with a cubic structure. The dielectric response of the polycrystalline CSCTO yielded three semi-circles and are modelled by a series combination of three parallel RC circuits representing grain, grain boundary and electrode effect response. The activation energy, E_a value for the CSCTO is 0.31 eV and 0.73 eV for grain and grain boundary regions, respectively.

ACKNOWLEDGEMENTS

The authors gratefully acknowledge the research grant given by the Ministry of Science, Technology and Innovation, Malaysia (MOSTI), under the Fundamental Research vote no. (5523122) and the Department of Physics, Universiti Putra Malaysia.

REFERENCES

Bochu, B., Deschizeaux, M.N., Joubert, J.C., Collomb, A., Chenavas, J. and Marezio, M. (1979). Synthese et caraterisation d'une serie de titanates perowskites isotypes de [$CaCu_3$] (Mn_4)$O_{12,}$ *J. Solid State Chem, 29,* 291–298.

Ohwa, H., Iwata, M. and Ishibashi, Y. (2004). Dielectric properties in $ACu_3Ti_4O_{12}$ (A = Ca, Sr, Ba). *Ferroelectrics, 301,* 185-189.

Subramanian, M.A., Li, D. and Duan, N. (2000). High dielectric constant in $ACu_3Ti_4O_{12}$ and $ACu_3Ti_4Fe_{12}$ phases, *J. Sol. St. Chem. 151,* 323-325.

Jha, P. Arora, P. and Ganguli, A.K. (2003). Polymeric citrate precursor route to the synthesis of the high dielectric constant oxide, $CaCu_3Ti_4O_{12.}$ *Materials Letters, 57*(16-17), 2443 - 2446.

Guillemet-Fritsch, S., Lebey, T., Boulos, M. and Durand, B. (2006). Dielectric properties of $CaCu_3Ti_4O_{12}$ based multiphase ceramics. *Journal of the European Ceramic Society, 26*(7), 1245-1257.

Sinclair, D.C., Adams, T.B., Morrison, F.D. and West, A.R. (2002). $CaCu_3Ti_4O_{12.}$ One-step internal barrier layer capacitor. *Applied Physics Letters, 80*(12), 2153.

ISSN: 0128-7680
Pertanika J. Sci. & Technol. **17 (1)**: 137 – 147 (2009)

Physicochemical Characterisation and Substrate Specificity of Purified β-1,6-glucanase from *Trichoderma longibrachiatum*

Muskhazli Mustafa*, Nor Azwady Abd. Aziz, Anida Kaimi, Nurul Shafiza Noor, Salifah Hasanah Ahmad Bedawi and Nalisha Ithnin
Department of Biology, Faculty of Science, Universiti Putra Malaysia, 43400 UPM, Serdang, Selangor, Malaysia
**E-mail: muskhazli@science.upm.edu.my*

ABSTRACT

The β-1,6-glucanases are ubiquitous enzymes which appear to be implicated in the morphogenesis and have the ability to become virulence factor in plant-fungal symbiotic interaction. To our knowledge, no report on ß-1,6-glucanases purification from *Trichoderma longibrachiatum* has been made, although it has been proven to have a significant effect as a biocontrol agent for several diseases. Therefore, the aim of this study was to purify β-1,6-glucanase from *T. longibrachiatum* T28, with an assessment on the physicochemical properties and substrate specificity. β-1,3-glucanase enzyme, from the culture filtrate of *T. longibrachiatum* T28, was successively purified through precipitation with 80% acetone, followed by anion-exchange chromatography on Neobar AQ and chromatofocusing on a Mono P HR 5/20 column. (One β-1,6-glucanase) band at 42kDa in size was purified, as shown by the SDS-PAGE. The physicochemical evaluation showed an optimum pH of 5 and optimum temperature of 50°C for enzyme activity with an ability to maintain 100% enzyme stability. Enzyme activity was slightly reduced by 10-20% in the presence of 20 mM of Zn^{2+}, Ca^{2+}, Co^{2+}, Mg^{2+}, Cu^{2+}, Mn^{2+} and Fe^{2+}. The highest β-1,6-glucanase hydrolysis activity was obtained on pustulan due to the similarity of β-glucosidic bonds followed by laminarin, glucan and cellulose. Therefore, it can be concluded that the characterization of ß-1,6-glucanase secreted by *T. longibrachiatum* in term of molecular weight, responsed to selected physicochemical factors and the substrate specificity are approximately identical to other *Trichoderma sp.*

Keywords: β-1,6-glucanase, characterisation, metal ion, pH, purification, substrate specificity, *Trichoderma longibrachiatum*

INTRODUCTION

Filamentous fungi of the genus *Trichoderma* have long been recognized as the agents for the biocontrol of plant diseases (Ridout *et al.*, 1988) which can directly impact mycelia or the survival propagules of other fungi through the production of toxic secondary metabolites (Benitez *et al.,* 2004), formation of specialized structures (Sarrocco *et al.,* 2006) and secretion of cell wall degrading enzymes (Noronha and Ulhoa, 1996). The most common cell wall degrading enzymes are chitinase, ß-1,3-glucanase, ß-1,6-glucanase and proteinases (Haran *et al.*, 1995; Haran *et al.*, 1996; Lorito *et al.*, 1996). The secretion of these enzymes was proposed to be regulated by catabolite repression (Lorito *et al.,* 1996) and the presence of fungal cell walls (Djonovic *et al.,* 2006). Chitin and ß-1,3-glucans were considered as the major components in the cell wall, while β-1,6-glucan represented relatively minor components of

Received: 11 January 2007
Accepted: 8 April 2008
*Corresponding Author

the fungal cell walls (Lora *et al.*, 1995) and plants were found to lack β-1,6-glucan altogether (Inbar and Chet, 1994). Due to this factor, chitinase and ß-1,3-glucanase have been proposed as the key enzymes in mycoparasitism against phytopathogenic fungi (Elad *et al.,* 1982), whereas less attention has been given to the function of ß-1,6-glucanase.

The existence of ß-1,6-glucanase has been known for almost five decades (Delgado-Jarana *et al.*, 2000). Endo-ß-1,6-glucanase was shown to act cooperatively with chitinase to hydrolyse fungal cell walls of *B. cinerea, Gibberella fujikuroi, Phytophthora syringe* and *Saccharomyces cerevisiae* (de la Cruz *et al.*, 1993). The β-1,6-glucanases are ubiquitous enzymes which appear to be implicated in the morphogenesis such as the synthesis of β-1,6-glucan of cell walls in *S. cerevisiae* (Cid *et al.*, 1995) and *S. commune* (Khun *et al.,* 1990), mobilisation of an extracellular storage glucan (Stasinopoulos and Seviour, 1989), and digestive metabolism in invertebrates (Papavizas, 1985). In plant-fungal symbiotic interaction, ß-1,6-glucanase was identified as being secreted by *Trichoderma* sp. into the apoplast of the host grass; *Poa ampla*, upon attack by its endophytic fungus, *Neotyphodium* sp. (Moy *et al.,* 2002). Recently, ß-1,6-glucanase has also been shown to be a virulence factor in the interaction between the mycopathogen *Verticillium fungicola* and its host, *Agaricus bisporus* (Amey *et al.,* 2003).

Even though ß-1,6-glucanases have been purified from several filamentous fungi, including *Penicillium brefeldianum* (Schep *et al.,* 1984), *Acermonium* sp. (Martin *et al.,* 2006), *Acremonium persicinum* (Pitson et al., 1996) *Saccharomycopsis fibuligera* (Mulenga and Berry, 1994) and *T. harzianum* (de la Cruz *et al.,* 1995), their physiological function has not been conclusively studied. The current knowledge on ß-1,6-glucanases is still limited to the studies on biochemical and lytic properties of purified enzymes (Montero *et al.*, 2005).

To our knowledge, no report on ß-1,6-glucanases purification from *T. longibrachiatum* has been made, although it has been proven to have a significant effect as a biocontrol agent for groundnut rot (Sreenivasaprasad and Manibhusanrao, 1990; 1993) and coffee pulp (Onsando and Waudo, 1992). Therefore, the aim of this study was to purify β-1,6-glucanase from *T. longibrachiatum* T28. In the current study, the physicochemical properties and the substrate specificity of the purified β-1,6-glucanase were also assessed.

MATERIALS AND METHODS

Strains and Growth Conditions

The *T. longibrachiatum* T28 was obtained from Plant Systematic and Microbe Laboratory, Biology Department, Universiti Putra Malaysia and maintained on the Malt Yeast Glucose Agar (MYG) slant.

The Preparation of Crude Culture

The preparation of the test strain culture was carried out using the sub-cultured *T. longibrachiatum* T28 from the slant agar to the MYG plate culture and incubated at 32°C. After 4 days, $1x10^7$ spores.ml^{-1} of *T. longibrachiatum* T28 were prepared and added into Trichoderma Complete Medium (pH 5.5), which was supplemented with 0.5% (w/v) glucose. The seed cultures were then shaken (180rpm) at 32°C for 24 hours, before the seed cultures were filtered and washed thoroughly with sterile distilled water. After that, the seed cultures were transferred into the Trichoderma Minimal Medium (pH 5.5; 1.0% w/v *Pleurotus sajor-caju* mycelium) and shaken at 180rpm at 32°C for another 72 hours. The culture filtrate was collected, dialysed against distilled water, for at least 24 hours at 4°C before it was ready to be used for enzyme purification. The β-1,6-glucanase activity and protein concentration were determined as below.

Enzyme Assays

β-1,6-glucanase activity was determined using the method described by Somogyi (1952) in measuring the amount of reducing sugars released from pustulan. One enzymatic unit (U) of β-1,6-glucanase activity is defined as the amount of enzyme which releases 1μmol of glucose in 1 hour at 45°C.

The determination of protein was performed using Bio-Rad protein assay kit, based on the method by Bradford (1976). The mixture of distilled water and Bio-Rad reagent was used as control, and the standard curve for the protein was plotted using bovine serum albumin in the range of 0-20μg.

β-*glucanase Purification*

Unless indicated, all the steps in the purification process were carried out according to the method used by Muskhazli *et al.* (2005) and performed at 4°C. The purification process was performed in three steps; these comprised of acetone precipitation, followed by anion-exchange step using Neobar AQ column and ended with chromatofocusing step performed on a Mono P HR 5/20 column. In each step, all the active fractions were pooled and dialysed against distilled water for 24h at 4°C before they were assayed for β-1,6-glucanase activity and protein content. Discontinuous sodium dodecyl sulfate-polyacrylamide gel electrophoresis (SDS-PAGE) was also carried out on the collected fraction, according to Laemmli (1970), i.e. using 10% acrylamide gels and stained with Coomasie R-250 brilliant blue (Sigma). Low molecular range standard proteins were used to determine the molecular mass.

Physicochemical Parameters and Substrate Specificity

The optimal temperature for β-1,6-glucanase activity, was determined by measuring the reducing sugars released, after 30 minutes of incubation at the temperatures between 25°C-75°C, i.e. at an increment of 5°C. Meanwhile, the temperature stability for the β-1,6-glucanase activity was examined by maintaining the purified β-1,6-glucanase for 1 hour at the temperatures between 25°C-75°C, at the increment of 5°C, before the β-1,3-glucanase activity was determined.

The effect of pH on the enzyme activity was determined by varying the pH of the reaction mixture between pH 4-8, at the increment of 1 pH unit. The pH of the mixture was adjusted to the intended pH, with 50mM sodium citrate buffer. The stability of the pH was determined by incubating the purified β-1,6-glucanase enzyme, at pH 4-8 for 1 hour at 37°C, before the pH was changed to pH 5, prior to the activity determination of β-1,6-glucanase.

In addition, the effects of several metal ions on the activity of β-1,6-glucanase were also investigated. The metal ions used for this study were Zn^{2+}, Co^{2+}, Ca^{2+}, Mn^{2+}, Mg^{2+}, Fe^{2+} and Cu^{2+}. Twenty millimolar (20mM) of metal ion solution, in sodium acetate buffer pH 5.5, was prepared and added into the purified β-1,6-glucanase enzyme before the activity was determined.

The β-1,6-glucanase activity, on several substrates, was also determined. These included pustulan (1.0% w/v), laminarin (1.0% w/v), cellulose (1.0% w/v) and glucose (1.0% w/v). Each substrate was prepared in 0.05M sodium acetate buffer pH 5.5.

RESULTS AND DISCUSSION

β-*glucanase purification*

Acetone precipitation, at 80% saturation, was found to be capable of recovering 58.70% of the total β-1,6-glucanase activity from the culture filtrates. The precipitated protein was

dialysed, dissolved in distilled water, and labelled as crude enzyme. The crude enzyme, from *T. longibrachiatum* T28, showed β-1,6-glucanase activities at 20.61U. The elution pattern for the anion exchange chromatography of the crude enzyme fraction is shown in *Fig. 1a.* Based on the data presented in the figure, fractions 4-10 is shown to correspond in protein and β-1,6-glucanase activity. This pooled fraction was later designated as T28 (G1), and it has β-1,6-glucanase activity of 8.85U, i.e. equivalent to 25.21% of the total activity (Table 1). The analysis of the pooled fractions, using the SDS-PAGE, showed that 5 bands virtually appeared for T28 (G1), with the molecular weight aproximately at 31kDa, 45kDa, 66.2kDa, 96kDa and 97.4kDa *(Fig. 1c).* Meanwhile, the elution profiles for T28 (G1), during chromatofocusing, are depicted in *Fig. 1b*, and from this, only one major peak for β-1,6-glucanase activity was obtained from fractions 49-51, which comprised 8.43% of the total enzyme activity (2.96U). The analysis of the pool, corresponding to these fractions using the SDS-PAGE, revealed only one major band with a calculated molecular mass of about 45kDa (*Fig. 1c*). The existence of the purified β-1,6-glucanase, in the range of 41kDa to 53kDa, has been reported previously. The molecular weight sizes of ß-1,6-glucanase, from different species, have been reported to be in the range of 41kDa to 53kDa. These include ß-1,6-glucanase from *T. viride* with a molecular weight of 45kDa (Nobe *et al.*, 2003), *T. harzianum* at 46kDa (Moy *et al.*, 2002) and 47kDa (Montero *et al.*, 2005). Several other isoforms or sub-units of β-1,6-glucanase from *T. harzianum* with different catalytic activities, molecular weights and substrate specificities have also been previously reported; these were with different molecular weights of 43kDa and 51kDa (de La Cruz, 1995).

TABLE 1
Summary of the purification steps and enzyme activity for each step involved in a typical purification of β-1,6-glucanase

Steps	Fractions	Enzyme activity (U)	Yield (%)
Culture filtrate		35.11	100
Acetone precipitation		20.61	58.70
Anion exchange	4-10	8.85	25.21
Chromatofocusing	49-51	2.96	8.43

However, the difference in the molecular weight of the purified β-1,6-glucanase is not new because the molecular mass of β-glucanase has appeared to vary between species and also within species (Pitson *et al.*, 1993). Nevertheless, it is not known whether the existence of the isoform or different molecular weights of this enzyme was the product of or as a result of the same or separated β-1,6-glucanase genes. According to Mrsa *et al.* (1993), one of the reasons for the differences is attributed to the anomalous migration of protein in the gels rather than to the post-translation processing of the polypeptide chain, and sometimes, the type of growth substrate used can also influence the number of bands on the SDS-PAGE (Vazquez-Garciduenas *et al.,* 1998) or the activation of a specific gene (Montero *et al.,* 2005). Furthermore, according to Matsuzawa *et al.* (1996), species, the type of reactions (exo- or endo-) and the method of purification may also impose effect on characterization, even for the purified β-glucanase of the same type.

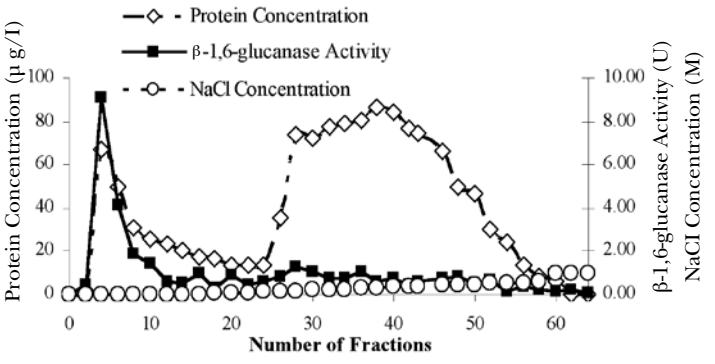

(a)

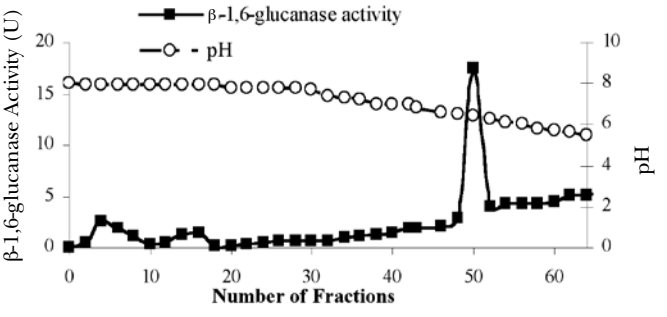

(b)

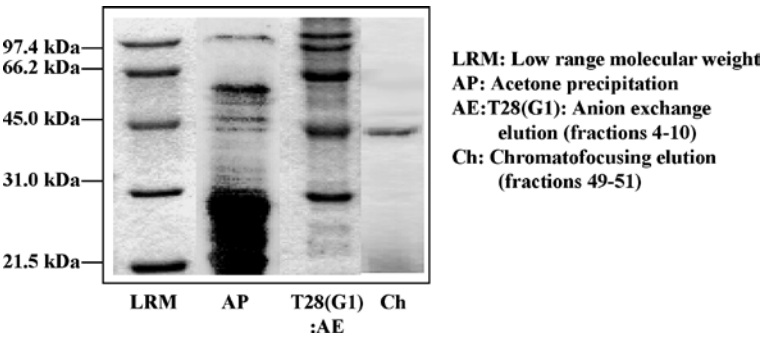

(c)

Fig. 1: The purification of T. longibrachiatum *T28 β-1,6-glucanases (a) Elution profile of the crude culture after anion exchange (Neobar AQ exchanger column), eluted with a 0 to 0.5M NaCl gradient with fractions 4-10 as T28 (G1); (b) Elution profile of T28 (G1) after chromatofocusing on mono P HR 5/20 with a 8.5 to 5.5 pH gradient; (c) SDS-PAGE (10%) of protein from pooled peaks and stained with Coomassie blue. LRM=Low range standard molecular weight; AP=Acetone precipitation; AE:T28(G1)=Anion exchange elution fractions 4-10; Ch= Chromatofocusing elution fractions 49-51*

Physicochemical Parameters and Substrate Specificity

In this study, the optimum temperature for the β-1,6-glucanase activity was found to be 50°C. The enzyme showed a rapid reduction in its stability, i.e. from 100% to only 40%, when the temperature was increased from 50°C to 55°C. Enzyme was found to be inactive and unstable at the temperature above 70°C (*Fig. 2a*), and was completely inactivated at 75°C; this was probably due to the thermal denaturation of the enzyme. Meanwhile, the optimal activity, for the short-term incubation, was often seen at the temperatures ranging from 30°C to 50°C; nevertheless, many fungal β-glucanases appeared to be stable at the temperatures up to 50°C to 60°C (Pitson *et al.*, 1993). β-1,6-glucanase for *T. longibrachiatum* T28 was shown to have the same optimal temperature and stabilisation temperature to the purified β-1,6-glucanase from *T. harzianum* (de la Cruz *et al.*, 1995; Hiura *et al.,* 1987) and *T. viride* (Nobe *et al.*, 2003). One simple conclusion which could be made from this was that even though *T. longibrachiatum* was categorised as warm climate fungi (Danielson and Davey, 1973), the enzyme itself could not function in extreme temperatures. However, Bodenmann (1985) explained that the effect of temperature could be stabilised by the substrate in the culture through the 'padding effect' which resisted the heat.

The optimal activity of the fungal β-glucanase usually appears in acidic conditions, which is often between pH 4.0 to 6.0, and according to Pitson *et al.* (1993), most of the fungal β-glucanases have a broad optimum pH. As shown in *Fig. 2b*, there was a clear influence of pH on the enzyme activity, with β-1,6-glucanase enzyme shown to be the most active at pH

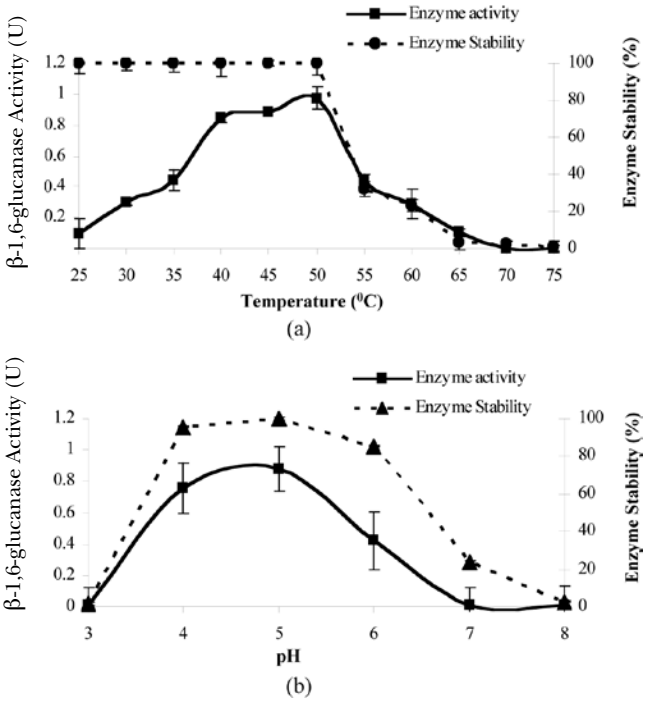

Fig. 2: The effect of physicochemical parameters, (a) temperature and (b) pH, on the activity and stability of the purified β-1,6-glucanase in T. longibrachiatum *T28. Each value of the β-1,6-glucanase stability is represented as a percentage compared to control, which is taken as 100%*

5.0. Meanwhile, this enzyme was able to sustain the activity above 80% over a pH range of approximately 4-6. However, in some cases, enzyme stability can be sustained up to pH 9 in the absence of a substrate (Tangarone *et al.*, 1989). An acidic or alkaline concentration may have an impact on the nutrient transport mechanism, it may also cause enzyme structure or disintegrate while in extreme condition (Kubicek-Pranz, 1998).

Metal ion is necessary for the enzyme activity as an additional factor which is involved in the catalytic process, as oxidizing or reducing agent, and to maintain the enzyme configuration (Deane *et al.,* 1998). The effects of several known metal ion inhibitors, on the activity of the purified enzymes, are shown in Table 2. In overall, the β-1,6-glucanase activity was inhibited by these metal ions but only in the range of 10-20%. In particular, Cu^{2+} ion in the assay mixture gave the highest inhibition, at 34.5% for β-1,6-glucanase. Watanabe *et al.* (1988) explained that the inhibition effect in the context of enzyme-substrate complex. In certain conditions, the position of the metal ion in enzyme-substrate complex prevented the substrate to form a firm bound to the recognition site in β-1,6-glucanase enzyme for the substrate hydrolysis, and thus brought to a halt or reduction in the enzyme activity. The inhibition effect of the metal ions on the enzyme activity, which is similar to one in the finding of the current study, has also been reported previously. In specific, the enzyme activity was slightly inhibited (20-35%) when 1mM of Co^{2+}, Hg^{2+}, Cu^{2+}, Fe^{2+} and Fe^{3+} where added into the culture (Hiura *et al.,* 1987), while a significant inhibition on the enzyme activity was established with the presence of 1mM $HgCl_2$, $MnCl_2$, $KMnO_4$ (Tangarone *et al.,* 1989); 1% (w/v) SDS and 1% (w/v) β-mercaptoethanol (Thrane *et al.,* 1997).

Mycoparasitism in *Trichoderma* species was regulated by catabolite repression and carbon source starvation (Lorito *et al.,* 1996), which means that the β-1,6-glucanase activity was controlled by the carbon source as shown in Table 2. The purified β-1,6-glucanase has the ability to hydrolyse pustulan because most of the linkages are β-1,6-linked glucan. It also was found to be able to split the linkages for the non-specific substrates such as laminarin (β-1,3-glucan bonds) and cellulose (β-1,4-glucan bonds), but in relatively low capacity of 41.6% and 17.5% respectively, as compared to pustulan. A similar result, on the ability of β-1,6-glucanase from other *Trichoderma* species to hydrolyse the non β-1,6-linked substrate, has also been reported previously (de la Cruz *et al.*, 1995; Moy *et al.*, 2002; Nobe *et al.*, 2003). The ability to hydrolyse the non β-1,6-linked substrate may be due to the enzyme amino acid sequence (de la Cruz *et al.*, 1993). However, not all purified β-glucanase has this ability; for this, Vazquez-Garciduenas *et al.* (1998) found that the purified β-1,3-glucanase could only hydrolyse laminarin. Nonetheless, the existence of glucose in media caused almost 98% reductions in the enzyme activity due to the catabolite repression which led to less β-1,6-glucanase being secreted, while the accumulation of other carbon sources caused their starvation and this further led to a high enzyme activity (Montero *et al.,* 2005). Although purified enzyme has been indicated to have the ability to hydrolyse all the substrates (as shown in the results of this study), the type of linkages in the substrate or substrate specificity still possesses some influences on the enzyme activity. The highest activity was obtained when the enzyme hydrolyse substrate contained the same β-glucosidic bonds specific for the enzymes. The substrate specificity of each enzyme has a significant effect on the mycoparasitism performance for *Trichoderma* species (de la Cruz *et al.,* 1993) and as demonstrated by Djonovic *et al.* (2006), a high β-1,6-glucanse activity was found to be lower in *Rhizoctonia solani* as compared to *Pytium ultimum*, due to its cell wall, which is mainly fabricated with chitin and β-1,3-linked glucan (Bartnicki-Garcia, 1968). On the other hand, *P. ultimum* attained a high content of β-1,6-linked glucan in its cell wall, giving a significant effect on the β-1,6-glucanse activity.

TABLE 2
The effect of metal ions (20mM) and 1% (w/v) of different substrates on β-1,6-glucanase activity in *T. longibrachiatum* T28

		Enzyme activity (U) ± s.d*	Relative activity (%)**
Metal ions (20mM)	None	0.97 ± 0.300	100
	Zn^{2+}	0.87 ± 0.180	89.6
	Ca^{2+}	0.87 ± 0.764	90.2
	Co^{2+}	0.73 ± 0.461	75.5
	Mg^{2+}	0.69 ± 0.277	71.2
	Cu^{2+}	0.63 ± 0.731	65.5
	Mn^{2+}	0.79 ± 0.688	81.9
	Fe^{2+}	0.78 ± 0.423	80.6
Substrate (1% w/v)	Pustulan	0.97 ± 0.300	100
	Laminarin	0.04 ± 0.539	41.6
	Cellulose	0.17 ± 0.216	22.5
	Glucose	0.0001 ± 0.132	0.12

*The results are the mean values of triplicate tests ± standard deviation.

**Relative activity (%) is expressed as a percentage compared to control, which is taken as 100%.

CONCLUSIONS

In conclusion, all the results obtained in this experiment showed that ß-1,6-glucanase secreted by *T. longibrachiatum,* possessed a molecular weight size and it also responded to selected physicochemical factors and substrate, which are almost similar to other *Trichoderma sp.*

ACKNOWLEDGEMENTS

The authors gratefully acknowledged the Ministry of Science, Technology and Innovation Malaysia for the research grant, which was given under the Fundamental Research Program (05-11-02-0060F) and the staff of PS&M Laboratory, Biology Department, Universiti Putra Malaysia.

REFERENCES

Amey, R.C., Mills, P.R., Bailey, A. and Foster, G.D. (2003). Investigating the role of a *Verticillium fungicola* β-1,6-glucanase during infection of *Agaricus bisporus* using targeted gene disruption. *Fungal Genetic and Biology, 39.* 264–275.

Bartnicki-Garcia, S. (1968). Cell wall chemistry, morphogenesis and taxonomy of fungi. *Annual Review of Microbiology, 22,* 87-109.

Benitez, T., Rincon, A.M., Limon, M.C. and Codon, A.C. (2004). Biocontrol mechanisms of *Trichoderma* strains. *International Microbiology,* 7, 249–260.

Bodenmann, J. (1985). Extracellular enzymes of *Phytophthora infestans* – endocellulase, beta-glucosidase and 1,3-beta-glucanase. *Canadian Journal Microbiology, 31,* 75-82.

Bradford, M. (1976). A rapid and sensitive method for the quantification of microgram quantities of protein utilizing the printciple of protein-dye binding. *Analytical Biochemistry, 72*, 248-254.

Cid, V.J., Duran, A., Del Rey, F., Snyder, M.P., Nombela, C. and Sanchez, A. (1995). Molecular basis of cell integrity and morphogenesis in *Saccharomyces cerevisiae. Microbiological Reviews, 59*, 345-386.

Danielson, R.M. and Davey, C.B. (1973). The abundance of *Trichoderma* propagules and distribution of species in forest soil. *Soil Biology and Biochemistry, 5*, 485-494.

de la Cruz, J., Rey, M., Lora, J.M., Hidalgo-Gallego, A., Dominguez, F., Pintor-Toro, J.A., Llobell, A. and Benitez, T. (1993). Carbon source control on β-glucanases, chitobiase and chitinase from *Trichoderma harzianum. Archives of Microbiology, 159*, 316-322.

de la Cruz, J., Pintor-Taro, J.A., Benitez, T. and Llobell, A. (1995). Purification and characterization of an endo-ß-1,6-glucanase from *Trichoderma harzianum* that is related to its mycoparasitism. *Journal of Bacteriology, 177,* 1864-1871.

Deane, E.E., Whipps, J.M., Lynch, J.M. and Peberdy, J.F. (1998). The purification and characterization of a *Trichoderma harzianum* exochitinase. *Biochimica et Biophysica Acta, 1383*, 101-110.

Delgado-Jarana, J., Pintor-Toro, J.A. and Benitez, T. (2000). Overproduction of ß-1,6-glucanase in *Trichoderma harzianum* is controlled by extracellular acidic proteases and pH. *Biochimica et Biophysica Acta, 1481*, 289–296.

Djonovic, S., Pozo, M.J. and Kenerley, C.M. (2006). Tvbgn3, a ß-1,6-glucanase from the biocontrol fungus *Trichoderma virens,* is involved in mycoparasitism and control of *Pyhtium ultimum. Applied and Environmental Microbiology, 72,* 7661-7670.

Elad, Y., Chet, I. and Henis, Y. (1982). Degradation of plant pathogenic fungi by *Trichoderma harzianum. Canadian Journal of Microbiology, 28,* 719-725.

Haran, S., Schickler, H., Oppenheim, A. and Chet, I. (1995). New components of the chitinolytic system of *Trichoderma harzianum. Mycological Research, 99*, 441-446.

Haran, S., Schickler, H. and Chet, I. (1996). Molecular mechanisms of lytic enzymes involved in the biocontrol activity of *Trichoderma harzianum. Microbiology, 142*, 2321-2331.

Hiura, N., Nakajima, T. and Matsuda, K. (1987). Purification and some properties of an endo-β-1,6-glucanase from *Neurospora crassa. Agricultural and Biological Chemistry, 51*, 3315-3321.

Inbar, J. and Chet, I. (1994). A newly isolated lectin from the plant pathogenic fungus *Sclerotium rolfsii*: purification, characterization and role in mycoparasitism. *Microbiology, 140*, 651-657.

Khun, P.J., Trinci, A.P.J., Jung, M.J., Goosey, M.W. and Copping, L.G. (1990). *Biochemistry of Cell Walls and Membranes in Fungi* (p. 25-30). Berlin: Springer-Verlag.

Kubicek-Pranz, E.M. (1998). Nutrition, cellularstructure and basic metabolic pathways in *Trichoderma* and *Gliocladium.* In C.P. Kubicek and G.E. Harman (Eds.), *Trichoderma and Gliocladium* (p. 95-119). New York: Taylor and Francis.

Laemmli, U.K. (1970). Cleavage of structural proteins during the assembly of the head of bacteriophage T4. *Nature, 227*, 680-685.

Lora, M.J., de la Cruz, J., Benitez, T., Llobell, A. and Pintor-Toro, J.A. (1995). Molecular characterization and heterologous expression of an endo-1,6-β-glucanase gene from the mycoparasitic fungus *Trichoderma harzianum. Molecular and General Genetics, 247*, 639-645.

Lorito, M., Farkas, V., Rebuffat, S., Bodo, B. and Kubicek, C.P. (1996). Cell wall synthesis is a major target of mycoparasitic antagonism by *Trichoderma harzianum. Journal of Bacteriology, 178*, 6382-6385.

Martin, K.L., Unkles, S.E., McDougall, B.M. and Seviour, R.J. (2006). Purification and characterization of the extracellular β-1,6-glucanases from the fungus *Acremonium* strain OXF C13 and isolation of the genes encoding these enzymes. *Enzyme and Microbial Technology, 38,* 351–357.

Matsuzawa, T., Amano, Y., Kubo, M. and Kandat, T. (1996). Mode of action of exo-β-1,3-glucanase from *Trichoderma pseudokoningii* TM37 on various β-D-glucans. *Journal of Fermentation and Bioengineering, 74*, 261-267.

Montero, M., Sanz, L., Rey, M., Monte, E. and Llobell, A. (2005). BGN16.3, a novel acidic β-1,6-glucanase from mycoparasitic fungus *Trichoderma harzianum* CECT 2413. *The FEBS Journal, 272,* 3441–3448.

Moy, M., Li, H.J.M., Sullivan, R., White, J.F. and Belanger, F.C. (2002). Endophytic fungal β-1,6-glucanase expression in the infected host grass. *Plant Physiology, 130,* 1298–1308.

Mrsa, V., Klebl, F. and Tanner, W. (1993). Purification and characterization of the *Saccharomyces cerevisiae* BGL2 gene product, a cell wall endo-1,3-β-glucanase. *Journal of Bacteriology, 175*, 2102-2106.

Mulenga, D.K. and Berry, D.R. (1994). Isolation and characterization of a unique endo-beta-1,6-glucanase from the yeast *Saccharomycopis fibuligera* NCYC 451. *Microbios, 80,* 143–154.

Muskhazli, M., Salfarina, R., Nalisha, I. and Nor Farizan, T. (2005). Purification and characterization of β-1,3-glucanase from *Trichoderma harzianum* BIO 10671. *Pertanika Journal of Tropical Agriculture Science, 28,* 23-31.

Nobe, R., Sakakibara, Y., Fukuda, N., Yoshida, N., Ogawa, K. and Suiko, M. (2003). Purification and characterization of laminaran from *Trichoderma viride. Bioscience, Biotechnology and Biochemistry, 67*, 1349-1357.

Noronha, C.F. and Ulhoa, C.J. (1996). Purification and characterization of an endo-B-1,3-glucanase from *Trichoderma harzianum. Canadian Journal of Microbiology, 42*, 1039-1044.

Onsando, J.M. and Waudo, S.W. (1992). Effect of coffee pulp on *Trichoderma* spp. in Kenyan tea soils. *Tropical Pest Management, 38*, 376-381.

Papavizas, G.C. (1985). *Trichoderma* and *Gliocladium*: biology, ecology and the potential for biocontrol. *Annual Review of Phytopathology, 23*, 23-54.

Pitson, S.M., Sevior, R.J. and Mc Dougal, B.M. (1993). Non-celluloytic fungal β-glucanase: their physiology and regulation. *Enzyme and Microbial Technology, 15,* 178-192.

Pitson, S.M., Seviour, R.J., McDougall, B.M., Stone, B.A. and Sadek, M. (1996). Purification and characterization of an extracellular (1–6)-beta-glucanase from the filamentous fungus *Acremonium persicinum. The Biochemical Journal, 316,* 841–846

Ridout, C.J., Coley-Smith, J.R. and Lynch, J.M. (1988). Fraction of extracellular enzymes from a mycoparasitic strain of *Trichoderma harzianum. Enzyme and Microbial Technology, 10*, 180-186.

Sarrocco, S., Mikkelsen, L., Vergara, M., Jensen, D.F., Lubeck, M. and Vannacci, G. (2006). Histopathological studies of sclerotia of phytopathogenic fungi parasitized by a GFP transformed *Trichoderma virens* antagonistic strain. *Mycological Research, 110,* 179–187.

Schep, G.P., Shepard, M.G. and Sullivan, P.A. (1984). Purification and properties of a beta-1,6-glucanase from *Penicillium brefeldianum. The Biochemical Journal, 223*, 707–714.

Somogyi, M. (1952). Notes on sugar determination. *The Journal of Biological Chemistry, 195,* 19-23.

Sreenivasaprasad, S. and Manibhushanrao, K. (1990). Antagonistic potential of *Gliocladium virens* and *Trichoderma longibrachiatum* to phytopathogenic fungi. *Mycopathologia, 109*, 19-26.

Sreenivasaprasad, S. and Manibhushanrao, K. (1993). Efficiency of *Gliocladium virens* and *Trichoderma longibrachiatum* as biological control agents of groundnut root and stem rot diseases. *International Journal of Pest Management, 39*, 167-171.

Stasinopoulos, S.J. and Seviour, R.J. (1989). Exopolysaccharide formation by isolates of *Cephalosporium* and *Acremonium. Mycological Research, 92*, 55–60.

Tangarone, B., Royer, J.C. and Nakas, J.P. (1989). Purification and characterization of an endo-(1,3)-β-D-Glucanase from *Trichoderma longibrachiatum. Applied and Environmental Microbiology, 55,* 177-184.

Thrane, C., Tronsmo, A. and Jensen, D.F. (1997). Endo-1,3-β-glucanase and cellulase from *Trichoderma harzianum*: purification and partial characterization, induction of and biological activity against plant pathogenic *Pythium* spp. *European Journal of Plant Pathology, 103,* 331-344.

Vazquez-Garciduenas, A., Leal-Morales, C.A. and Herrera-Estrella, A. (1998). Analysis of the β-1,3-glucanolytic system of the biocontrol agent *Trichoderma harzianum. Applied and Environmental Microbiology, 64*, 1442-1446.

Watanabe, R., Ogasawara, N., Tanaka, H. and Uchiyama, T. (1988). Effect of fungal lytic enzymes and non-ionic detergents on the actions of some fungicides against *Pyricularia oryzae. Agricultural and Biological Chemistry, 52*, 895-901.

ISSN: 0128-7680
Pertanika J. Sci. & Technol. **17 (1)**: 149 – 154 (2009)

Alkaloids from *Piper nigrum* and *Piper betle*

C.M. Lim[1], G.C.L. Ee[1*], M. Rahmani[1] and C.F.J. Bong[2]
[1]Department of Chemistry, Faculty of Science, Universiti Putra Malaysia, 43400 UPM, Serdang, Selangor, Malaysia
[2]Department of Crop Science, Faculty of Agriculture & Food Sciences, Universiti Putra Malaysia, Bintulu Campus, 97008 Bintulu, Sarawak, Malaysia
[*]E-mail: gwen@fsas.upm.edu.my

ABSTRACT

An investigation, on the roots of *Piper nigrum* and the aerial parts of *Piper betle*, has yielded several alkaloids. The dried root sample of *Piper nigrum* was extracted using various solvents in increasing polarity. The dried aerial part of *Piper betle* was extracted using the Soxhlet extraction method. The alkaloids isolated were pellitorine **(1)**, (*E*)-1-[3',4'-(Methylenedioxy)cinnamoyl]piperidine **(2)**, piperine **(3)**, piperolactam D **(4)**, cepharadione A **(5),** and 2,4-tetradecadienoic acid isobutyl amide **(6)**. These compounds were isolated using chromatographic methods, while the elucidation of the structures was carried out using MS, IR and NMR techniques. The extracts of *Piper nigrum* and *Piper betle* were also tested for cytotoxicity activities. This is the first report on (*E*)-1-[3',4'-(Methylenedioxy)cinnamoyl] piperidine **(2)** from *Piper nigrum* as a natural product.

Keywords: *Piper nigrum*, *Piper betle*, alkaloids, cytotoxicity

INTRODUCTION

The genus *Piper* belongs to the Piperaceae family and it has over 700 species distributed in both hemispheres. The Piperaceae family is a source of many biologically active phytochemicals with great potential for medicinal and agricultural uses. Species in the genus *Piper* have a wide array of secondary metabolite compounds, particularly alkaloids and amides (Scott *et al.*, 2005). *Piper nigrum* is one of the more well-known species because of its high commercial, economical, and medicinal properties. It is known that *Piper nigrum* has biological activities such as CNS stimulant, analgesic, antipyretic and antifeedent activities (Miyakado *et al.*, 1979). Meanwhile, *Piper betle* possesses a variety of medicinal properties. The leaves of *Piper betle* can be used as a traditional remedy to treat stomach ailments and infections, as well as a general tonic. The leaves of *Piper betle* can also be used to stop bleeding by applying the leaves directly onto the wound. This paper reports the isolation of the alkaloid components pellitorine (**1**) and (*E*)-1-[3', 4'-(Methylenedioxy)cinnamoyl]piperidine **(2),** as well as the discovery of bioactive extracts from both plant samples being studied.

MATERIALS AND METHODS

Plant Material

The roots of *Piper nigrum* were collected from Sri Aman, in Sarawak, Malaysia. The aerial parts of *Piper betle* were obtained from Kedah, Malaysia.

Received: 11 January 2008
Accepted: 8 April 2008
[*]Corresponding Author

General

Infrared spectra were measured in NaCl pellet on a Perkin-Elmer FTIR Spectrum BX spectrometer. EIMS were recorded on a Shidmazu GCMS-QP5050A spectrometer. The NMR spectra were obtained using Unity INOVA 500 MHz NMR/JEOL 400 MHz FTNMR spectrometer using tetramethylsilane (TMS) as internal standard. The ultra violet spectra were recorded in $CHCl_3$ on a Shidmazu UV-160A, UV-Visible Recording Spectrophotometer.

Extraction and Isolation

The dry powdered roots of *Piper nigrum* (4.8kg) were extracted repeatedly with distilled petroleum ether thrice, for seventy two hours at room temperature. This was followed by the extraction in chloroform and finally in ethanol. All the extracts were dried in vacuo to obtain crude extracts. The ethanol extract was then added to a large quantity of 5% aqueous hydrochloric acid. After that, the acidic solution was filtered using kieselghur to remove the non-alkaloidal substances. The filtrate was then basified with concentrated ammonia solution to pH 10. The liberated alkaloids were extracted exhaustively with chloroform. Then, the chloroform extract was washed with distilled water and dried over anhydrous sodium sulphate. The acid-base treated ethanol extract was obtained by removing the solvent under reduced pressure. The extract after evaporation yielded an oily extract (0.53g). The crude extract was chromatographed over silica gel (120-230 mesh) column and fractions were collected in 100 ml aliquots. Fractions 10-26 gave pellitorine **(1),** and (*E*)-1-[3', 4'-(Methylenedioxy) cinnamoyl] piperidine **(2)**. The dried sample of the aerial parts of *Piper betle* underwent the Soxhlet extraction using hexane, chloroform and methanol. All extracts were dried under reduced pressure.

Pellitorine **(1).** White crystals with melting point 60-62°C (Lit. 69°C, Rosario, *et al.*, 1996). UV ($CHCl_3$) λ_{max} nm (log ε):292(1.87), 236(0.48), 212(0.53), 264(0.27), 220(0.31). IR υ_{max} cm^{-1} (NaCl): 3300 (N-H group), 2926, 2864, 1656(C=O), 1624, 1550, 1460, 1368, 1260, 1160, 994. EIMS m/z (rel. int.): 223(43), 208(10), 180(7), 166(8), 151(100), 110(12), 96(55), 81(50), 67(21), 53(18). For NMR data, *see* Table 1).

(*E*)-1-[3', 4'-[Methylenedioxycinnamoyl] piperidine **(2).** White crystals with melting point 74-76°C (Lit. 83°C, Schobert *et al.*, 2001). UV ($CHCl_3$) λ_{max} nm (log ε): 325(2.46), 235(0.82), 397(0.01), 251(0.60). IR υ_{max} cm^{-1} (NaCl): 3460, 2934, 2858, 1642, 1598, 1494, 1444, 1354, 1248, 1134, 1034, 978, 930, 810. EIMS m/z (rel. int.): 259(57), 175(73), 148(30), 145(100), 138(17), 117(33), 89(66), 84(86), 63(31). For NMR data, *see* Table 2).

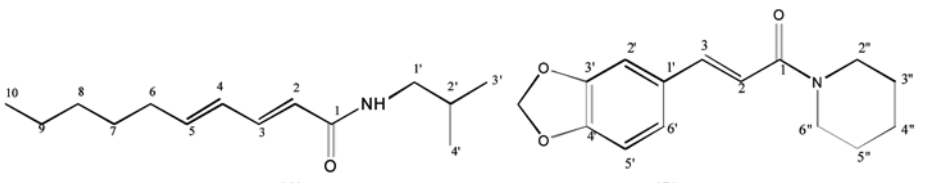

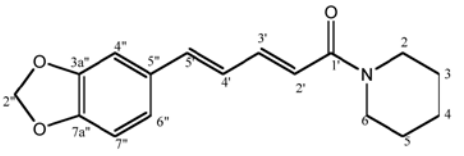

(3)

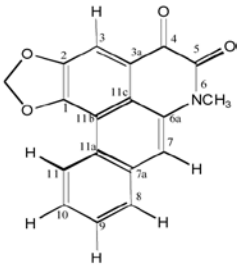

(4)

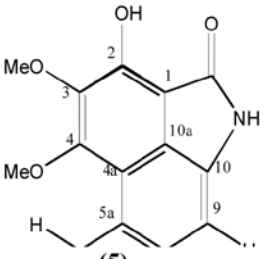

(5)

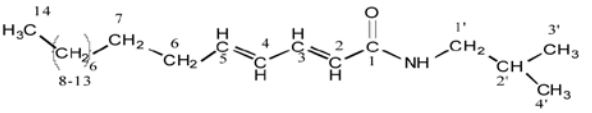

(6)

TABLE 1
NMR data for pellitorine **(1)**

Position	^{1}H NMR, δ	^{13}C NMR, δ	HMBC
1	-	166.45	7.19 (H-3) (^{3}J), 5.79 (H-2) (^{2}J), 3.16 (H-1') (^{3}J)
2	5.79 (1H, d, *J*=15.0Hz)	121.70	6.09 (H-4) (^{3}J)
3	7.19 (1H, dd, *J*=15.0,11.0Hz)	141.26	5.79 (H-2) (^{2}J)
4	6.09 (1H, m)	128.16	2.13 (H-6) (^{3}J)
5	6.12 (1H, m)	128.16	2.13 (H-6) (^{2}J)
6	2.13 (2H, m)	32.87	1.38 (H-7) (^{2}J),1.29 (H-8) (^{3}J)
7	1.38 (2H, m)	28.44	2.13 (H-6) (^{2}J)
8	1.29 (2H, m)	31.31	1.38 (H-7) (^{2}J),2.13 (H-6) (^{3}J)
9	1.29 (2H, m)	22.42	0.89 (H-10) (^{2}J),1.29(H-8) (^{2}J)
10	0.89 (3H, m)	13.96	1.29 (H-9) (^{2}J)
1'	3.16 (2H, dd, *J*=6.4, 12.8 Hz)	46.89	1.76 (H-2') (2*J*), 0.91 (H-3') (^{3}J), 0.93(H-4') (^{4}J)
2'	1.76 (1H,m)	28.58	0.91 (H-3') (^{2}J), 0.93(H-4') (^{2}J)
3'	0.91 (3H, d, 6.4 Hz)	20.08	1.76 (H-2') (^{2}J), 3.16(H-1') (^{3}J)
4'	0.93 (3H, d, 6.4 Hz)	20.08	1.76 (H-2') (^{2}J), 3.16 (H-1') (^{3}J)
N-H	5.76 (br s)	-	-

TABLE 2
NMR data for (*E*)-1-[3',4'-(Methylenedioxy)cinnamoyl]piperidine **(2)**

Position	^{1}H NMR, δ	^{13}C NMR, δ	HMBC
2"	3.57 (2H, br s)	43.30	1.58-1.69 (H-3",H-4") (^2J,^3J)
3"		25.56	1.58-1.69 (H-4", H-5") (^2J, ^3J)
4"	1.58 - 1.69 (6H, m)	24.60	1.58-1.69 (H-3", H-5') (^2J)
5"		26.69	1.58-1.69 (H-4", H-3") (^2J,^3J)
6"	3.64 (2H, br s)	46.92	1.58-1.69 (H-5") (^2J), (H-4") (^3J)
1	-	165.38	7.03 (H-2) (^2J), 7.54(H-3) (^3J)
2	7.03 (1H, d. *J*=13.3 Hz)	123.52	7.54 (H-3) (^2J)
3	7.54 (1H, d, *J*=13.3 Hz)	141.89	6.97 (H-2') (^3J), 7.03 (H-2) (^2J)
1'	-	129.87	6.78 (H-6') (^2J), 7.54 (H-3) (^2J)
2'	6.97 (1H br d, *J*=1.8 Hz)	106.27	7.54 (H-3) (^3J)
3'		148.12	5.98 (OCH_2O) (^3J), 6.97 (H-2') (^2J), 6.71 (H-5') (^3J)
4'	-	148.76	5.98 (OCH_2O) (^3J), 6.97 (H-2') (^3J), 6.71 (H-5') (^2J)
5'	6.71 (1H, br d, *J*=8.2 Hz)	115.63	
6'	6.78 (1H, br d, *J*=8.2 Hz)	108.41	7.54 (H-3) (^3J)
OCH_2O	5.98 (2H, s)	101.33	-

RESULTS AND DISCUSSION

Pellitorine **(1)**, white crystals, and with molecular formula $C_{14}H_{25}NO$ exhibited a parent molecular ion peak at m/z 223 in the EI-MS spectrum. The infrared spectrum showed a strong absorption band at 3300 cm^{-1}, which accounted for the NH group. Another strong absorption band, observed at 1656 cm^{-1}, belong to the C=O of the amide group. The ^{1}H NMR spectrum of pellitorine showed three doublet signals at δ5.79 (*J*=14.7 Hz) for H-2, 0.91 (*J*=6.4 Hz) for H-3' and 0.93 (*J*=6.4 Hz) for H-4'. Two multiplet signals, which appeared at δ 6.09 and 6.12, were due to the olefinic protons at C-4 and C-5. Meanwhile, a multiplet occurring at a very upfield region at δ1.76, was due to the proton at C-2', coupling with the adjacent protons in the isobutyl moiety. A broad singlet at δ5.76 was attributed to NH. The ^{13}C NMR spectrum gave a total of 14 peaks and most of the carbon peaks appeared at the upfield region. The amide carbonyl carbon resonating at δ166.45(C-1) was further confirmed by DEPT spectra. A ^3J correlation between δ166.45 (C-1) and δ3.16 (H-1') was observed and this validated the position of the isobutyl group. The location of olefinic protons was confirmed by a ^3J correlation of the carbonyl carbon at δ166.45 with the proton

at δ5.79. The chemical shifts of the proton and carbon NMR spectra were compared with the values in the literature, and all the values for the ^{1}H and ^{13}C NMR spectra were found to be in agreement. Hence, this compound was identified as deca-2*E*,4*E*-dienoic acid isobutyl amide, which is also known as pellitorine, previously isolated from *Cissampelos glaberrima* (Rosario *et al.*, 1996).

(*E*)-1-[3',4'-(Methylenedioxy)cinnamoyl]piperidine **(2)** was isolated as white crystals, and its molecular formula of $C_{15}H_{17}NO_3$ was determined by EIMS (m/z 259). The infrared spectrum showed absorptions at 3460 cm^{-1} and 1642 cm^{-1}, indicating the presence of NH and C=O. The ^{1}H NMR spectrum displayed signals for the equivalent methylene groups, α to the nitrogen atom at δ3.57, which was for H-2" and δ3.64 for H-6." Three downfield signals, observed at δ6.97 (1H, brd, *J*=1.8 Hz), δ6.71 (1H, brd, *J*=8.2 Hz) and δ 6.78 (1H, brd, *J*=8.2 Hz) were assigned to H-2', H-5' and H-6', respectively. The ^{1}H-^{1}H correlation was determined using a COSY spectrum. The COSY gave ^{4}J coupling between H-2' and H-6.' At the same time, the ^{3}J coupling between H-2 and H-3 was also observed in the COSY spectrum. The ^{13}C NMR spectrum was assigned using a combination of the DEPT, HMQC and HMBC experiments. From the HMQC spectrum, no correlations were observed for C-1, C-1', C-3' and C-4'. Hence, these carbons are not attached to any protons and are quaternary carbons. Meanwhile, a total of 6 methylene carbons, 5 methine carbons and 4 quaternary carbons were observed from the DEPT spectrum. Long range couplings were also observed between the cinnamoyl carbonyl carbon at δ165.38 and protons H-3 and H-2. C-4' was found to correlate with the -OCH_2O- group protons. A ^{2}J correlation was observed between C-1 and H-2. Moreover, a ^{3}J correlation between C-1 and H-3 was observed in the HMBC spectrum. All the ^{13}C NMR and ^{1}H NMR values are given in Table 2. As a result, this compound was assigned as (*E*)-1-[3',4'-(Methylenedioxy)cinnamoyl]piperidine**(2)**, which was previously synthesized by Schobert *et al.* (2001).

The structures of the other four alkaloids were determined by making comparisons of the spectral data with that of the published data - piperine**(3)** (Park *et al.*, 2002), piperolactam D**(4)** (Olsen *et al.*, 1993), cepharadione A**(5)** (Desai *et al.*, 1988; Wijeratne *et al.*, 1995) and 2,4-tetradecadienoic acid isobutyl amide**(6)** (Greger *et al.*, 1981).

The extracts of *Piper nigrum* and *Piper betle* were also tested for cytotoxic activities. For this purpose, the extracts of *Piper nigrum* were tested on HL60 (Human promyelocytic leukemia cells). The petroleum ether and chloroform extracts were bioactive against HL 60 cell line, with a high inhibitory concentration of less than 30 µg/ml. The ethyl acetate extract gave no activity. The petroleum ether extract gave an IC_{50} value of 11.2 µg/ml, and the IC_{50} value of chloroform extract was found to be 9.8 µg/ml. Meanwhile, the crude extracts of *Piper betle* were tested on HeLa cell line (the human epithelial cells derived from the cervical cancer cells). The crude hexane extract gave an IC_{50} value of 17.6 µg/ml, while the chloroform and methanol extracts were found to be not bioactive towards the HeLa cell line.

ACKNOWLEDGEMENTS

The authors wish to thank Dr Jegak Uli for the collection of the plant samples, Mr Johadi Iskandar for the recording of the NMR spectra, and UPM for the financial support.

REFERENCES

Desai, S.J., Prabhu, B.R. and Mulchandani, N.B. (1988). Aristolactams and 4,5-dioxoaporphines from *Piper Longum. Phytochemistry, 5,* 1511-1515.

Greger, H., Grenz, M. and Bohlmann, F. (1981). Amides from *Achillea* species and *Leucocyclus formosus*. *Phytochemistry*, *11*, 2579-2581.

Miyakado, M., Nakayama, I. and Yoshioka, H. (1979). The piperaceae amides I: structure of pipercide, a new insecticidal amide form *Piper nigrum* L. *Agriculture and Biological Chemistry, 43*, 1609-1611.

Olsen, C.E., Tyagi, O.D., Boll, P.M., Hussaini, F.A. Parmer, S.V., Sharma, N.R., Taneja, P. and Jain, S.C. (1993). An aristolactam from *Piper acutisleginum* and revision of the structures of piperolactam B and D. *Phytochemistry*, *2*, 518-520.

Park, I.K., Lee, S.G., Shin, S.C., Park, J.D. and Ahn, Y.J. (2002). Larvicial activity of isobutylamides identified in *Piper nigrum* fruits against three mosquito species. *Journal of Agricultural and Food Chemistry*, *50*, 1866-1870.

Rosario, S.L., Silva, A.J. and Parente, J.P. (1996). Alkamides from *Cissampelos glaberrima. Planta Medica*, *62*, 376-377.

Schobert, R., Siegfried, S. and Gordon, G.J. (2001). Three-component synthesis of (*E*)-α,β-unsaturated amides of the piperine family. *Journal of Chemical Society, Perkin Trans, 1*, 2393-2397.

Scott, I.M., Puniani, E., Jensen, H., Livesey, J.F., Poveda, L., Vindas, P.S., Durst, T. and Arnason, J.T. (2005). Analysis of Piperaceae germplasm by HPLC and LCMS: a method for isolating and identifying unsaturated amides from *Piper* spp extracts. *Journal of Agricultural and Food Chemistry*, *53*, 1907-1913.

Wijeratne, E.M.K, Gunantilaka, A.A.L., Kingstan, D.G.I., Haltiwanger, R.C. and Eggleston, D.S. (1995). Artabotrin: A novel bioactive alkaloid from *Artabotrys zeylanicus. Tetrahedron, 51*, 7877-7882.

ISSN: 0128-7680
Pertanika J. Sci. & Technol. **17 (1)**: 155 – 161 (2009)

Synthesis and Evaluation of a Molecularly Imprinted Polymer for Pb(II) Ion Uptake

Nor Azah Yusof*, Appri Beyan, Md. Jelas Haron and Nor Azowa Ibrahim
Department of Chemistry, Faculty of Science, Universiti Putra Malaysia, 43400 UPM, Serdang, Selangor, Malaysia
**E-mail: azah@science.upm.edu.my*

ABSTRACT

A molecularly imprinted polymer (MIP), with the ability to bind Pb(II) ion, was prepared using the non-covalent molecular imprinting methods and evaluated as a sorbent for the Pb(II) ion uptake. 4-vinylbenzoic acid was chosen as the complexing monomer. The imprinted polymer was synthesized by radical polymerization. The template (Pb(II) ions) was removed using 0.1 M HCl. As a result, the efficient adsorption was found to occur at pH 7. The result also showed the applicability of the Langmuir model for the sorption, with the maximum sorption capacity of 204.08 μg/mg.

Keywords: Ion imprinting, molecular recognition, Pb(II) removal, metal extraction

INTRODUCTION

Imprinted polymerization is a process in which monomers are polymerized in a solution containing the specific analyte to produce imprinted polymer, which is selective towards the target analyte. Imprinted polymers are highly cross-linked molecules, which are bearing 'tailor-made' binding sites for the target analyte. Imprinted polymers are easy to prepare, stable, inexpensive and can be reused. The selection of an ion imprinted polymer was done based on the coordination geometry and coordination number of the ions, as well as their charges and sizes (Mayes and Whitcombe, 2005). A number of studies have been carried out on ion imprinting polymers involving various metal ions (Ebru *et al.*, 2006; Handan *et al.*, 2005; Hiroyuki *et al.*, 1977; Mostafa *et al.*, 2007; Muge *et al.*, 2004; Ridvan *et al.*, 2007, Kosuke *et al.*, 2005), but no studies have so far reported on the removal of Pb(II) in the literature.

Pb(II) is a toxic metal of continuing occupational and environmental concern, with a wide variety of adverse effects. This means that Pb(II) is a general protoplasmic poison, which is cumulative, slow acting and subtle, and produces a variety of symptoms. Like other heavy metals, it has an affinity for sulphur. Though it exerts much of its activity through sulfohydryl inhibition, Pb(II) also interacts with carboxyl and phosphoryl groups. The element interferes with heme synthesis (Elinde and Friberg, 1980).

In this study, ion imprinted polymer was used to study on the Pb^{2+} uptake in aqueous environment. For this purpose, 4-vinylbenzoic acid was chosen as the complexing monomer. The imprinted polymer was synthesized by radical polymerization. The template (Pb(II) ions) was removed using 0.1 M HCl. After removing Pb^{2+}, the imprint polymer was evaluated for its binding capability towards Pb^{2+} in the aqueous environment, and compared with the non-imprinted polymer. A study on the pH for the binding to occur was also carried out.

Received: 11 January 2008
Accepted: 8 April 2008
*Corresponding Author

Meanwhile, the study on the interaction between the template (Pb^{2+}) and the monomer was carried out using the FTIR.

EXPERIMENTAL

Materials

4-Vinylbenzoic acid (4VBA), ethylene glycol dimethacrylate acid (EGDMA) and benzoylperoxide (BPO) were obtained from Fluka (Switzerland). All other chemicals were of reagent grade and purchased from Merck (Germany). Deionised water was used throughout the experiment.

(a) The preparation of Pb^{2+}- imprinted polymer

Radical polymerization was used for the preparation of the Pb^{2+}- imprinted polymer. For this purpose, 1.00 mmol of $Pb(NO_3)_2$ was dissolved in a mixture of water:ethanol (1:3), and 4.0 mmol of 4VBA was added, and this was followed by 20.0 mmol of EGDMA. After that, 50 mg of BPO was added and the mixture was bubbled with N_2 for 10 minutes. Polymerization was conducted for 24 hours in water bath at 70°C, with constant stirring. The obtained imprinted polymer was washed with ethanol and water to remove unreacted monomer or diluents. The polymer was also crushed, ground and sieved prior to storage.

(b) Adsorption studies

The adsorption of Pb(II) ions from the aqueous solutions was investigated in the batch experiments. The effects of the initial Pb(II) ion concentration, pH of the medium on the adsorption rate, and the adsorption capacity were studied. The suspensions were brought to the desired pH by adding sodium hydroxide and nitric acid. The concentration of the metal ions, in the aqueous phases after the desired treatment periods, was measured using an ICP-AES. The experiments were performed in three replicates.

The adsorption values were calculated as the differences in the Pb(II) ion concentration of the pre- and post-adsorption solutions divided by the weight of the dry imprinted polymer. The adsorbed Pb(II) ions were desorbed by treating them with HCl solution. The Pb(II) adsorbed imprinted polymer were placed in the desorption medium and stirred continuously at 600 rpm at room temperature for 2 hours. The final Pb(II) ion concentration, in the aqueous phase, was determined by the ICP-AES.

(c) The characterization of the imprinted polymer

The FTIR spectra of 4VBA and the imprinted polymer were obtained using the FTIR spectrophotometer. The imprinted polymer particles (about 0.1 g) were thoroughly mixed with KBr, pressed into a pellet and the FTIR spectrum was recorded.

RESULTS AND DISCUSSION

The Characterization of the Imprinted Polymer

Cross-linked imprinted and non-imprinted particles were spherical in shape, with a size ranged from 63-90 μm in diameter. The FTIR spectrum (*Fig. 1*) of 4VBA has the characteristic of carbonyl band at 1724 cm^{-1} and weak O-H stretching at 3300 cm^{-1}. The FTIR spectrum (*Fig. 1*) for Pb^{2+}– imprinted polymer has a strong characteristic stretching of

hydrogen bonded alcohol, and O-H around 3400 cm^{-1}, indicating an interaction between Pb^{2+} and the O-H group. There is also a shift for carbonyl band, which indicates an interaction of coordinate covalent between Pb^{2+} and the carbonyl group.

Adsorption Rate

Fig. 2 shows the time dependence of the adsorption capacities of the Pb(II) ions towards imprinted polymer as a function of time. As can be seen here, Pb^{2+} adsorption increased with the time during the first 20 min, and the levels off as equilibrium was most probably due to geometric shape memory between Pb^{2+} ions and Pb^{2+}cavities in the imprinted polymer structure. The removal of the template (Pb^{2+}) from the polymeric matrix created several cavities of complementary size, shape and chemical functionality to the template.

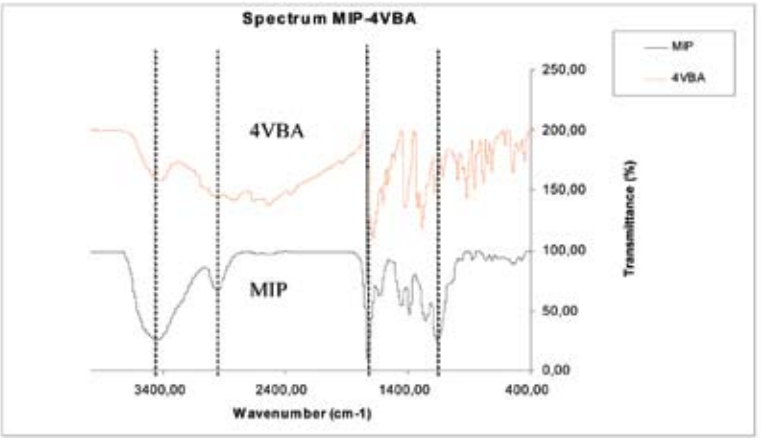

Fig. 1: FTIR Spectra for monomer (4VBA) and Pb^{2+}-imprinted polymer

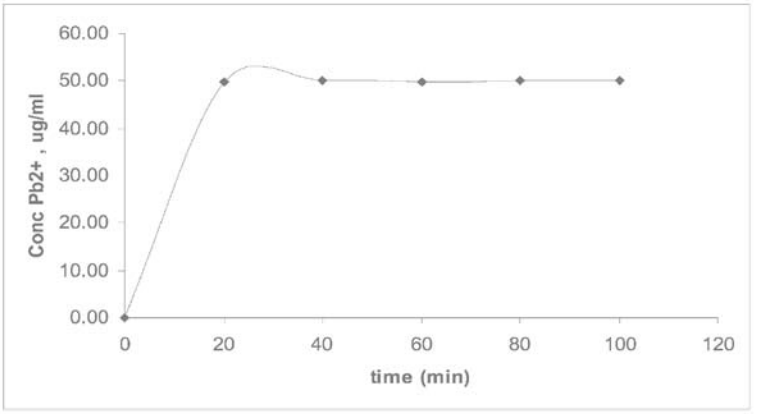

Fig. 2: Time dependence of the adsorption capacities of lead ions towards imprinted polymer

The Effects of the Initial Concentration of the Pb(II) Ion

Fig. 3 shows the dependence of the equilibrium concentration on the adsorbed amount of the Pb^{2+} ions into the imprinted polymer. The adsorption values were found to increase with the increasing concentration of Pb^{2+} ions, and a saturation value was achieved at Pb^{2+} ion concentration of 250 µg/ mL. The level off represented the saturation of the active binding cavities on the imprinted polymer. Meanwhile, the maximum adsorption capacity for Pb^{2+} ions was 150 µg/ mg dry weight of Pb^{2+}-imprinted polymer.

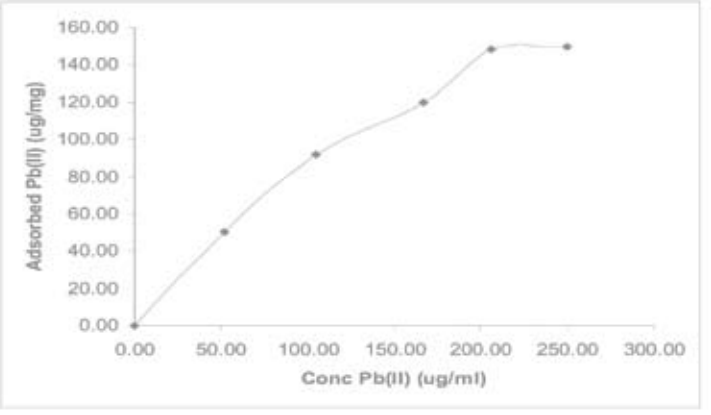

Fig. 3: Effects of the initial concentration of lead(II) ion

Adsorption Isotherm

An adsorption isotherm was used to characterize the interactions of each molecule with the adsorbents. This provided a relationship between the concentration of the molecules in the solution and the amount of ions adsorbed on the solid phase when the two phases were at equilibrium. The Langmuir adsorption model assumes that the molecules are adsorbed at a fixed number of well-defined sites, each of which is capable of holding only one molecule. These sites are also assumed to be energetically equivalent and distant from each other, so that there are no interactions between molecules adsorbed on adjacent sites (Sibel *et al.*, 2007).

During the batch experiments, the adsorption isotherms were used to evaluate the adsorption properties. For the systems considered, the Langmuir model was found to be applicable in interpreting Pb(II) ion adsorption on the Pb^{2+}-imprinted polymer. As a result, the Langmuir adsorption model was found to fit better as compared to the Freundlich model for this system. The correlation coefficient (R^2) was 0.9931. The maximum adsorption capacity and the Langmuir constant were calculated to be 204.08 µg/mg and 0.02 mL/µg, respectively. Both the Langmuir and Freundlich plots are respectively displayed in *Fig. 4* and *5*. The constants are summarized in Table 1.

The Effects of pH

Metal ion adsorption onto specific adsorbents is pH dependent. The effect of the pH on the Pb^{2+} ion adsorption of Pb^{2+}-imprinted polymer is shown in Table 2. The Pb^{2+}-imprinted

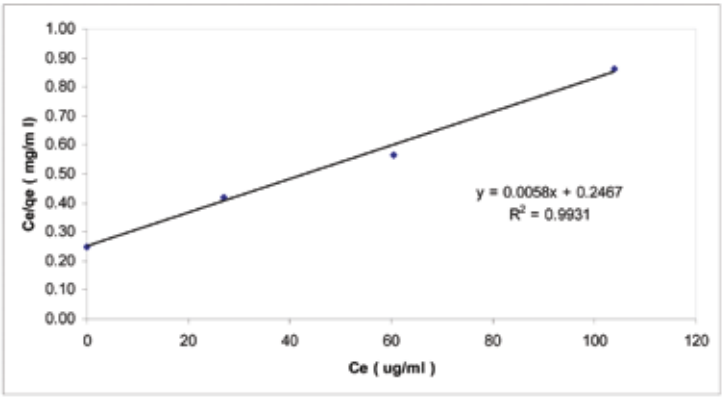

Fig. 4: The Langmuir plot for the adsorption of Pb(II) by fabricated MIP

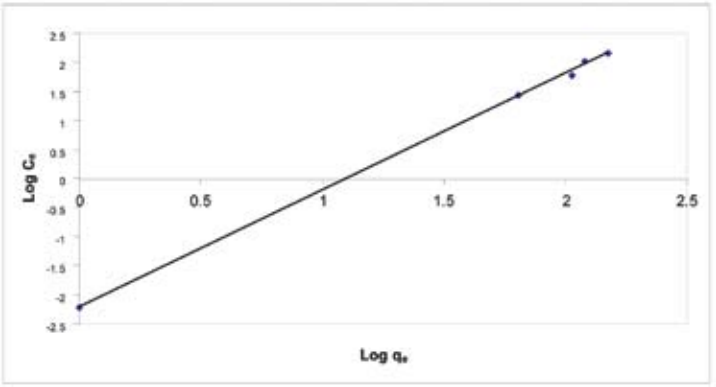

Fig. 5: The Freundlich plot for the adsorption of Pb(II) by fabricated MIP

polymer exhibited a low affinity in acidic concentrations (pH < 5.0) and a high affinity at pH 7.0. Muge *et al.* (2007), who fabricated ion imprinted beads for molecular recognition based mercury removal from human serum, also discovered a low affinity in acidic concentrations (pH < 5.0) and a high affinity at pH 7.0. This is due to the protonation of the carboxyl group in the polymer at low pH, indicating the inhibition of the complex formation between the recognition site (carboxyl group) and Pb(II) ion. pH higher than 7.0 was not tested due to the formation of precipitate between a high concentration of hydroxide ion and Pb(II) ion.

TABLE 1
Calculated value of Langmuir and Freundlich constants

	Experimental, q (ug/mg)	Langmuir constants			Freundlich constants		
		q_m(ug/mg)	b	r^2	K_F	n	r^2
MIP	148.78	204.08	0.02	0.993	0.006	0.496	0.979

TABLE 2
The effect of pH on the Pb^{2+} ion adsorption of Pb^{2+}-imprinted polymer

pH	Binding Capacity,ug/mg (MIP)
1	0.00
2	0.00
3	0.00
4	9.56
5	15.52
6	26.88
7	46.88

CONCLUSIONS

Molecularly imprinted beads, which were spherical in shape, were prepared using the radical polymerization. The average size of the beads was controlled to be between 63 and 140 μm in diameter. The adsorption was relatively fast and the time required to reach the equilibrium condition was about 20 min. The maximum adsorption capacity, for Pb^{2+} ions, was 150 μ/g dry weight of the imprinted polymer. The fast adsorption equilibrium was most probably due to the high complex and geometric affinity between the Pb^{2+} ions and Pb^{2+} cavities in the beads structure. The adsorption values was increased with the increasing concentration of Pb^{2+} ions, and the saturation value was achieved at the ion concentration of 250 μg/mL. This represented the saturation of the active binding cavities on the Pb^{2+}-imprinted polymer. The adsorption time was found to be 30 min. Therefore, Pb^{2+}-imprinted polymer can be used a number of times, without decreasing their adsorption capacities significantly.

ACKNOWLEDGEMENT

The author would like to acknowledge the Ministry of Science, Technology and Innovation of Malaysia for funding this research through the research grant, Science Fund 03-01-04-SF0138 and studentship to one of the authors.

REFERENCES

Andac, M., Mirel, S., Senel, S., Ridvan, S., Ersoz, A. and Denzli, A. (2007). Ion-imprinted beads for molecular recognition based mercury removal from human serum. *Biological Macromolecules, 40,* 159-166.

Andac, M., Ridvan, S. and Denizli, A. (2004). Molecular recognition based cadmium removal from human plasma. *Journal Of Chroamatography B, 811,* 119-126.

Araki, K., Maruyama, T., Kamiya, T. and Goto, M. (2005). Metal ion-selective membrane prepared by surface molecular imprinting. *Journal of Chromatography B, 818,* 141-145.

Birlik, E., Ersoz, A., Acikkalp, E., Denizli, A, Ridvan, S. (2006). Cr (III) imprinted polymeric beads: Sorption and preconcentration studies. *Journal of Hazardous Materials* (in Press).

B¨uy¨uktiryaki, S., Ridvan, S., Denizli, A. and Ers¨oz, A. (2007). Mimicking receptor for methyl mercury pre-concentration based on ion-imprinting. *Talanta, 71,* 699-705.

Elinde, C.G. and Friberg, L. (1980). *Handbook on the Toxicology of Metals*. Amsterdam: Elsevier North-Holland Biomedical Press.

Liu, Y., Chang, X., Wang, S., Guo, Y., Din, B. and Meng, S.M. (2004). Solid-phase extraction and pre-concentration of cadmium(II) in aqueous solution with Cd(II)-imprinted resin (poly-Cd(II)-DAAB-VP) packed columns. *Analytica Chimica Acta, 519*, 173-179.

Mayes, A.G. and Whitcombe, M.J. (2005). Synthetic strategies for the generation of molecularly imprinted organic polymers. *Advanced drug Delivery Reviews, 57*, 1742-1778.

Mostafa K., Yadollah Y., Ensieh G., Javad F. and Mojtaba S. (2007). Imprinted polymer particles for selenium uptake: Synthesis, characterization and analytical applications. *Analytica Chimica Acta, 581*, 208-213.

Nishide, H., Deguchi, J. and Thuchida, E. (1977). Adsorption of metal ions on cross linked poly(4-vinylpyridine) resin prepared with a metal ion as template. *Journal of Polymer Science, 15,* 3023-3029.

Ridvan, S., Birlik, E., Ersoz, A., Yilmaz, F., Gedikbey, T. and Denizli, A. (2003). Preconcentration of Copper on Ion-selective imprinted polymer microbeads. *Analytica Chimica Acta, 480*, 251-258.

Yavuz, H., Ridvan, S. and Denizli, A. (2005). Iron removal from human plasma based on molecular recognition using imprinted beads. *Materials Science & Engineering C, 25,* 521-528.

ISSN: 0128-7680
Pertanika J. Sci. & Technol. **17 (1)**: 163 – 171 (2009)

Some Explicit Conditions for a Stationary Representation of the Unilateral Second-Order Spatial ARMA Model

Saidatulnisa Abdullah and Mahendran Shitan*
Department of Mathematics, Faculty of Science, Universiti Putra Malaysia, 43400 UPM, Serdang, Selangor, Malaysia
**E-mail: mahen698@gmail.com*

ABSTRACT

The analysis of the spatial data has been carried out in many disciplines such as demography, meteorology, geology and remote sensing. The spatial data modelling is important because it recognizes the phenomenon of spatial correlation in field experiments. Three main categories of the spatial models, namely, the simultaneous autoregressive (SAR) models (Whittle, 1954), the conditional autoregressive (CAR) models (Bartlett, 1971), and the moving average (MA) models (Haining, 1978) have been studied. Whittle (1954) presented a form of bilateral autoregressive (AR) models, whereas Basu and Reinsel (1993) considered the *first-order* autoregressive moving average (ARMA) model of the quadrant type. Awang, N. and Mahendran Shitan (2003) presented the second-order ARMA model, and established some explicit stationary conditions for the model. When fitting the spatial models and making prediction, it is assumed that, the properties of the process would not change with sites. Properties like stationarities have to be assumed, and for this reason, it was therefore imperative that the researchers had made certain that the process was stationary. This could be achieved by providing the explicit stationarity conditions for the model. The explicit conditions, for a stationary representation of the *second-order* spatial unilateral ARMA model denoted as ARMA(2,1;2,1), have been established (Awang, N. and Mahendran Shitan, 2003) and in this paper, some explicit conditions are established for a stationary representation of the *second-order* spatial unilateral ARMA model, denoted as ARMA(2,2;2,2).

Keywords: ARMA model, spatial model, stationarity

INTRODUCTION

In this study, some conditions for stationarity are established for a more general second-order autoregressive moving average model:

$$Y_{ij} = \alpha_1 Y_{i-l,j} + \alpha_2 Y_{i,j-1} + \alpha_3 Y_{i-l,j-1} + \alpha_4 Y_{i-2,j} + \alpha_5 Y_{i-2,j-1} + \alpha_6 Y_{i,j-2} + \alpha_7 Y_{i-1,j-2} + \alpha_8 Y_{i-2,j-2} + \varepsilon_{ij} + \theta_1 \varepsilon_{i-1,j} + \theta_2 \varepsilon_{i,j-1} + \theta_3 \varepsilon_{i-1,j-1}$$

$$+\theta_4 \varepsilon_{i-2,j} + \theta_5 \varepsilon_{i-2,j-1} + \theta_6 \varepsilon_{i,j-2} + \theta_7 \varepsilon_{i-1,j-2} + \theta_8 \varepsilon_{i-2,j-2}, \quad (1)$$

where Y_{ij}, the value at the site (i,j), is a finite autoregesssion of the values at the sites, which lie in the lower quadrant of (i,j), for $i = 1,..., m$, $j = 1,..., n$ and ε_{ij} are a collection of independent random variables, with $E(\varepsilon_{ij}) = 0$ and Var $(\varepsilon_{ij}) = \sigma^2$.

Received: 11 January 2008
Accepted: 8 April 2008
*Corresponding Author

In Section 2, sufficient and necessary conditions for the existence of a stationary representation of the model in (1) are established. In Section 3, the conclusions are drawn.

THE CONDITIONS FOR THE SECOND-ORDER ARMA SPATIAL MODEL

First, the backward shift operators B_1 and B_2 were defined effectively as $B_1 Y_{ij} = Y_{i-1,j}$ and $B_2 Y_{i,j-1} = Y_{i,j-1}$. Equation (1) can then be written as follows:

$$(1- \alpha_1 B_1 - \alpha_2 B_2 - \alpha_3 B_1 B_2 - \alpha_4 B_1^2 - \alpha_5 B_1^2 B_2 - \alpha_6 B_2^2 - \alpha_7 B_1 B_2^2 - \alpha_8 B_1^2 B_2^2)\ Y_{ij}$$

$$= (1+ \theta_1 B_1 + \theta_2 B_2 + \theta_3 B_1 B_2 + \theta_4 B_1^2 + \theta_5 B_1^2 B_2 + \theta_6 B_2^2 + \theta_7 B_1 B_2^2 + \theta_8 B_1^2 B_2^2)\ \varepsilon_{ij} \quad (2)$$

Equation (2) can be written more compactly as;

$$\Phi(B_1, B_2)\, Y_{ij} = \Theta(B_1, B_2)\, \varepsilon_{ij} \quad (3)$$

where

$$\Phi(B_1, B_2) = (1 - \alpha_1 B_1 - \alpha_2 B_2 - \alpha_3 B_1 B_2 - \alpha_4 B_1^2 - \alpha_5 B_1^2 B_2 - \alpha_6 B_2^2 - \alpha_7 B_1 B_2^2 - \alpha_8 B_1^2 B_2^2)$$

and

$$\Theta(B_1, B_2) = (1 + \theta_1 B_1 + \theta_2 B_2 + \theta_3 B_1 B_2 + \theta_4 B_1^2 + \theta_5 B_1^2 B_2 + \theta_6 B_2^2 + \theta_7 B_1 B_2^2 + \theta_8 B_1^2 B_2^2)$$

Proposition. For the model defined as in (1), if none of the roots of $\Phi(z_1, z_2) = 1 - \alpha_1 z_1 - \alpha_2 z_2 - \alpha_3 z_1 z_2 - \alpha_4 z_1^2 - \alpha_5 z_1^2 z_2 - \alpha_6 z_2^2 - \alpha_7 z_1 z_2^2 - \alpha_8 z_1^2 z_2^2 = 0$ lie within the closed unit polydisc $(|z_1| \le 1, |z_2| \le 1)$ then

(i) $|\alpha_6| - |\alpha_2| < 1$,

(ii) $|\alpha_3 + \alpha_2 + \alpha_5| > |\alpha_7 + \alpha_6 + \alpha_8 + \alpha_4 + \alpha_1 - 1|$,

(iii) $|\alpha_3 - \alpha_2 - \alpha_5| > |\alpha_7 - \alpha_6 - \alpha_8 - \alpha_4 + \alpha_1 + 1|$,

(iv) $|\alpha_4| - |\alpha_1| < 1$,

(v) $|\alpha_3 + \alpha_1 + \alpha_7| > |\alpha_5 + \alpha_4 + \alpha_8 + \alpha_6 + \alpha_2 - 1|$,

(vi) $|\alpha_3 - \alpha_1 - \alpha_7| > |\alpha_5 - \alpha_4 - \alpha_8 - \alpha_6 + \alpha_2 + 1|$,

Proof of Proposition:
(a) Sufficiency

(i) Since $\Phi(z_1, z_2) \neq 0$ for all $|z_1| \le 1, |z_2| \le 1$ it implies that for $z_1 = 0, \Phi(z_1, z_2) \neq 0$ for $|z_2| \le 1$. The roots of $\Phi(0, z_2)$ $= 1 - \alpha_2 z_2 - \alpha_6 z_2^2 = 0$ is given by $z_2 = \dfrac{-\alpha_2 \pm \sqrt{\alpha_2^2 + 4\alpha_6}}{2\alpha_6}$. However, it is required that $|z_2| > 1$. Therefore,

$$z_2 = \frac{-\alpha_2 \pm \sqrt{\alpha_2^2 + 4\alpha_6}}{2\alpha_6} > 1.$$

This will give:

$$\left|\frac{-\alpha_2 \pm \sqrt{\alpha_2^2 + 4\alpha_6}}{2\alpha_6}\right| > 1,$$

$$\left|-\alpha_2 \pm \sqrt{\alpha_2^2 + 4\alpha_6}\right| > 2|\alpha_6|\ ,$$

$$\left(-\alpha_2 \pm \sqrt{\alpha_2^2 + 4\alpha_6}\right)^2 > 4\alpha_6^2\ ,$$

$$\alpha_2^2 + \alpha_2^2 + 4\alpha_6 \mp 2\alpha_2\sqrt{\alpha_2^2 + 4\alpha_6} > 4\alpha_6^2\ ,$$

$$\mp 2\alpha_2\sqrt{\alpha_2^2 + 4\alpha_6} > 4\alpha_6^2 - 2\alpha_2^2 - 4\alpha_6\ ,$$

$$4\alpha_2{}^2(\alpha_2{}^2 + 4\alpha_6) > 16\alpha_6{}^4 + 4\alpha_2{}^4 + 16\alpha_6{}^2 - 16\alpha_2{}^2\alpha_6{}^2 - 32\alpha_6{}^3 + 16\alpha_2{}^2\alpha_6\,,$$

$$16\alpha_6{}^4 + 16\alpha_6{}^2 - 16\alpha_6{}^2\alpha_2{}^2 - 32\alpha_6{}^3 < 0,$$

$$\alpha_6{}^2 + 1 - \alpha_2{}^2 - 2\alpha_6 < 0,$$

$$(\alpha_6 - 1)^2 < \alpha_2{}^2,$$

$$|\alpha_6 - 1| < |\alpha_2|,$$

$$|\alpha_6| - 1 < |\alpha_2|, \text{ and finally}$$

$$|\alpha_6| - |\alpha_2| < 1.$$

This establishes condition (i).
(ii) Taking $z_1 = 1$ implies that,
$\Phi(1, z_2) = 1 - \alpha_1 - \alpha_2 z_2 - \alpha_3 z_2 - \alpha_4 - \alpha_5 z_2 - \alpha_6 z_2{}^2 - \alpha_7 z_2{}^2 - \alpha_8 z_2{}^2$. The roots of $\Phi(1, z_2) = 0$ are given by:

$$z_2 = \frac{-(\alpha_2 + \alpha_3 + \alpha_5) \pm \sqrt{(\alpha_2 + \alpha_3 + \alpha_5)^2 + 4(\alpha_6 + \alpha_7 + \alpha_8)(1 - \alpha_1 - \alpha_4)}}{2(\alpha_6 + \alpha_7 + \alpha_8)}$$

However it is required that $|z_2| > 1$. Hence, this will give:

$\left|-(\alpha_2 + \alpha_3 + \alpha_5) \pm \sqrt{(\alpha_2 + \alpha_3 + \alpha_5)^2 + 4(\alpha_6 + \alpha_7 + \alpha_8)(1 - \alpha_1 - \alpha_4)}\right| > 2|\alpha_6 + \alpha_7 + \alpha_8|$, which will lead to:

$z_1 = -1$, the roots of $> |\alpha_7 + \alpha_6 + \alpha_8 + \alpha_4 + \alpha_1 - 1|$.

This establishes condition (ii).
(iii) Taking $z_1 = -1$, the roots of $\Phi(-1, z_2) = 1 + \alpha_1 - \alpha_2 z_2 + \alpha_3 z_2 - \alpha_4 - \alpha_5 z_2 - \alpha_6 z_2{}^2 + \alpha_7 z_2{}^2 - \alpha_8 z_2{}^2 = 0$ is given by:

$$z_2 = \frac{-(\alpha_2 - \alpha_3 - \alpha_5) \pm \sqrt{(\alpha_3 - \alpha_2 - \alpha_5)^2 - 4(\alpha_7 - \alpha_6 - \alpha_8)(1 + \alpha_1 - \alpha_4)}}{2(\alpha_7 - \alpha_6 - \alpha_8)} .$$

However, it is required that $|z_2|>1$. This will give:

$\left|-(\alpha_3 - \alpha_2 - \alpha_5) \pm \sqrt{(\alpha_3 - \alpha_2 - \alpha_5)^2 - 4(\alpha_7 - \alpha_6 - \alpha_8)(1 + \alpha_1 - \alpha_4)}\right| > 2|\alpha_7 - \alpha_6 - \alpha_8|$, which leads to:

$$|\alpha_3 - \alpha_2 - \alpha_5| > |\alpha_7 - \alpha_6 - \alpha_8 - \alpha_4 + \alpha_1 + 1|.$$

This establishes condition (iii).

(iv) Taking $z_2 = 0$, the roots $z_1 = \frac{-\alpha_1 \pm \sqrt{\alpha_1^2 + 4\alpha_4}}{2\alpha_4}$ requires that $|z_1|>1$.

This produces the following:

$$4\alpha_1^2(\alpha_1^2 + 4\alpha_4) > 16\alpha_4^4 + 4\alpha_1^4 + 16\alpha_4^2 - 16\alpha_1^2\alpha_4^2 - 32\alpha_4^3 + 16\alpha_1^2\alpha_4,$$

$$16\alpha_4^4 + 16\alpha_4^2 - 16\alpha_1^2\alpha_4^2 - 32\alpha_4^3 < 0,$$

$$\alpha_4^2 + 1 - \alpha_1^2 - 2\alpha_4 < 0,$$

$$(\alpha_4 - 1)^2 < \alpha_1^2,$$

$$|\alpha_4 - 1| < |\alpha_1|, \text{ but}$$

$$|\alpha_4| - |1| < |\alpha_4 - 1|, \text{ therefore}$$

$$|\alpha_4| - 1 < |\alpha_1|,$$

$$|\alpha_4| - |\alpha_1| < 1.$$

This establishes condition (iv).

(v) Taking $z_2 = 1$ implies that:
$\Phi(z_1,1) = 1 - \alpha_1 z_1 - \alpha_2 - \alpha_3 z_1 - \alpha_4 z_1^2 - \alpha_5 z_1^2 - \alpha_6 - \alpha_7 z_1 - \alpha_8 z^2$. The roots of $\Phi(z_1,1) = 0$ are given by: $z_1 = \frac{-(\alpha_1 + \alpha_3 + \alpha_7) \pm \sqrt{(\alpha_1 + \alpha_3 + \alpha_7)^2 + 4(\alpha_4 + \alpha_5 + \alpha_8)(1 - \alpha_2 + \alpha_6)}}{2(\alpha_4 + \alpha_5 + \alpha_8)}$.

However, we require that $|z_1|>1$. This will give:

$$\left|-(\alpha_1 + \alpha_3 + \alpha_7) \pm \sqrt{(\alpha_1 + \alpha_3 + \alpha_7)^2 + 4(\alpha_4 + \alpha_5 + \alpha_8)(1 - \alpha_2 + \alpha_6)}\right| > 2|\alpha_4 + \alpha_5 + \alpha_8|,$$

which leads to:

$$|\alpha_3 + \alpha_1 + \alpha_7| > |\alpha_5 + \alpha_4 + \alpha_8 + \alpha_6 + \alpha_2 - 1|.$$

This establishes the condition (v).

(vi) Taking $z_2 = -1$ implies that:
$\Phi(z_1, -1) = 1 - \alpha_1 z_1 + \alpha_2 + \alpha_3 z_1 - \alpha_4 z_1^2 + \alpha_5 z_1^2 - \alpha_6 - \alpha_7 z_1 - \alpha_8 z_1^2$. The roots of $\Phi(z_1,-1) = 0$ are given by:

$$z_1 = \frac{-(\alpha_3 - \alpha_1 - \alpha_7) \pm \sqrt{(\alpha_3 - \alpha_1 - \alpha_7)^2 - 4(\alpha_5 - \alpha_4 - \alpha_8)(1 + \alpha_2 - \alpha_6)}}{2(\alpha_5 - \alpha_4 - \alpha_8)}.$$

However, it is required that $|z_1| > 1$. This will give:

$\left|-(\alpha_3 - \alpha_1 - \alpha_7) \pm \sqrt{(\alpha_3 - \alpha_1 - \alpha_7)^2 - 4(\alpha_5 - \alpha_4 - \alpha_8)(1 + \alpha_2 - \alpha_6)}\right| > 2|\alpha_5 - \alpha_4 - \alpha_8|$, which leads to:

$$|\alpha_3 - \alpha_1 - \alpha_7| > |\alpha_5 - \alpha_4 - \alpha_8 - \alpha_6 + \alpha_2 + 1|.$$

This establishes condition (vi).

(b) *Necessity*
In (3), if $\Phi(z_1,z_2) = 0$ has root (w_1, w_2), then:

$$(1 - \alpha_1 w_1 - \alpha_2 w_2 - \alpha_3 w_1 w_2 - \alpha_4 w_1^2 - \alpha_5 w_1^2 w_2 - \alpha_6 w_2^2 - \alpha_7 w_1 w_2^2 - \alpha_8 w_1^2 w_2^2) = 0.$$

This gives

$$w_2 = \frac{-(\alpha_2 + \alpha_3 w_1 + \alpha_5 w_1^2) \pm \sqrt{(\alpha_2 + \alpha_3 w_1 + \alpha_5 w_1^2)^2 - 4(\alpha_6 + \alpha_7 w_1 + \alpha_8 w_1^2)(\alpha_1 w_1 + \alpha_4 w_1^2 - 1)}}{2(\alpha_6 + \alpha_7 w_1 + \alpha_8 w_1^2)} \quad (4)$$

Equation (4) can also be rewritten as, $w_2 = \frac{-b_2 \pm \sqrt{b_2^2 - 4a_2 c_2}}{2a_2}$, where:

$a_2 = \alpha_6 + \alpha_7 \mathrm{Re}(w_1) + \alpha_8 |w_1|^2$, $b_2 = \alpha_2 + \alpha_3 \mathrm{Re}(w_1) + \alpha_5 |w_1|^2$ and $c_2 = \alpha_1 \mathrm{Re}(w_1) + \alpha_4 |w_1|^2 - 1$.

Let $|w_1|$, and write $w_1 = r \exp(i\phi)$, where $0 \le r \le 1$, $0 \le \phi \le 2\pi$.
We than has:
$|r \exp(i\phi)| < 1$ or $|r| < 1$. This is equivalent to $-1 < r < 1$.
The researchers need to establish that no roots of $\Phi(z_1, z_2) = 0$ lie within the closed unit polydisc, and hence, it we need to show that:

$|w_2| > 1$ or $|w_2|^2 > 1$.

For $|w_2|^2 > 1$, we have $\left|\frac{-b_2 \pm \sqrt{b_2^2 - 4a_2 c_2}}{2a_2}\right|^2 > 1$, or $b_2^2 > (a_2 + c_2)^2$. This means the following is needed:

$$(\alpha_2 + \alpha_3 \mathrm{Re}(w_1) + \alpha_5 |w_1|^2)^2 > (\alpha_6 + \alpha_7 \mathrm{Re}(w_1) + \alpha_8 |w_1|^2 + \alpha_1 \mathrm{Re}(w_1) + \alpha_4 |w_1|^2 - 1)^2$$

or

$$\alpha_2^2 + \alpha_3^2 r^2 + \alpha_5^2 r^4 + 2(|\alpha_2 \alpha_3| r + |\alpha_2 \alpha_5| r^2 + |\alpha_3 \alpha_5| r^3) > \alpha_6^2 + \alpha_7^2 r^2 + \alpha_8^2 r^4 + 2(|\alpha_6 \alpha_7| r + |\alpha_7 \alpha_8| r^3 + |\alpha_6 \alpha_8| r^2)$$

$$+\alpha_1^{\,2} r^2 + \alpha_4^{\,2} r^4 + 1 + 2\,(|\alpha_1\alpha_4| r^3 - |\alpha_1| r - |\alpha_4| r^2)$$
$$+ 2(|\alpha_1\alpha_6| r + |\alpha_4\alpha_6| r^2 - |\alpha_6| + |\alpha_1\alpha_7| r^2 + |\alpha_4\alpha_7| r^3 - |\alpha_7| r + |\alpha_1\alpha_8| r^3 + |\alpha_4\alpha_8| r^4 - |\alpha_8| r^2)$$

Nevertheless, it is sufficient to show that:

$$\alpha_2^{\,2} - \alpha_6^{\,2} - 1 + 2\,|\alpha_6| > M,$$

where $M = \sup_{0 \le r \le 1} f(r)$

$$= \sup_{0 \le r \le 1} \{\alpha_7^{\,2} r^2 + \alpha_8^{\,2} r^4 + 2(|\alpha_6\alpha_7| r + |\alpha_7\alpha_8| r^3 + |\alpha_6\alpha_8| r^2)$$
$$+ \alpha_1^{\,2} r^2 + \alpha_4^{\,2} r^4 + 2(|\alpha_1\alpha_4| r^3 - |\alpha_1| r - |\alpha_4| r^2)$$
$$+ 2(|\alpha_1\alpha_6| r + |\alpha_4\alpha_6| r^2 + |\alpha_1\alpha_7| r^2 + |\alpha_4\alpha_7| r^3 - |\alpha_7| r + |\alpha_1\alpha_8| r^3 + |\alpha_4\alpha_8|\alpha_7| r^4 - |\alpha_8| r^2)$$
$$- \alpha_3^{\,2} r^2 - \alpha_5^{\,2} r^4 - 2(|\alpha_2\alpha_3| r + |\alpha_2\alpha_5| r^2 + |\alpha_3\alpha_5| r^3)\}$$

The function $f(r)$ may attain its minimum over, $0 \le r \le 1$ at $r = 0$, in which case $\alpha_2^{\,2} - \alpha_6^{\,2} - 1 + 2\,|\alpha_6| > 0$, or $|\alpha_6| - |\alpha_2| < 1$, is needed, and this follows condition (i):
Similarly, the function $f(r)$ may attain its maximum over $0 \le r \le 1$ at $r = 1$, in which, the following is needed:

$$\alpha_2^{\,2} - \alpha_6^{\,2} - 1 + 2|\alpha_6| > \alpha_7^{\,2} + \alpha_8^{\,2} + 2\,(|\alpha_6\alpha_7| + |\alpha_7\alpha_8| + |\alpha_6\alpha_8|)$$
$$+ \alpha_1^{\,2} + \alpha_4^{\,2} + 2(|\alpha_1\alpha_4| - |\alpha_1| - |\alpha_4|)$$
$$+ 2(|\alpha_1\alpha_6| + |\alpha_4\alpha_6| + |\alpha_1\alpha_7| + |\alpha_4\alpha_7| - |\alpha_7| + |\alpha_1\alpha_8| + |\alpha_4\alpha_8| - |\alpha_8|) - \alpha_3^{\,2} - \alpha_5^{\,2}$$
$$- 2\,(|\alpha_2\alpha_3| + |\alpha_2\alpha_5| + |\alpha_3\alpha_5|).$$

This can also be re-expressed as:

$$\alpha_2^{\,2} + \alpha_3^{\,2} + \alpha_5^{\,2} + 2(|\alpha_2\alpha_3| + |\alpha_2\alpha_5| + |\alpha_3\alpha_5| > \alpha_6^{\,2} + \alpha_7^{\,2} + \alpha_8^{\,2} + \alpha_1^{\,2} + \alpha_4^{\,2} + 1$$
$$+ 2(|\alpha_6\alpha_7| + |\alpha_7\alpha_8| + |\alpha_4\alpha_7| + |\alpha_1\alpha_7| - |\alpha_7|)$$
$$+ 2(|\alpha_6\alpha_8| + |\alpha_4\alpha_6| + |\alpha_1\alpha_6| - |\alpha_6|)$$
$$+ 2\,(|\alpha_4\alpha_8| + |\alpha_1\alpha_8| - |\alpha_8|) + 2|\alpha_1\alpha_4| - 2|\alpha_4| - 2|\alpha_1|).$$

From the above $|\alpha_3 + \alpha_2 + \alpha_5| > |\alpha_7 + \alpha_6 + \alpha_8 + \alpha_4 + \alpha_1 - 1|$, can be obtained, and this follows condition (ii).

The function $f(r)$ may also attain its maximum over $0 \le r \le 1$ at $r = 1$, in which the following is needed:

$$\alpha_2^{\,2} - \alpha_6^{\,2} - 1 - 2|\alpha_6| > \alpha_7^{\,2} + \alpha_8^{\,2} + 2\,(-|\alpha_6\alpha_7| - |\alpha_7\alpha_8| + |\alpha_6\alpha_8|)$$
$$+ \alpha_1^{\,2} + \alpha_4^{\,2} + 2(-|\alpha_1\alpha_4| + |\alpha_1| - |\alpha_4|)$$
$$+ 2(-|\alpha_1\alpha_6| + |\alpha_4\alpha_6| + |\alpha_1\alpha_7| - |\alpha_4\alpha_7| + |\alpha_7| - |\alpha_1\alpha_8| + |\alpha_4\alpha_8| - |\alpha_8|) - \alpha_3^{\,2} - \alpha_5^{\,2}$$
$$- 2\,(-|\alpha_2\alpha_3| + |\alpha_2\alpha_5| - |\alpha_3\alpha_5|).$$

This can also be re-expressed as:

$$\alpha_2^{\,2} + \alpha_3^{\,2} + \alpha_5^{\,2} - 2(|\alpha_2\alpha_3| - |\alpha_2\alpha_5| + |\alpha_3\alpha_5| > \alpha_7^{\,2} + \alpha_6^{\,2} + \alpha_8^{\,2} + \alpha_1^{\,2} + \alpha_4^{\,2} + 1$$
$$+ 2(-|\alpha_6\alpha_7| - |\alpha_7\alpha_8| + |\alpha_1\alpha_7| - |\alpha_4\alpha_7| + |\alpha_7|)$$
$$+ 2(|\alpha_6\alpha_8| - |\alpha_1\alpha_6| + |\alpha_4\alpha_6| - |\alpha_6|)$$
$$+ 2\,(-|\alpha_1\alpha_8| + |\alpha_4\alpha_8| - |\alpha_8|) + 2(-|\alpha_1\alpha_4| + |\alpha_1|) - 2|\alpha_4|.$$

From this $|\alpha_3 - \alpha_2 - \alpha_5| > |\alpha_7 - \alpha_6 - \alpha_8 + \alpha_1 - \alpha_4 + 1|$, can be obtained and this follows condition (iii).

To provide proofs of necessity for conditions (iv) – (vi), (3) will be considered if $\Phi(z_1, z_2) = 0$ has roots (w_1, w_2), then

$$(1 - \alpha_1 w_1 - \alpha_2 w_2 - \alpha_3 w_1 w_2 - \alpha_4 w_1^2 - \alpha_5 w_1^2 w_2 - \alpha_6 w_2^2 - \alpha_7 w_1 w_2^2 - \alpha_8 w_1^2 w_2^2) = 0.$$

This gives

$$w_1 = \frac{-(\alpha_1 + \alpha_3 w_2 + \alpha_7 w_2^2) \pm \sqrt{(\alpha_1 + \alpha_3 w_2 + \alpha_7 w_2^2)^2 - 4(\alpha_4 + \alpha_5 w_2 + \alpha_8 w_2^2)(\alpha_2 w_2 + \alpha_6 w_2^2 - 1)}}{2(\alpha_4 + \alpha_5 w_2 + \alpha_8 w_2^2)} \tag{5}$$

Equation (5) can also be rewritten as $w_1 = \frac{-b_1 \pm \sqrt{b_1^2 - 4a_1 c_1}}{2a_1}$, where:

$a_1 = \alpha_4 + \alpha_5 \mathrm{Re}(w_2) + \alpha_8 |w_2|^2$, $b_1 = \alpha_1 + \alpha_3 \mathrm{Re}(w_2) + \alpha_7 |w_2|^2$ and $c_1 = \alpha_2 \mathrm{Re}(w_2) + \alpha_6 |w_2|^2 - 1$.

Let $|w_2| \leq 1$, and write $w_2 = r \exp(i\phi)$, where $0 \leq r \leq 1$, $0 \leq \phi \leq 2\pi$.

Since $|r \exp(i\phi)| < 1$ or $|r| < 1$, This is equivalent to $-1 < r < 1$.

Similarly, it is crucial to establish that no roots of $\Phi(z_1, z_2) = 0$ lie within the closed unit polydisc, and for this reason, it is therefore important to show that:

$|w_1| > 1$ or $|w_1|^2 > 1$.

For $|w_1|^2 > 1$, $\left| \frac{-b_1 \pm \sqrt{b_1^2 - 4a_1 c_1}}{2a_1} \right|^2 > 1$, or $b_1^2 > (a_1 + c_1)^2$ is achieved.

This means, the following is required:

$$(\alpha_1 + \alpha_3 \mathrm{Re}(w_2) + \alpha_7 |w_2|^2)^2 > (\alpha_4 + \alpha_5 \mathrm{Re}(w_2) + \alpha_8 |w_2|^2 + \alpha_2 \mathrm{Re}(w_2) + \alpha_6 |w_2|^2 - 1)^2$$

or

$$\begin{aligned}
&\alpha_1^2 + \alpha_3^2 r^2 + \alpha_7^2 r^4 + 2(|\alpha_1 \alpha_3| r + |\alpha_1 \alpha_7| r^2 + |\alpha_3 \alpha_7| r^3) > \\
&\alpha_4^2 + \alpha_5^2 r^2 + \alpha_8^2 r^4 + \alpha_2^2 r^2 + \alpha_6^2 r^4 + 1 \\
&+ 2(|\alpha_4 \alpha_5| r + |\alpha_4 \alpha_8| r^2 + |\alpha_2 \alpha_4| r + |\alpha_4 \alpha_6| r^2 - |\alpha_4|) \\
&+ 2(|\alpha_5 \alpha_8| r^3 + |\alpha_2 \alpha_5| r^2 + |\alpha_5 \alpha_6| r^3 - |\alpha_5| r) \\
&+ 2(|\alpha_2 \alpha_8| r^3 + |\alpha_6 \alpha_8| r^4 - |\alpha_8| r^2) \\
&+ 2(|\alpha_2 \alpha_6| r^3 - |\alpha_2| r) - 2|\alpha_6| r^2
\end{aligned}$$

It is sufficient that to show that:

$$\begin{aligned}
&\alpha_1^2 - \alpha_4^2 + 2|\alpha_4| - 1 > M, \text{ where } M = \sup_{0 \leq r \leq 1} f(r) = \sup_{0 \leq r \leq 1} \{\alpha_5^2 r^2 + \alpha_8^2 r^4 + \alpha_2^2 r^2 + \alpha_6^2 r^4 \\
&+ 2(|\alpha_4 \alpha_5| r + |\alpha_4 \alpha_8| r^2 + |\alpha_2 \alpha_4| r + |\alpha_4 \alpha_6| r^2) \\
&+ 2(|\alpha_5 \alpha_8| r^3 + |\alpha_2 \alpha_5| r^2 + |\alpha_5 \alpha_6| r^3 - |\alpha_5| r) \\
&+ 2(|\alpha_2 \alpha_8| r^3 + |\alpha_6 \alpha_8| r^4 - |\alpha_8| r^2) \\
&+ 2(|\alpha_2 \alpha_6| r^3 - |\alpha_2| r) - 2\alpha_6 r^2 - \alpha_3^2 r^2 - \alpha_7^2 r^4 \\
&- 2(|\alpha_1 \alpha_3| r + |\alpha_1 \alpha_7| r^2 + |\alpha_3 \alpha_7| r^3)\}
\end{aligned}$$

The function $f(r)$ may attain its minimum over $0 \le r \le 1$ at $r = 0$, in which $\alpha_1^2 - \alpha_4^2 + 2|\alpha_4| - 1 > 0$ or $|\alpha_4| - |\alpha_1| < 1$ is needed, and this follows condition (iv).

In addition, the function $f(r)$ may attain its maximum over $0 \le r \le 1$, in which the following is needed:

$$\begin{aligned}
&\alpha_1^2 - \alpha_4^2 + 2|\alpha_4| - 1 > \alpha_5^2 + \alpha_8^2 + \alpha_2^2 + \alpha_6^2 \\
&+ 2(|\alpha_4\alpha_5| + |\alpha_4\alpha_8| + |\alpha_2\alpha_4| + |\alpha_4\alpha_6|) \\
&+ 2(|\alpha_5\alpha_8| + |\alpha_2\alpha_5| + |\alpha_5\alpha_6| - |\alpha_5|) \\
&+ 2(|\alpha_2\alpha_8| + |\alpha_6\alpha_8| - |\alpha_8|) \\
&+ 2(|\alpha_2\alpha_6| - |\alpha_2|) - 2\alpha_6 + \alpha_3^2 - \alpha_7^2 \\
&+ 2(|\alpha_1\alpha_3| + |\alpha_1\alpha_7| + |\alpha_3\alpha_7|)
\end{aligned}$$

This can also be re-expressed as:

$$\begin{aligned}
&\alpha_1^2 + \alpha_3^2 + \alpha_7^2 + 2(|\alpha_1\alpha_3| + |\alpha_1\alpha_7| + |\alpha_3\alpha_7| > \alpha_4^2 + \alpha_5^2 + \alpha_8^2 + \alpha_2^2 + \alpha_6^2 + 1 \\
&+ 2(|\alpha_4\alpha_5| + |\alpha_4\alpha_8| + |\alpha_2\alpha_4| + |\alpha_4\alpha_6| - |\alpha_4|) \\
&+ 2(|\alpha_5\alpha_8| + |\alpha_2\alpha_5| + |\alpha_5\alpha_6| - |\alpha_5|) \\
&+ 2(|\alpha_2\alpha_8| + |\alpha_6\alpha_8| - |\alpha_8|) + 2(|\alpha_2\alpha_6| - 2|\alpha_2| - 2|\alpha_6|).
\end{aligned}$$

From this $|\alpha_1 + \alpha_3 + \alpha_7| > |\alpha_4 + \alpha_5 + \alpha_8 + \alpha_2 + \alpha_6 - 1|$, can be obtained, and this is based on condition (v).

The function $f(r)$ may also attain its maximum over $0 \le r \le 1$ at $r = -1$, in which the following is needed:

$$\begin{aligned}
&\alpha_1^2 - \alpha_4^2 + 2|\alpha_4| - 1 > \alpha_5^2 + \alpha_8^2 + \alpha_2^2 + \alpha_6^2 \\
&+ 2(-|\alpha_4\alpha_5| + |\alpha_4\alpha_8| - |\alpha_2\alpha_4| + |\alpha_4\alpha_6|) \\
&+ 2(-|\alpha_5\alpha_8| + |\alpha_2\alpha_5| - |\alpha_5\alpha_6| + |\alpha_5|) \\
&+ 2(-|\alpha_2\alpha_8| + |\alpha_6\alpha_8| - |\alpha_8|) \\
&+ 2(-|\alpha_2\alpha_6| + |\alpha_2|) - 2|\alpha_6| - \alpha_3^2 - \alpha_7^2 \\
&- 2(-|\alpha_1\alpha_3| + |\alpha_1\alpha_7| - |\alpha_3\alpha_7|)
\end{aligned}$$

This can be re-expressed as:

$$\begin{aligned}
&\alpha_1^2 + \alpha_3^2 + \alpha_7^2 + 2(-|\alpha_1\alpha_3| + |\alpha_1\alpha_7| - |\alpha_3\alpha_7|) > \alpha_4^2 + \alpha_5^2 + \alpha_8^2 + \alpha_2^2 + \alpha_6^2 + 1 \\
&+ 2(-|\alpha_4\alpha_5| - |\alpha_5\alpha_8| - |\alpha_5\alpha_6| + |\alpha_2\alpha_5| + |\alpha_5|) \\
&+ 2(|\alpha_4\alpha_8| + |\alpha_4\alpha_6| - |\alpha_2\alpha_4| - |\alpha_4|) \\
&+ 2(|\alpha_6\alpha_8| - |\alpha_2\alpha_8| - |\alpha_8|) + 2(-|\alpha_2\alpha_6| - |\alpha_6|) + 2|\alpha_2|).
\end{aligned}$$

From the above, $|\alpha_3 - \alpha_1 - \alpha_7| > |\alpha_5 - \alpha_4 - \alpha_8 - \alpha_6 + \alpha_2 + 1|$ can be obtained; this follows condition (vi).

CONCLUSIONS

In this study, some explicit conditions were established for the existence of a stationary representation of the more general second-order unilateral spatial ARMA model, as discussed in Section 2.

The previous models being studied were mostly of the first-order, that is, only the nearest neighbouring sites are used to model the value of a particular site. In some situations, it is

not enough to merely use just the neighbouring values to model the value of a certain site or describe the spatial correlations in the data. Therefore, not only a second-order spatial model is necessary, it can also serve as an alternative to depict the spatial correlation of the data on a regular grid. However, the estimation of the parameters of such a model must be done in such a way that the conditions (set out in Section 2) do not contradict and that the parameters of the model should be maximised with bounded constraints.

REFERENCES

AWANG, N. and MAHENDRAN SHITAN. (2003). Some explicit stationary conditions for the unilateral second-order spatial ARMA model. *Proc. 1st Internat. Conf. on Research and Education in Mathematics (*pp. 96-99), Bangi, Selangor.

BARTLETT, M.S. (1971). Physical nearest neighbour models and non-linear time series. *J. Appl. Prob.*, *8,* 222-232.

BASU, S. and REINSEL, G.C. (1993). Properties of the spatial unilateral first-order ARMA Model. *Adv. Appl. Prob.*, *25*, 631 - 648.

HAINING, R.P. (1978). The moving average model for spatial interaction, *Tran. Inst. Br. Geog.*, *3,* 202-225.

WHITTLE, P. (1954). On stationary processes in the plane. *Biometrika*, *41,* 434 - 449.

ISSN: 0128-7680
Pertanika J. Sci. & Technol. **17 (1)**: 173 – 181 (2009)

Corn Cobs and Sugar Cane Waste as a Viscosivier in Drilling Fluid

Sonny Irawan*, Ahmad Zakuan Ahmad Azmi and Mohd. Saaid
Department of Geoscience and Petroleum Engineering,
Universiti Teknologi PETRONAS, Bandar Seri Iskandar,
31750 Tronoh, Perak, Malaysia
**E-mail: drsonny_irawan@petronas.com.my*

ABSTRACT

The present project investigated the potential of utilizing corncobs and sugar cane waste as viscosivier in drilling fluid. For this purpose, the synthetic-based drilling fluid, Sarapar 147, was used as the base fluid. Both the materials were subjected to pre-treatment of drying, dehumidifying, grinding and sieving process prior to rheological tests. The rheological tests were conducted in accordance with the API 13B specifications to measure mud density, plastic viscosity, yield point, 10-second and 10-minute gel strength. The study found that plastic viscosity and yield point had a direct relationship with the amount of materials added. To drill fluid additive with corn cobs, the density, plastic viscosity and yield point were increased when the amount of additives were increased. Based on these experiments, both additives were found to have the potential to be used as additive in drilling fluid. In particular, they were able to improve its rheological properties by increasing the density, plastic viscosity and yield point. The suitable concentration for the corn cobs and sugar cane is 6.45 lb/bbl and 9.43 lb/bbl, respectively.

Keyword: Drilling fluid, rheology, additives, corn cobs, sugar cane

INTRODUCTION

Wells are drilled through different formations which require different mud properties to achieve the optimum penetration and stable borehole conditions. Therefore, the design of a particular mud program needs to take into consideration a number of factors such as the availability of additives, temperature and contamination. Generally, drilling fluid can be classified into two categories, water based fluids (WBF) and non-aqueous based fluid (NABF). The NABF can be further divided into sub-categories, namely oil-based fluids (OBF), enhanced mineral oil-based fluids (EMOBF) and synthetic-based fluids (SBF). The NABF has been widely used because of its superior performance in drilling operations. However, due to an environmental issue in the use of OBF, it was changed to SBF. The purpose of developing SBF was to cater difficult drilling targets and the capability in reducing environmental impacts (McKee, 1995). The SBF is synthesized from the components of petroleum products or has non-hydrocarbon derivatives (Imran, 2006). Drilling and production discharges to the marine environment present different environmental concerns to those in the offshore areas. Among the potential impacts to the marine environment include toxicity, bioaccumulation and biological oxygen demand (BOD).

Received: 25 February 2008
Accepted: 28 May 2008
*Corresponding Author

Agriculture is one of the main economic activities in Malaysia. The industry produces a large amount of wastes, which could be utilized for other better purposes. From the perspective of oil and gas industry, this agriculture waste can be reused in formulating drilling fluids. Furthermore, most agriculture waste is harmless to both human and the environment. In this study, corn cobs and sugar cane waste, two examples of the waste, derived from the local agriculture activities, were explored for their practical use as viscosivier in drilling fluid. These wastes were extracted to be used as loss circulation materials and viscosivier in drilling fluid formulation. Samples of mud added with the treated waste materials were subjected to rheological measurement and lost circulation. The rheological properties, measured with a rotational viscometer, are commonly used to indicate solid build-up flocculation or deflocculation of solids, lifting and suspension capabilities, as well as to calculate hydraulics of a drilling fluid. At a given temperature and pressure, fluids are characterized by their behaviour under transient conditions, as manifested by their response time to change conditions of flow.

METHODOLOGY

The experiment was conducted in accordance with the standards stipulated in the American Petroleum Institute - API 13B-2, and recommended by the Practice Standard Procedure for Testing Oil-Based Drilling Fluid. Sarapar 147, which is the product from Shell, was used as the base fluid in the present study.

The Preparation of Additives

First, sugar cane waste was dried so as to remove leaves and other particles. Next, the sugar cane stalks were squeezed, bagasse, to release sap and sugar water. The same procedures were repeated for corn cobs. Corn kernels were to obtain the cobs. Both additives were dehumidified in an oven for 24 hours at 70°C. A Mortar Grinder was used to grind the additives into small pieces. Then, a Sieve Shaker was used separately obtain the desired particle size of 125-500 microns.

The Preparation of the Mud Sample

In this study, the Hamilton Beach Multi mixer was used extensively to prepare the mud samples. The oil-water ratio was set at 70:30, as recommended by the API 13B. Firstly, the required volume of Sarapar 147 was poured into the mixing container, followed by primary emulsifier and secondary emulsifier. Next, the required mass of lime was added, followed by Brine (calcium chloride + water) and additives. In the final step, the required amount of bentonite was mixed and stirred. These mixing stages are illustrated in *Fig. 1.*

Properties Measured

Three parameters were measured to assess the rheological performance of the prepared mud samples. These were density (lb/gal), plastic viscosity (cP) and gel strength (cP).

(i) Density

The procedure was to fill the cup with mud and put it on the lid. The excess mud was wiped off from the lid. The rider was moved along the arm till a balance was obtained, before the density (lb/gal) reading was recorded.

(ii) Plastic Viscosity and Yield Point

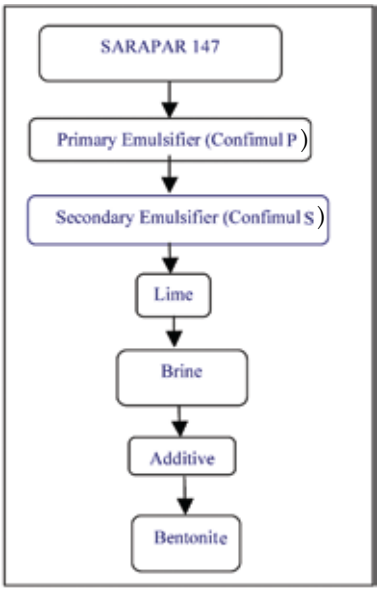

Fig. 1: Flowchart of the mud mixing process

Fann Viscometer Model 35SA was used for the rheology test. The temperature of the mud sample was within 120°F ± 2°F throughout the tests. For this part, the mud sample was kept at 120°F ± 2°F throughout the test. The thermal cup was filled with 2/3 full of the mud sample. The thermal cup was placed on the viscometer stand and the rotary sleeve was immersed into the thermal cup. The mud sample was then heated at 120 ± 2°F. The dial reading was taken when the viscometer was run at 600 rpm. The speed was then changed to 300 rpm and the dial reading was taken. The dial reading was also taken for 200 rpm, 100 rpm, 6 rpm and 3 rpm. The characteristics, which can be obtained from this procedure, are Plastic Viscosity (PV) and Yield Point (YP).

(iii) Gel Strength – 10 Seconds & 10 Minutes

For the 10-second gel strength measurement, the viscometer was turned to 600 rpm for 10 seconds, and the toggle was switched off and the mud was allowed to stand for 10 seconds. After 10 seconds, the viscometer was run at 3 rpm and the maximum dial reflection was recorded. For the 10- minute gel strength reading, the same procedures were applied, but it was allowed to operate for 10 minutes (API Standard 13 B, 1995).

RESULTS AND DISCUSSION

Mud Density

In the experiment, the mud density was intentionally set around 8 lb/gal to observe any changes. From the experiment conducted, it was shown in *Fig. 2* that the mud density would increase when the amount of additives was increased. For the mud additives added in 125-microns and 500-microns corn cobs, the trends of density were found to remain

the same. Initially, both corn cobs sizes were indicated to have the same density until the amount of 0.013 lb was achieved. Further addition of additives would cause the curve to diverge. As for the 500 microns of the particle size, the increment might be due to the solid content as the size was larger as compared to 125 microns. In this study, a small amount of additives was found to significantly increase the mud density.

Fig. 3 shows the density of the mud added with sugar cane waste. It was found to have the same measurement density trend as that of the corn cobs added mud. Thus, it can be stated that the amount has a direct relationship with the density of the mud. However, the particle size was found to yield lesser effect. For this, it was observed that the density was almost similar throughout the addition of the additives. The densities started to increase when the amount of corn cobs or sugar canes exceeded 0.013 lb.

Plastic Viscosity

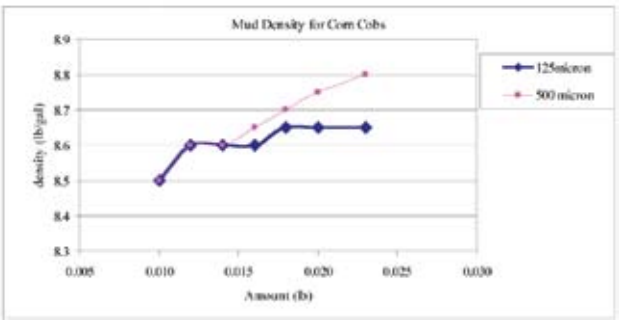

Fig. 2: Mud density of corn cobs

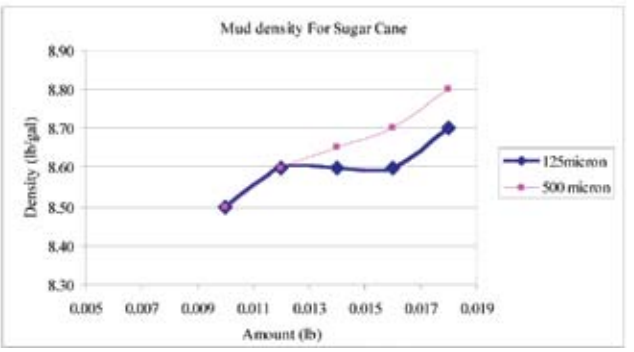

Fig. 3: Mud density of sugar cane

Fig. 4 shows that the plastic viscosity of mud added increased linearly with the amount of corn cobs added. Without any additive, which was the base sample, it gave a reading of 19 cP when 0.011 lb of additive was added; the plastic viscosity was measured up to 22 cP. At the amount of 0.022 lb, it gave a reading of 24.5 cP for 125 microns and 26 cP for 500 microns. Further

increment of the corn cobs would decrease the value of the plastic viscosity. As expected, 500 microns showed a slightly higher value of plastic viscosity as compared to 125 microns due to its particle size. The larger the particle, the more viscous of the fluid would be.

Fig. 5 illustrates the trend of plastic viscosity for mud added sugar cane. Unlike the corn cobs, sugar cane additives experienced its optimum value in the earlier amount of the addition. It was observed that the amount 0.011 lb initially added to the additives and the plastic viscosity increased as compared to the base fluid, which was 16 cP. Interestingly, the trend was found to be still valid if the amount of 0.012 lb was added. However, it started to decrease at 0.013 lb. If the additives were continuously added, the curves of the graph would tend to decrease. The curve of 500 microns gave a higher reading as compared to 125 microns due to its particle size. Based on the observation of both the figures (4 and 5), there must be an optimum of plastic viscosity value for the formulation to work affectively. As for the corn cobs, the optimum value was found to be around 0.019 lb and this was about 0.013 lb for sugar cane

Yield Point

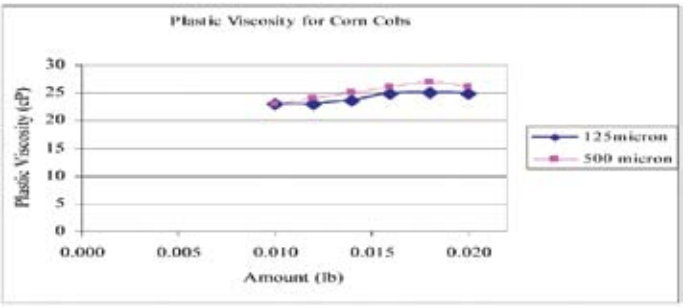

Fig. 4: Plastic viscosity for corn cobs additive

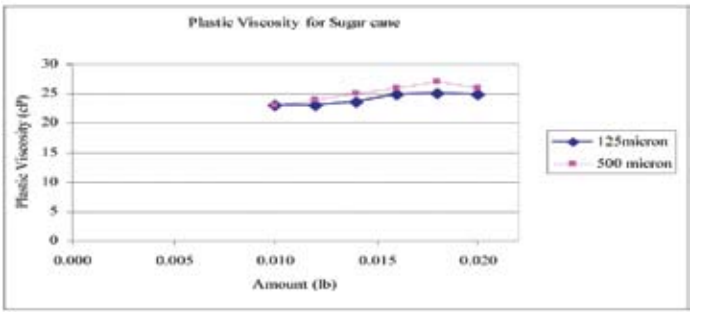

Fig. 5: Plastic viscosity for sugar cane additive

From *Fig. 6*, the value yield point decreased as the amount increased for corn cobs, in both sizes. For the 125 and 500 microns, the minimum reading was revealed at 0.022. It important to highlight that further increment of the amount of additives would cause the

curve to keep on decreasing.

Based on *Fig. 7*, the trend of graph for sugar cane was found to behave better when compared with the corn cob curves. It basically showed the same trend, with a reduction in the yield point as the amount was increased. The 500 microns was found to have a lower value compared to 125 microns. This was due to the fact that there is more solid content in the fluid sample of 125 microns as compared to 500 microns, thus decreased the distances between inter-particles. Further increment of the amount would result in the value of yield point to decrease. The yield point is sensitive to the electrochemical environment, indicating the need for chemical treatment. The yield point might be reduced by the addition of substances which neutralize electric charges such as thinning agent and by addition of chemicals to precipitate the contaminants.

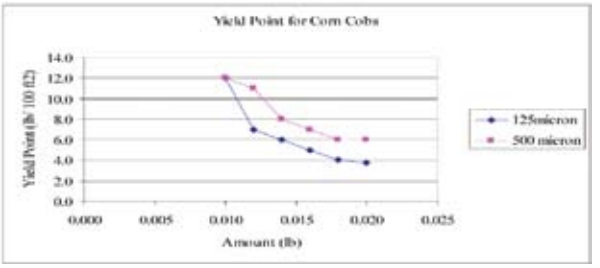

Fig. 6: Yield point for corn cobs

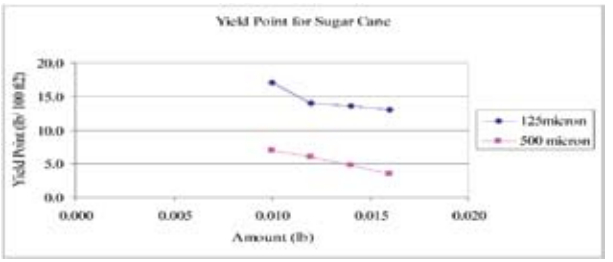

Fig. 7: Yield point for sugar cane

Gel Strength

For the corn cobs in the sizes of 125 and 500 microns, the highest value was found at the amount of 0.011 lb, while the lowest value was at the amount of 0.022 lb, as shown in *Figs. 8* and *9*. A similar trend was also obtained for the sugar cane additives depicted in *Figs. 9* and *10*. For both the additives, the particle size of 500 microns showed a higher value as compared to 125 microns. The trends of the graph, for the gel strength of both additives, are almost identical with the yield point graph. This could probably due to the attractive forces in the mud system.

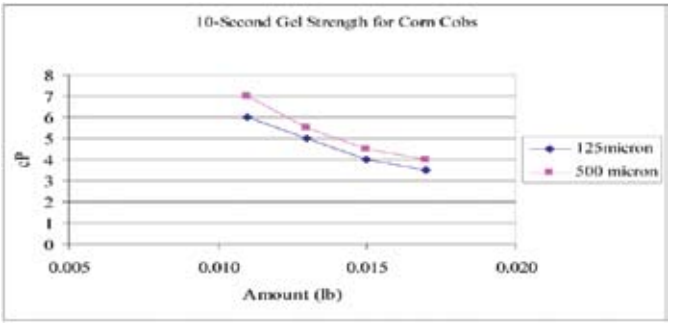

Fig. 8: 10 second gel strength for corn cobs

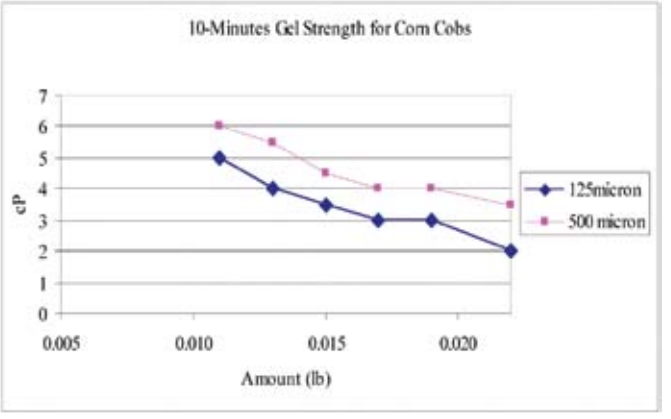

Fig. 9: 10 minutes gel strength for corn cobs

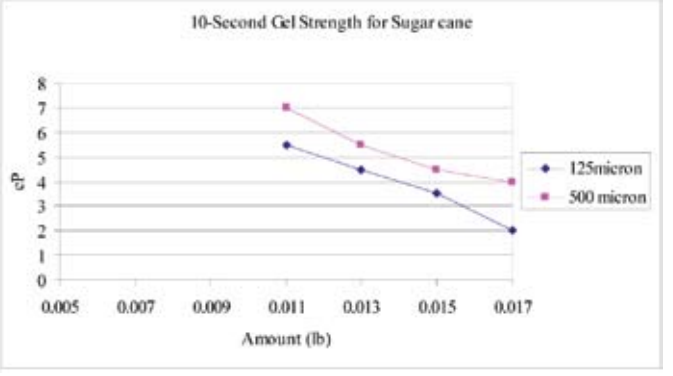

Fig. 10: 10 seconds gel strength for sugar cane

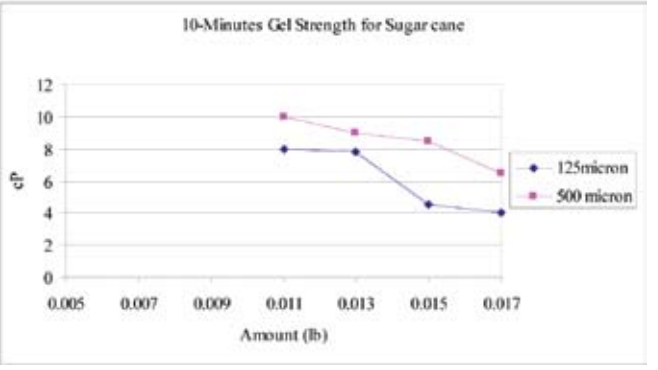

Fig. 11: 10 minutes gel strength for sugar cane

CONCLUSIONS

The present study found that corn cobs and sugar cane could serve as a viscosifier. The plastic viscosity was found to have a direct relationship with the added amount. On the contrary, the yield point and gel strength showed a reverse relationship with the added amount. The optimum value or the best concentration was obtained at the amount of 0.019 lb for the corn cobs, and this was 0.013 for the sugar cane, with the concentration of 9.43 lb/bbl for corn cobs and 6.45 lb/bbl for sugar cane.

REFERENCES

American Petroleum Institute (1995). *API Specification 13B - API Recommended Practice Standard Procedure for Field Testing Oil-Based Drilling Fluids* (3rd. ed). Dallas, Texas:

Devereux, S. (1998). *Practical Well Planning and Drilling Manual.* Oklahoma: PennWell Book.

Doyle *et al.* (1999). *Drilling and Production Discharges in the Marine Environment.* UK: Blakie Academic & Professional.

Faidzal, H. Hassan. (2004). Palm oil derivative as drilling fluid formulation. MSc. Dissertation, Universiti Teknologi Petronas.

Hemphill, T. (1998). Prediction of rheological behaviour of ester-based drilling fluid under downhole conditions. SPE International Petroleum Conference and Exhibition of Mexico, 5-7 March 1998. SPE Paper No: 35330., Tabasco.

Imran, M. (2006). Investigating the blended ester based blend with commercially available mud additives. MSc. Dissertation, Universiti Teknologi Petronas.

Gray, G.R and Darley, H.C.H. (1983). *Compositional and Properties of Oil Well Drilling Fluid.* (4th Ed). Texas: Gulf Publishing Company.

McKee *et al.* (1995). A New development towards improved synthetic-based mud performance. *SPE/IADC Drilling Conference* (p: 612-616) in Amsterdam, 28 Feb-March 1995. SPE/IADC 29405. Amsterdam.

Online Library. (2006). Sugar cane additive for filtration control in well working compositions. Retrieved 4th November 2006, from http://www.freepatentsonline.com/7094737.html

Online Library. (2006). Lost circulation material with rice fraction. Retrieved 4 November, 2006, from http://www.freepatentsonline.com/5118664.html

Wojtanowicz, A.K. (1999). *Environment Control Technology in Petroleum Drilling and Production.* UK: Blackie Academic & Professional.

Zevallos, L. *et al.* (1996). Synthetic-based fluids enhance environment and drilling performance in deepwater locations. *International Petroleum Conference & Exhibition of Mexico,* (pp. 235-242) Tabasco, 5-7 March 1996. SPE 35329.

ISSN: 0128-7680
Pertanika J. Sci. & Technol. **17 (1)**: 183 – 189 (2009)

Chemical Extraction and Separation from the Amoxicillin Plant's Waste-Stream

M. Mohammadi, G.D. Najafpour* and A.A. Ghoreyshi
Faculty of Chemical Engineering, Noushirvani
University of Technology, Babol, Iran
**E-mail: najafpour8@yahoo.com*

ABSTRACT

In the production of amoxicillin for the activation of amoxicillin molecule, hydrolysis takes place at the final stage. In the hydrolysis, the side branch of the amoxicillin molecule, which is not activated, is debranched, and methyl aceto-acetate is easily separated from the amoxicillin molecule. It is highly desired to recycle methyl aceto-acetate as the chemical compound which is needed for the reformation of Dane salt. The main objective of this project was to carry out the liquid-liquid extraction for the recovery of methyl aceto-acetate from the waste stream. For this purpose, diluted ammonia solution was used as a solvent for the chemical extraction, and methyl aceto-acetate was extracted from the waste stream. The liquid-liquid extraction was carried out, while the pH was adjusted to 9.56 by adding ammonia solution. The extraction was repeated in three consecutive stages to enhance the yield in this process. The samples were taken from each stage of separation for GC analysis. The result obtained from the organic chemical extraction using ammonia in three consecutive stages of extraction with overall removal efficiency of 75%. The extraction process was accompanied with distillation for chemical recovery. Similarly, the undesired remaining organics were successfully extracted from the waste stream by distillation. The yield and partition coefficients of the extraction process were calculated based on the chemical analysis obtained from the GC results.

Keywords: Amoxicillin, distribution coefficients, extraction, methyl aceto- acetate, phase separation

INTRODUCTION

In the process of amoxicillin production, hydrolysis is applied at the final stage for the activation of antibiotic product. As a result of the reaction, methyl aceto-acetate is formed. In the waste stream, a number of solvents can easily be wasted along with other chemicals. Waste stream processing is needed for the recovery of fine chemicals for the prevention of environmental pollution and also improving economical feasibility of the production plant. Amoxicillin is one of the major ß-lactam antibiotics, which possesses a high spectrum of activity, high solubility, high rate of absorption, and chemical stability under acid conditions (Gonçalves *et al.*, 2005). Amoxicillin is a well-known antibiotic obtained after a sequence of reactions from 6-α-aminoacyl-penicillin (6-APA). It is a semi-synthetic penicillin antibiotic with a broad spectrum of bactericidal activity against a wide range of common gram-positive and gram-negative pathogens. Amoxicillin is usually the drug of choice within the class because it is easily absorbed, following oral administration, than other ß-lactam antibiotics. In specific, it has a low capacity for protein binding and is widely distributed in various tissues

Received: 23 January 2008
Accepted: 16 May 2008
*Corresponding Author

after absorption. Like all ß-lactam antibiotics, it prevents the formation of the bacterial cell wall by interfering with the final stage of peptidoglycan synthesis (Considine, 1974; Gonçalves *et al.*, 2002 & 2005; Katzung, 1998; Zayed and Abdallah, 2005; Jager *et al.*, 2007).

The preparation process of a 6-APA derivative comprises of a number of steps, which are very practical in antibiotic production (Diago and Ludescher, 1995 & 1998). The first step is the preparation of a mixed carboxylic acid anhydride by creating a reaction between Dane salt and an acylating agent, in a solvent which is water-immiscible or sparingly soluble in water such as methyl isobutyl-ketone, n-butyl acetate, isobutyl acetate and methylene chloride (Diago and Ludescher, 1995 & 1998; Centellas *et al.*, 1999). The first step of the reaction is shown in Table 1. For the preparation of Dane salt, the amine group of phenylglycine is temporarily protected by the formation of the corresponding enamine. From the reaction of phenylglycine with an alkyl aceto-acetate (such as methyl or ethyl aceto-acetate), Dane salt is formed in the presence of a base. The protected compound known as Dane salt has a general formula of R_1-$CHNHR_2COO^-$, where R_1 denotes an appropriate side chain (e.g. phenyl, 4-hydroxyphenyl or 1, 4-cyclohexadien-1-yl) and R_2 denotes alkyl, preferably C_{1-8} alkyl (Cabre *et al.*, 1999).

In the process of protecting 6- APA at the second stage, it is reacted with triethylamine, as shown in Table 1. The third step is the acylation reaction of the compound obtained from the first step with the protected 6-APA or a derivative of 6-APA in free acid or salt form (Diago and Ludescher, 1995 & 1998; Centellas *et al.*, 1999). A summary of the acylation reaction is also shown in Table 1. The ß-lactam ring in 6-APA is easily cleaved in aqueous phase; it is most preferable to carry out the reaction in a non-aqueous solvent system such as methylene chloride (Bender, 1979).

The fourth step involves the hydrolysis of enamine function, which was resulted from the product obtained from the previous acylation reaction. The hydrolysis was carried out with diluted solution of organic acid, or inorganic acid such as diluted aqueous hydrochloric acid, at a low temperature (Bender, 1979; Diago and Ludescher, 1995 & 1998). Methyl aceto-acetate is the by-product of the hydrolysis reaction. The diluted acid has created two phases, organic and aqueous phases. The librated methyl aceto-acetate is found in the organic phase, while the antibiotic remains in the aqueous phase. The final step is the crystallization of amoxicillin, obtained in the aqueous phase, with the use of chemical techniques (Bender, 1979). The chemical structure and action of hydrolysis and crystallization steps are shown in Table 1.

In the process of amoxicillin production, methyl aceto-acetate was formed from the acid hydrolysis of deactivated form of amoxicillin molecule (Bender, 1979). It is important to highlight that methyl aceto-acetate exists in the organic phase. The recovery of certain chemicals, such as methyl aceto-acetate from the organic phase, has an economical impact which makes the process economically feasible. Methyl aceto-acetate is one of the most consumable esters in the pharmaceutical industries and agricultural uses (Othmer, 1997; Boyd and Morrison, 2007). In addition, methyl aceto-acetate is also used in the preparation of "Dane Salt" which is used in the production of synthetic penicillin (Smith, 1963; Schweitzer, 1997). Therefore, the recovery of methyl aceto-acetate, in the production of antibiotic, is essential and makes the process more economical to reform Dane salt. Similarly, the recovery of methyl aceto-acetate also has an environmental impact. In particular, environmental pollution may occur if these chemicals are not recovered from the waste stream.

TABLE 1
The preparation process of Amoxicillin from 6-APA and Dane salt (Cabre *et al.*, 1999)

Preparation stages	Formulation
1. The formation of mixed anhydride	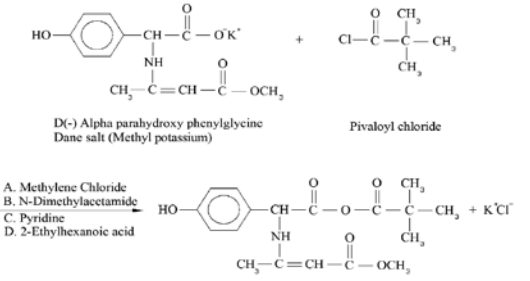
2. Protection of 6-APA	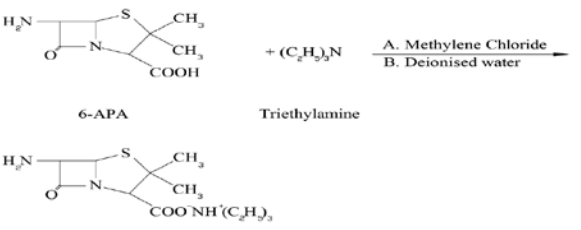
3. Acylation reaction of protected 6-APA and mixed anhydride	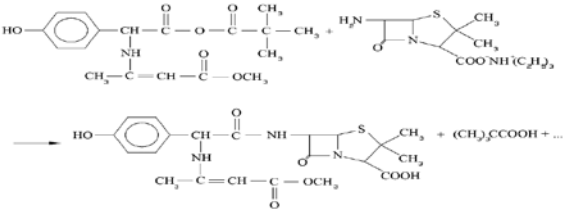
4. Hydrolysis of enamine function	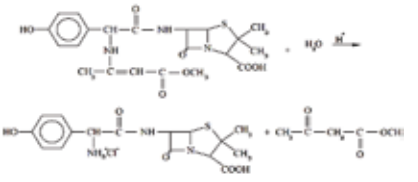
5. Crystallization	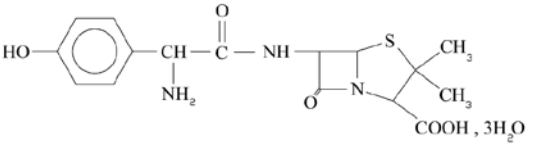

The objective of the present research work was to recover and reuse the downstream waste obtained from Antibiotic Company, Sari, in Iran. The samples were analyzed and the organic chemicals were successfully separated and recovered using the fractional separation. Finally, most of the methyl aceto-acetate was recovered by the use of the extraction process, which was followed by distillation.

MATERIALS AND METHODS

The standard chemicals used were supplied by Merck. The waste sample was obtained from the waste stream of amoxicillin plant, Antibiotic Company, Sari, Iran. The Gas Chromatograph (GC), was equipped with the capillary column TRB-G43 and FID detector, Varian, Model 3800 (USA) and Rotavapor Laborota Model 4001 Heidolph (Germany) for distillation, were used in each stage of the separation process.

The waste stream consists of methyl aceto-acetate, pivalic acid, N, N-dimethyl acetamid, 2-ethyl hexanoic acid, isopropyl alcohol and methylene chloride. In the first stage of the separation process, an alkaline solution, such as $NaHCO_3$ or ammonium solution was introduced to the mixture to extract acid compounds and amide from the waste stream. After separating the organic phase from the aqueous phase, methyl aceto-acetate was found in the organic phase.

Three consecutive stages of extraction were required to increase the efficiency of the process. At final stage, volatile chemical such as methylene chloride was recovered using a common distillation process.

Material balances were conducted at each stage of the separation process, and each product stream was analyzed using the GC, FID and a 30m capillary column (TRB-G43) for the identification and quantitative analysis of the chemical compositions. The detector and injector temperatures were set at 240°C and 220°C, respectively. For this purpose, the temperature programming was specifically used to run the GC. The column temperature was kept at 35°C for 5 minutes, then it was increased to 40°C, with a rate of 1°C/min. In the second stage of the temperature programming, the temperature was increased to 230°C, with a rate of 6°C/min . The carrier gas for the GC was nitrogen, with a flow rate of 30 ml/min. The GC was operated using the software known as star chromatography workstation. The run time for each sample was 41.67 min.

RESULTS AND DISCUSSION

The recovery of methyl aceto-acetate was carried out for the economical feasibility of the operating process. Meanwhile, methyl aceto-acetate needs to remain in the reaction and preferable from the environmental view point. As explained in the process description in the earlier section, the recovered methyl aceto-acetate could easily be converted into Dane salt, which is used in the preparation of the antibiotic. Furthermore, the recovery of methyl aceto-acetate is reduced in the effluent in order to eliminate the organic pollutants. The oily residues, which are retained after the solvent recovery, have to be disposed as schedule wastes or incinerated. In the recovery process of methyl aceto-acetate from the amoxicillin production plant, the waste stream mixture may contain a number of components. Both the waste sample and the extracted samples were analyzed using the GC. The boiling points and the chemical composition of the waste stream are shown in Table 2.

TABLE 2
The chemical composition of waste stream for amoxicillin plant

Chemical compound	Boiling point (°C)	Weight percent
Methylene chloride (MCH)	39.8	39.2271
N,N-Dimethyl acetamide (DMAC)	166	5.5092
Iso propyl alcohol (IPA)	82.3	4.6351
Pivalic acid (PIVA)	164	30.4195
2-Ethylhexanoic acid (2EHA)	226	0.6567
Methyl aceto-acetate (MAA)	164	19.5523

Since some of the compounds (DMAC, PIVA and MAA) in the waste stream have close boiling points, distillation is therefore not a suitable technique to separate all the chemicals which exist in the wastes. Hence, liquid extraction was implemented to separate all the components and recover methyl aceto-acetate.

Alkaline condition is required for the phase separation; Boyd and Morrison (2007) state that strong alkaline solution may cause cleavage of the methyl aceto-acetate to methanol and acetic acid. Ammonia was selected due to its mild alkaline condition and a suitable change in the pH of the solution. In addition, ammonia is found to be capable of extracting all the organic acids into aqueous phase. Ammonia solution was introduced as a chemical agent in extracting solvent, which was meant to extract acids and other undesired chemicals from the organic phase. Fresh feed of the organic waste from amoxicillin plant, one litre was mixed with 160 ml of 9 molar ammonia solutions, diluted with distilled water and the total volume was reached to 2 litres for equal volume of solvent to feed ratio. As a result, alkaline condition with pH of 9.56 was obtained. Aqueous and organic phases were distinctly separated after a few minutes of mixing and settling. The weight percentage of all the chemical species in the aqueous and organic phases, after the three stages of extraction using ammonia solution, are presented in Table 3.

In the first stage of extraction, the highest and lowest distribution coefficients were devoted to pivalic acid and methyl aceto-acetate. This means "most" of the pivalic acid was retained in the aqueous phase and the methyl aceto-acetate was kept in the organic phase along with methylene chloride. In the next stage of extraction, more methyl aceto-acetate was extracted into the organic phase, along with volatile solvent like methylene chloride. To extract all the acid residues, more amide and alcohol "extraction" was repeated for three consecutive stage of extraction. The overall process yield calculation was based on the mass ratio of the final to the initial methyl aceto-acetate. The process yield of 75% was obtained based on the analysis. The results showed that ammonia was very efficient for the extraction of most of the acids found in the organic phase as well as most of the amide and alcohol.

Finally, the low boiling point compounds such as methylene chloride were eliminated in a single stage distillation. Methyl aceto-acetate, with the purity of 93.82%, was obtained from the distillation process. The weight percentages of all the chemicals, in the distillate and residual phases after distillation, are shown in Table 4.

TABLE 3
The chemical analysis of the aqueous and organic phases, with ammonia extraction from amoxicillin waste

Chemical compound	Original sample	Aqueous phase	Organic phase	Distribution coefficient
	Weight percent	Weight percent	Weight percent	
The first stage of extraction with ammonia solution				
Isopropyl alcohol	4.635	9.136	4.125	2.214
Methylene chloride	39.226	4.083	57.975	0.07
Pivalic acid	30.420	77.815	0.566	137.216
Methyl aceto-acetate	19.552	1.366	31.775	0.043
N,N-dimethylacetamide	5.510	6.823	5.550	1.229
2-Ethylhexanoic acid	0.657	0.777	0.007	115.791
Sum.	100.000	100.000	100.000	
The second stage of extraction with ammonia solution				
Isopropyl alcohol	4.125	30.24	1.814	16.673
Methylene chloride	57.975	19.78	63.319	0.313
Pivalic acid	0.566	1.95	0.301	6.606
Methyl aceto-acetate	31.775	21.25	31.363	0.677
N,N-dimethylacetamide	5.550	26.78	3.147	8.511
2-Ethylhexanoic acid	0.007	0.000	0.056	0
The third stage of extraction with ammonia solution				
Isopropyl alcohol	1.814	25.230	0.836	30.168
Methylene chloride	63.319	30.022	62.442	0.481
Pivalic acid	0.301	4.245	0.027	157.211
Methyl aceto-acetate	31.363	25.888	34.618	0.748
N,N-dimethylacetamide	3.147	14.615	2.040	7.163
2-Ethylhexanoic acid	0.056	0.000	0.037	0
Sum.	100.000	100.000	100.000	

TABLE 4
Chemical analysis of the distillate and residue from distillation column

Chemical compound	Original sample Weight percent	Weight percent in distillate	Weight percent in residue
Isopropyl alcohol	0.836	2.468	0.017
Methylene chloride	62.442	93.481	0.658
Pivalic acid	0.027	0.000	0.000
Methyl aceto-acetate	34.618	3.806	93.818
N,N-dimethylacetamide	2.040	0.245	5.507
2-Ethylhexanoic acid	0.037	0.000	0.000
Sum.	100.000	100.000	100.000

CONCLUSIONS

From the waste stream processing of the amoxicillin production plant, the chemical compounds such as methyl aceto-acetate was recovered. The process set up was managed in a manner that part of the chemicals was extracted by adding ammonia solution. Distillation was also applied in the final stage. In this study, it was found that the overall process efficiency of 75 percent was achieved for the recovery of methyl aceto-acetate.

ACKNOWLEDGEMENTS

The work was made possible through the support of Faculty of Chemical Engineering, Biotechnology Centre and Nano-Bio Lab, Noushirvani University of Technology, Babol, Iran. The authors wish to acknowledge the research team, led by Mr. Safei at Antibiotic Company, Sari, Iran, for their cooperation and encouragement throughout the present research. Special thanks to Professor M. Tajbaksh, Faculty of Chemistry, University of Mazandaran, Babolsar, Iran, for his valuable assistant at the Organic Chemistry Lab.

REFERENCES

Bender, R.H.W. (1979). United States Patent on Dane salt and process for preparing aminopenicillins therefrom. Patent No.: 4231954, www.freepatentsonline.com

Boyd, R.N. and Morrison, R.T. (2007). *Organic Chemistry* (6th Ed.). New York: McGraw Hill.

Cabre, J., Centellas, V., Diago, J., Esteve, A. and Serrat, J. (1999). US Patent on Process for separating pivalic acid from spent reaction mixtures. Patent No.: 5990351

Centellas, V., Diago, J. and Ludescher, J. (1999). United States Patent on Silylation process, Patent No.: 5998610

Considine D.M. (1974). *Chemical and Process Technology Encyclopaedia.* New York: McGraw Hill,

Diago, J. and Ludescher, J. (1995). United States Patent on Processes for the production of 6-alpha-aminoacyl-penicillin and 7-alpha. Patent No.: 5840885

Diago, J. and Ludescher, J. (1998). United States Patent on Beta lactam production. Patent No.: 5719276

Gonçalves, L.R.B., Lafuente, R.F., Guisán, J.M. and Giordano, R.L.C. (2002). The role of 6-aminopenicillanic acid on the kinetics of Amoxicillin enzymatic synthesis catalyzed by penicillin G acylase immobilized onto glyoxyl-agarose. *Enzyme and Microbial Technology, 31,* 464–471.

Gonçalves, L.R.B., Giordano, R.L.C. and Giordano, R.C. (2005). Mathematical modelling of batch and semi batch reactors for the enzymic synthesis of Amoxicillin. *Process Biochemistry, 40,* 247–256.

Jager, S.A.W., Jekel, P.A. and Janssen, D.B. (2007). Hybrid penicillin acylases with improved properties for synthesis of β-lactam antibiotics. *Enzyme and Microbial Technology, 40,* 1335–1344.

Katzung, B.G. (1998). *Basic and Clinical Pharmacology* (7th Ed.). Appleton & Lange.

Kirk Othmer. (1997). *Encyclopaedia of Chemical Technology* (4th Ed., Vol. 4, 3 & 14). New York: John Wiley & Sons.

Schweitzer, P.A. (1997). *Handbook of Separation Techniques for Chemical Engineering.* New York: McGraw Hill.

Smith, B.D. (1963). *Design of Equilibrium Stage Processes.* New York: McGraw Hill.

Zayed, M.A. and Abdallah, S.M. (2005). Synthesis and structure investigation of the antibiotic Amoxicillin complexes of d-block elements. *Spectrochimica Acta Part A 61,* 2231–2238.

ISSN: 0128-7680
Pertanika J. Sci. & Technol. **17 (1)**: 191 – 199 (2009)

Biosorption of Pb (II) Ions by Immobilized Cells of *Pycnoporus sanguineus* in a Packed Bed Column

Mashitah Mat Don*, Yus Azila Yahaya and Subhash Bhatia
School of Chemical Engineering, Universiti Sains Malaysia,
Engineering Campus, Seri Ampangan,
14300 Nibong Tebal, Penang, Malaysia
**E-mail: chmashitah@eng.usm.my*

ABSTRACT

The removal of heavy metals like lead, copper and cadmium from wastewater streams is an important environmental issue. The capability of immobilized *Pycnoporus sanguineus* (*P. sanguineus*), a white-rot macrofungi to remove heavy metals from aqueous solution in a packed bed column was investigated. Lead (Pb (II)) biosorption by immobilized cells of *P. sanguineus* was investigated in a packed bed column. The experiments were carried out by considering the effect of bed height (5-13 cm), flow rate (4-12 ml min^{-1}) and initial lead (II) concentration (50-300 mg L^{-1}). The breakthrough profiles showed that the saturation of metal ions was achieved faster for 5 cm bed height and 12 ml min^{-1} influent flow rate. However, the breakthrough time decreased as the initial metal concentration increased from 50 to 300 mg L^{-1}. The column was regenerated using 0.1M HCl solution and biosorption-desorption studies were carried out for 2 cycles. The results showed that the breakthrough time decreased as the number of cycle was proceeded.

Keywords: Biosorption, breakthrough curve, column, desorption, fungus, immobilization, lead, *Pycnoporus sanguineus*

ABBREVIATIONS

C_o	initial concentration (mg L^{-1})
C	outlet concentration (mg L^{-1})
F	flow rate (ml min^{-1})
H	bed height (cm)
M	mass of biosorbent (g)
m_{ad}	total adsorbed Pb (II) (mg)
m_d	metal mass desorbed (mg)
m_{total}	total amount of metal feed to the column (mg)
Q	metals uptake capacity (mg g^{-1})
R	total metal removal (%)
t	time (min)
t_b	breakthrough time (hr)
t_e	exhaustion time (hr)

Received: 28 January 2008
Accepted: 20 May 2008
*Corresponding Author

INTRODUCTION

To date, various treatment technologies have been introduced for an efficient removal of heavy metals from an industrial effluent. One of these technologies is biosorption process, which utilizes biological materials including fungi, algae, bacteria and yeast, to accumulate metal ions from wastewater (Arica *et al.*, 2001). Conventional methods such as chemical precipitation, electrochemical treatment, membrane technology and ion exchange processes may be inefficient and expensive when operated at low metal concentration (1-100 mg L^{-1}) (Cruz *et al.*, 2004; Malkoc and Nuhoglu, 2006). Some of these treatments produced toxic sludge which may cause further disposal problem. Since these biological materials are abundant and capable to adsorb metal ions, biosorption process has emerged as an alternative method used in removing heavy metal over conventional methods (Cordero *et al.*, 2004; Cruz *et al.*, 2004). Application of fungi, as a biosorbent in heavy metals removal, has received a great attention (Mittar *et al.*, 1992; Arica *et al.*, 2003).

Many fungal species, such as *Aspergillus niger*, *Rhizopus* sp., *Saccharomyces* spp., *Mucor* sp and *Phanerochaete crysosporium,* have extensively been studied as a potential biosorbent in metal ions removal (Kapoor and Viraraghavan, 1997; Say *et al.*, 2001; Kim *et al.*, 2003; Yan and Viraraghavan, 2003). For an efficient use of biosorbents in heavy metal removal in an industrial operation, these free fungal cells were immobilized in carbohydrate-based polymers including alginate, chitin, chitosan and carboxymethyl cellulose (Jianlong *et al.*, 2000; Arica *et al.*, 2003). These immobilized cells offer several advantages, including minimal clogging in continuous systems (Ting and Sun, 2000; Arica *et al.*, 2001; Bayramoglu *et al.*, 2003), which is easy to separate from the reaction system and can be regenerated and reused (Arica *et al.*, 2001; Annadurai *et al.*, 2007).

Mashitah *et al.* (1999) reported that the non-living biomass, known as *Pycnoporus sanguineus* (*P. sanguineus*), or white rot fungi, is one of the potential biosorbent for Pb (II), Cu (II) and Cd (II) biosorption. However, the utilization of *P. sanguineus* cells, in an immobilized system, is lessly reported. Therefore, this study was carried out to determine the potential of the live immobilized cells of *P. sanguineus* to adsorb Pb (II) ions in a packed bed column.

MATERIALS AND METHODS

Microorganism, Medium and Growth Conditions

P. sanguineus, which is capable of adsorbing heavy metals was obtained from the Forest Research Institute Malaysia (FRIM), located in Kepong, Selangor. The culture was maintained by a weekly transfer on malt extract agar slant, incubated at 30°C for 6 days, after which they were stored at 4°C until required.

The composition of the medium used comprised of glucose 20 g L^{-1}, yeast extract 10g L^{-1} and malt extract 10 g L^{-1}. The pH of the medium was adjusted to pH 9, prior to autoclaving at 121°C (1.5 bar) for 15 minutes.

Cell suspension was prepared by inoculating a stock culture of *P. sanguineus* onto the malt extract agar plates, and incubated at 27°C for 6 days. The formed mycelium mat was scraped using a sterile blade and mixed with 10 ml sterile Tween 20 solution prior putting it into a sterile sampling bottle (100 ml). The sampling bottle was then vortexed for 3 minutes so that the mycelium would evenly be distributed in the liquid.

15 ml of the cell suspension was inoculated into an Erlenmeyer flask containing 135 ml of the production medium. The flask was incubated in a rotary shaker at 30°C, 150 rpm for 66 hr. The sample was then harvested and centrifuged at 3500 rpm for 4 minutes.

The Preparation of Immobilized Cells

The sodium alginate beads were prepared by dropping a mixture of sodium alginate solution and *P. sanguineus* cells into 2% (w/v) $CaCl_2$ solution under magnetic stirring (slow) at room temperature. The beads were stirred in this solution for 30 minutes. Successively, they were collected by filtration, washed three times with sterile deionized water and stored in Tris-HCl buffer pH 7 at 4°C until used.

The Preparation of Metal Ions

The metal solutions were prepared by diluting 1000 mg L^{-1} of Pb $(NO_3)_2$ solutions with deionized water to a desired concentration ranged between 50 to 300 mg L^{-1}. For each of the solutions, the initial concentrations of the metals and samples after the biosorption treatment, were determined using an Atomic Absorption Spectrometer (Model Shimadzu AA 6650).

The Biosorption Procedures

The biosorption studies were performed in a jacketed glass column (length 60 cm, i.d. 4 cm) at room temperature. The immobilized beads were packed into it using a wet packing technique. The bed was supported and closed using glass wool plugs to ensure a good liquid distribution at the top and bottom of the column. *Fig. 1* below shows the experimental set up used in the present study. The experiments were carried out to study the effects of the following variables, (i) bed height (5-13 cm), (ii) flow rate (4-12 ml min^{-1}) and (iii) initial Pb (II) concentration (50-300 mg mL^{-1}).

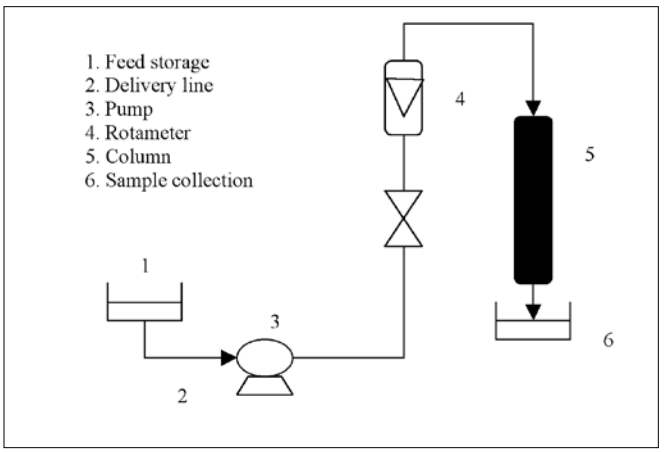

Fig. 1: Experimental set up for the biosorption studies in fixed bed column

In a typical experiment, a known Pb (II) ion concentration feed (100 mg L^{-1}) was pumped at a fixed flow rate into the column with a known bed height. Samples were collected periodically and analyzed for the Pb (II) concentration, using the Atomic Absorption Spectrometer (AAS) until saturation was reached in the column. The breakthrough curve was obtained by plotting C/C_o against time or outlet concentration, and C against time (t). The operation of the column was stopped when the effluent Pb (II) concentration

exceeded a value of 99.5% of the initial feed concentration. The total quantity of the metal mass, biosorbed in the column (m_{ad}), was calculated from the area above the breakthrough curve (outlet concentration, C versus time, t) and multiplied by the flow rate. Dividing the metal mass (m_{ad}) by the mass of biosorbent (M) resulted in the metal uptake capacity (Q) (Volesky *et al.*, 2003; Padmesh *et al.*, 2005). The breakthrough time (t_b) was the time at which metal concentration in the effluent reached 0.01% of the initial feed concentration and exhaustion time (t_e), and at which metal concentration exceeded 99.5 % of the initial feed concentration, respectively.

The total adsorbed Pb (II), m_{ad} (mg) in the column for a given Pb (II) concentration and the flow rate, is calculated as:

$$m_{ad} = \frac{F}{1000}\int_{t=0}^{t=t_{total}} C_{ad}\, dt \tag{1}$$

Meanwhile, the total amount of the metal feed to the column (m_{total}; mg) is:

$$m_{total} = \frac{C_o F t_e}{1000} \tag{2}$$

The mass transfer zone can be calculated using the following Eq. (3):

$$\Delta t = t_e - t_b \tag{3}$$

The total metal removal, R (%) with respect to flow volume is given as:

Total metal removal,
$$R(\%) = \frac{m_{ad}}{m_{total}} \times 100 \tag{4}$$

The metal mass desorbed, m_d (mg) can be calculated from the elution curve (C versus t) and the elution efficiency is given as:

$$E(\%) = \frac{m_d}{m_{ad}} \times 100 \tag{5}$$

Loaded biosorbents with metal ions were regenerated with 0.1 M HCl by pumping it in a down-flow operation of the column. After the regeneration, the biosorption studies were carried out again. This biosorption-regeneration was repeated two times in order to investigate the biosorption capacity of the immobilized cells. The continuous experiments were conducted at room temperature (30°C).

RESULTS AND DISCUSSION

The Effect of the Bed Height

Fig. 2 presents a breakthrough curve for the Pb (II) biosorption onto the immobilized cells of *P. sanguineus* at different bed heights of 5, 9 and 13 cm, respectively. The concentration of the Pb (II) solution was fixed at 100 mg L^{-1} and pH 4 for all the bed heights studied. The

preliminary results showed that pH 4 was an optimum pH for Pb (II) removal. It was fed into the column and maintained at 4 ml min^{-1}. The results showed that the Pb (II) uptake was increased from 11.51 to 19.65 mg g^{-1}, as the bed height was increased from 5 to 13 cm. With the increase of the bed height, more binding sites were available for the biosorption to occur (Vijayaraghavan *et al.*, 2005). The saturation of the immobilized cells of *P. sanguineus* was achieved nearly 38 hours at 5 cm bed height. However, at a higher bed height (13 cm), the saturation was obtained after 144 hours. Malkoc and Nuhoglu (2006) stated that higher bed height would result in broadened mass transfer zone, thus increased the saturation period for the metals onto immobilized cells.

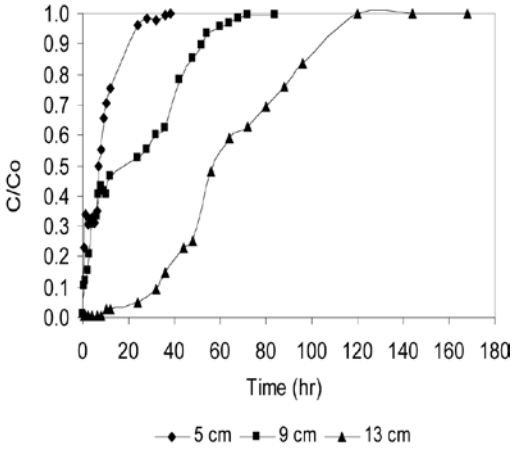

Fig. 2: The breakthrough curves of the Pb (II) biosorption onto immobilized cells of P. sanguineus *at different bed heights (Condition: 100 mg L^{-1} Pb (II), flow rate: 4 ml min^{-1}, pH 4.0)*

The Effect of the Flow Rate

Fig. 3 presents the breakthrough curve of the Pb (II) biosorption in a column at the different flow rates which ranged from 4 to 12 ml min^{-1}. The experiments were carried out at a constant initial Pb (II) concentration (100 mg L^{-1}), pH 4 and 9 cm bed height. The result (*Fig. 3*) revealed that the Pb (II) uptake was decreased with the increase in the flow rate. This was due to the insufficient contact time for the Pb (II) ions to be adsorbed by the immobilized cells of *P. sanguineus* (Ko *et al.*, 2000; Vijayaraghavan *et al.*, 2005). As illustrated in *Fig. 3,* a steeper breakthrough curve was observed at a flow rate of 12 ml min^{-1}, when the breakthrough time decreased. A similar phenomenon was reported on cobalt (II) and nickel (II) biosorption by seaweeds and heavy metals removal in fixed bed column by *P. sanguineus*, respectively (Zulfadhly *et al.*, 2001; Vijayaraghavan *et al.* 2005).

The Effect of the Initial Metal Concentrations

Fig. 4 shows the breakthrough profiles of the Pb (II) biosorption at different initial Pb (II) concentrations with bed height 9 cm, and the flow rate of 4 ml min^{-1} and pH 4. When the initial Pb (II) concentration was increased from 50 to 300 mg L^{-1}, the Pb (II) uptake was also found to increase from 21.74 to 25.73 mg g^{-1}. At a higher initial Pb (II) concentration, the biosorbent was saturated earlier, thus resulted in a faster breakthrough and exhaustion time (Zulfadhly *et al.*, 2001; Malkoc and Nuhoglu, 2006). At a lower concentration of Pb

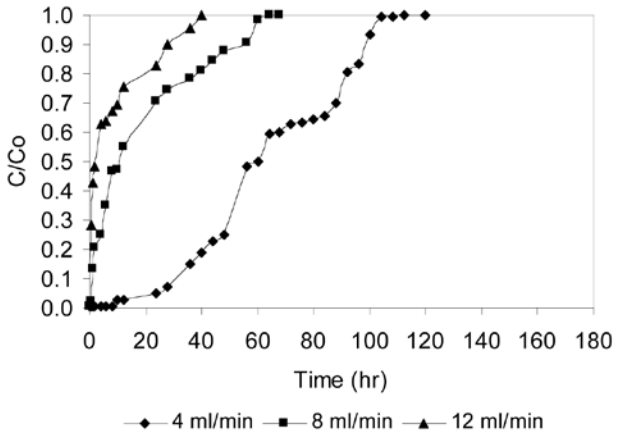

Fig. 3: Breakthrough curves of Pb (II) biosorption onto immobilized cells of P.sanguineus *at different flow rates (Condition: 100 mg L^{-1} Pb (II), bed height= 9 cm, pH 4.0)*

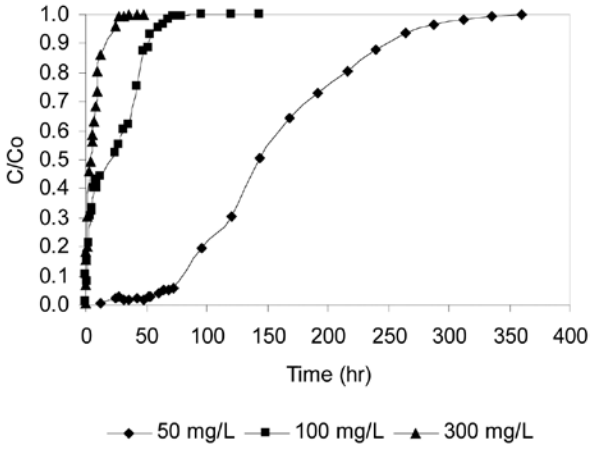

Fig. 4: The breakthrough curves of Pb (II) biosorption onto immobilized cells of P. sanguineus *at different initial Pb (II) concentrations (Condition: 100 mg L^{-1} Pb (II), bed height= 9 cm, pH 4.0)*

(II) solution, less driving force was observed between the metal ions and the immobilized cells of *P. sanguineus,* resulting in a broadened mass transfer zone (Malkoc and Nuhoglu, 2006). The adsorption efficiency, at different bed heights, flow rates and initial metal concentrations, is presented in Table 1.

Regeneration

Regeneration of biosorbent after biosorption process is very important to reduce the process cost in a continuous operation (Vijayaraghavan *et al.*, 2005). *Fig. 5* shows the desorption curve of the Pb (II) ions through a packed bed of *P. sanguineus* by passing 0.1 M HCl as an elution agent. The biosorbents were reused up to two biosorption-desorption cycles. It was observed that the elution efficiency was up to 85% for a complete recovery of Pb (II) ions and more than 20 L of 0.1 M HCl was used. After two biosorption-desorption cycles,

TABLE 1
Adsorption efficiency at different bed heights, flow rates and initial metal concentrations

C_o (mg L^{-1})	*H* (cm)	*F* (ml min^{-1})	Adsorption efficiency (%)
100	5	4	81
100	9	4	74
100	13	4	65
100	9	8	19
100	9	12	15
50	9	4	60
300	9	4	89

a significant biosorbent weight loss was observed, and this suggested that it was no longer suitable to be used in the next cycle. As reported by a few researchers, cells that were exposed to an acidic elutant might face a physical-chemical damage of the biosorbent structure which resulted in both weight loss and reduction of the biosorption capacity in a subsequent cycle (Tuzun *et al.*, 2005; Vijayaraghavan *et al.*, 2005). These can be seen as tabulated in Table 2. The comparison of the Pb (II) biosorption by various biosorbents is shown in Table 3.

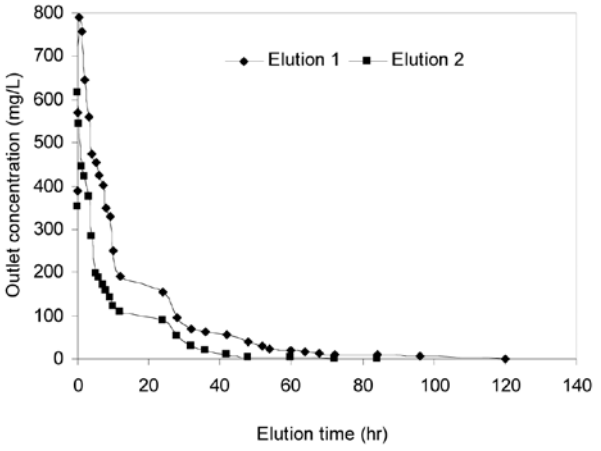

Fig. 5: The breakthrough curves of Pb (II) desorption

TABLE 2
Elution parameters for two biosorption-desorption cycles

Metal	Cycle No	Uptake capacity (mg g^{-1})	Metal removal (%)	Time for Elution (hr)	Elution efficiency (%)
Pb	1	25.7	88.8	120	85
	2	21.0	75.6	84	50

TABLE 3
Comparison of Pb (II) biosorption by various biosorbents

Metal	Biosorbent	Metal Removal (%)	Elution efficiency (%)	Reference
Pb	Immobilized *P. sanguineus*	88.8	85	This study
	Aspergillus niger beads	50	99	Kapoor and Viraraghavan, 1998
	Immobilized bacterial Biomass		98	Chang *et al.* 1998
	Calcium treated Anaerobic biomass	50	80	Hawari and Mulligan, 2006
	Immobilized *Microcytis aeruginosa*	80	80	Jian *et al.* 2005

CONCLUSIONS

The biosorption of the Pb (II) ions was examined using immobilized cells of *P. sanguineus* in a packed bed column, and the following conclusions are therefore summarized: Immobilized cells of *P. sanguineus* cell were found to be capable of removing 88.8 % of Pb (II) ions from aqueous solutions.

The increase in bed height and initial Pb (II) concentration increased the metals uptake in the column. The contact time in the column, at a higher flow rate, resulted in a decrease of the metal uptakes. The column regeneration, using 0.1 M HCl, was carried out for two biosorption-desorption cycles; the results indicated a significant biosorbent weight loss.

ACKNOWLEDGEMENT

The authors acknowledge Universiti Sains Malaysia (Acc No: 6035132) for the financial support of this research.

REFERENCES

Annadurai, G., Lai, Y.L. and Jiunn, F.L. (2007). Biodegradation of phenol by *Pseudomonas pictorium* on immobilized with chitin. *African Journal of Biotech, 6*(3), 296-303.

Arica, M.Y., Arpa, C., Ergene, A., Bayramoglu, G. and Genc, O. (2003). Ca-alginate as a support for Pb (II) and Zn (II) biosorption with immobilized *Phanerochaete chrysosporium. Carbohydrate Polymer, 52*, 167-174.

Arica, M.Y., Kacar, Y. and Genc, O. (2001). Entrapment of white-fungus *Trametes versicolor* in Ca alginate beads: Preparation and biosorption kinetic analysis for cadmium removal from an aqueous solution. *Biores. Technol, 80*: 121-129.

Bayramoglu, G., Bektas, S. and Arica, M.Y. (2003). Biosorption of heavy metals on immobilized white-rot fungus *Trametes versicolor. J. Hazard. Mater, B101*, 285-300.

Chang J.S., Huang, J.C., Chang C.C. and Tarn, T. (1998). Removal and recovery of lead fixed-bed biosorption with immobilized bacterial biomass. *Wat. Sci. Technol.*, *38*, 171-178.

Cordero, B., Lodeiro, P., Herrero, R. and Sastre de Vicente, M.E. (2004). Biosorption of cadmium by *Fucus spiralis*. *Environ. Chem.*, *1*, 180-187.

Cruz, C.C.V., Da Costa, A.C.A., Henriques, C.A. and Luna, A.S. (2004). Kinetic modelling and equilibrium studies during cadmium biosorption by dead *Sargassum* sp. biomass. *Biores. Technol.*, *91*, 249-257.

Hawari, A.H. and Mulligan, C.N. (2006). Heavy metals uptake mechanisms in a fixed-bed column by calcium-treated anaerobic biomass. *Process. Biochem.*, *41*, 187-198.

Jian, Z.C., Xian, C.T., Jun, X., Tao, Z. and Zhi, L.L. (2005). Biosorption of lead, cadmium and mercury by immobilized *Microcystis aeruginosa* in a column. *Process. Biochem.*, *40*, 3785-3679.

Jianlong, W., Horan, N., Stentiford, E. and Yi, Q. (2000). The radial distribution and bioactivity of *Pseudomonas* sp immobilized in calcium alginate gel beads. *Process. Biochem.*, *35*, 465-469.

Kapoor, A. and Viraraghavan, T. (1997). Heavy metal biosorption sites in *Aspergillus niger*. *Biores. Technol.*, *61*, 221-227.

Kapoor, A. and Viraraghavan, T. (1998). Removal of heavy metals from aqueous solution using immobilized fungal biomass in continuous mode. *Wat. Res*, *32*, 1968-1977.

Kim, S.K., Park, C.B., Koo, Y.M. and Yun, H.S. (2003). Biosorption of cadmium and copper ions by *Tricoderma reesei* RUT C30. *J. Ind. Eng. Chem.*, *9*, 403-406.

Ko, D.C.K., Porter, J.F. and McKay, G. (2000). Optimised correlations for the fixed-bed adsorption of metal ions on bone char. *Chem. Eng. Sci.*, *55*, 5819-5829.

Malkoc, E. and Nuhoglu, Y. (2006). Removal of Ni (II) ions from aqueous solutions using waste of tea factory: Adsorption on a fixed-bed column. *J. Hazard. Mater.*, *B135*, 328-336.

Padmesh, T.V.N., Vijayaraghavan, K., Sekaran, G. and Velan, M. (2005). Batch and column studies on biosorption of acid dyes on fresh water macro alga *Azolla filiculoides*. *J. Hazard Mater, B125*, 121-129.

Say, R., Denizli, A. and Arica, M.Y. (2001). Biosorption of cadmium (II), lead (II) and copper (II) with the filamentous fungus *Phanerochaete chrysosporium*. *Biosres. Technol.*, *76*, 67-70.

Ting, Y.P. and Sun, G. (2000). Use of polyvinyl alcohol as a xall entrapment matrix for copper biosorption by yeast cells. *J. Chem. Technol. Biotechnol.*, *75*, 541-546.

Tuzun, I., Bayramoglu, G., Yalcin, E., Basaran, G., Celik, G. and Arica, Y.M. (2005). Equilibrium and kinetic studies on biosorption of Hg (II), Cd (II) and Pb (II) ions onto microalgae *Chlamydomonas reinhardtii*. *J. Environ. Manage. 77*, 1-8.

Vijayaraghavan, K., Jegan, K., Palanivelu, K. & Velan, M. (2005). Biosorption of copper, cobalt and nickel by marine green alga *Ulva reticulate* in a packed column. *Chemosphere.*, *60*, 419-426.

Volesky, B., Weber, J. and Park, J.M. (2003). Continuous-flow metal biosorption in a regenerable *Sargassum* column. *Wat. Res*, *37*, 297-306.

Yan, G. and Viraraghavan, T. (2001). Heavy metal removal in a biosorption column by immobilized *M. rouxii* biomass. B*iores. Technol.*, *78*, 243-249.

Yan, G. and Viraraghavan, T. (2003). Heavy metal removal from aqueous solution by fungus *Mucor rouxii*. *Wat. Res*, *37*, 4486-4496.

Zulfadhly, Z., Mashitah, M.D. and Bhatia, S. (2001). Heavy metals removal in fixed-bed column by the macro fungus *Pycnoporus sanguineus*. *Environ. Pollut.*, *112*, 463-470.

Pertanika

Our goal is to bring high quality research to the widest possible audience

Journal of Science & Technology

INSTRUCTIONS TO AUTHORS

(Manuscript Preparation & Submission Guidelines)

Revised January 2009

We aim for excellence, sustained by a responsible and professional approach to journal publishing.
We value and support our authors in the research community.

Please read the guidelines and follow these instructions carefully; doing so will ensure that the publication of your manuscript is as rapid and efficient as possible. The Editorial Board reserves the right to retum manuscripts that are not prepared in accordance with these guidelines.

About the Journal

Pertanika is an international peer-reviewed journal devoted to the publication of original papers, and it serves as a forum for practical approaches to improving quality in issues pertaining to tropical agriculture and its related fields. Pertanika Journal of Tropical Agricultural Science began publication in 1978. In 1992, a decision was made to streamline Pertanika into three journals to meet the need for specialised journals in areas of study aligned with the interdisciplinary strengths of the university. The revamped, Pertanika Journal of Science and Technology (JST) is now focusing on research in science and engineering, and its related fields. Other Pertanika series include Pertanika Journal of Tropical Agricultural Science (JTAS); and Pertanika Journal of Social Sciences and Humanities (JSSH).

JST is published in **English** and it is open to authors around the world regardless of the nationality. It is currently published two times a year i.e. in **January** and **July**.

Goal of Pertanika

Our goal is to bring the highest quality research to the widest possible audience.

Quality

We aim for excellence, sustained by a responsible and professional approach to journal publishing. JST is an international journal indexed in EBSCO.

Future vision

We are continuously improving access to our journal archives, content, and research services. We have the drive to realise exciting new horizons that will benefit not only the academic community, but society itself.

We also have views on the future of our journals. The emergence of the online medium as the predominant vehicle for the 'consumption' and distribution of much academic research will be the ultimate instrument in the dissemination of the research news to our scientists and readers.

Aims and scope

Pertanika Journal of Science and Technology aims to provide a forum for high quality research related to science and engineering research. Areas relevant to the scope of the journal include: *bioinformatics, bioscience, biotechnology and bio-molecular sciences, chemistry, computer science, ecology, engineering, engineering design, environmental control and management, mathematics and statistics, medicine and health sciences, nanotechnology, physics, safety and emergency management*, and related fields of study.

Editorial Statement

Pertanika is the official journal of Universiti Putra Malaysia. The abbreviation for Pertanika Journal of Science & Technology is *Pertanika J. Sci. Technol.*

Guidelines for Authors

Publication policies

Pertanika policy prohibits an author from submitting the same manuscript for concurrent consideration by two or more publications. It prohibits as well publication of any manuscript that has already been published either in whole or substantial part elsewhere.

Editorial process

Authors are notified on receipt of a manuscript and upon the editorial decision regarding publication.

Manuscript review: Manuscripts deemed suitable for publication are sent to the Editorial Advisory Board members and/or other reviewers. We encourage authors to suggest the names of possible reviewers. Notification of the editorial decision is usually provided within to eight to ten weeks from the receipt of manuscript. Publication of solicited manuscripts is not guaranteed. In most cases, manuscripts are accepted conditionally, pending an author's revision of the material.

Author approval: Authors are responsible for all statements in articles, including changes made by editors. The liaison author must be available for consultation with an editor of *The Journal* to answer questions during the editorial process and to approve the edited copy. Authors receive edited typescript (not galley proofs) for final approval. Changes **cannot** be made to the copy after the edited version has been approved.

Please direct all inquiries, manuscripts, and related correspondence to:

The Executive Editor
Pertanika Journals
Research Management Centre (RMC)
4th Floor, Administration Building
Universiti Putra Malaysia
43400 UPM, Serdang, Selangor
Malaysia
Phone: + (603) 8946 6192
Fax: + (603) 8947 2075
ndeeps@admin.upm.edu.my

or visit our website at http://rmc.upm.edu.my/pertanika for further information.

Manuscript preparation

Pertanika accepts submission of mainly four types of manuscripts. Each manuscript is classified as **regular** or **original** articles, **short communications**, **reviews**, and proposals for **special issues**. Articles must be in **English** and they must be competently written and argued in clear and concise grammatical English. Acceptable English usage and syntax are expected. Do not use slang, jargon, or obscure abbreviations or phrasing. Metric measurement is preferred; equivalent English measurement may be included in parentheses. Always provide the complete form of an acronym/abbreviation the first time it is presented in the text. Contributors are strongly recommended to have the manuscript checked by a colleague with ample experience in writing English manuscripts or an English language editor.

Linguistically hopeless manuscripts will be rejected straightaway (e.g., when the language is so poor that one cannot be sure of what the authors really mean). This process, taken by authors before submission, will greatly facilitate reviewing, and thus publication if the content is acceptable.

The instructions for authors must be followed. Manuscripts not adhering to the instructions will be returned for revision without review. Authors should prepare manuscripts according to the guidelines of Pertanika.

1. Regular article
Definition: Full-length original empirical investigations, consisting of introduction, materials and methods, results and discussion, conclusions. Original work must provide references and an explanation on research findings that contain new and significant findings.

Size: Should not exceed 5000 words or 8-10 printed pages (excluding the abstract, references, tables and/or figures). One printed page is roughly equivalent to 3 type-written pages.

2. Short communications
Definition: Significant new information to readers of the Journal in a short but complete form. It is suitable for the publication of technical advance, bioinformatics or insightful findings of plant and animal development and function.

Size: Should not exceed 2000 words or 4 printed pages, is intended for rapid publication. They are not intended for publishing preliminary results or to be a reduced version of Regular Papers or Rapid Papers.

3. Review article
Definition: Critical evaluation of materials about current research that had already been published by organizing, integrating, and evaluating previously published materials. Re-analyses as meta-analysis and systemic reviews are encouraged. Review articles should aim to provide systemic overviews, evaluations and interpretations of research in a given field.

Size: Should not exceed 4000 words or 7-8 printed pages.

4. Special issues
Definition: Usually papers from research presented at a conference, seminar, congress or a symposium.

Size: Should not exceed 5000 words or 8-10 printed pages.

5. Others
Definition: Brief reports, case studies, comments, Letters to the Editor, and replies on previously published articles may be considered.

Size: Should not exceed 2000 words or up to 4 printed pages.

With few exceptions, original manuscripts should not exceed the recommended length of 6 printed pages (about 18 typed pages, double-spaced and in 12-point font, tables and figures included). Printing is expensive, and, for the Journal, postage doubles when an issue exceeds 80 pages. You can understand then that there is little room for flexibility.

Long articles reduce the Journal's possibility to accept other high-quality contributions because of its 80-page restriction. We would like to publish as many good studies as possible, not only a few lengthy ones. (And, who reads overly long articles anyway?) Therefore, in our competition, short and concise manuscripts have a definite advantage.

Format

The paper should be formatted in one column format with the figures at the end. A maximum of eight keywords should be indicated below the abstract to describe the contents of the manuscript. Leave a blank line between each paragraph and between each entry in the list of bibliographic references. Tables should preferably be placed in the same electronic file as the text. Authors should consult a recent issue of the Journal for table layout.

There is no need to spend time formatting your article so that the printout is visually attractive (e.g. by making headings bold or creating a page layout with figures), as most formatting instructions will be removed upon processing.

Manuscripts should be typewritten, typed on one side of the ISO A4 paper with at least 4cm margins and double spacing throughout. Every page of the manuscript, including the title page, references, tables, etc. should be numbered. However, no reference should be made to page numbers in the text; if necessary, one may refer to sections. Underline words that should be in italics, and do not underline any other words.

Authors are advised to use Times New Roman 12-point font. Be especially careful when you are inserting special characters, as those inserted in different fonts may be replaced by different characters when converted to PDF files. It is well known that 'μ' will be replaced by other characters when fonts such as 'Symbol' or 'Mincho' are used.

We recommend that authors prepare the text as a **Microsoft Word** file.

1. Manuscripts in general should be organised in the following order:

    - **Page 1: Running title.** (Not to exceed 60 characters, counting letters and spaces). This page should **only** contain your running title/ full title of your paper. In addition, the **Subject areas** most relevant to the study must be indicated on this page. Select one or two subject areas (refer to the *Scope Form).*
      A **list** of number of **black and white / colour figures and tables** should also be indicated on this page**.** Figures submitted in color will be printed in colour. See "*5. Figures & Photographs"* for details.

    - **Page 2: Author(s) and Corresponding author information.** This page should **repeat** the title of your paper with name(s) of all the authors, institutions and corresponding author's name, institution and full address (Street address, telephone number (including extension), hand phone number, fax number and e-mail address) for editorial correspondence.

      Authors' addresses. Multiple authors with different addresses must indicate their respective addresses separately by superscript numbers:

      George Swan[1] and Nayan Kanwal[2]
      [1]Department of Biology, Faculty of Science, Duke University, Durham, North Carolina, USA.
      [2]Research Management Centre, Universiti Putra Malaysia, Serdang, Malaysia.

    - **Page 3**: This page should **repeat** the title of your paper with only the **Abstract** (the abstract should be less than 250 words for a Regular Paper and up to 100 words for a Short Communication). **Keywords** must also be provided on this page (Not more than eight keywords in alphabetical order).
    - **Page 4 and subsequent pages**: This page should begin with the **Introduction** of your article and the rest of your paper should follow from page 5 onwards.

    Abbreviations. Define alphabetically, other than abbreviations that can be used without definition. Words or phrases that are abbreviated in the introduction and following text should be written out in full the first time that they appear in the text, with each abbreviated form in parenthesis. Include the common name or scientific name, or both, of animal and plant materials.

    Footnotes. Current addresses of authors if different from heading.

2. **Text.** Regular Papers should be prepared with the headings **Introduction**, **Materials and Methods**, **Results and Discussion, Conclusions** in this order. Short Communications should be prepared according to "*8. Short Communications."* below.
3. **Tables.** All tables should be prepared in a form consistent with recent issues of Pertanika and should be numbered consecutively with Arabic numerals. Explanatory material should be given in the table legends and footnotes. Each table should be prepared on a separate page. (Note that when a manuscript is accepted for publication, tables must be submitted as data - .doc, .rtf, Excel or PowerPoint file- because tables submitted as image data cannot be edited for publication.)

4. **Equations and Formulae.** These must be set up clearly and should be typed triple spaced. Numbers identifying equations should be in square brackets and placed on the right margin of the text.

5. **Figures & Photographs.** Submit an original figure or photograph. Line drawings must be clear, with high black and white contrast. Each figure or photograph should be prepared on a separate sheet and numbered consecutively with Arabic numerals. Appropriate sized numbers, letters and symbols should be used, no smaller than 2 mm in size after reduction to single column width (85 mm), 1.5-column width (120 mm) or full 2-column width (175 mm). Failure to comply with these specifications will require new figures and delay in publication. For electronic figures, create your figures using applications that are capable of preparing high resolution TIFF files acceptable for publication. In general, we require **300 dpi or higher resolution for coloured and half-tone artwork** and **1200 dpi or higher for line drawings**. For review, you may attach low-resolution figures, which are still clear enough for reviewing, to keep the file of the manuscript under 5 MB. Illustrations may be produced at extra cost in colour at the discretion of the Publisher; the author could be charged Malaysian Ringgit 50 for each colour page.

6. **References.** Literature citations in the text should be made by name(s) of author(s) and year. For references with more than two authors, the name of the first author followed by 'et al.' should be used.

   Swan and Kanwal (2007) reported that …
   The results have been interpreted (Kanwal et al. 2009).

   - References should be listed in alphabetical order, by the authors' last names. For the same author, or for the same set of authors, references should be arranged chronologically. If there is more than one publication in the same year for the same author(s), the letters 'a', 'b', etc., should be added to the year.
   - When the authors are more than 11, list 5 authors and then et al.
   - Do not use indentations in typing References. Use one line of space to separate each reference. For example:
     - Jalaludin, S. (1997a). Metabolizable energy of some local feeding stuff. *Tumbuh, 1,* 21-24.
     - Jalaludin, S. (1997b). The use of different vegetable oil in chicken ration. *Mal. Agriculturist, 11,* 29-31.
     - Tan, S.G., Omar, M.Y., Mahani, K.W., Rahani, M., Selvaraj, O.S. (1994). Biochemical genetic studies on wild populations of three species of green leafhoppers *Nephotettix* from Peninsular Malaysia. *Biochemical Genetics*, *32,* 415 - 422.
   - In case of citing an author(s) who has published more than one paper in the same year, the papers should be distinguished by addition of a small letter as shown above, e.g. Jalaludin (1997a); Jalaludin (1997b).
   - Unpublished data and personal communications should not be cited as literature citations, but given in the text in parentheses. 'In press' articles that have been accepted for publication may be cited in References. Include in the citation the journal in which the 'in press' article will appear and the publication date, if a date is available.

7. **Examples of other reference citations**:
   Monographs: Turner, H.N. and Yong, S.S.Y. (2006). *Quantitative Genetics in Sheep Breeding*. Ithaca: Cornell University Press.

   Chapter in Book: Kanwal, N.D.S. (1992). Role of plantation crops in Papua New Guinea economy. In Angela R. McLean (Eds.), *Introduction of livestock in the Enga province PNG* (p. 221-250). United Kingdom: Oxford Press.

   Proceedings: Kanwal, N.D.S. (2001). Assessing the visual impact of degraded land management with landscape design software. In N.D.S. Kanwal and P. Lecoustre (Eds.), *International forum for Urban Landscape Technologies* (p. 117-127). Lullier, Geneva, Switzerland: CIRAD Press.

8. **Short Communications** should include **Introduction, Materials and Methods, Results and Discussion, Conclusions** in this order. Headings should only be inserted for Materials and Methods. The abstract should be up to 100 words, as stated above. Short Communications must be 5 printed pages or less, including all references, figures and tables. References should be less than 30. A 5 page paper is usually approximately 3000 words plus four figures or tables (if each figure or table is less than 1/4 page).

   *Authors should state the total number of words (including the Abstract) in the cover letter. Manuscripts that do not fulfill these criteria will be rejected as Short Communications without review.

STYLE OF THE MANUSCRIPT

Manuscripts should follow the style of the latest version of the Publication Manual of the American Psychological Association (APA). The journal uses British spelling and authors should therefore follow the latest edition of the Oxford Advanced Learner's Dictionary.

SUBMISSION OF MANUSCRIPTS

All articles submitted to the journal **must comply** with these instructions. Failure to do so will result in return of the manuscript and possible delay in publication.

The **four copies** of your original manuscript, four sets of photographic figures, as well as a CD with the **electronic copy in MS Word** (including text and figures) together with a **cover letter**, **declaration form**, **referral form A**, **scope form** need to be enclosed. They are available from the Pertanika's home page at http://rmc.upm.edu.my/pertanika or from the Executive Editor's office upon request.

Please do **not** submit manuscripts directly to the editor-in-chief or to the UPM Press. All manuscripts must be **submitted through the executive editor's office** to be properly acknowledged and rapidly processed:

Dr. Nayan KANWAL
Executive Editor
Research Management Centre (RMC)

4th Floor, Administration Building
Universiti Putra Malaysia
43400 UPM, Serdang, Selangor, Malaysia
email: ndeeps@admin.upm.edu.my; tel: + 603-8946 6192
fax: + 603 8947 2075

Authors should retain copies of submitted manuscripts and correspondence, as materials can not be returned.

Cover letter

All submissions must be accompanied by a cover letter detailing what you are submitting. Papers are accepted for publication in the journal on the understanding that the article is original and the content has not been published or submitted for publication elsewhere. This must be stated in the cover letter.

The cover letter must also contain an acknowledgement that all authors have contributed significantly, and that all authors are in agreement with the content of the manuscript.

The cover letter of the paper should contain (i) the title; (ii) the full names of the authors; (iii) the addresses of the institutions at which the work was carried out together with (iv) the full postal and email address, plus facsimile and telephone numbers of the author to whom correspondence about the manuscript should be sent. The present address of any author, if different from that where the work was carried out, should be supplied in a footnote.

As articles are double-blind reviewed, material that might identify authorship of the paper should be placed on a cover sheet.

Note When your manuscript is received at Pertanika, it is considered to be in its final form. Therefore, you need to check your manuscript carefully before submitting it to the executive editor (see also **English language editing** below).

Electronic copy

Preparation of manuscripts on a CD or DVD is preferable and articles should be prepared using MS Word. File name(s), the title of your article and authors of the article must be indicated on the CD. The CD must always be accompanied by four hard-copies of the article, and the content of the two must be identical. The CD text must be the same as that of the final refereed, revised manuscript. CDs formatted for IBM PC compatibles are preferred, as those formatted for Apple Macintosh are not acceptable. Please do not send ASCII files, as relevant data may be lost. Leave a blank line between each paragraph and between each entry in the list of bibliographic references. Tables should be placed in the same electronic file as the text. Authors should consult a recent issue of the Journal for table layout.

Peer review

In the peer-review process, three referees independently evaluate the scientific quality of the submitted manuscripts. The Journal uses a double-blind peer-review system. Authors are encouraged to indicate in **referral form A** the names of three potential reviewers, but the editors will make the final choice. The editors are not, however, bound by these suggestions.

Manuscripts should be written so that they are intelligible to the professional reader who is not a specialist in the particular field. They should be written in a clear, concise, direct style. Where contributions are judged as acceptable for publication on the basis of content, the Editor or the Publisher reserves the right to modify the typescripts to eliminate ambiguity and repetition and improve communication between author and reader. If extensive alterations are required, the manuscript will be returned to the author for revision.

The editorial review process

What happens to a manuscript once it is submitted to Pertanika? Typically, there are seven steps to the editorial review process:

1. The executive editor and the editorial board examine the paper to determine whether it is appropriate for the journal and should be reviewed. If not appropriate, the manuscript is rejected outright and the author is informed.
2. The executive editor sends the article-identifying information having been removed, to three reviewers. Typically, one of these is from the Journal's editorial board. Others are specialists in the subject matter represented by the article. The executive editor asks them to complete the review in three weeks and encloses two forms: (a) referral form B and (b) reviewer's comment form along with reviewer's guidelines. Comments to authors are about the appropriateness and adequacy of the theoretical or conceptual framework, literature review, method, results and discussion, and conclusions. Reviewers often include suggestions for strengthening of the manuscript. Comments to the editor are in the nature of the significance of the work and its potential contribution to the literature.
3. The executive editor, in consultation with the editor-in-chief, examines the reviews and decides whether to reject the manuscript, invite the author(s) to revise and resubmit the manuscript, or seek additional reviews. Final acceptance or rejection rests with the Editorial Board, who reserves the right to refuse any material for publication. In rare instances, the manuscript is accepted with almost no revision. Almost without exception, reviewers' comments (to the author) are forwarded to the author. If a revision is indicated, the editor provides guidelines for attending to the reviewers' suggestions and perhaps additional advice about revising the manuscript.
4. The authors decide whether and how to address the reviewers' comments and criticisms and the editor's concerns. The authors submit a revised version of the paper to the executive editor along with specific information describing how they have answered' the concerns of the reviewers and the editor.
5. The executive editor sends the revised paper out for review. Typically, at least one of the original reviewers will be asked to examine the article.
6. When the reviewers have completed their work, the executive editor in consultation with the editorial board and the editor-in-chief examine their comments and decide whether the paper is ready to be published, needs another round of revisions, or should be rejected.
7. If the decision is to accept, the paper is sent to that Press and the article should appear in print in approximately two to three months. The Publisher ensures that the paper adheres to the correct style (in-text citations, the reference list, and tables are typical areas of concern, clarity, and grammar). The authors are asked to respond to any queries by the Publisher. Following these corrections, page proofs are mailed to the corresponding authors for their final approval. At this point, only essential changes are accepted. Finally, the article appears in the pages of the Journal and is posted on-line.

English language editing
Authors are responsible for the linguistic accuracy of their manuscripts. Authors not fully conversant with the English language should seek advice from subject specialists with a sound knowledge of English. The cost will be borne by the author, and a copy of the certificate issued by the service should be attached to the cover letter.

Author material archive policy
Authors who require the return of any submitted material that is rejected for publication in the journal should indicate on the cover letter. If no indication is given, that author's material should be returned, the Editorial Office will dispose of all hardcopy and electronic material.

Copyright
Authors publishing the Journal will be asked to sign a declaration form. In signing the form, it is assumed that authors have obtained permission to use any copyrighted or previously published material. All authors must read and agree to the conditions outlined in the form, and must sign the form or agree that the corresponding author can sign on their behalf. Articles cannot be published until a signed form has been received.

Lag time
The elapsed time from submission to publication for the articles averages 5-6 months. A decision of acceptance of a manuscript is reached in 2 to 3 months (average 9 weeks).

Back issues
Single issues from current and recent volumes are available at the current single issue price from UPM Press. Earlier issues may also be obtained from UPM Press at a special discounted price. Please contact UPM Press at penerbit@putra.upm.edu.my or you may write for further details at the following address:

UPM Press
Universiti Putra Malaysia
43400 UPM, Serdang
Selangor Darul Ehsan
Malaysia.

Pertanika

Our goal is to bring high quality research to the widest possible audience

Pertanika is Indexed in Scopus & EBSCO

Pertanika is an international peer-reviewed leading journal in Malaysia which began publication in 1978. The journal publishes in three different areas — Journal of Tropical Agricultural Science (JTAS); Journal of Science and Technology (JST); and Journal of Social Sciences and Humanities (JSSH).

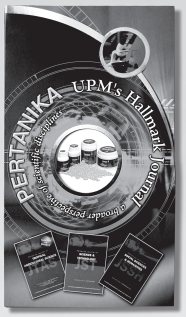

JTAS is devoted to the publication of original papers that serves as a forum for practical approaches to improving quality in issues pertaining to tropical agricultural research or related fields of study. It is published twice a year in **February** and **August**.

JST caters for science and engineering research or related fields of study. It is published twice a year in **January** and **July**.

JSSH deals in research or theories in social sciences and humanities research with a focus on emerging issues pertaining to the social and behavioural sciences as well as the humanities, particularly in the Asia Pacific region. It is published twice a year in **March** and **September**.

Why should you publish in Pertanika Journals?

Benefits to Authors

PROFILE: our journals are circulated in large numbers all over Malaysia, and beyond, in Southeast Asia. Recently, we have widened our circulation to other overseas countries as well. We will ensure that your work reaches the widest possible audience in print and online, through our wide publicity campaigns held frequently, and through our constantly developing electronic initiatives through e-pertanika and Pertanika Online.

QUALITY: Our double-blind peer refereeing procedures are fair and open, and we aim to help authors develop and improve their work. Pertanika JTAS is now over 30 years old; this accumulated knowledge has resulted in Pertanika JTAS being indexed by Scopus (Elsevier).

AUTHOR SERVICES: we provide a rapid response service to all our authors, with dedicated support staff for each journal, and a point of contact throughout the refereeing and production processes. Our aim is to ensure that the production process is as smooth as possible, is borne out by the high number of authors who publish with us again and again.

LAG TIME & REJECTION RATE: the elapsed time from submission to publication for the articles in Pertanika averages 6-8 months. A decision of acceptance of a manuscript is reached in 1 to 3 months (average 7 weeks).

Our journals have a 30% rejection rate of its submitted manuscripts, many of the papers fail on account of their substandard presentation and language (frustrating the peer reviewers).

Call for Papers

Pertanika invites you to explore frontiers from all fields of science and technology to social sciences and humanities. You may contribute your scientific work for publishing in UPM's hallmark journals either as a ***regular article***, ***short communications***, or a ***review article*** in our forthcoming issues. Papers submitted to this journal must contain original results and must not be submitted elsewhere while being evaluated for the Pertanika Journals.

Submissions in English should be accompanied by an abstract not exceeding 300 words. Your manuscript should be no more than 6,000 words or 10-12 printed pages, including notes and abstract. Submissions should conform to the Pertanika style, which is available at www.rmc.upm.edu.my/pertanika or by mail or email upon request.

Papers should be double-spaced 12 point type (Times New Roman fonts preferred). The first page should include the title of the article but no author information. Page 2 should repeat the title of the article together with the names and contact information of the corresponding author as well as all the other authors. Page 3 should contain the abstract only. Page 4 and subsequent pages to have the text - Acknowledgments - References - Tables - Legends to figures – Figures, etc.

Questions regarding submissions should only be directed to the Executive Editor, Pertanika Journals.

Remember, ***Pertanika is the resource to support you in strengthening research and research management capacity***.

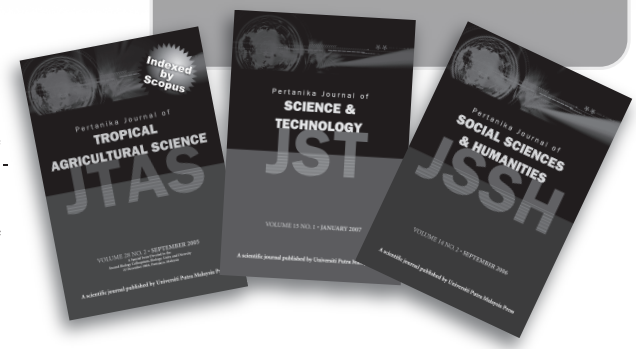

An Award Winning International-Malaysian Journal

FEB. 2008

Mail your submissions to:

The Executive Editor
Pertanika Journals
Research Management Centre (RMC)
Publication Division
4th Floor, Administration Building
Universiti Putra Malaysia
43400 UPM, Serdang, Selangor, Malaysia

Tel: +603-8946 6192
ndeeps@admin.upm.edu.my
www.rmc.upm.edu.my/pertanika

Selected Articles from the World Engineering Congress 2007
Guest Editors: Siti Mazlina Mustapa Kamal, Farah Saleena Taip and Siti Aslina Hussain

Selected Articles from the Science Seminar 2007
Guest Editorial Board: W. Mahmood Mat Yunus, Nor' Aini Mohd Fadzillah, Abdul Halim Abdullah, Hishamuddin Zainuddin, Mahendran a/l Shitan and Shamarina Shohaimi

Selected Articles from the 21st Symposium of Chemical Engineers 2007
Guest Editors: Zurina Zainal Abidin, Intan Salwani Ahamad and Robiah Yunus

Pertanika Journal of Science & Technology
Volume 17 (1) Jan. 2009

Contents

Regular Articles

Research Management Centre (RMC)
4th Floor, Administration Building
Universiti Putra Malaysia
43400 UPM Serdang
Selangor Darul Ehsan
Malaysia

http://www.rmc.upm.edu.my
E-mail : pertanika@rmc.upm.edu.my
Tel : +603 8946 6185/ 6192
Fax : +603 8947 2075

UPM Press
Universiti Putra Malaysia
43400 UPM Serdang
Selangor Darul Ehsan
Malaysia

http://penerbit.upm.edu.my
E-mail : penerbit@putra.upm.edu.my
Tel : +603 8946 8855/8854
Fax : +603 8941 6172

ISSN 0128-7680
01
9 770128 768083